DEVELOPMENT OF CRITERIA AND TEST METHODS FOR EYE AND FACE PROTECTIVE DEVICES

David A. LaMarre
American Optical Corporation
14 Mechanic Street
Southbridge, Massachusetts 01550

Contract No. 210-75-0058

FINAL REPORT

U.S. DEPARTMENT OF HEALTH, EDUCATION, AND WELFARE
Public Health Service
Center for Disease Control
National Institute for Occupational Safety and Health
Division of Physical Sciences and Engineering
Cincinnati, Ohio 45226

August, 1977

DISCLAIMER

The contents of this report are reproduced herein as received from the contractor.

The options, findings, and conclusions expressed herein are not necessarily those of the National Institute for Occupational Safety and Health, nor does mention of company names or products constitute endorsement by the National Institute for Occupational Safety and Health.

NIOSH Project Officer: Keith Crouch, Ph.D.
Principal Investigator: David A. LaMarre

CONTENTS

CONTENTS

CONTENTS

ABSTRACT

Eye and face protection devices required by OSHA for use by industrial employees must comply with the performance and design specifications of American National Standards Institute Standard Practice for Occupational and Educational Eye and Face Protection ANSI Z87.1-1968. Some of the requirements and test methods of Z87.1 have been unchanged for many years or are not clearly defined, hence there exists a need to determine whether performance requirements are adequate and to improve test methods.

Following description of a program of analytical and experimental work on three specific aspects of eye and face protection devices, recommendations are presented for significant changes in attenuation properties of light-absorptive materials such as welding plates, for a high-speed impact test employing a pointed missile, and for improved test methods for optical attributes.

This report was submitted in fulfillment of Contract No. 210-75-0058 by American Optical Corporation under the sponsorship of the National Institute for Occupational Safety and Health.

ACKNOWLEDGEMENTS

We wish to express our gratitude to the following persons for their contributions during this program: Neill M. Brandt, who performed the experimental impact testing and the statistical analysis of the resulting data; Fred N. Winters, Jr. and James A. Reilly for their assistance in assessing optical requirements for protectors; and Martin S. Dragon for analysis and recommendation of objective optical test methods. We wish particularly to thank Donald B. Whitney for helpful discussion and insight on many points.

INTRODUCTION

Occupational eye and face protective devices presently must conform to the requirements of ANSI Z87.1-1968. Since some of the requirements and test methods of Z87.1 have been unchanged for many years or are not clearly defined, there is a need to determine whether certain performance requirements are still adequate; and for improved test methods to allow more objective determination of conformance of present products to Z87.1 as well as to assist in determining efficacy of present and future products against a variety of hazards.

As a result of NIOSH evaluation of this situation, the contract called for effort in three specific areas:

1. Determination of the adequacy of Table 1 of Z87.1 which calls out required amounts of absorption of ultraviolet, visible, and infrared radiation for protectors used by welders, furnace workers, and others;

2. Evaluation and recommendation of an impact-resistance test method utilizing a projectile more representative of some hazardous missiles that occur in factory environments - e.g., machine shops - than the slow-moving smooth steel spheres of various sizes required by Z87.1;

3. Determination of the adequacy, based on human visual needs, of the optical tolerances for eye and face protectors, recommendation of objective test methods for optical properties where possible rather than the present subjective methods of Z87.1, and for classification of defects of types commonly found in optical materials used in protectors.

The three tasks under this contract correspond to the three areas above. The three tasks are essentially unrelated technically, and so the summary and recommendations for each task are given at the end of the task.

TASK 1

INTRODUCTION

The Contract calls for evaluation of the adequacy of Table 1 on page 24 of the American National Standard Institute Z87.1-1968 Standard for Occupational and Educational Eye and Face Protection with respect to its applicability in the current industrial environment and for modifications as necessary to that Table. In the sections below, the strengths and shortcomings of Table 1 of Z87.1 will be discussed as will new knowledge and products which could affect Table 1.

Table 1 of Z87.1 calls out shade numbers of absorbing lenses and the required transmittances for these shade numbers in the ultraviolet, visible, and infrared portions of the spectrum based on the only good absorbing lens materials in wide use at the time the table was first generated, during or before the 1930's.† These absorptive materials were glasses containing various amounts of ferrous and ferric iron which gave them their characteristic green or yellow-green appearance in transmission. The ferrous ions determined the amount of infrared absorption and absorption at the red end of the visible region, while the ferric ions gave the ultraviolet absorption and the absorption at the blue end of the visible. By adjusting the ratio of ferrous to ferric ions and the total iron concentration it was possible to make glasses of all shade numbers from 1.5 to 14 listed in the table. (For the low shade numbers it was sometimes necessary to add cerium to the glasses to get sufficient ultraviolet absorption). So transmission curves for all these early lens materials were similar in shape with the transmission scale changed depending upon the shade number of the lens. These iron-containing glasses have a long history of providing adequate protection for industrial users. Because of this it is reasonable to ask why the Table may need revisions or additions.

The reasons why Table 1 of Z87.1 needs revision fall into two broad categories. The first category consists of technical shortcomings in the Table itself and in the Z87.1

---

† See, for example, National Bureau of Standards Handbook H24, 1938.

approach to absorptive eye protection which is embodied in the Table and Appendix A.2 of that standard. The second category consists of a number of new factors affecting eye protection needs.

An obvious deficiency of Table 1 of Z87.1 is the fact that it places no limits on ultraviolet transmission in the region from 200 nm to 300 nm which is known to be very effective in damaging the cornea (photokeratitis). This may not have been a serious shortcoming when the only available materials were the green iron-doped glasses since by their nature they would transmit very little ultraviolet radiation in this region as compared to their visual transmittance, but since different glasses and new plastics are becoming available for absorbing lenses it does not automatically follow that these would have the same high absorption. It is very likely that the values given in Table 1 for maximum ultraviolet transmission are not low enough for the higher shade numbers since with most of the green glasses the values of transmission actually achieved are much lower than those called for in the Table; hence, the protection value of the product may have been derived from this property of the glasses rather than from meeting the values set up in the Table, which represented the practical limit of measurement capability many years ago. This fact has been recognized in Table 4 of the ISO Draft Standard for welding filters (ISO/TC 94/SC6, April 1973) where much lower limits for UV transmission are set.

Another shortcoming in Table 1 of Z87.1 is that all infrared radiation from 700 nm to the limits of glass transmission is lumped into one integrated measurement. It is now known that the wavelength region from 700 to approximately 1300 nm is transmitted through the ocular media and is absorbed in significant doses in the retina, while radiation of wavelength greater than approximately 1300 nm is absorbed before reaching the retina. Hence, allowable infrared transmittance of the filters should be split into two values for the two wavelength regions as has been done in the ISO draft standard just mentioned.

When choosing an absorbing lens or plate the tendency is to pick the shade which allows comfortable viewing of the work. If modern powerful arc sources or high intensity lamps vary considerably from older sources in the ratio of ultraviolet or infrared to visible emission, then it must be examined whether the ultraviolet and infrared attenuation levels are sufficiently low in Table 1 for given values of luminous transmittance. In addition, the green glasses have a transmission curve in the visible region which is

closely centered on the photopic eye sensitivity curve. As a consequence, the green glasses as a class transmit a minimum of radiation in the visible region for their given values of luminous transmittance (or shade). A modern welding plate whose transmission in the visible region is peaked, for example, in the blue (to suppress red and yellow flare characteristic of the arc in some welding processes) can admit more radiation in the visible region to the eye for a given shade number than does a green iron-doped glass, particularly if the arc emission peaks in the UV or blue rather than in the green.

There now exist glass and plastic welding plates, some of which have metallic coatings, which meet the standards of Table 1 of Z87.1 but which in some cases allow markedly different ratios of ultraviolet, visible, and infrared radiation to be transmitted than do the traditional iron-doped green glass plates. In addition, there are a number of glasses and plastic materials which, while not necessarily new, can provide very effective absorption in certain regions of the spectrum and which may offer more useful and pleasant-to-wear protection than green glass for some applications.

Table 1 and Appendix A.2 of Z87.1 taken together may be considered as general purpose recommendations for eye protection from radiation. Since Z87.1 is now binding because of adoption by OSHA, if it is desired to provide protection for the eye from any portion of the UV, visible, or infrared, then lenses from Table 1 should be used. The rigidity of this requirement allows no room for use of more specialized absorptive materials which might perform suitably for certain radiation hazards without having the drawbacks of the green glasses. If, for instance, protection from ultraviolet radiation only is wanted and visible attenuation is not desirable, then cerium-containing glasses may offer sufficient protection. If all that is necessary is attenuation in the visible with modest amounts of ultraviolet and infrared absorption, then neutral gray glasses might be used and they would better preserve color balance for the wearer. Again, there exist today so-called "heat screen" glasses which are quite effective at filtering out infrared but which have relatively high luminous transmittance. The ISO/TC 94/SC6 Draft Standard recognizes some of these lenses and sets requirements for them.
If a user can determine his radiation source characteristics, then there may be better solutions for particular problems than those given in Table 1 of Z87.1 and the user should be allowed to adopt these improved solutions provided they can be shown to be safe.

New light sources have appeared on the industrial scene since the 1930's. Welding arcs now operate at higher currents and wattages and consequently with higher amounts of radiation emitted than ever before. This may become increasingly the case for two reasons. First,the adoption of smoke-extractor welding guns removes the cloud of absorptive smoke around the weld area and second, it appears to be economically advantageous to increase productivity by increasing the welding wattage even further. Xenon arc lamps, tungsten halogen lamps, electronic photoflash units and high intensity carbon arcs have all been developed in recent years. On the other hand, light-duty welding processes where wattages may be only a few hundred watts have also been developed in recent years. It may be that these economically-attractive fastening methods are being handicapped by the requirement that the welder wear a welding helmet when all that may be necessary is a modest amount of ultraviolet and visible absorption. This more comfortable protection might be adequately provided by faceshields over spectacles or by the use of various types of goggles.

Finally, much work has been done in recent years to quantify the Maximum Permissible Exposures (MPEs) for the human eye to optical radiation.

As a consequence, then, of the possible shortcomings of Table 1 listed above, and the factors of new sources of optical radiation, new knowledge of MPEs, and new eye protection materials, the work on this task was divided into three subtasks:

1. Recommend Maximum Permissible Exposures for the industrial situation.

2. Study emitted optical radiation from welding arcs and other light sources; and

3. Recommend revisions to Table 1 of Z87.1

In order to organize calculations for these tasks, a formalism akin in spirit to that of photometry was devised which should allow improved future knowledge about MPEs or source data to be utilized directly for updating requirements for absorptive plates.

SUBTASK 1: RECOMMENDED MAXIMUM PERMISSIBLE EXPOSURES (MPEs)

United States and Foreign MPEs

First work under this Subtask consisted mainly of literature study. As a result of flashblindness considerations with the advent of nuclear bombs, the advent of lasers, and NASA's need to provide eye protection in space where the shielding effect of atmospheric gases is absent, much scientific work has been done in the last three decades to quantify threshold values for damage for the human eye. A very thorough review of this work may be found in a paper by Sliney and Freasier entitled "Evaluation of Optical Radiation Hazards."[2] This paper contains a list of ninety references to earlier work. More recently Pitts has published a paper, "The Human Ultraviolet Action Spectrum,"[3] which updates knowledge in the 200 to 300 nm region. Because few measurements have been made of eye sensitivity to optical radiation in the 300 to 400 nm region, NIOSH is presently funding a program of measurements by Dr. Pitts at the Univ. of Houston. Recent communication with Dr. Pitts reveals that these data are not yet available for use in this project.

All the scientific work of recent years referred to above was distilled into standards or guides for the safe use of lasers. The latest versions are "Threshold Limit Values for Chemical Substances and Physical Agents in the Workroom Environment with Intended Changes for 1976"[4] issued by the American Conference of Government Industrial Hygienists (ACGIH), and the American National Standard for the Safe Use of Lasers, ANSI Z136.1-1976[5]. At this time the TLVs* (Threshold Limit Values - ACGIH terminology) and MPEs (Maximum Permissible Exposures - ANSI terminology) are the same, and are given in Tables 1 and 2.

Table 1 gives the MPEs for direct viewing of a laser beam; it applies when light sources subtend small angles at the eye. Because of the thermal conductivity of the retina and surrounding materials and other effects, the numerical definition of "small angle" is time-dependent. For purposes of industrial exposures, it is adequate to note that the angle which marks the borderline between use of Table 1 (small angular subtense of source at eye) and Table 2 (large angular subtense) is 15 milliradians for a 1 second exposure and 24 milliradians for exposure time 10 seconds or greater - for more detail, see Figure 1, which is an expanded portion of Fig. 3 of ANSI Z136.1-1976[5].

---

* TLV is a registered trademark of ACGIH.

TABLE 1. Maximum Permissible Exposure (MPE) for Direct Ocular Exposures, Intrabeam Viewing, from a Laser Beam

Wavelength, λ (μm)	Exposure Duration, t (s)	Maximum Permissible Exposure (MPE)	
Ultraviolet			
0.200-0.302	10^{-2}-3×10^{4}	3×10^{-3} J·cm^{-2}	
0.303	"	4×10^{-3} "	In no case shall the total irradiance, over all the wavelengths within the UV spectral region, be greater than 1 watt per square centimeter upon the cornea.
0.304	"	6×10^{-3} "	
0.305	"	1.0×10^{-2} "	
0.306	"	1.6×10^{-2} "	
0.307	"	2.5×10^{-2} "	
0.308	"	4.0×10^{-2} "	
0.309	"	6.3×10^{-2} "	
0.310	"	1.0×10^{-1} "	
0.311	"	1.6×10^{-1} "	
0.312	"	2.5×10^{-1} "	
0.313	"	4.0×10^{-1} "	
0.314	"	6.3×10^{-1} "	
0.315-0.400	10^{-9}-10	$0.56t^{1/4}$ J·cm^{-2}	
0.315-0.400	10-10^{3}	1J·cm^{-2}	
0.315-0.400	10^{3}-3×10^{4}	1×10^{-3}W·cm^{-2}	
Visible and Near-Infrared			
0.400-0.700	10^{-9}-1.8×10^{-5}	5×10^{-7}J·cm^{-2}	
0.400-0.700	1.8×10^{-5}-10	$1.8t^{3/4}\times10^{-3}$ "	
0.400-0.550	10-10^{4}	10×10^{-3} "	
0.550-0.700	10-T_1	$1.8t^{3/4}\times10^{-3}$ "	
0.550-0.700	T_1-10^{4}	$10C_B\times10^{-3}$ "	
0.400-0.700	10^{4}-3×10^{4}	$C_B\times10^{-6}$W·cm^{-2}	
0.700-1.059	10^{-9}-1.8×10^{-5}	$5C_A\times10^{-7}$J·cm^{-2}	
0.700-1.059	1.8×10^{-5}-10^{3}	$1.8C_At^{3/4}\times10^{-3}$ "	
1.060-1.400	10^{-9}-5×10^{-5}	5×10^{-6} "	
1.060-1.400	5×10^{-5}-10^{3}	$9t^{3/4}\times10^{-3}$ "	
0.700-1.400	10^{3}-3×10^{4}	$320C_A\times10^{-6}$W·cm^{-2}	
Far-Infrared			
1.4-10^{3}	10^{-9}-10^{-7}	10^{-2}J·cm^{-2}	
	10^{-7}-10	$0.56t^{1/4}$J·cm^{-2}	
	>10	0.1W·cm^{-2}	

C_A, C_B, and T_1 are defined at the end of Table 2.

TABLE 2. Maximum Permissible Exposure (MPE) for Viewing a Diffuse Reflection of a Laser Beam or an Extended Source Laser

Wavelength, λ (μm)	Exposure Duration, t (s)	Maximum Permissible Exposure (MPE)
Ultraviolet		
0.200-0.400	Same as Table 1	
Visible		
0.400-0.700	10^{-9}-10	$10t^{1/3}$ J·cm^{-2}·sr^{-1}
0.400-0.550	10-10^4	21 J·cm^{-2}·sr^{-1}
0.550-0.700	10-T_1	$3.83t^{3/4}$ J·cm^{-2}·sr^{-1}
0.550-0.700	T_1-10^4	$21C_B$ J·cm^{-2}·sr^{-1}
0.400-0.700	10^4-3×10^4	$2.1C_B\times10^{-3}$ W·cm^{-2}·sr^{-1}
Near Infrared		
0.700-1.400	10^{-9}-10	$10C_At^{1/3}$ J·cm^{-2}·sr^{-1}
0.700-1.400	10-10^3	$3.83C_At^{3/4}$ J·cm^{-2}·sr^{-1}
0.700-1.400	10^3-3×10^4	$0.64C_A$ W·cm^{-2}·sr^{-1}
Far-Infrared		
1.4-10^3	Same as Table 1	

DEFINITIONS

$C_A = 10^{[(\lambda-0.700)/0.515]}$ 0.700 μm $\leq \lambda \leq$ 1.060 μm

$= 5$ 1.060 μm $\leq \lambda \leq$ 1.400 μm

$C_B = 1$ 0.400 μm $\leq \lambda \leq$ 0.550 μm

$= 10^{[15(\lambda-0.550)]}$ 0.550 μm $\leq \lambda \leq$ 0.700 μm

$T_1 = 10$s 0.400 μm $\leq \lambda \leq$ 0.550 μm

$= 10^{[1+20(\lambda-0.550)]}$ 0.550 μm $\leq \lambda \leq$ 0.700 μm

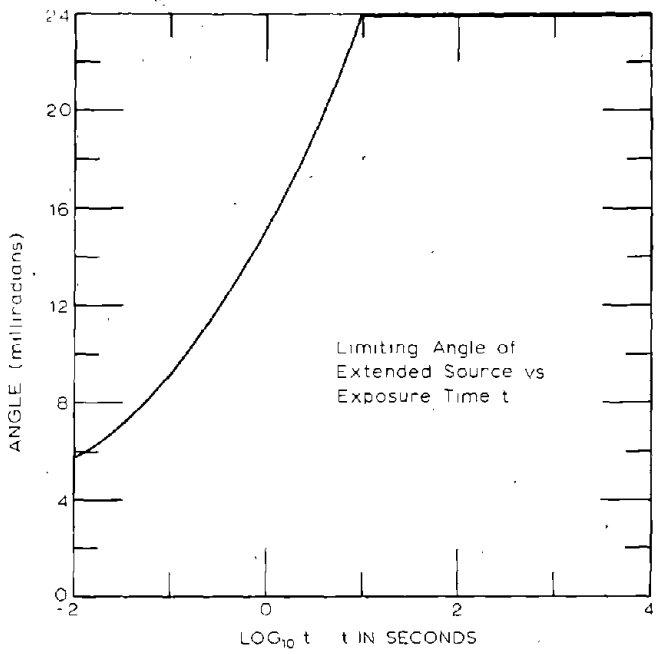

Figure 1. Limiting angle of extended source versus exposure time, t

It will perhaps help to orient the reader if we mention that it appears that welding arcs and arc lamps will usually be governed by Table 1, whereas sources of large angular extent, such as some melting furnaces, heat-treat furnaces, arc lamps with associated optics, etc. will be governed by Table 2.

Before going into the matter of how the laser MPEs can be used for industrial eye protection, it is worth examining another approach to laser eye protection.

The International Organization for Standardization (ISO) is currently considering a Fourth Draft Proposal ISO/TC 94/SC 6/WG 3 for "Filters and Eye Protectors Against Laser Radiation." The ISO draft divides the spectrum into only two spectral regions and contains very simple recommendations for MPEs:

TABLE 3. ISO RECOMMENDATION FOR MAXIMUM PERMISSIBLE EXPOSURE

Laser Type	Actual working time and pulse lengths respectively	MPE 200nm to 1.4μm	MPE 1.4μm to 1mm
CW laser	more than 0.1s	5×10^{-6} W/cm^2	0.1 W/cm^2
Pulsed laser	1μs to 0.1s	5×10^{-7} J/cm^2	0.01 J/cm^2
Giant pulse laser	1ns to 1μs	5×10^{-8} J/cm^2	Not yet established

It is evident that the ISO MPEs are a much simpler set with which to deal than are those given in Tables 1 and 2. This point will be considered further, but before doing so we feel it to be worthwhile to develop a set of definitions and analytical expressions which will be useful for further work in Task 1.

Weighting Incident Power by its Relative Efficiency for Causing Biological Damage

Given MPEs as a function of wavelength and time such as in the Tables above, it is a relatively straightforward job to calculate protection required for a given laser which will normally operate at one wavelength, a few wavelengths, or a relatively restricted band of wavelengths. For industrial eye protection, most sources will emit in much or all of the spectrum from 200 nm to 4 μm, and it becomes necessary to weight the incident power by its efficiency for producing biological effects. This is a common method of analysis, and is used, for instance, in the ACGIH guideline for occupational exposure to ultraviolet radiation.[4]

For future work in Task 1 we will need to consider two types of effects caused by optical radiation:

1. The light-producing effects which are related to the radiant power by the luminous efficiency function and are analyzed using photometric concepts and units, and,

2. the effects producing biological damage which are related to the optical radiation by the MPEs. As far as we know, these are not formally covered by a measurement system analogous to photometry.

Because the photometric system has become the accepted way to deal with light calculations, we believe it may be easier for future work on this contract to set up a formalism for MPE calculations similar to the photometric system; experience has shown us that it is easy to get confused when too many informal calculations are required, since the MPEs are functions of wavelength, time, and source angular size.

First we recall the photometric relations for spectral sensitivity;*

$$K(\lambda) = K_m V(\lambda) \qquad (1)$$

---

* c.f. Color in Business, Science, and Industry[6], p. 467

where $K(\lambda)$ = luminous efficiency at wavelength λ in lumens/watt (lm/W)

K_m = maximum luminous efficiency, 680 lm/W at λ = 555 nm, where $V(\lambda) = 1$

$V(\lambda)$ = relative photopic luminous efficiency function

and for obtaining luminous flux

$$F = K_m \int_\lambda P(\lambda) V(\lambda) d\lambda \qquad (2)$$

where F = Luminous flux, in lumens

$P(\lambda)$ = spectral radiant flux (power) at the wavelength λ, W/nm

We note that the luminous efficiency $K(\lambda)$ is given by the luminous flux divided by the corresponding radiant flux. The relative photopic luminous efficiency function $V(\lambda)$ is shown in Figure 2. (Since we will be dealing with situations involving plenty of light, we need only the photopic curve; also, since critical color matching is not our problem, the relative luminous efficiency $V(\lambda)$ for the 1931 CIE observer (Figure 2) will be used throughout).

Turning now to the MPE situation, we define for small sources governed by Table 1,

$Z(\lambda,t)$ = MPE at wavelength λ for exposure time t, W/cm^2 (3)

(We will leave the development of a formalism for large sources until later.)

We then define a "relative ocular bio-damage efficiency function" S as

$$S(\lambda,t) = \frac{Z(\lambda_o,t)}{Z(\lambda,t)} \quad \text{unitless} \qquad (4)$$

where λ_o is a reference wavelength which remains to be chosen. $S(\lambda,t)$ is then the analog of $V(\lambda)$. Now $V(\lambda)$ has been defined to be equal to 1 at the wavelength of peak visual sensitivity (555 nm), which is convenient but not essential. Because a key factor in the choice of industrial eye protection filters is a person's ability to see well enough to perform his job, we will be concerned in Subtasks 2 and 3 with the ratios of attenuation required for eye protection in various spectral regions to that required in the visible region for comfortable effective vision. For this reason, and because of the

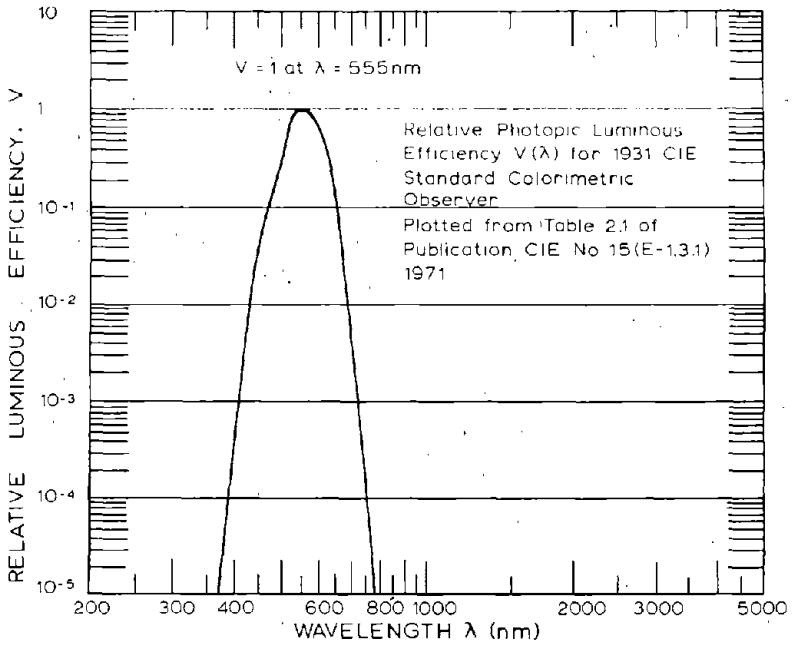

Figure 2. Relative photopic luminous efficiency V(λ) for 1931 CIE Standard Colorimetric Observer

particular breakdown of Tables 1 and 2 into spectral regions, we will choose

$$\lambda_o = 549 \text{ nm} . \tag{5}$$

From (4) and (5),

$$S(549, t) = 1. \tag{6}$$

It is worthwhile to have a convenient name for the quantity of irradiance (W/cm^2) which equals the MPE. For this purpose we define

1 biowatt/cm^2 = amount of power per square centimeter ("bio-irradiance") required to equal the MPE when the MPE is specified as an irradiance (W/cm^2). (7)

For example, from Table 1 when $t = 10^4$s and $\lambda = 549$ nm, the MPE = $Z(549, 10^4) = 10$ mJ/cm^2. This corresponds to an average irradiance of

$$\frac{10\times10^{-3} \text{ J/cm}^2}{10^4 \text{s}} = 10^{-6} \text{ W/cm}^2 \tag{8}$$

so under these conditions 1 biowatt (bioW) = 10^{-6}W.

(As noted after Eq. (3), for the present we will neglect the question of what to do when the MPE is defined as a radiance in W/cm sr). The biowatt corresponds to the lumen, the amount of power required to cause a given sensation of light anywhere in the visible region of the spectrum. Corresponding to Eq. (1) we may write

$$Q(\lambda,t) = Q_o(t)S(\lambda,t) \tag{9}$$

where $S(\lambda,t)$ is given by (4)

$$Q_o(t) = \frac{1}{Z(\lambda_o,t)} \text{ bioW/W} \tag{10}$$

$= $ reference bio-damage efficiency at the chosen wavelength $\lambda_o = 549$ nm

$Q(\lambda,t) = $ bio-damage efficiency at wavelength λ for exposure time t (11)

and finally, in correspondence to Eq. (2), we obtain exposure in bio-irradiance (bioW/cm^2) from

$$D = Q_o(t) \int_\lambda E(\lambda)S(\lambda,t)d\lambda \tag{12}$$

where $D = $ biologically-weighted irradiance, in bioW/cm^2

$E(\lambda) = $ spectral irradiance at wavelength λ, W/cm^2 nm. (13)

We have purposefully neglected dependence of $E(\lambda)$ on t since this dependence should not be important for future work. Note that if it had seemed desirable, Q_o, the reference bio-damage efficiency, could have been defined independent of t so as to more closely parallel K_m, but if $Q(\lambda,t)$ were to have the same meaning then $S(\lambda,t)$ would have changed greatly as t changed. To repeat, we will be considering ratios of power in different spectral bands to that in the visible band, so we feel more comfortable keeping $S = 1$ in the middle of the visible for any t and letting Q_o be the quantity which is strongly time dependent.

To illustrate the concepts of this section we have prepared graphs showing $S(\lambda,t)$ calculated from Eq. (4) and Table 1*

---

* Except that we have used 10 mW/cm^2 as the MPE for the 1.4 μm to 1 mm region, t > 10s, rather than 0.1 W/cm^2 given in Table 1. This will be discussed later.

for a range of times of interest for industrial non-laser exposures - see Figures 3-7, which are plotted to the same scale as Figure 2.

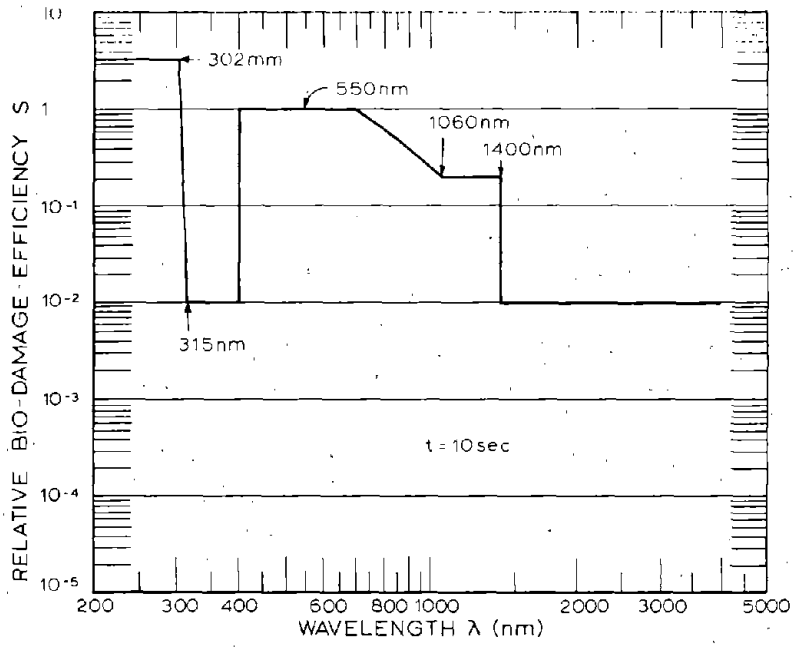

Figure 3. Relative bio-damage efficiency for t = 10 seconds for small sources (Table 1) vs wavelength

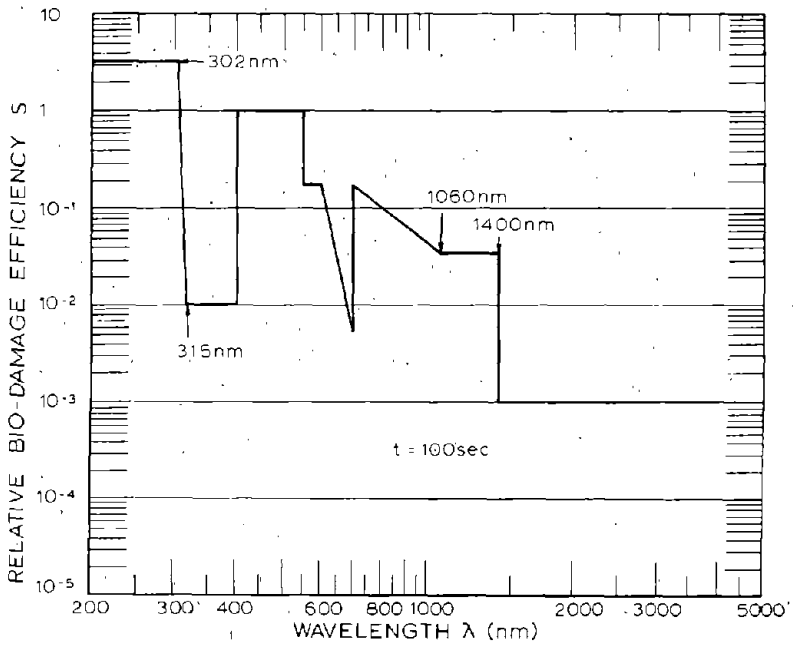

Figure 4. Relative bio-damage efficiency for t = 100 seconds for small sources (Table 1) vs wavelength

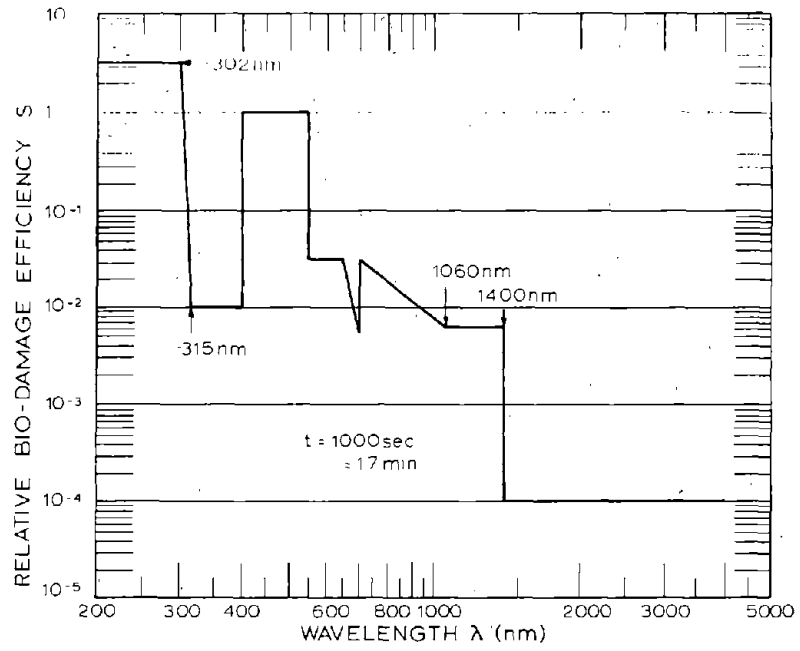

Figure 5. Relative bio-damage efficiency for t = 1000 seconds for small sources (Table 1) vs wavelength

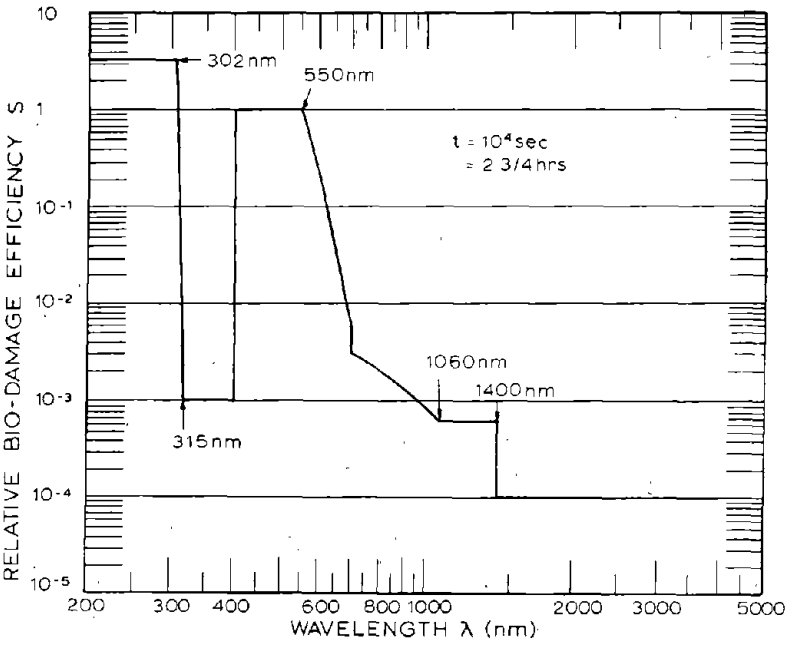

Figure 6. Relative bio-damage efficiency for t = 10^4 seconds for small sources (Table 1) vs wavelength

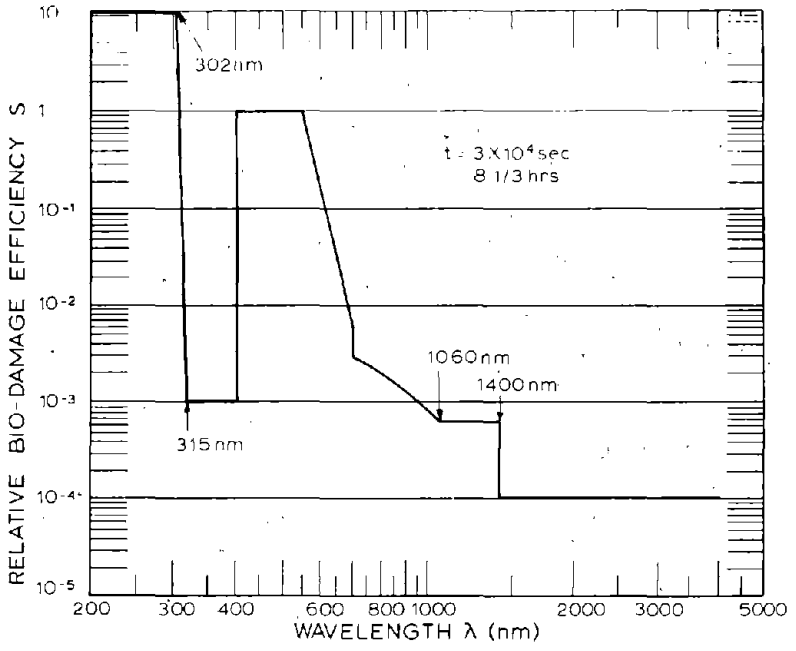

Figure 7. Relative bio-damage efficiency for $t = 3 \times 10^4$ seconds for small sources (Table 1) vs wavelength

The behavior of $Q_o(t)$ as a function of time is shown in Figure 8, from Eq. (10) and Table 1. General features of Figures 3-7 are:

1. Low relative bio-damage efficiency S("sensitivity") in the near ultraviolet and infrared regions as compared to the far UV and visible regions,

2. general similarity of the curve shapes as a function of time, and

3. decreasing relative sensitivity S in the red end of the visible and the IR as exposure time increases.

As a result of the definitions of S, Q, Q_o, D, etc. above, the MPE for exposure to a spectrally discrete source of small angular size, such as a laser beam is simply 1 bioW/cm^2. This occurs because the biowatt incorporates time and wavelength dependence of eye sensitivity to damage. For evaluating laser exposures, the biowatt scheme offers no advantages over direct use of Tables 1 and 2. For the case where sources emit over a large continuous wavelength range, it is hoped that use of the biowatt scheme will allow simple statements of MPEs analogous to (Ref. 2, page 14) "the authors feel that a reasonable upper limit for long-term viewing of a luminous source is of the order of 1 cd/cm^2." The same drudgery lies behind the

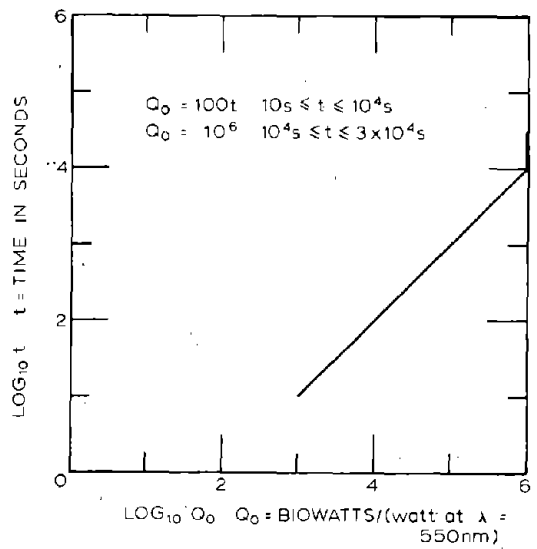

Figure 8. Reference bio-damage efficiency Q_o vs time, t

biowatt as behind the candela (lumen/steradian) except that there may be more drudgery behind the biowatt because the situation is more complicated.

Choice of Basic Maximum Permissible Exposures

In Section A the ANSI-ACGIH and the ISO Fourth Draft recommendations for MPEs were tabulated. For future work under this contract we choose the ANSI-ACGIH recommendations as shown in Tables 1 and 2. Reasons for rejection of the ISO recommendations of Table 3 are that:

1. the relative bio-damage efficiency S is much too high in the near UV and near IR, where it equals that in the visible and far UV,

2. the ISO MPEs are not time-dependent for times greater than 0.1s, which is the region of interest for us, and

3. the ISO MPEs would allow greater irradiance in the visible and far UV than the ANSI-ACGIH set for times greater than 2×10^3s; for example, for t = 10^4s (2-3/4 hours), approximately 7 times more in the far UV and 2-1/2 times in the visible, assuming a spectrally neutral source, E(λ) a constant. Conversely, for $t < 2\times10^3$s, the ISO MPEs allow less exposure for times of interest to us.

While we are not familiar with the genesis of the ISO recommendations, it appears that primary considerations in their development were simplicity and concern for relatively short exposure times. The ISO MPEs make it relatively easy to determine attenuation factors for laser eye protection but may be overly restrictive when one confronts the problem of filter-plate attenuation for short time exposures of the order of minutes and overly permissive for long time exposures of the order of hours.

The only change in Table 1 is the MPE given in the last line. That line is replaced by

$$1.4\text{-}10^3 \text{ nm} \qquad t > 10s \qquad \text{MPE} = 10 \text{ mW/cm}^2 \qquad (14)$$

as mentioned in an earlier footnote. This change takes into account the recommendation of Sliney and Freasier (Ref. 2, Page 15) and guidelines currently being evolved for welding eye protection by the Project Committee on Radiation of the American Welding Society.

Choice of Maximum Permissible Exposures for Spectrally Broad-Band Sources

There is one basic difference between the relative visual sensitivity curve of Figure 2 and the relative bio-damage sensitivity curves of Figures 3-7. The relative visual sensitivity $V(\lambda)$ measures the relative efficiency of radiant energy of different wavelengths for producing one effect, light. The relative bio-damage sensitivity $S(\lambda,t)$ measures the relative efficiency of different wavelengths for producing several damage effects:

1. Photokeratitis or keratoconjunctivities from UV in the 200-315 nm region. This effect is well established and is caused by absorption in the cornea and surrounding tissues.

2. Cataracts after chronic long-term exposure to visible, IR in the 700-1400 nm region, and possibly UV in the 315-400 nm region. In all these wavelength regions energy is absorbed (and hence heat produced near or in the crystalline lens of the eye) by the aqueous, iris, or lens. In addition, photochemical effects caused by UV may act to produce cataracts.

3. Chorioretinal injury - retinal burns in severe cases - caused by energy reaching the retina in the 360-1400 nm band.

4. Corneal heating, from IR wavelengths longer than about 1400 nm.

References 2 and 3 give much more information on the four effects listed above. With the simplifications inherent in the comments above, the eye effects break into two basic groups, corneal (effects 1 and 4 above) and intraocular (effects 2 and 3). As a result, we might propose something like the MPEs given in Table 4 for industrial exposure.

Let's look at the assumptions and problems of proposing Table 4 as MPEs.

First, we could assume that the effects of corneal absorption from 200-315 nm and from 1.4 μm - 1 mm are independent and assign an MPE for 1 bioW/cm^2 for each region rather than combining the two. But, we are not aware of any data on this

TABLE 4. MAXIMUM PERMISSIBLE EXPOSURE (MPE) FOR NON-LASER SOURCES[a]

Spectral Region	Maximum Permissible Exposure (MPE)
A. SOURCES OF SMALL ANGULAR SIZE	
315 nm to 1.4 μm	1 bioW/cm^2
200 nm to 315 nm PLUS 1.4 μm to 1 mm	1 bioW/cm^2
B. SOURCES OF LARGE ANGULAR SIZE	
315 nm to 1.4 μm	1 bioW/cm^2 sr
200 nm to 315 nm PLUS 1.4 μm to 1 mm	1 bioW/cm^2
C. SOURCES OF ANY ANGULAR SIZE	
360 nm to 830 nm*	1 cd/cm^2 for times 10s or greater

(a) Sources are classified as small or large by whether their size falls below or above the curve in Figure 1.

* The CIE[7] defines the V(λ) function, and hence the visible spectrum, between 360 nm and 830 nm, but notes that for most purposes in colorimetry the range of 380 nm to 780 nm is adequate. For approximate calculations the range 400 to 700 is often used.

subject so, for safety's sake, a conservative approach of keeping the sum of the energy absorbed in the cornea from both bands equal to the amount known to be safe for either band is preferable.

It is now common practice to consider total energy in the 400 nm-1.4 μm band when considering intraocular effects such as retinal damage or cataract formation. Having combined the 200-315 nm and 1.4 μm - 1 mm bands, if we then consider 400 nm - 1.4 μm together, what happens to the band remaining at 315-400 nm? Is it worth setting up a separate MPE for that band where, as far as is known now, the eye's bio-damage sensitivity is rather low? Table 4 shows that we don't think so; our reasons are as follows. Partial recent information from Pitts tends to indicate that the short wavelength end of the band does not affect the cornea much and so must be transmitted at least to the aqueous, while the CIE data (Figure 2) show that energy begins to reach the retina in perceptible amounts at the long wavelength end of the band. Therefore, it seems most appropriate to combine the 315-400 nm band with the 400-1400 nm band as an intraocular band. It is conceivable to think that current studies may lead, for instance, to creation of a third spectral region involved primarily in formation of cataracts, where wavelengths in the near UV and near IR, which are absorbed considerably by the anterior elements of the eye and the crystalline lens, require their own combined MPE.

We have also made one further addition to Table 4 which is not a direct outgrowth of Tables 1 and 2, and that is the addition of an MPE for source luminance ("brightness") of 1 cd/cm^2 for exposure times greater than 10 seconds. Sliney and Freasier (Ref. 2, p. 14) "feel that a reasonable upper limit for long-term viewing of a luminous source is of the order of 1 cd/cm^2," and recent conversations with Mr. Sliney show that number to still be his best estimate.* The purpose of this luminance MPE is to guard against retinal damage or possible safety hazards such as after-images from visually-very-efficient sources. The 1 cd/cm^2 number may, for interest, be compared to the luminance of a standard cool white fluorescent lamp, 0.7 cd/cm^2, or that of a 60W "soft white" incandescent light bulb, 3 cd/cm^2.

For completeness, Tables1 and 2 with the changes we propose for non-laser sources are given as Tables 5 and 6. Tables 4, 5, 6, and Figure 1, together with the definitions and equations of Section B above (and their analogs for extended sources to be listed below) constitute the MPEs and the computational methods which we plan to use in Tasks 2 and 3.

---

* See also Ref. 4, p. 90.

TABLE 5. Maximum Permissible Exposure (MPE)
For Viewing a Small Source

Wavelength, λ (μm)	Exposure Duration, t (s)	Maximum Permissible Exposure (MPE)	
Ultraviolet			
0.200-0.302	10^{-2}-3×10^{4}	3×10^{-3} J·cm^{-2}	
0.303	"	4×10^{-3} "	In no case shall the total irradiance, over all the wavelengths within the UV spectral region, be greater than 1 watt per square centimeter upon the cornea.
0.304	"	6×10^{-3} "	
0.305	"	1.0×10^{-2} "	
0.306	"	1.6×10^{-2} "	
0.307	"	2.5×10^{-2} "	
0.308	"	4.0×10^{-2} "	
0.309	"	6.3×10^{-2} "	
0.310	"	1.0×10^{-1} "	
0.311	"	1.6×10^{-1} "	
0.312	"	2.5×10^{-1} "	
0.313	"	4.0×10^{-1} "	
0.314	"	6.3×10^{-1} "	
0.315-0.400	10^{-9}-10	$0.56t^{1/4}$ J·cm^{-2}	
0.315-0.400	10-10^{3}	1J·cm^{-2}	
0.315-0.400	10^{3}-3×10^{4}	1×10^{-3}W·cm^{-2}	
Visible and Near-Infrared			
0.400-0.700	10^{-9}-1.8×10^{-5}	5×10^{-7}J·cm^{-2}	
0.400-0.700	1.8×10^{-5}-10	$1.8t^{3/4}\times10^{-3}$ "	
0.400-0.550	10-10^{4}	10×10^{-3} "	
0.550-0.700	10-T_1	$1.8t^{3/4}\times10^{-3}$ "	
0.550-0.700	T_1-10^{4}	$10C_B\times10^{-3}$ "	
0.400-0.700	10^{4}-3×10^{4}	$C_B\times10^{-6}$W·cm^{-2}	
0.700-1.059	10^{-9}-1.8×10^{-5}	$5C_A\times10^{-7}$J·cm^{-2}	
0.700-1.059	1.8×10^{-5}-10^{3}	$1.8C_At^{3/4}\times10^{-3}$ "	
1.060-1.400	10^{-9}-5×10^{-5}	5×10^{-6} "	
1.060-1.400	5×10^{-5}-10^{3}	$9t^{3/4}\times10^{-3}$ "	
0.700-1.400	10^{3}-3×10^{4}	$320C_A\times10^{-6}$W·cm^{-2}	
Far-Infrared			
1.4-10^{3}	10^{-9}-10^{-7}	10^{-2}J·cm^{-2}	
	10^{-7}-10	$0.56t^{1/4}$J·cm^{-2}	
	>10	1.0×10^{-2}W·cm^{-2}	

C_A, C_B, and T_1 are defined at the end of Table 6.

TABLE 6. Maximum Permissible Exposure (MPE)
For Viewing an Extended Source

Wavelength, λ (μm)	Exposure Duration, t (s)	Maximum Permissible Exposure (MPE)
Ultraviolet		
0.200-0.400	Same as Table 1	
Visible		
0.400-0.700	10^{-9}-10	$10t^{1/3}$ J·cm^{-2}·sr^{-1}
0.400-0.550	10-10^{4}	21J·cm^{-2}·sr^{-1}
0.550-0.700	10-T_1	$3.83t^{3/4}$ J·cm^{-2}·sr^{-1}
0.550-0.700	T_1-10^{4}	$21C_B$J·cm^{-2}·sr^{-1}
0.400-0.700	10^{4}-3×10^{4}	$2.1C_B\times10^{-3}$W·cm^{-2}·sr^{-1}
Near Infrared		
0.700-1.400	10^{-9}-10	$10C_At^{1/3}$ J·cm^{-2}·sr^{-1}
0.700-1.400	10-10^{3}	$3.83C_At^{3/4}$ J·cm^{-2}·sr^{-1}
0.700-1.400	10^{3}-3×10^{4}	$0.64C_A$W·cm^{-2}·sr^{-1}
Far-Infrared		
1.4-10^{3}	Same as Table 1	

DEFINITIONS

$C_A = 10^{[(\lambda-0.700)/0.515]}$ $\quad 0.700\ \mu m \leq \lambda \leq 1.060\ \mu m$

$= 5 \quad 1.060\ \mu m \leq \lambda \leq 1.400\ \mu m$

$C_B = 11 \quad 0.400\ \mu m \leq \lambda \leq 0.550\ \mu m$

$= 10^{[15(\lambda-0.550)]} \quad 0.550\ \mu m \leq \lambda \leq 0.700\ \mu m$

$T_1 = 10s \quad 0.400\ \mu m \leq \lambda \leq 0.550\ \mu m$

$= 10^{[1+20(\lambda-0.550)]} \quad 0.550\ \mu m \leq \lambda \leq 0.700\ \mu m$

Two more points should be raised before ending this discussion of Subtask 1.

Throughout the previous pages it has been implicitly assumed that it is reasonable to take a set of MPEs specified for lasers and to apply them to other types of sources of optical radiation. To the best of our knowledge this approach is sound for the following reasons:

1. The laser MPEs were established by considering relevant data from all types of sources, laser and non-laser, from both laboratory exposures, accidental exposures, and epidemiological studies of industrial and natural (outdoor) exposures. For example, Pitts data[3] obtained using an incoherent light source are a key basis for the laser MPE's the 200-300 nm band.

2. It seems intuitively reasonable to the writer that non-laser sources which are generally incoherent and of relatively low spectral radiance (watts/cm^2 steradian nanometer) would have less tendency to cause exotic interference or field effects, higher-order effects, or "high-Q" photochemical effects than laser sources.

For these two reasons, we view the use of modified laser MPEs as a conservative approach to dealing with non-laser sources.

Finally, a few words about the terms "biowatt," "bio-irradiance," etc. These are simply convenient terms which occurred readily in thinking about the problems above, but their use may bother some people for various reasons. We hope their real meaning is clear from the text and definitions; if the concepts they embody have any value then better names could be found.

Computation of Exposure for Sources of Large Angular Extent

For extended sources in spectral regions where the MPEs are given as radiances, the equations and definitions (3) to (7) and (9) to (14) need minor modification. The analogous information is presented here, with primes denoting analogous quantities or definitions to those given above.

$$Z'(\lambda,t) = \text{MPE at wavelength } \lambda \text{ for exposure time } t \qquad (3')$$

$$S'(\lambda,t) = \frac{Z'(\lambda_o,t)}{Z'(\lambda,t)} \qquad (4')$$

$$\lambda_o = 549 \text{ nm} \qquad (5')$$

$$S'(549,t) = 1 \qquad (6')$$

1 biowatt/cm^2 steradian

= amount of power per square centimeter per unit solid angle ("bio-radiance") required to equal the MPE when the MPE is specified as a radiance (W/cm^2 sr) (7')

$$Q'(\lambda,t) = Q_o'(t)S'(\lambda,t) \qquad (9')$$

where

$$Q_o'(t) = \frac{1}{Z'(\lambda_o,t)} \text{ bioW/W} \qquad (10')$$

$Q'(\lambda,t)$ = bio-damage efficiency at wavelength λ for exposure time t (11')

$$D' = Q_o'(t) \int_\lambda N(\lambda)S'(\lambda,t)d\lambda \qquad (12')$$

where

D' = biologically-weighted radiance in bioW/cm sr

$N(\lambda)$ = spectral radiance at wavelength λ, W/cm^2 sr nm (13')

SUBTASK 2: STUDY WELDING AND LIGHT SOURCE DATA

Approach Chosen

Preliminary investigation had shown that the optical spectra from welding and cutting processes vary widely in spectral distribution and intensity. For this reason and others to be mentioned later it was felt that the best approach to recommending absorption levels for filter plates was to develop in this subtask one (or more, if necessary) "worst-case envelope spectrum" and then to use the spectrum in conjunction with the MPEs recommended in Table 4, to calculate necessary attenuation for welding filters in different spectral regions. It was also felt to be worthwhile for later use to first develop numerically the bio-irradiance D in various wavelength regions which would result from a source of uniform spectral radiance. Hence the work to be reported next is divided into three parts:

1. Quantify bio-irradiance D resulting from a source of uniform spectral radiance,
2. Analyze literature on sources,
3. Propose worst-case envelope spectrum or spectra.

Bio-irradiance From a Spectrally Uniform Source

A source of uniform spectral radiance will produce at the observer a spectrally-uniform irradiance

$$E(\lambda) = \alpha \text{ W/cm}^2 \text{ nm}^* \tag{14}$$

where α is a constant. From eq. (12), this irradiance will result in a bio-irradiance D of

$$D = \alpha\, Q_o(t) \int_\lambda S(\lambda,t)\, d\lambda. \tag{15}$$

Evaluation of (15) using the formalism of eqs. 3-13 is a tedious task so we will show this explicitly for one value of t and then list the results for the range of times of interest.

Consider the case for $t = 10^4$ sec ($\approx$2 3/4 hrs.). From Table 5, and eq. (3),

---

* The calculations below are carried out using nm as unit of wavelength rather than μm purely as a matter of convenience.

$$Z(549\ \text{nm},\ 10^4\ \text{sec}) = 10\ \text{mJ/cm}^2 \qquad (16)$$

$$\therefore Z(549, 10^4) = \frac{1 \times 10^{-2}\ \text{J/cm}^2}{10^4\ \text{s}} = 10^{-6}\ \text{W/cm}^2 \qquad (17)$$

So from eq. (10),

$$Q_o(10^4) = \frac{1}{10^{-6}}\ \text{bioW/W}$$

$$= 10^6\ \text{bioW/W} \qquad (18)$$

We now calculate the relative bio-damage efficiency function S from eq. (4) and evaluate the integral (2) for each of the wavelength bands which we designate as follows:

Wavelength Region	Name	Abbreviated Name
200-315 nm	Far UV	FUV
315-400 nm	Near UV	NUV
400-700 nm	Visible	VIS
700-1400 nm	Near IR	NIR
1400-5000 nm	Far IR	FIR
315-1400 nm	Retinal	RET
200-315 nm PLUS 1400-5000 nm	Corneal	COR

The designations above were chosen because the wavelength regions we are using are derived from U.S. laser standards and do not correspond exactly to the C.I.E. designations of UV-A, UV-B, etc. and we wish to avoid possible confusion. The cut-off at 5000 nm for the FIR region was chosen because it corresponds to the long-wavelength transmission limit for present commercial absorptive glasses and plastics as far as we know. As discussed previously, the band designated above as "Retinal" is more properly called "intraocular" but it is felt that "Retinal" more easily conveys the general idea. We'll evaluate the contribution to D of each of the first 5 bands above; values for RET and COR are obtained by addition.

FUV 200-315 nm

From eqs. (3) and (4), and Table 5,

$$S(200\text{-}302,\ 10^4) = \frac{Z(549,\ 10^4)}{Z(200\text{-}302,\ 10^4)} \tag{19}$$

$$= \frac{10^{-6}\ W/cm^2}{(3 \times 10^{-3}\ J/cm^2)/10^4 s}$$

$$= 3.33 \tag{20}$$

and similarly, dropping the time identification,

S(303)	= 2.50	S(309)	= .16
" 304	= 1.67	" 310	= .10
" 305	= 1.00	" 311	= .06
" 306	= .63	" 312	= .04
" 307	= .40	" 313	= .03
" 308	= .25	" 314	= .01
		" 315	= .001

(21)

So from eq. (2),

$$D(FUV) = \alpha\ Q_o(10^4) \int_{200}^{315} S(\lambda) d\lambda. \tag{22}$$

Using the trapezoidal rule for integration,

$$D(FUV) = \alpha\ Q_o \left[(302\text{-}200)(3.33) + \sum_{303}^{314} S(\lambda) + \tfrac{1}{2} S(302) + \tfrac{1}{2} S(315)\right]$$

$$= 349\ \alpha\ Q_o\ \text{bioW/cm}^2 \tag{23}$$

NUV 315-400 nm

Again from Table 5, FQR,

$$Z(315\text{-}400,\ 10^4) = 10^{-3}\ W/cm^2,$$

hence

$$S = \frac{10^{-6}\ w/cm^2}{10^{-3}\ w/cm^2} = 10^{-3} \tag{24}$$

So $D(NUV) = \alpha\ Q_o\ [(400-315)(10^{-3})]$

$= 0.085\ \alpha\ Q_o$ bioW/cm^2 (25)

VIS 400-700 nm

Again from Table 5, FQR,

$Z(400\text{-}700,\ 10^4) = C_B\ \mu W/cm^2$

where $C_B = 1, \qquad 400 \leq \lambda \leq 550$

$= 10^{[.015(\lambda-550)]}$* $\qquad 550 \leq \lambda \leq 700$

So $S = \dfrac{10^{-6}\ W/cm^2}{C_B\ \mu W/cm^2} = \dfrac{1}{C_B}$

Hence $D(VIS) = \alpha\ Q_o \displaystyle\int_{400}^{700} \frac{1}{C_B}\ d\lambda$

$= \alpha\ Q_o \left[(500-400) + \displaystyle\int_{550}^{700} 10^{-[.015(\lambda-550)]}\, d\lambda\right]$

$= \alpha\ Q_o\ (150 + 28.8)$

$= 179\ \alpha\ Q_o$ bioW/cm^2 (26)

NIR 700-1400 nm

$Z(700\text{-}1400,\ 10^4) = 320\ C_A\ \mu W/cm^2$

where $C_A = 10^{[(\lambda-700)/515]}$* $\qquad 700 \leq \lambda \leq 1060$

$= 5 \qquad 1060 \leq \lambda \leq 1400$

Hence $S = \dfrac{10^{-6}\ W/cm^2}{320\ C_A\ \mu W/cm^2} = \dfrac{1}{320\ C_A}$

---

* These expressions for C_A and C_B are those given at the end of Table 6 recast for nanometers rather than micrometers.

So

$$D(NIR) = \frac{\alpha\, Q_o}{320}\left[\int_{700}^{1060} 10^{-[(\lambda-700)/515)]}\, d\lambda + \frac{(1400-1060)}{5}\right]$$

$$= \frac{\alpha\, Q_o}{320}\,(179 + 68)$$

$$= 0.77\ \alpha\ Q_o\ \text{bioW/cm}^2 \qquad (27)$$

FIR 1400-5000 nm

$$Z(1400\text{-}5000,\ 10^4) = 10\ \text{mW/cm}^2$$

$$S = \frac{10^{-6}\ \text{W/cm}^2}{10\ \text{mW/cm}^2} = 10^{-4}$$

$$D(FIR) = \alpha\ Q_o\ (5000\text{-}1400)\ 10^{-4}$$

$$= 0.36\ \alpha\ Q_o\ \text{bioW/cm}^2 \qquad (28)$$

The values for D(RET) and D(COR) are obtained by adding results (25), (26), (27), and (23), (28), respectively. The values obtained above for $t = 10^4$ s and other values of t of interest are tabulated in Table 7 below and graphed in Figure 9.

For example, the bio-irradiance in the visible region, D(VIS), from a source producing uniform spectral irradiance of 1 $\mu W/cm^2$ nm for 1000 seconds would be, from eq. (15) and Table 7;

$$D(VIS) = \alpha\ Q_o(t) \int_{400}^{700} S(\lambda)\ d\lambda$$

$$= (1 \times 10^{-6}\ \text{W/cm}^2\text{nm})(10^5\ \text{bioW/W})(154\ \text{nm})$$

$$= 15.4\ \text{bioW/cm}^2 \qquad (29)$$

As another example, the bio-irradiance in the Retinal band produced by the same source in 10^4 seconds would be

$$D(RET) = \alpha\ Q_o(t) \int_{315}^{1400} S(\lambda)\ d\lambda$$

$$= (1 \times 10^{-6}\ \text{W/cm}^2\ \text{nm})(10^6\ \text{bioW/W})(180\ \text{nm})$$

$$= 180\ \text{bioW/cm}^2. \qquad (30)$$

TABLE 7. Bio-damage irradiance D in different spectral bands in units of $\alpha\ Q_o(t)$ bioW/cm^2 and $Q_o(t)$ for various times t in seconds from a source producing uniform spectral irradiance α W/cm^2 nm, for sources of angular size less than 24 mr ("Small sources" - see Fig. 1).

t / Spectral Band	10	10^2	10^3 ($\approx$17 min.)	10^4 ($\approx 2\frac{3}{4}$ hrs.)	3×10^4 ($\approx 8\frac{1}{3}$ hrs.)
FUV	349	349	349	349	1041
NUV	.85	.85	.85	.085	.085
VIS	300	164	154	179	179
NIR	247	43	7.7	.77	.77
FIR	360	36	3.6	.36	.36
RET	548	208	163	180	180
COR	709	385	353	349	1041
Q_o(bioW/W)	10^3	10^4	10^5	10^6	10^6

As a final example, the same source acting for 10 seconds would produce an exposure in the Retinal band of

$$D(RET) = (1 \times 10^{-6}\ W/cm^2\ nm)(10^3\ bioW/W)(548\ nm)$$

$$= 0.548\ bioW/cm^2 \qquad (31)$$

Finally, for comparison purposes, we list the illuminance I, lumens/cm^2, which would result from the irradiance of α W/cm^2 nm at the cornea. From eq. (2) the luminous flux per unit area, illuminance I, is given by

$$\frac{F}{A} = I = \alpha\ K_m \int_{360}^{830} V(\lambda)\,d\lambda \qquad (32)$$

where A = area and the other symbols are defined with eqs. 1 and 2. Now it is shown at the end of Table 2.1 of Publication CIE No. 15(E-1.3.1) 1971[7] that

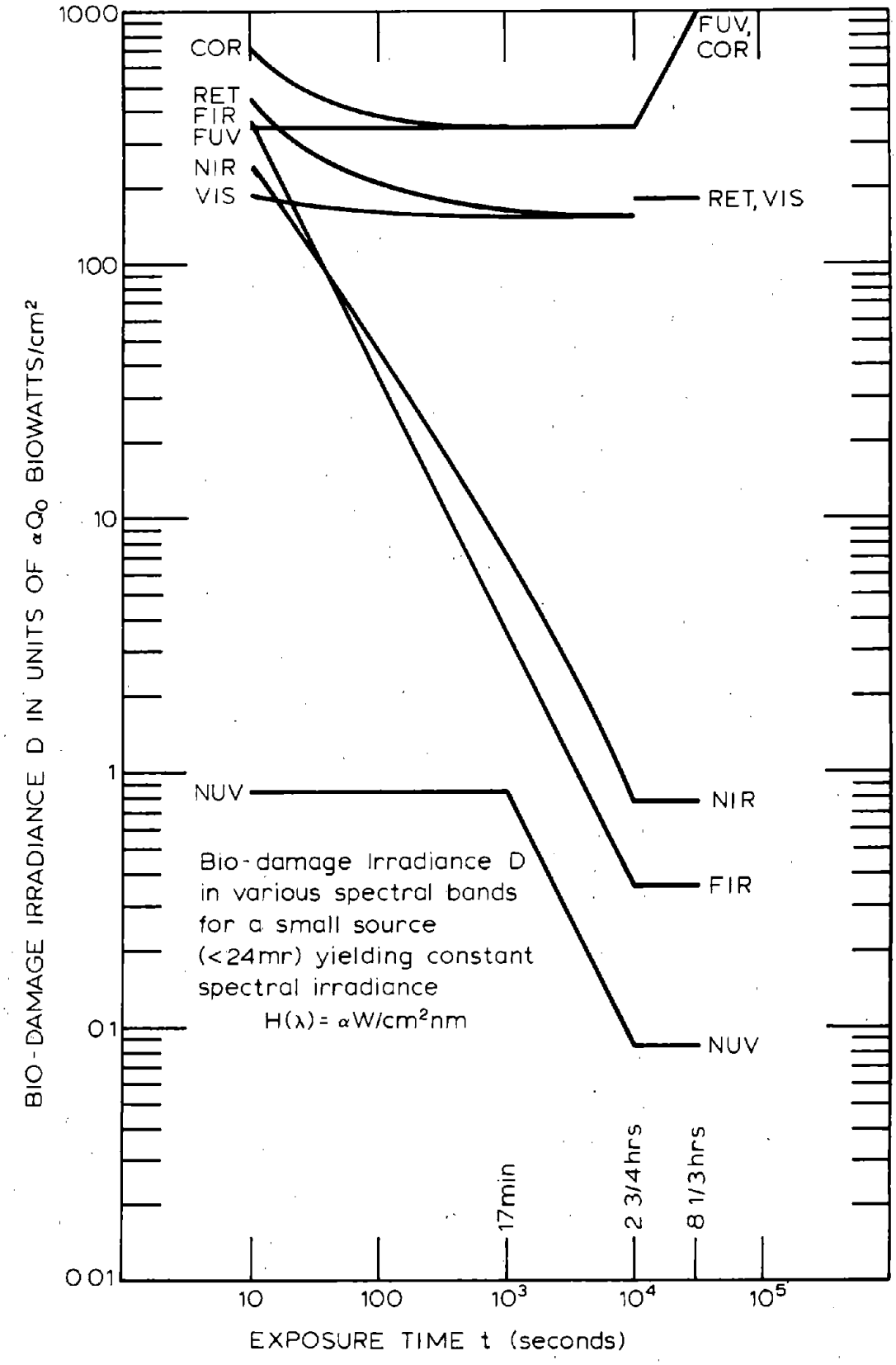

Figure 9. Bio-damage irradiance in various spectral bands vs. exposure time t.

$$\int_{360}^{830} V(\lambda)\, d\lambda = 107 \text{ nm} \qquad (33)$$

so eq. (32) becomes

$$I = (680\ \ell m/W)(107\ nm)(\alpha\ W/cm^2\ nm)$$

Hence

$$I = 7.28 \times 10^4 \alpha\ \ell m/cm^2 \qquad (34)$$

a fact which will be used later.

This concludes the evaluation of bio-irradiance from a spectrally uniform source.

Analysis of Light Source Data

In this section we will deal primarily with radiation from welding and cutting processes since it turns out that these processes, taken as a group, represent the worst sources for which protection must be provided. Other sources will be discussed briefly as necessary.

We have studied the data on welding arc sources from References 8-12 and they are not as complete as desirable. Nevertheless, the monumental work of Sutter, et al[8] probably allows an adequate assessment of worst-case source emission.

Sutter measured the irradiance at a known distance from a large number of welding and cutting processes, conducting a total of 715 tests. Processes studied were tungsten-inert gas welding, metal-inert gas welding, metal-active gas welding, arc metal welding, plasma welding, and plasma cutting. Currents utilized ranged from 0.3A to 600A. Shielding gases used were CO_2; a mixture of 15% CO_2, 5% O_2, 80% Ar; ArS_3; Ar plus 6.5% H_2; Ar plus 40% H_2, Ar plus 8% N_2; Ar; He. Welds were carried out on mild steel, alloy steel, AlSi, AlMg, and copper, using common commercial choices of electrode size, electrode material, current, and shielding gas.

For approximately 30 cases a detailed spectral emittance curve was measured from 320 nm to 2000 nm. For all of the 715 cases Sutter measured total irradiance (W/cm^2) at a distance of 50 cm from the arc within each of the following wavelength bands:

320-400 nm
400-750 nm
750-1300 nm
750-2000 nm.

In addition, the illuminance in lux ($\ell m/m^2$), the irradiance beyond 780 nm transmitted through 4 mm and 20 mm of water, and the luminance of the brightest portion of the arc were measured.

Unfortunately, Sutter did not make measurements of UV in the photokeratitic region from 200 to 320 nm. When one considers that Sutter's primary interest was welder eye protection, and the large amount of work which he and his coworkers carried out, and the fact that large values of optical attenuation are easy to obtain in the 200-320 nm region, this omission becomes very reasonable.

After examining the 30 complete spectra published by Sutter and the dozen or so spectra shown in References 9-12, it is apparent that the spectra are generally very rich in detail, with many "spikes" of maximum intensity 10 to 100 times that of the surrounding continuum. For the purposes of assessing absorption requirements for filters, it is adequate to work with averages of irradiance over wavelength bands for the following reasons:

1. It appears to be impractical to have specialized eye protection filters for the many different processes, so each shade of filter will be used with many different processes; for this reason, no attempt was made in calculating the ratios below to differentiate between different types of welding processes. This is consistent with welding plate usage today.

2. The processes are very sensitive to many conditions; for example, in addition to the parameters mentioned above, Sutter's data show a strong dependence of output on arc length - the distance between electrode tip and work,

3. The maximum permissible exposure (MPE) levels being recommended (Tables 4, 5, 6 of FQR) are effectively averaged for wavelength bands,

4. Sizeable safety factors will need to be incorporated in calculations to account for processes which have not been measured and processes not yet invented.

Taking all the data tabulated by Sutter, one can calculate the ratios of irradiance or other data at 50 cm distance for different wavelength bands. Results of doing this are listed below. The forms of the ratios have been chosen so that the maximum values will be utilized to devise a composite "worst-case" envelope spectrum for welding and cutting processes; the minimum values are listed simply for the

reader's interest since, together with the maximum values, they illustrate the extreme variability between processes.

Irradiance ratios:

$$\text{Max.}\ \frac{E(320\text{-}400)\ (W/cm^2)}{E(400\text{-}750)\ (W/cm^2)} = 22 \qquad (35)$$

$$\text{Min.}\quad " \qquad " \qquad = 0.038 \qquad (36)$$

$$\text{Max.}\ \frac{E(750\text{-}1300)\ (W/cm^2)}{E(400\text{-}750)\ (W/cm^2)} = 6.9 \qquad (37)$$

$$\text{Min.}\quad " \qquad " \qquad = 0.11 \qquad (38)$$

$$\text{Max.}\ \frac{E(750\text{-}2000)\ (W/cm^2)}{E(400\text{-}750)\ (W/cm^2)} = 11 \qquad (39)$$

$$\text{Min.}\quad " \qquad " \qquad = 0.22 \qquad (40)$$

Mixed ratios: irradiance to illuminance

$$\text{Max.}\ \frac{E(320\text{-}400)\ (W/cm^2)}{I\ (\ell m/cm^2)} = 0.13\ \ W/\ell m. \qquad (41)$$

$$\text{Min.}\quad " \qquad " \qquad = 2.2 \times 10^{-4}\ W/\ell m. \qquad (42)$$

$$\text{Max.}\ \frac{E(400\text{-}750)\ (W/cm^2)}{I\ (\ell m/cm^2)} = 0.0150\ \ W/\ell m. \qquad (43)$$

$$\text{Min.}\quad " \qquad " \qquad = 0.00327\ W/\ell m. \qquad (44)$$

$$\text{Max.}\ \frac{E(750\text{-}1300)\ (W/cm^2)}{I\ (\ell m/cm^2)} = 0.053\ W/\ell m. \qquad (45)$$

$$\text{Min.}\ \frac{E(750\text{-}1300)\ (W/cm^2)}{I\ (\ell m/cm^2)} = 5.2 \times 10^{-4}\ W/\ell m. \qquad (46)$$

For purposes of developing a worst-case source envelope spectrum, it is convenient if ratios of the type above are for the same wavelength bands as those corresponding to the MPEs. Assuming that the sources are of uniform spectral emittance in each wavelength band, the maximum ratios given above can be converted to

$$\text{Max.}\ \frac{E(315\text{-}400)}{E(400\text{-}700)} = 27 \qquad (47)$$

$$\text{Max.}\ \frac{E(700\text{-}1400)}{E(400\text{-}700)} = 10 \qquad (48)$$

$$\text{Max.}\ \frac{E(700\text{-}2000)}{E(400\text{-}700)} = 13 \qquad (49)$$

$$\text{Max.}\ \frac{E(315\text{-}400)}{I} = 0.14\ \text{W/ℓm.} \qquad (50)$$

$$\text{Max.}\ \frac{E(400\text{-}700)}{I} = 0.0129\ \text{W/ℓm.} \qquad (51)$$

$$\text{Max.}\ \frac{E(700\text{-}1400)}{I} = 0.068\ \text{W/ℓm.} \qquad (52)$$

From (48) and (49).

$$\text{Max.}\ \frac{E(1400\text{-}2000)}{E(400\text{-}700)} = 3 \qquad (53)$$

Results (47) to (53) come from taking the extreme values of Sutter's data. Other spectra in References 9-12 yield values less than the maxima given above.

We will return later to the question of values of irradiance ratios which should be used for the far-UV (FUV) region and the region from 2000 nm to 5000 nm. From (47) through (53) we will now calculate the relative irradiance and illuminance produced by a "worst-case" welding arc. For our purposes a "worst-case" arc is defined as one characterized by the maximum ratios of (47) through (53).

We assume the arc produces a uniform spectral irradiance β_o W/cm^2 nm from 400 nm - 700 nm, the VIS region. Then

$$E(400\text{-}700) = 300\ \beta_o\ \text{W/cm}^2 \qquad (54)$$

Assuming that within each spectral band the source spectral irradiance is constant, the ratio (47) is satisfied when the spectral irradiance in the near UV, β(NUV) is given by

$$\beta(\text{NUV}) = \frac{(300\ \beta_o\ \text{W/cm}^2)(27)}{400\text{-}315} = 95.3\ \beta_o\ \text{W/cm}^2\ \text{nm} \qquad (55)$$

Similarly, from (48),

$$\beta(\text{NIR}) = \frac{(300\ \beta_o\ \text{W/cm}^2)(10)}{1400-700} = 4.29\ \beta_o\ \text{W/cm}^2\ \text{nm}. \tag{56}$$

From (34), the source of uniform spectral radiance in the visible would produce an illuminance of

$$I = 7.28 \times 10^4\ \beta_o\ \text{ℓm/cm}^2, \tag{57}$$

but (51) tells us that the arc of least luminous efficiency is characterized by

$$E = \frac{300\ \beta_o\ \text{W/cm}^2}{0.0129\ \text{W/ℓm}} = 2.33 \times 10^4\ \beta_o\ \text{ℓm/cm}^2 \tag{58}$$

and hence, since

$$\frac{2.33 \times 10^4}{7.28 \times 10^4} = 0.32 \tag{59}$$

has approximately 1/3 the luminous efficiency of an equal energy source.

Eqs. (54) to (59) characterize a worst-case arc source, as inferred from the data of Sutter and others (Refs. 8-12), for the RETINAL region which is composed of NUV, VIS, and NIR. Three additional factors must be taken into account before an analysis of required welding-plate attenuation can be completed:

1. Source radiation characteristics in the FUV (200-315 nm) and FIR (1400-5000 nm) regions,

2. Source size characteristics, and

3. Any safety factors which it may be desirable to include.

Worst-Case Welding Arc

The very limited data available suggest that the average spectral irradiance produced by a source in the FUV region is not greater than 5 times that from the NUV region. If we round the value of 95.2 in (42) to 100, then we will assume that

$$\beta(\text{FUV}) = 500\ \beta_o\ \text{W/cm}^2\ \text{nm}. \tag{60}$$

Turning to the problem of the FIR, we will assume that the irradiance which gives the result (40) is constant out to 5000 nm; mathematically, that

$$\frac{E(1400\text{-}5000)}{E(400\text{-}700)} = \frac{5000\text{-}1400}{2000\text{-}1400}\,\frac{E(1400\text{-}2000)}{E(400\text{-}700)}$$

$$= 18. \qquad (61)$$

This gives

$$\beta(\text{FIR}) = \frac{300\ \beta_o\ \text{W/cm}^2\ (18)}{5000\text{-}1400} = 1.5\ \beta_o\ \text{W/cm}^2. \qquad (62)$$

We should emphasize that the assumptions expressed by (47) and (49) must be largely guesswork because of the lack of data.

For welding arcs, we can gain some information on arc sizes from Sutter's data since he has measured the luminance L as well as the illuminance I from the arcs he studied. Since his measurements were made at 50 cm distance, and since his sources were sufficiently small, we can find source area A_s from

$$I = \frac{L\ A_s}{d^2} \qquad (63)$$

where d ≡ distance = 50 cm. Calculation of A_s from Sutter's data yields values ranging from 0.021 cm^2 to 3.55 cm^2 for the effective source area in visible light. We will not choose a source size now to characterize the worst-case arc but instead will consider the effect of different source sizes in the analysis of Subtask 3.

When safety factors are considered, it should be remembered that there is an implicit safety factor resulting from use of the maximum ratios of irradiance measured in various wavelength bands to that measured in the visible, as in (22), (24), and (26). We prefer not to utilize any additional safety factors until the analysis of Subtask 3.

To summarize, the worst-case welding arc chosen for future use is assumed to have a different uniform spectral irradiance β within each of the 5 wavelength bands, these values being related to the value β_o of spectral irradiance in the visible region as follows:

TABLE 8. Worst-Case Welding Arc.

Spectral irradiance β(W/cm^2 nm) in each spectral region in terms of the spectral irradiance β_o(W/cm^2 nm) in the visible region. β and β_o are assumed constant in each region.

Wavelength Region	Spectral Irradiance β W/cm^2 nm	Notes
FUV (200-315 nm)	500 β_o	Eq. (60)
NUV (315-400 nm)	100 β_o	Eq. (55), value rounded
VIS (400-700 nm)	β_o	Eq. (54)
NIR (700-1400 nm)	5 β_o	Eq. (56), value rounded
FIR (1400-5000 nm)	2 β_o	Eq. (62), value rounded

This completes the analysis of welding arc data. Since lasers are not being considered in this work, the remaining types of light source common in industry are incandescent sources of varying sizes such as lamps for lighting, heat lamps, and furnaces used for melting and heat treating. These incandescent sources may be approximated by blackbodies of varying emissivities to an accuracy sufficient for us[2] and calculations will be made for specific cases as needed in future work on Subtask 3.

To conclude this subtask, it should be noted that Clark[13,14,15] has conducted a thorough investigation of infrared radiation from welding arcs in a series of papers which form the basis for allowed infrared welding plate transmittances in the Australian standard AS Z45-1967. Results of Clark's studies will be compared with those utilizing the worst-case-welding arc of Table 8 in Subtask 3.

SUBTASK 3. REVISE TABLE 1 OF Z87.1-1968

Bio-Irradiance From the Worst-Case Welding Arc

Using the results shown in Tables 7 and 8, we can calculate the bio-damage irradiance D for various times t which would be produced by the Worst-Case Welding Arc (WCWA) in each of the spectral bands of interest from a source producing uniform spectral irradiance α W/cm^2 nm in the visible region.

For example, for t = 10^4 sec, from Table 7,

$$D(VIS) = 179\ \alpha\ Q_o(t) \tag{64}$$

while for the near UV region, from Table 7, a source of uniform spectral irradiance α would cause a bio-damage irradiance of

$$D(NUV) = 0.085\ \alpha\ Q_o(t) \tag{65}$$

However, WCWA is, from Table 8, 100 times as spectrally radiant in the near UV as in the visible, so for the WCWA

$$D(NUV) = 8.5\ \alpha\ Q_o t \tag{66}$$

Comparison of eqs. (1) and (3) shows that WCWA would produce 8.5/179 = 0.0475 times as much bio-damage irradiance in the near UV region as in the visible for t = 10^4 sec.

In a similar way we can calculate, for all spectral regions and times shown in Tables 7 and 8, the relative bio-damage irradiance produced by WCWA. Results are shown in Table 9.

For example, a WCWA which produces a bio-damage irradiance D of 1 bioW/cm^2 in the visible region for t = 10^3s would produce 1133 bioW/cm^2 in the far UV region according to Table 9, provided the WCWA was a small source. As another example, a WCWA producing uniform spectral irradiance at the eye in the visible region of α W/cm^2 nm would, from Tables 7 and 9, produce a bio-damage irradiance D in the near IR in 10^2s of

$$D(NIR) = 1.31\ (164)\alpha\ Q_o(10^2)$$

$$= 1.31\ (164)\ \alpha(10^4) = 2.15 \times 10^6\ \alpha\ \text{bioW/cm}^2 \tag{67}$$

TABLE 9. Relative bio-damage irradiance D in different spectral bands for various times t produced by the Worst-Case Welding Arc of Table 2, SQR. Values are normalized by assigning a value of 1 to the bio-damage irradiance D produced in the visible region. This table is for small sources.

time t (sec) / Spectral Band	10	10^2	10^3 (≈17 min.)	10^4 (≈$2\frac{3}{4}$ hrs.)	3×10^4 (≈$8\frac{1}{3}$ hrs.)
FUV	582	1064	1133	975	2908
NUV	0.283	0.518	0.552	0.0475	0.0475
VIS	1	1	1	1	1
NIR	4.12	1.31	0.250	0.0215	0.0215
FIR	2.40	0.439	0.0468	0.0040	0.0040
RET	5.21	2.83	1.80	1.07	1.07
COR	584	1064	1133	975	2908

since the source would produce

$$D(VIS) = 164\ \alpha\ Q_O(10^2) \qquad (68)$$

as shown by Table 7, and the ratio D(NIR)/D(VIS) = 1.31 from Table 9.

Optical Density Requirements for Welding Eye Protection

The absorption characteristics of a welding filter should be that it is dark enough to afford comfortable viewing and that it should protect adequately from all optical radiation. This general notion needs to be quantified, however, if we are to make numerical recommendations for absorption.

Let us suppose that a filter is being used to view a WCWA for a time t and that the optical density (OD)

$$OD \equiv \log_{10} \frac{1}{T},\ T = \text{external transmittance} \qquad (69)$$

is such that a bio-irradiance of 1 bioW/cm^2 is produced by energy in the visible region. If all other energy were absorbed by the filter, this bio-irradiance would be the maximum desirable value. Any practical filter will, however, increase the value of D above 1 bioW/cm^2 because of transmittance in the NUV and NIR portions of the retinal band. Similarly, contributions from the FUV and FIR regions will contribute to a bio-irradiance value for the corneal band.

In order to be able to quantify, we will assume that for viewing a Worst-Case Welding Arc:

Assumption 1: Filter absorption should be such that the contributions of the NUV and NIR regions are equal and do not together exceed 10% of the contribution from the VIS region in the bio-irradiance for the RET band.

Assumption 2. Filter absorption should be such that the contributions of the FUV and FIR bands are equal and that their sum, for the COR band, is equal to that for the RET band.

These are important assumptions since they determine much of the numerical outcome of calculations to follow. Why do we choose these particular assumptions?

Our state of knowledge (or ignorance) at this time combined with our early decision to set maximum permissible exposures for the COR and RET bands gives us no preference for either band being less harmful than the other, so we weight them equally. Similar thinking brings about the choice of equal contributions from the FUV and FIR bands of the COR band and for the NUV and NIR bands of the RET band. Finally, we assume that the VIS contribution may be chosen as high as is safe (i.e., corresponds to the MPE for that time period) by a welder when he selects his welding plate, so we arbitrarily choose to require that the contribution from NUV and NIR be an order of magnitude less than that from VIS in the sum for the RET band.

With the two key assumptions above, we can now calculate the additional optical density in each spectral region beyond that required in the VIS region. As an example, consider the column for t = 10^2s in Table 9. If the OD of the filter is such that D = 1 unit for the VIS region, then D for the NUV should not exceed 0.05 unit, but would amount to 0.518 unit unless the OD of the filter in the NUV region were greater than in the VIS region. So the relative transmittance of the filter in the NUV compared to the VIS should be

$$0.05/0.518 = 0.0965 \qquad (70)$$

or the increase in OD in the NUV from that in the VIS band should be, from (6),

$$\log_{10} \frac{1}{0.0965} = 1.02 \qquad (71)$$

In a similar way we can calculate the increase in OD for each band for the cases of Table 9. The results are shown in Table 10.

TABLE 10. Increase in Optical Density (OD) above that for the VIS band required in each spectral band for various times t for welding filters confirming to Assumptions 1 and 2 above used to view Worst-Case Welding Arcs. (Negative values in the table correspond to cases where less OD is required than for the VIS band). This table is for small sources.

time t (sec) / Spectral Band	10	10^2	10^3 ($\approx$17 min.)	10^4 ($\approx 2\frac{3}{4}$ hrs.)	3×10^4 ($\approx 8\frac{1}{3}$ hrs.)
FUV	3.03	3.29	3.31	3.25	3.72
NUV	.75	1.02	1.04	- .02	- .02
VIS	0	0	0	0	0
NIR	1.92	1.42	.70	- .37	- .37
FIR	.64	- .10	-1.07	-2.14	-2.14

As an example of the meaning of Table 10, if a WCWA were viewed for 100 sec. and a filter of OD = 3.0 was required to obtain a Maximum Permissible Exposure in the VIS band, then the OD required under our assumptions in the NIR band would be 3.0 + 1.42 = 4.42.

Examination of Table 10 would suggest that the attenuation of welding filters should vary with time in bands other than the VIS band. This would be so if the welder was wearing a plate of OD just sufficient to produce the MPE in the VIS band for the time domain listed, say 10 s., but not sufficient to reduce exposure to the MPE in 100 s, for example. As far as we know, however, the vast majority of production welders wear filters which avoid retinal problems and visual discomfort when used

for welding times of 10 to 3 x 10^4s. Let us learn what we can from this.

Consider the largest source allowed by the small-source MPE's and upon which Table 2 is based. This is a 24 mr source, which we will assume is 1.2 cm in diameter viewed at a distance of 50 cm., and produces the largest irradiance (as a function of source size) compared to its luminance allowable in the small-source case. Source area A_s is then

$$A_s = \frac{\pi(1.2)^2}{4} = 1.13 \text{ cm}^2$$

Referring to eq. (63),

$$I = \frac{L\, A_s}{d^2} \tag{72}$$

let us assume that source luminance L = 1 cd/cm^2, the MPE for luminance given in Table 4. Then illuminance I is

$$I = \frac{1(1.13)}{50^2} = 4.52 \times 10^{-4} \text{ ℓ/cm.}$$

Now, from eq. (34), a source which produces a constant spectral irradiation of α W/cm^2 nm produces an illuminance

$$I = 7.28 \times 10^4\ \alpha \text{ ℓm/cm}^2$$

So the value of α, say α_o, for a 24 mr source of uniform spectral irradiance to have luminance of 1 cd/cm^2 is found by equating the two expressions immediately above:

$$7.28 \times 10^4\ \alpha_o = 4.52 \times 10^{-4}$$

$$\alpha_o = 6.21 \times 10^{-9} \text{ W/cm}^2 \text{ nm} \tag{73}$$

Using Table 7, we know that this source would produce as bio-damage irradiance in the VIS band if viewed continuously for 10^4s:

$$D = 179\ \alpha_o Q_o(t)$$

$$= 179\ (6.21 \times 10^{-9})(10^6) = 1.11 \text{ bioW/cm}^2, \tag{74}$$

an amount slightly in excess of the MPE. But if viewed for 10 s., the source would produce

$$D = 300\ \alpha_o Q_o(t)$$

$$= 300\ (6.21 \times 10^{-9})(10^3) = 1.86 \times 10^{-3}\ \text{bioW/cm}^2, \quad (75)$$

an amount less than 1/500 of the MPE.

It seems to us very unlikely that a welder would tolerate a filter which caused the arc to have a luminance of more than 500 cd/cm^2, a luminance which corresponds to viewing the tungsten filament of an ordinary incandescent lamp with a clear glass bulb. This point will be discussed more later.

For the source characterized by eq. (73) we can list D for times of interest.

TABLE 11. Bio-irradiance in the visible region, D(VIS), versus time produced by continuous viewing of a circular source of uniform spectral irradiance and 24 mr angular size which has a luminance of 1 cd/cm^2.

time (sec)	D(VIS) (bioW/cm^2)
10	1.86×10^{-3}
10^2	1.02×10^{-2}
10^3	9.56×10^{-2}
10^4	1.11
3×10^4	1.11

Before we can finally use the calculations above to make a recommendation for welding plate attenuation, we must consider one more attribute of the WCWA - its size. Following Eq. (63), we noted that the largest source in Sutter's arc data had an effective source area of 3.55 cm^2. If viewed at a distance of 50 cm., a reasonable working distance in welding, this would correspond to a circular source of angular subtense of 42.5 mr, which is larger than the 24 mr for the largest "small source". Does this mean that we must start calculations for large sources all the way back at a point corresponding to Eq. (19) and develop "large source" tables corresponding to everything we did for small sources from that point? Fortunately, no, as we will explain.

For the restricted time domain of 10s to 3 x 10^4s which we are considering in this welding analysis, the dividing value, 24 mr, between large and small sources remains constant. It is a characteristic of the MPEs with which we started in this time domain that the radiance of a 24 mr source which would produce an irradiance equal to the small-source MPE in the VIS and NIR bands is also equal to the radiance of the large-source MPE to within 5%. The reader can check this computationally, but the key factors to note are that the MPEs for VIS and NIR of Table 6 are in a constant ratio (2100/sr) to those of Table 5, and 2100 is nearly the reciprocal of A_s/d^2 which relates radiance and irradiance for a circular source of 24 mr size.

As a result, the increases in optical density listed in Table 10 hold for larger source sizes for the VIS and NIR bands, since they were calculated for cases of maximum allowable irradiance from any small source, including 24 mr which also corresponds to the cases of maximum source radiance for large sources.

The use of the 1 cd/cm^2 luminance MPE and the WCWA keeps maximum radiance constant as source size increases, but irradiance increases as source sizes exceed 24 mr, which affects the necessary increases in OD of Table 10 in the NUV, FUV, and FIR bands. We have seen above that the largest source found by Sutter had an area of 3.55 cm^2 and that a 24 mr source at 50 cm distance had an area of 1.13 cm^2. We will assume that the largest WCWA appears circular as viewed and has an area of 4(1.13 cm^2) and is viewed at 50 cm and so has an angular size of 2(24) or 48 mr. This assumption means that the values for the NUV, FUV, and FIR bands of Table 10 should be increased by 0.6, since an OD of 0.6 corresponds to a factor of 4.

This ends the consideration of large size sources started after Table 11. We return now to the discussion preceding Table 11.

Table 11 and Table 10 taken together can easily be made to show that the most stringent requirement on OD increases in bands over that in the VIS band occurs for t = 3 x 10^4s and is the same as that for t = 10^4s except in the FUV band if maximum permissible source luminance is kept constant at 1 cd/cm^2. For instance, Table 11 shows that D(VIS) is only 1.86 x 10^{-3} bioW/cm^2 for t = 10s and a 1 cd/cm^2 source, so the OD increases in other bands could be lowered by the ratio of 1/1.86 x 10^{-3} which corresponds to an OD decrease of 2.73 and all bands would then require less OD than for t = 10^4s.

Our final assumption, then, is that long-term comfortable viewing for the welder corresponds to a luminance of 1 cd/cm^2 or less. In this case, the increases in OD listed for t = 10^4s,

when modified as indicated above in the NUV, FUV, and FIR to accommodate large sources, become our first-cut recommendation for welding filter plates after some rounding of values:

TABLE 12. Increase in Optical Density (OD) above that for the VIS band recommended for welding filter plates.

Spectral Band	Increase in OD
FUV	4.0
NUV	0.6
VIS	0
NIR	-0.4
FIR	-1.5

Two further factors need to be taken into account, however. Filters of low shade number, typically from 3 to 6 or 7, are commonly employed for viewing either quasi-blackbody radiation from furnaces or heat-treating ovens, or for gas welding, while filters of shades 1.5 to 3 are often used by arc welders' helpers. In a series of papers (Refs. 13, 14, 15), Clark has discussed these points and summarized them well in Ref. 15. Clark points out that furnaces and gas welding produce ratios of energy in the NIR band as compared to the visible which can be greater than those deduced for the WCWA and so has recommended lower transmittance in the NIR region for shades up to 6 than would result from application of Table 12. We agree with Clark's analysis which lead to the transmittances listed in Table 1 of the Australian standard AS Z45-1967. That table is reproduced here as Table 13.

Because of the method of measurement specified in ANSI Z87.1 using a Corning 2404 filter and a tungsten lamp to measure integrated infrared transmittance, there is a rough comparability of values in the Near Infrared column of Table 13 and those in the Maximum Infrared Transmittance column of Table 1 of ANSI Z87.1-1968. Maximum allowed IR transmittances in the Australian standard are noticeably lower for low shades than in Z87.1 and much lower in high shades, being quite close to those which would result from application of Table 12. With respect to NIR transmission, values given in the ISO standard ISO/TC 94/SC 6 (which are the same as those in the German standard DIN 4647 Blatt 1) are intermediate between those of the Australian and U.S. standards. The Table from

TABLE 13. Transmittance and Transmission values of various shades of welding filter lenses (from p. 52, AS Z45-1967, the Australian standard).

TRANSMITTANCE AND TRANSMISSION VALUES OF VARIOUS SHADES OF WELDING FILTER LENSES

Shade Number	Erythemal Ultra-violet Maximum Mean % Transmission	Luminous Transmission Factor %		Near Infrared 0.7 to 1.3 μm Maximum Mean % Transmission	Maximum % Transmittance in Range 1.3 to 2.0 μm
		Minimum	Maximum		
1.1	0.001	75	100	25	50
1.4	0.001	60	75	20	35
1.7	0.001	40	60	13	25
2	0.001	30	40	10	13
2.5	0.001	18	30	6.0	10
3	0.001	8.6	18	8.6	7
4	0.001	3.2	8.6	3.2	3
5	0.001	1.2	3.2	1.2	1.5
6	0.001	0.45	1.2	0.45	1.3
7	0.001	0.17	0.45	1.7	1.0
8	0.001	0.061	0.17	0.61	0.7
9	0.0005	0.023	0.061	0.23	0.6
10	0.0001	0.0086	0.023	0.086	0.4
11	0.00005	0.0032	0.0086	0.032	0.3
12	0.00001	0.0012	0.0032	0.012	0.3
13	0.00001	0.00045	0.0012	0.0045	0.2
14	0.000005	0.00016	0.00045	0.0016	0.1
15	0.000001	0.000061	0.00016	0.00061	0.1
16	0.0000005	0.000023	0.000061	0.00023	0.06

NOTES:

1. The mean transmission for any filter in the range 320 to 400 nm is to be less than half of the measured luminous transmission factor.
2. For an explanation of the values given in the table see Appendix B.

the ISO standard is shown below for background information.

The final recommendation we make will incorporate values consistent with the Australian standard for near infrared transmittance for shades 1.5 to 6; since that standard does not list requirements for a shade 1.5 filter, we will interpolate between the values for shades 1.4 and 1.7 of the Australian standard to derive numbers for shade 1.5 filters sold in the U.S.A.

TABLE 14. Transmission specifications for welding filters (Table 4 of ISO/TC 94/SC 6)

TRANSMISSION SPECIFICATIONS FOR WELDING FILTERS

Scale No.	UV - Max. Transmission $\tau_{(\lambda)}$		Transmission in Visible Spectrum τ_V		IR Transmission - Max. Mean Value τ_{NIR}	τ_{MIR}
	313 nm %	365 nm %	max. %	min. %	Near IR 1300-780 nm %	Mid.IR 2000-1300 nm %
1.2	0.0003	50	100	74.4	37	20
1.4	0.0003	35	74.4	58.1	33	19
1.7	0.0003	22	58.1	43.2	26	16
2.0	0.0003	14	43.2	29.1	21	13
2.5	0.0003	6.4	29.1	17.8	15	9.6
3	0.0003	2.8	17.8	8.5	12	8.5
4	0.0003	0.95	8.5	3.2	6.4	5.4
5	0.0003	0.30	3.2	1.2	3.2	3.2
6	0.0003	0.10	1.2	0.45	1.7	1.9
7	0.0003	0.037	0.45	0.17	0.81	1.2
8	0.0003	0.013	0.17	0.060	0.43	0.68
9	0.0003	0.0045	0.060	0.023	0.20	0.39
10	0.0003	0.0016	0.0023	0.085	0.10	0.25
11	Value less	0.00060	0.0085	0.0032	0.050	0.15
12	than or	0.00020	0.0032	0.0012	0.027	0.096
13	equal to	0.000076	0.0012	0.00045	0.014	0.060
14	transmis-	0.000027	0.00045	0.00017	0.007	0.04
15	sion fac-	0.0000094	0.00017	0.000060	0.003	0.02
16	tor for 365 nm	0.0000034	0.000060	0.000023	0.003	0.02

Additional Specifications:

(a) Between 210 and 313 nm, transmission must not exceed value permissible for 313 nm.

(b) Between 313 and 365 nm, transmission must not exceed value permission for 365 nm.

(c) Transmission at 405 nm must not exceed that measured at 560 nm.

The second factor which needs to be taken into account is the need to prevent excessive transmittance in the blue spectral region because of suspected photochemical effects from chronic blue-light exposure.* This has previously been dealt with to a slight degree by Additional Specification (C) in Table 14 (ISO standard), but certainly not by Table 1 of Z87.1, which allows transmittances of 405 nm comparable to the luminous transmittance for shades 1.5 to 6 and considerably higher than the luminous transmittance for shades 7 to 14. As a first step in closing this loophole in Z87.1 we recommend a method of setting a limit to the average over a small wavelength range so as to prevent a fortuitous narrow-band absorption near 435 nm from baulking our objective; we recommend that the maximum mean transmittance from 420 nm to 460 nm not exceed the luminous transmittance.

From Tables 12, 13, and 14 and the accompanying discussion we put down in Table 15 our recommended transmittances for general-purpose filters for eye protection. We shall now proceed to discuss that table.

The range of 1400 to 2000 nm for FIR transmittance limit is chosen because experience (Ref. 15) has shown it to be an adequate representation of the FIR region for protection purposes, and because it is relatively convenient for spectrophotometry.

Note 1 of Table 15 simply expresses the application of Table 12 in the FUV region. These allowed values are somewhat lower than allowed by the ISO and Australian standards but are roughly comparable; Z87.1 does not specify values in this region.

Note 2 regulating the NUV band only slightly more restrictive than would be given by Table 13. It is difficult to make an overall comparison of this NUV requirement with those of Table 14 or Z87.1 because those Tables require transmittance values only at 2 or 3 wavelengths in or near the NUV band. It appears that Note 2 allows somewhat more transmittance than Table 14 or Z87.1 for low shade numbers and much less transmittance for high shades. We have chosen the approach of Note 2 because it appears adequate in view of our knowledge of radiation sources and MPEs in the NUV region and yet is not overly restrictive with regard to introduction of products other than iron-containing glasses.

The reason for the requirement of Note 3 was discussed above.

---

* See Ref. 4, pp. 90-92.

TABLE 15. Recommended Transmittances of various shades of general-purpose eye protection filters.

Shade Number	Luminous Transmittance			Maximum Mean Transmittance, 700 nm to 1400 nm, %	Maximum Mean Transmittance, 1400 nm to 2000 nm, %
	Maximum %	Nominal %	Minimum %		
①	②	③	④	⑤	⑥
1.5	67	61.5	55	18	18
1.7	55	50.1	43	13	16
2.0	43	37.3	29	10	13
2.5	29	22.8	18.0	6.0	9.6
3	18.0	13.9	8.50	6.0	8.5
4	8.50	5.18	3.16	3.2	5.4
5	3.16	1.93	1.18	1.2	3.2
6	1.18	0.72	0.44	0.45	1.9
7	0.44	0.27	0.164	0.45	1.2
8	0.164	0.100	0.061	0.25	0.68
9	6.1(-2)	3.7(-2)	2.3(-2)	9.4(-2)	0.39
10	2.3(-2)	1.4(-2)	8.5(-3)	3.5(-2)	0.25
11	8.5(-3)	5.2(-3)	3.2(-3)	1.3(-2)	0.15
12	3.2(-3)	1.9(-3)	1.2(-3)	4.9(-3)	0.096
13	1.2(-3)	7.2(-4)	4.4(-4)	1.8(-3)	0.060
14	4.4(-4)	2.7(-4)	1.6(-4)	6.7(-4)	0.04
15	1.6(-4)	1.0(-4)	6.1(-5)	2.5(-4)	0.02
16	6.1(-5)	3.7(-5)	2.3(-5)	9.4(-5)	0.02

Notes:

1. Maximum mean transmittance, 200 nm to 315 nm, shall not exceed the Nominal Luminous Transmittance times 10^{-4}.

2. Maximum mean transmittance, 315 to 400 nm, shall not exceed 25% of the Nominal Luminous Transmittance.

3. Maximum mean transmittance, 420 to 460 nm, shall not exceed the Nominal Luminous Transmittance.

4. A transmittance entry such as 7.2(-4) in the table means 7.2×10^{-4} or 0.00072.

TABLE 15. (continued)

Notes: (continued)

5. Luminous Transmittance values are for the 1931 CIE Observer and CIE Illuminant A.

6. If the Nominal Luminous Transmittances listed in Column (3) are abbreviated as NLT, the mean transmittance requirements of Notes 1, 2, 3 may be written as, where $T(\lambda) \equiv$ transmittance at wavelength λ,

Note 1: $$\frac{1}{115}\int_{200}^{315} T(\lambda)d\lambda \leq (NLT) \times 10^{-4}$$

Note 2: $$\frac{1}{85}\int_{315}^{400} T(\lambda)d\lambda \leq 0.25 \times (NLT)$$

Note 3: $$\frac{1}{40}\int_{420}^{460} T(\lambda)d\lambda \leq NLT$$

Similarly, mean transmittances listed in Columns (5) and (6) are given by

$$\frac{1}{700}\int_{700}^{1400} T(\lambda)d\lambda, \quad \text{Column (5)}$$

and $$\frac{1}{600}\int_{1400}^{2000} T(\lambda)d\lambda, \quad \text{Column (6)}$$

Summary Discussion of Recommended Values for Filter Transmittance

Our recommended values shown in Table 15 are based on input from foreign standards (Tables 13 and 14), from Z87.1, and from our analysis of MPEs and welding arc spectra which resulted in Table 12. Overall, choices were made which make Table 15 the most strict requirement of those discussed except, as noted above, for low shade numbers in the NUV region. Results of the analysis of MPEs and the Worst-Case Welding Arc given in Table 12 are very broadly in approximate agreement with those of the ISO (and DIN) and Australian standards; all three approaches require much more attenuation in the FUV and infrared regions than does Z87.1. Tables 12, 13, 14, and 15 also divide the infrared into two regions depending on whether or not a substantial fraction of energy is transmitted to the posterior portion of the eye.

Table 15 might be said to have as an advantage the fact that it is based on wavelength regions the same as those used in ACGIH and ANSI Laser documents; conversely, these regions are slightly different than those presently used in industrial safety standards (Tables 13 and 14).

Table 15 represents our best judgment about requirements for transmittance for general-purpose eye protection. Depending on the relative advantages of having a separate U.S. standard, we believe that Table 15, or else the proposed ISO standard of Table 14, should be adopted in the U.S.A.

Welding Plate Transmittance

It seems sensible, after the long argument which has been presented here in favor of tighter transmittance requirements for eye protection filters, to examine whether these requirements are consistent with performance of the green iron-containing glasses used for many years in general-purpose industrial applications.

Figures 10, 11, and 12 show the optical density versus wavelength for typical 2" x 4 1/4" welding plates of shades 3, 6, and 10 made of iron-containing glasses. Optical density (OD, see eq. (69) above) is plotted to fully represent the tremendous range of transmittance encountered. The dashed lines represent lower limits of the OD in the spectral regions which they cover. It was necessary to thin plates to as little as 0.5 mm thick to obtain data for these figures.

It is interesting to note that the shade 3 and 10 samples appear to be a slightly different composition than the shade 6, as evidenced by slightly different peak shapes in the visible region and different ratios of OD at the peaks at 550 nm and the troughs at 1200 nm. These curves represent typical examples of the filters which have protected welders for many years, and they easily meet the requirements of Tables 13, 14, and 15. So we may say that welders and other industrial workers have been protected for many years by the fortuitous absorption properties of green iron-containing glasses rather than by materials in conformance to the values called out in Table 1 of Z87.1.

Special-Purpose Filter Materials

In our opinion, one weakness of Z87.1 is that it allows no absorptive lenses other than those called out by Table 1 of Z87.1. This would appear to be unfortunate in that there are applications where UV, visible, and IR protection may not all be needed at the same time as required by Table 1 of Z87.1. For instance, we know of situations where only UV or only IR absorption is necessary and where visible absorption is

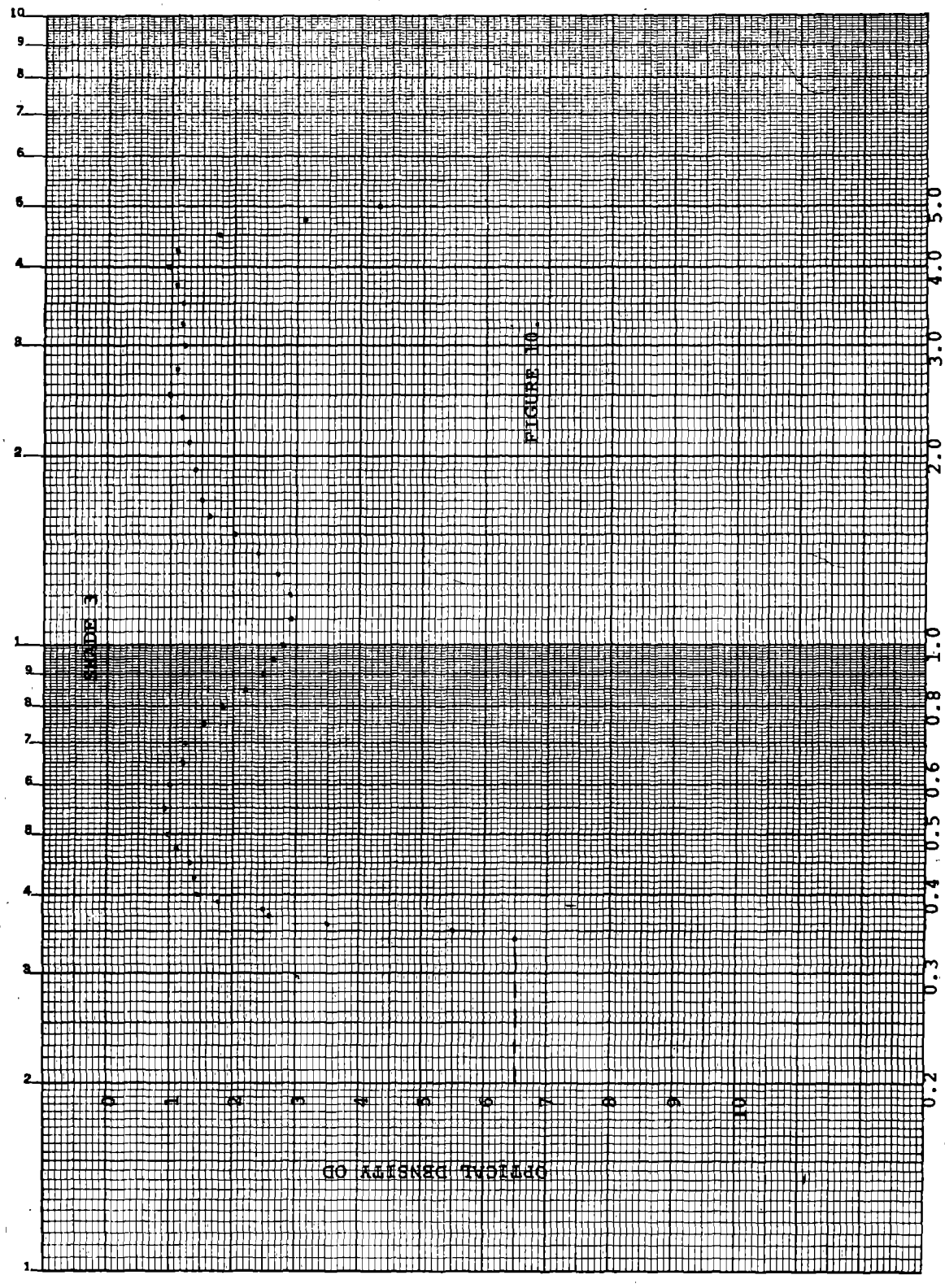

Figure 10. Optical Density vs. Wavelength for a Typical Shade 3 Welding Filter of Green Glass.

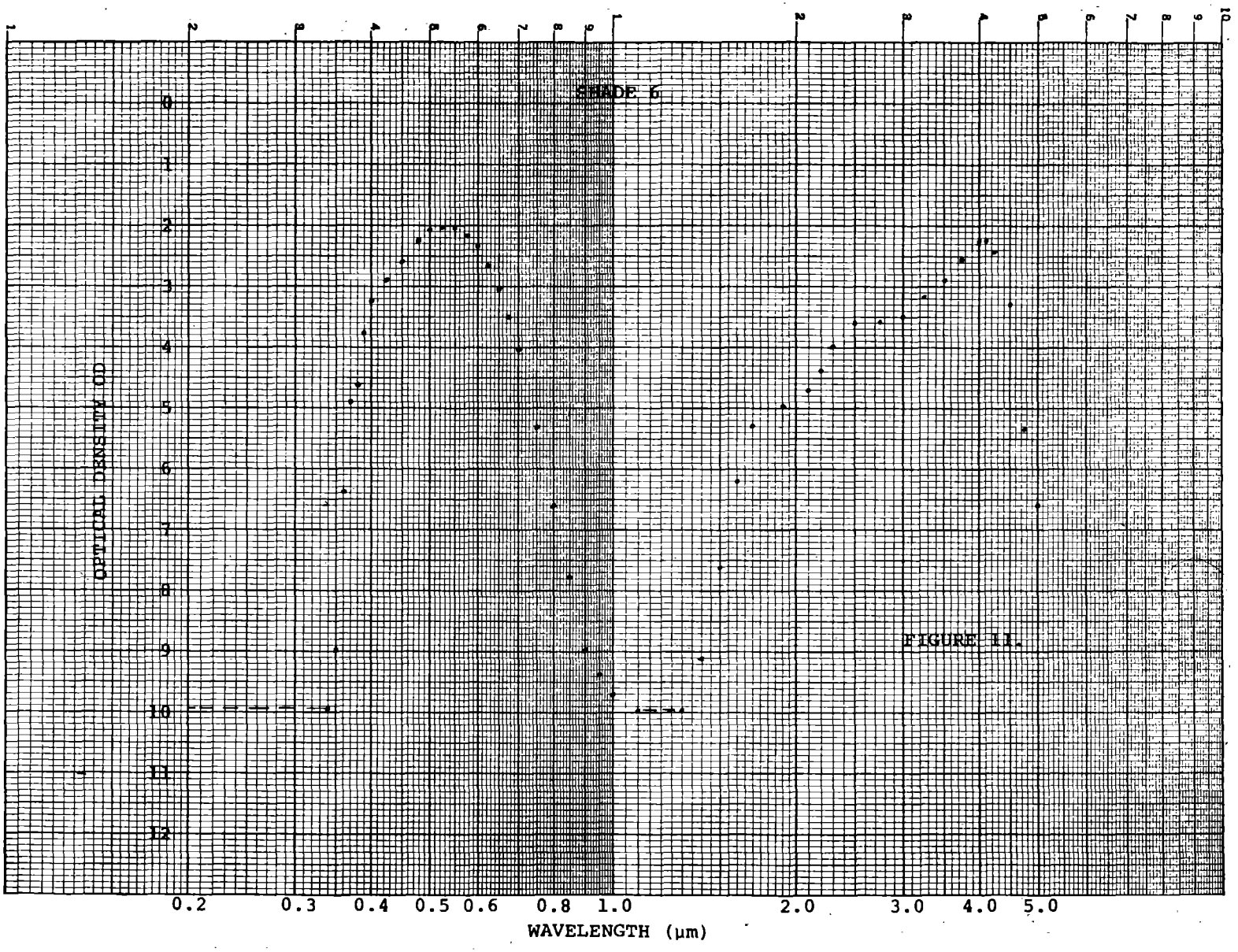

FIGURE 11.

Figure 11. Optical Density vs. Wavelength for a Typical Shade 6 Welding Filter of Green Glass.

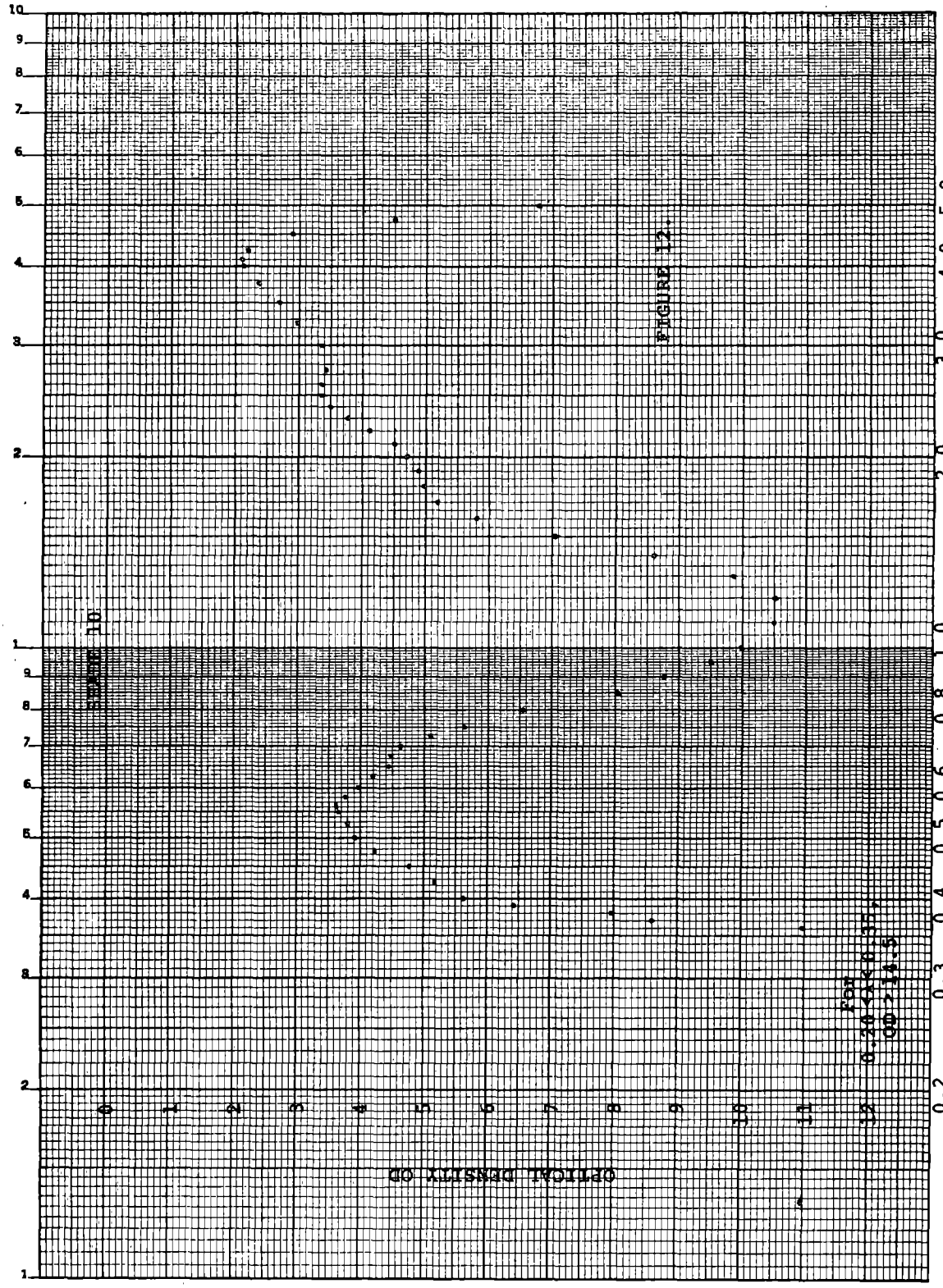

Figure 12. Optical Density vs. Wavelength for a Typical Shade 10 Welding Filter of Green Glass.

detrimental because of low overall illumination of the work area. We must give Z87.1 its due by realizing that in the past the knowledge of eye MPEs was fragmentary at best, and so the "green glass" approach was warranted. While MPEs for the eye are still undergoing revision, the tremendous amount of work in recent years has led to Tables 1 and 2, and we believe these MPEs are adequate to allow specification of absorptive lenses other than those having "green glass" properties. If radiation characteristics of the source are known, the use of some systematic scheme for calculating bio-damage exposure such as the one presented previously, together with the MPEs of Table 4, should allow adequate specification of filter absorption requirements for any specific situation. Materials with high luminous transmittance but strong absorption in either the UV or the IR would then become available for improved eye protection. Finally, the formalism of eqs. (2) to (13) allows straightforward if tedious evaluation of the effects of improved MPEs, new data for source optical radiation, new safety factors, etc. on recommended transmittances for eye protection.

TASK 2

INTRODUCTION

The contract calls for development of a ballistic test method for the purpose of classifying various eye and face protective devices on the basis of requirements for protection against impacts in the work place, such as would be caused by flying particles or other objects in a typical machine shop. Use of an anthropometric headform is required as a test fixture to hold the eye and face protective devices, but other variables such as mass, shape, and velocity of projectiles should be investigated as necessary. The contractor shall specify the tolerances involved in the test method, the expected repeatability in carrying out the tests, and shall furnish experimenal data in support of the ballistic test method in the final report.

This task consists of seven subtasks:

> SUBTASK 1. Select a missile; it was proposed to use the existing AO air gun. Specify the tolerances involved in the test method.
>
> SUBTASKS 2-6. After review and approval of the proposed test method, study the performance of safety spectacles, flexible mask goggles, cup goggles, welding helmets, and face shields, in that order.
>
> SUBTASK 7. Analyze the test results and method and report.

SUBTASK 1: SELECTION OF SUITABLE MISSILE

Background

Behind the effort of Subtask 1 lies considerable experience in impact resistance studies with spherical missiles. The breadth of this experience is illustrated in Figure 13, which presents the range of ball bearing sizes that have been used in air gun impact resistance studies over the past fifteen years at American Optical Corporation. Figure 14 pictures a typical breach-loading air gun used in these studies.

Figure 15 is a 1/2 μs exposure photograph of a 1 mm ball at 1000 ft/s impacting and fracturing a glass lens (an American Optical Corporation 3.4 mm thick air tempered industrial safety lens) made during some of these earlier studies. In Figure 16 the half microsecond exposure caught

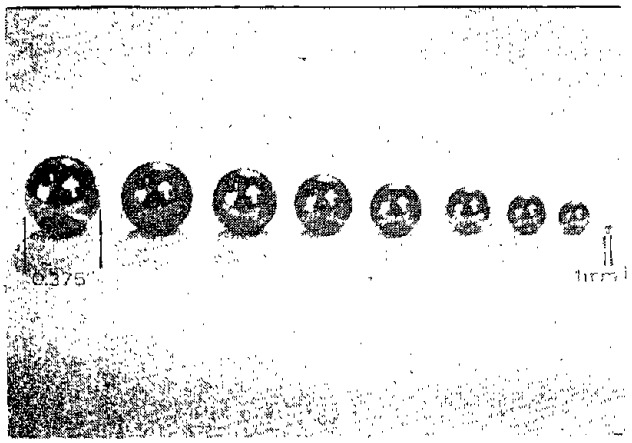

Figure 13. Various size ball bearing missiles used in air gun impact resistance studies.

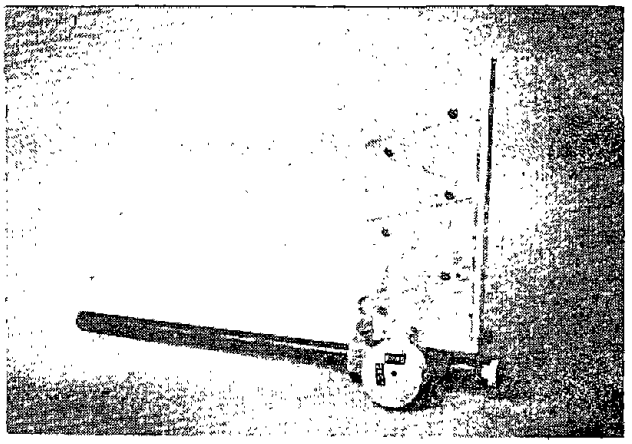

Figure 14. Typical breach-loading air gun used in impact resistance studies.

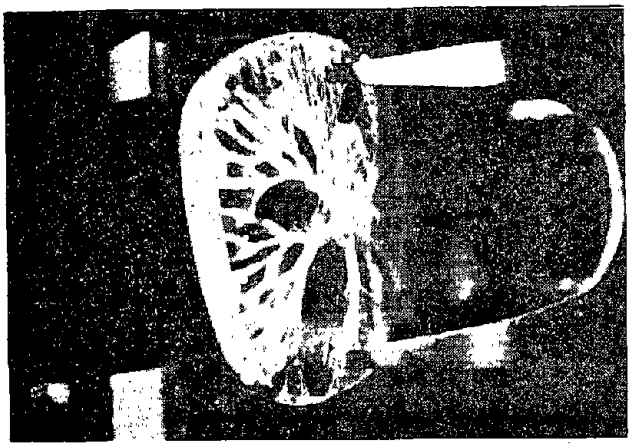

Figure 15. Photograph of 1 mm ball impacting and fracturing a glass lens. Arrow points toward ball.

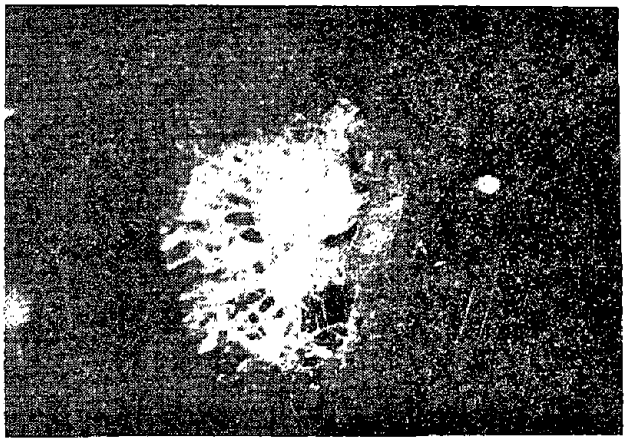

Figure 16. Photograph of 0.218 inch ball in rebound from a glass lens. Arrow points toward ball.

a 0.218 inch ball in rebound from fracturing a glass lens by 150 ft/s impact. This is a typical behavior. Although the safety lens is broken, and fine debris is ejected toward the eye, the primary small missile is usually repelled. Figure 17, a probability graph paper plot, provides a good concept of the 22 cal air gun impact resistance of three types of industrial eye protection lenses: air tempered glass, moderately brittle CR-39 plastic, and high strain limit plastic coated for scratch resistance (Gentex lens).

For contrast, Figure 18 presents a similar plot of the impact resistance to a 1-inch ball of lenses supported upon the Z87

base of air tempered glass, CR-39 plastic, and coated polycarbonate. Impact velocities in dropped ball tests rarely exceed 50 feet per second, somewhat lower than the minimum velocity encountered in 22 cal air gun tests of these materials. Note the reversal of relative impact resistance of air quenched glass and CR-39 for the two impact velocity ranges.

Data for Gentex polycarbonate lenses are missing from Figure 18 because it was not possible to break them in this test. Apparently, the reason for this is that the relatively brittle coating flakes loose from the Gentex lenses and so does not serve to initiate brittle failure at the low strain rates characteristic of the Z87.1 drop-ball test. Figure 17 shows the opposite effect for the Gentex lenses.

The "probability paper" graphs used in these impact studies have as abscissa a non-linear scale which represents the cumulative probability of occurrance for events. If these events, in this case breakage, follow a normal or Gaussian distribution the data will plot in a straight line. The slope of the straight line increases with the width of the normal distribution, while the + 1σ, - 1σ, + 2σ, - 2σ points (σ = standard deviation) occur at abscissa values of 84.1, 15.9, 97.6, 2.4, respectively.

Among the mass of experimental work done on high velocity impact resistance tests is that of Boeing Aircraft Corporation's Protective Equipment Specification 1-2.3.3 and 1-2.3.4 which employs a chisel-pointed missile. We found the test very unsatisfactory: (1) the missile was quite expensive to fabricate in our Machine Shop and each missile could be used but once because of damage suffered in its impact with a glass or plastic lens; (b) tumble of the missile in flight prevented impact with the axis of the missile normal, or near normal to the surface of the target lens. Figure 19 contains two 1/2 microsecond flash photos illustrating the problem.

Because any pointed missile will generally be used only once because of damage it receives in the impact, the missile choice is influenced by cost and ease of procurement. Because industrial sewing machine needles meet these two criteria and are available in a wide range of sizes and shapes, they were used for our initial scouting experiments. Benjamin air gun tufted darts are available in quantity and are relatively inexpensive, but the variation in their point geometry and weight moved us into the region of needles and suitable carriers.

Experimental Work

The first part of solution of the problem of selection of gun barrel and missile involved qualitative scouting of a variety of sewing machine needles and gun barrel bore sizes. The needles,

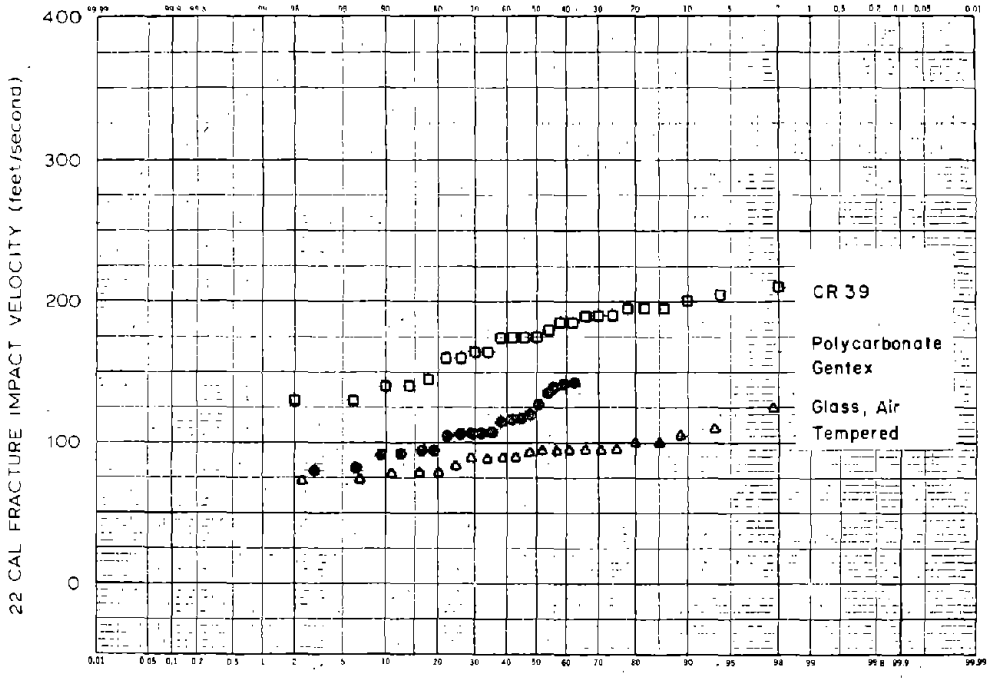

Figure 17. Probability graph of 22 cal air gun impact resistance of three types of industrial eye protection lenses

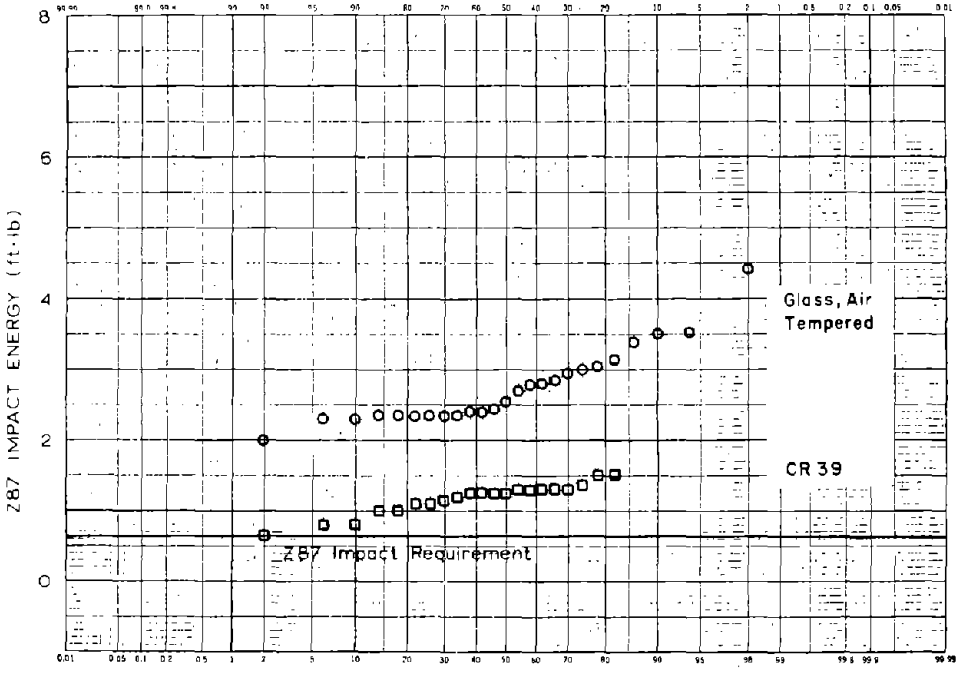

Figure 18. Probability graph of impact resistance to 1 inch ball on lenses supported on Z87.1 base

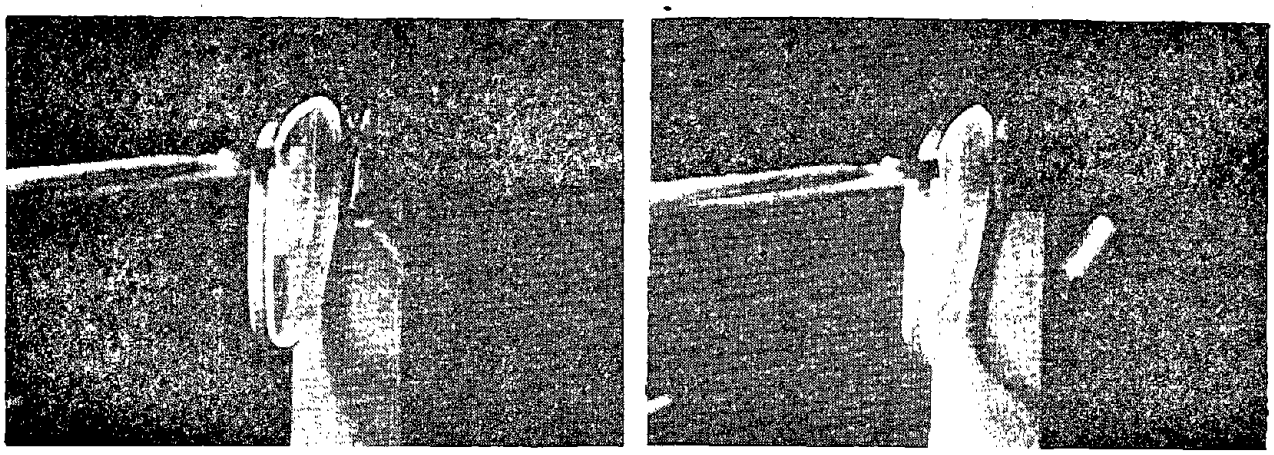

Figure 19. Photographs showing tumbling of missile using Boeing Aircraft Corporation test specification

see Figure 20, covered a moderately wide range of needles available for industrial sewing machines. The hypodermic tubing gun barrels found to be useful in addition to the regular gun barrels in our air gun arsenal are illustrated in Figure 21.

The needles, with and without a 0.218 inch carrier, were fired at both tempered glass and plastic eye protection devices in an effort to develop a generalized concept of the relations among missile mass, missile point, target material and missile velocity. Some form of missile that could simulate the general

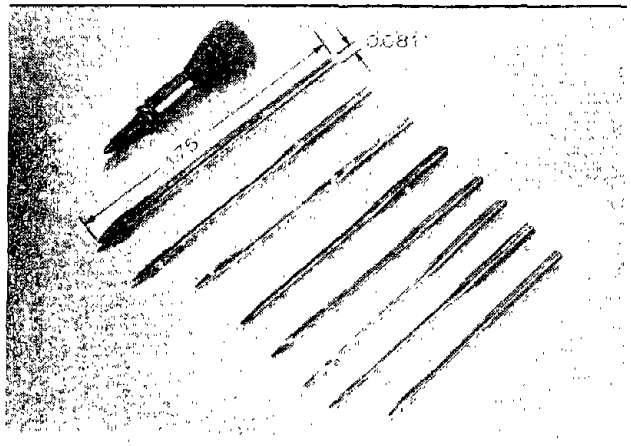

Figure 20. Needles available for industrial sewing machines considered for use as test missiles

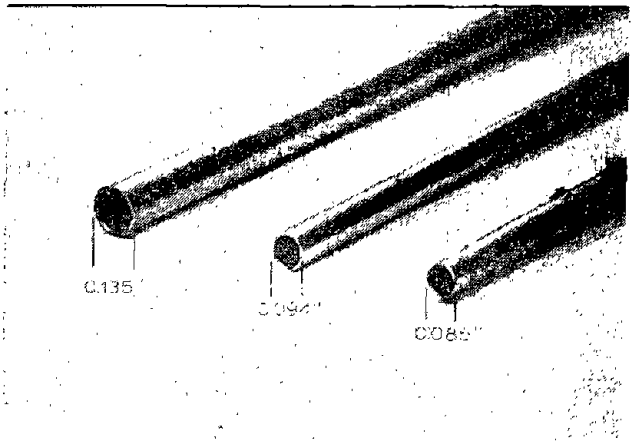

Figure 21. Range of hypodermic tubing gun barrels found to be useful for firing needles

type of missile hazard to be expected in an industrial shop - such as a fragment of a twist drill or tool bit - was a goal of this effort. A second goal was that the spectrum of missile velocities at which appreciable damage or destruction of the eye protector occur should be of such breadth as to allow some quantitative appraisal of relative protection offered by different materials and devices.

Results

Needles of the general size of home sewing machine needles, fired from appropriate small bore barrels were of such low mass that velocities in the 50 to 200 ft/s range caused little more than pitting of glass or of plastic lenses, (Figure 22). The larger Singer 200/25 (0.81g) pitted plastic and fractured tempered glass, see Figure 23.

When the mass of the missile was increased to about 1.6g by fitting the needle into a 0.218 inch diameter aluminum carrier, breakage of tempered glass and total penetration of plastic lenses occurred, (Figure 24). In this scouting experiment, fracture of glass by the 1.6g Singer 200/25 needle missile invariably occurred at much lower velocities than were required to puncture plastic lenses.

Our experience with our 22 cal and other ball size missile air guns indicated that the impact resistance of lenses to small high velocity (in excess of about 75 ft/s) missiles is almost completely independent of the lens supporting system. Nevertheless our scouting work did include firing, at about 200 ft/s, some needles loaded to 1.6g at safety glasses mounted upon anthropometric heads. Small diameter needles (Simanco 16) penetrated air tempered glass, Figure 25, and plastic,Figure 26, to sufficient depth to reach the eye itself.

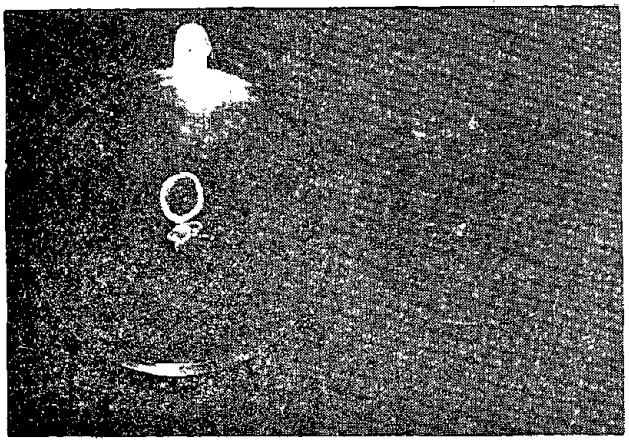

Figure 22. Pitting of glass (right) and plastic lenses by small mass needles in the 20 to 200 ft/s range

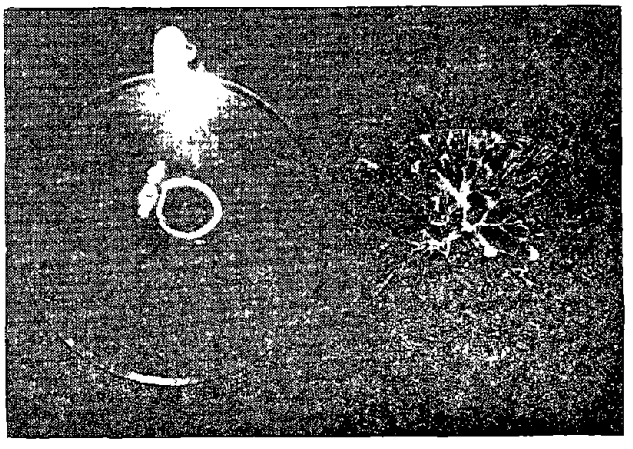

Figure 23. Pitted plastic lens (left) and fractured glass lens caused by Singer 200/25 needle

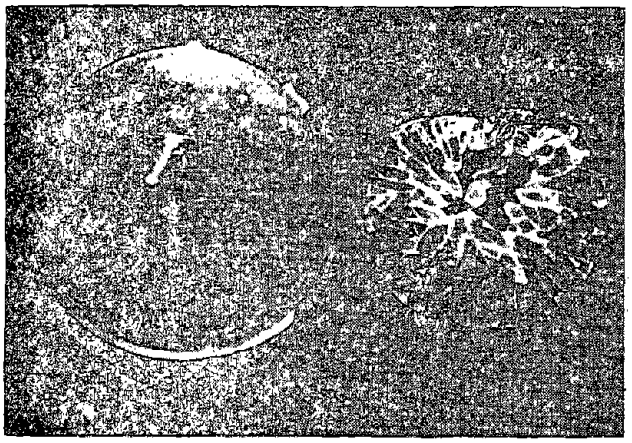

Figure 24. Total penetration of plastic lens and fracture of glass lens when needle mass was increased to 1.6g

While the anthropometric head may not be as necessary to provide realistic test results with high velocity low-mass missiles as with heavy slow-moving missiles, its use is highly recommended since:

1. it makes the test results as realistic as is practical; and

2. it solves in one stroke a large number of tedious and time-consuming problems of devising a series of holding fixtures for different products and then trying to figure out how realistic these tests are.

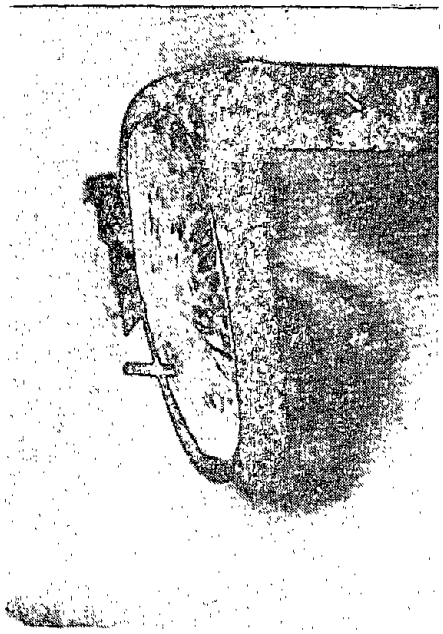

Figure 25. Side view of glass lens in frame showing needle penetrating eye

Figure 26. View of needles penetrating plastic lenses to a depth sufficient to reach the eyes

As a result of this scouting survey, the most appropriate missile appeared to be the 0.81g Singer 200/25 needle loaded in a 0.218 inch (22 cal) carrier.

1. The loaded needle is comparable to the mass (1.6g) and point of a missile that could occur in a Machine Shop.

2. The mass, by adjustment of the carrier size, and point, or by use of alternate needle points, can be altered if necessary to reconstruct an accident.

3. The needles are readily available to precise dimensions at low cost ($10.60 per 100 at this date).

4. The 0.218 carrier and needle can be fired in the existing 22 cal air gun.

5. The weighted needle appears to have impact characteristics that will provide quantitative distinction among glass and plastic materials in protective devices.

6. The use of needles alone was found to be impractical because their lightness and the small barrel diameters required would not yield sufficiently high velocities without helium as a propellent gas: the use of compressed air was judged more practical for routine test purposes.

The decision to use this needle and carrier remained dependent upon solution of one problem - a severe tendency for the missile to tumble after leaving the gun muzzle. This tumble action, illustrated in Figure 27, caused two detrimental types of behavior: (a) unreliable flight time measurement between the two timing gates, and (b) the axis of the missile to be non-normal to the target surface at the site of impact.

Modifications to the missile and air gun barrel were required to correct this tumble behavior. The carrier was lengthened from that shown in Figure 27, and the gun barrel was vented for a distance back from the muzzle to reduce the effect of muzzle blast as a cause of tumble. The timing gates were moved to the vented section of the barrel where the missile is guided but not accelerated so that the same section of the missile point activates both gates.

Results of these modifications resulted in the final choice of needle plus carrier as a Singer No. 135 x 17 needle, Size 200/25 (Fig. 28) for a replaceable point in a 0.218 inch diam., 1 5/8 inch long aluminum carrier drilled 1 17/32 inch deep with a 0.082 inch drill. The assembly weighs 3.20 gm (7.06×10^{-3} lb).

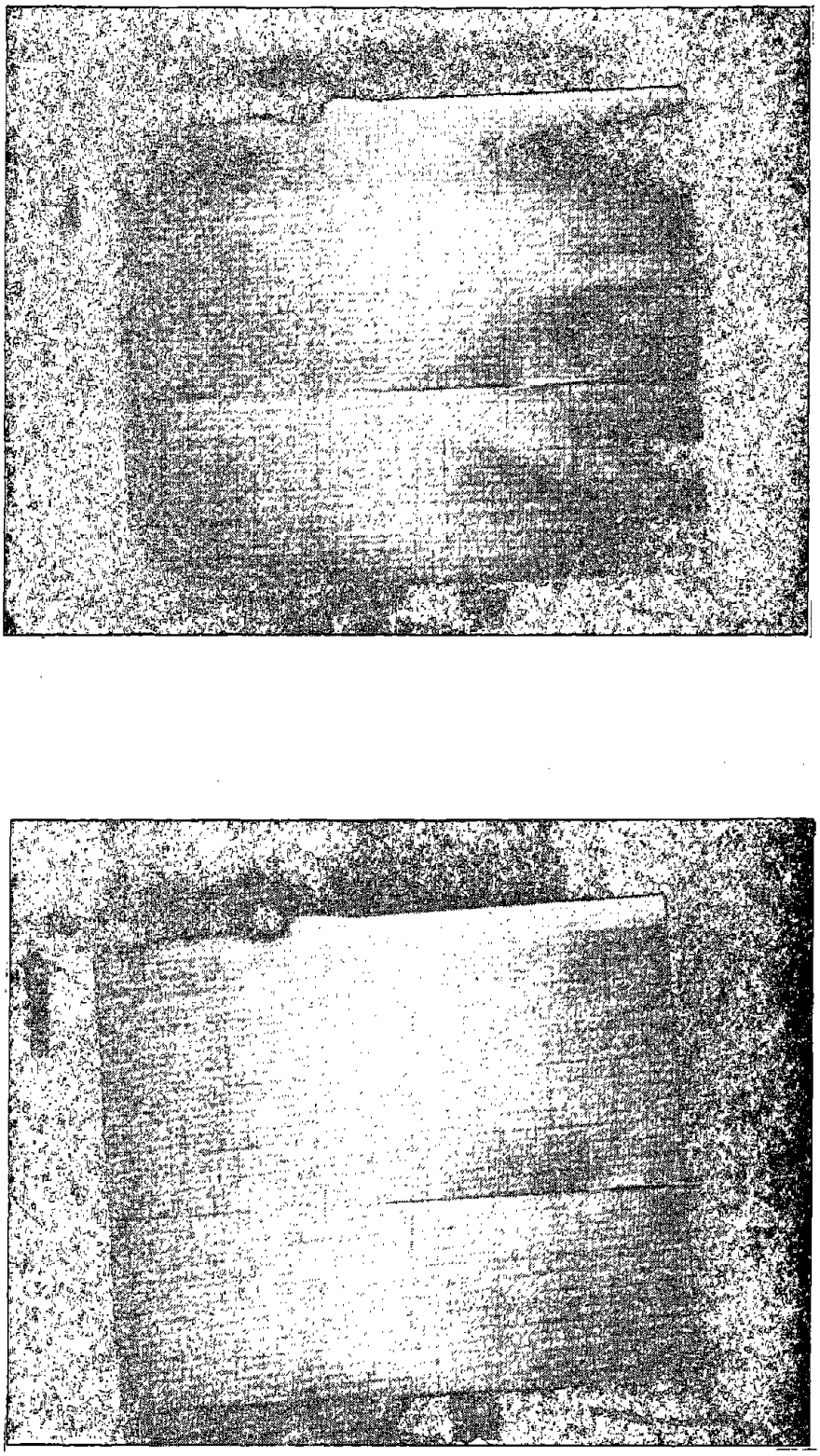

Figure 27. Photographs showing missile tumble with early aluminum carrier design.

LTR.	REVISED	BY	CHANGES

SEWING MACHINE NEEDLE #200/25

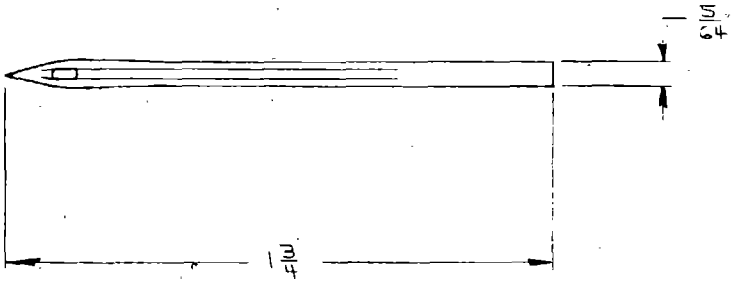

Figure 28. Singer No. 135x17 Needle Size 200/25.

LIMITS UNLESS SPECIFIED	AMERICAN OPTICAL CORPORATION						
DECIMALS ± .005							
FRACTIONS ± 1/64	MATERIAL						
ANGLES ± 0°30'							
SURFACE ROUGHNESS	DO NOT SCALE THIS DRAWING						
HARDNESS	SCALE		USED ON				
	DRAWN	BY	NO. REQ'D				
	CHECKED	BY					
SUPERSEDES	APPROVED	BY					

5099C

B.L.M. 10392

The carrier is shown in Figure 29 and the vented gun barrel for the 22 cal air gun in Figures 30 and 31. The missile shows negligible tumble at distances greater than 6 inches from the muzzle (Fig. 32) which is adequate for test purposes.

Repeatability of the Test Method

Although the actual missile velocity in each shot is determined with the timing device, a pressure-velocity curve is required to be able to select, in advance, the intended velocity of impact. Table 16 provides a tabulation of pressure, mean velocity, standard deviation (determined from probability paper plotting of twenty-five data points displayed in typical form in Figure 33), and coefficient of variance for the air pressure - missile velocity calibration of Barrel 220VB2. Figure 34 is the plotted curve of this calibration.

TABLE 16. PRESSURE-VELOCITY CALIBRATION OF 220 VENTED BARREL NO. 2 & SINGER 200/25 NEEDLE WITH 1 5/8" CARRIER

Pressure psi of air	V_{50} Mean ft/s	s_v Std. Dev. ft/s	% Coef. Var.
10	42.65	0.65	1.52
20	64.04	0.70	1.09
30	79.61	0.68	0.85
40	92.86	0.73	0.79
50	103.59	0.75	0.72
60	117.18	1.00	0.85
70	125.88	0.86	0.68
80	133.84	0.84	0.63

SUBTASK 2: SAFETY SPECTACLE PERFORMANCE

Subtasks 2 through 6 consisted of determining the impact resistance of various common types of eye and face protection products to the high speed needle-carrier combination.

Spectacles with Heat-Treated Glass Lenses

Safety spectacles with heat treated glass lenses were mounted upon the anthropometric head and impacted (using the staircase or Bruceton technique) until a sample of 25 specimens had

LTR.	REVISED	BY	CHA. ES

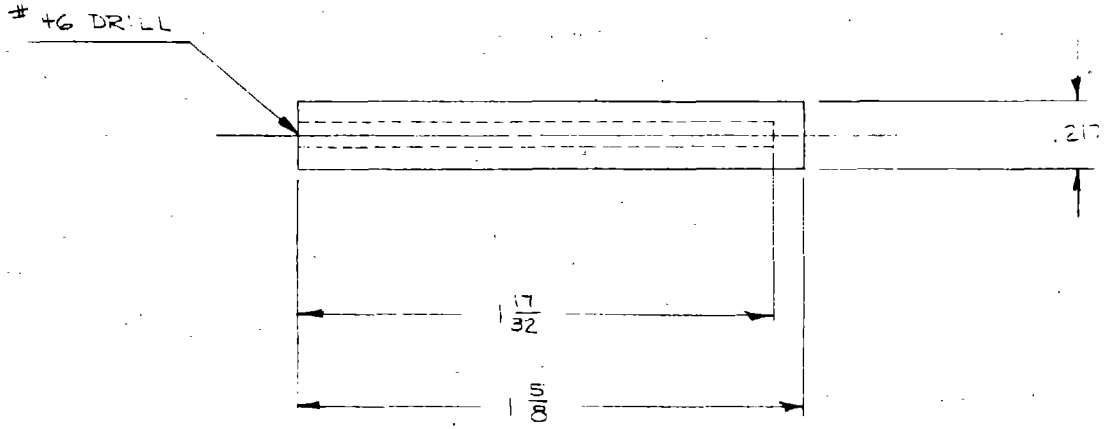

Figure 29. Aluminum Carrier for Singer Needle.

LIMITS UNLESS SPECIFIED	AMERICAN OPTICAL CORPORATION
DECIMALS ± .005	
FRACTIONS ± 1/64	MATERIAL
ANGLES ± 0°30'	
SURFACE ROUGHNESS	DO NOT SCALE THIS DRAWING
HARDNESS	SCALE / USED ON / DRAWN BY / NO. REQ'D / CHECKED BY
	APPROVED BY
SUPERSEDES	

8099C

B.L.M. 2779

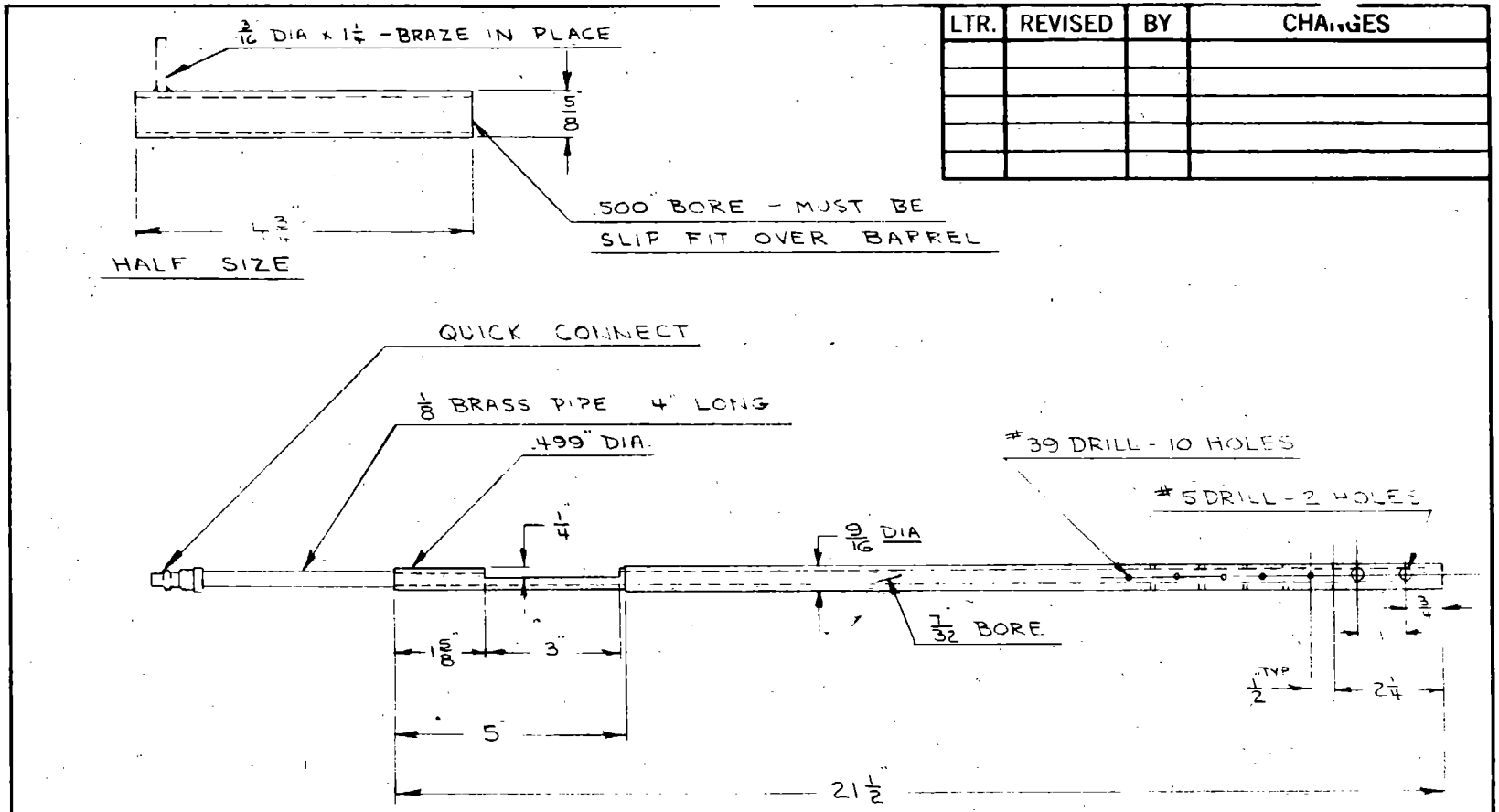

LTR.	REVISED	BY	CHANGES

LIMITS UNLESS SPECIFIED	AMERICAN OPTICAL CORPORATION						
DECIMALS ± .005							
FRACTIONS ± 1/64	MATERIAL						
ANGLES ± 0°30'							
SURFACE ROUGHNESS	DO NOT SCALE THIS DRAWING						
HARDNESS	SCALE		USED ON				
	DRAWN	BY	NO. REQ'D				
	CHECKED	BY					
SUPERSEDES	APPROVED	BY					

5099C

B.L.M. 10392

Figure 30. Modified Crossman "180" Pellgun Barrel.

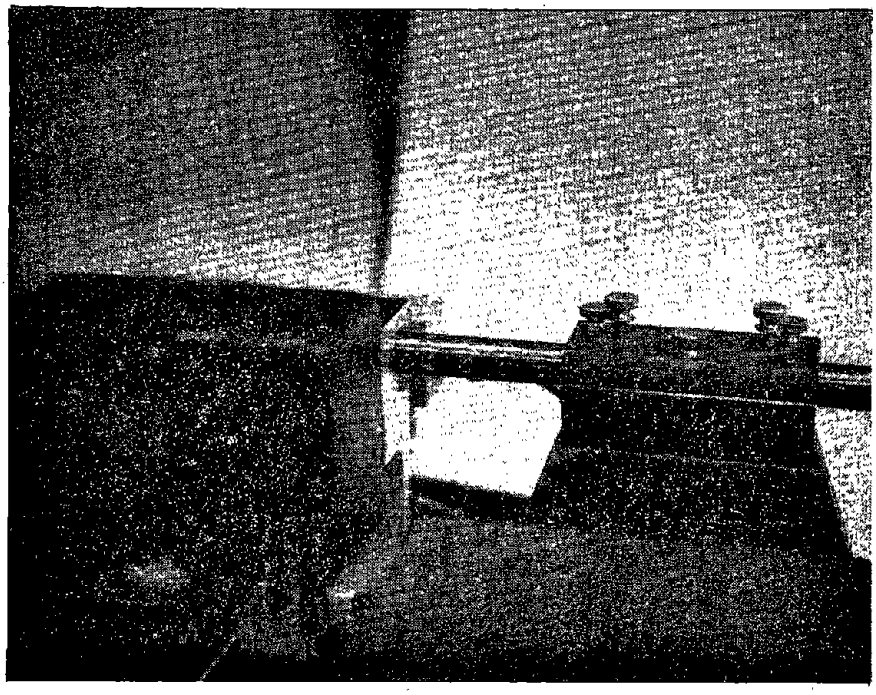

Figure 31. Vented region of barrel to reduce effects of muzzle blast upon missile flight.

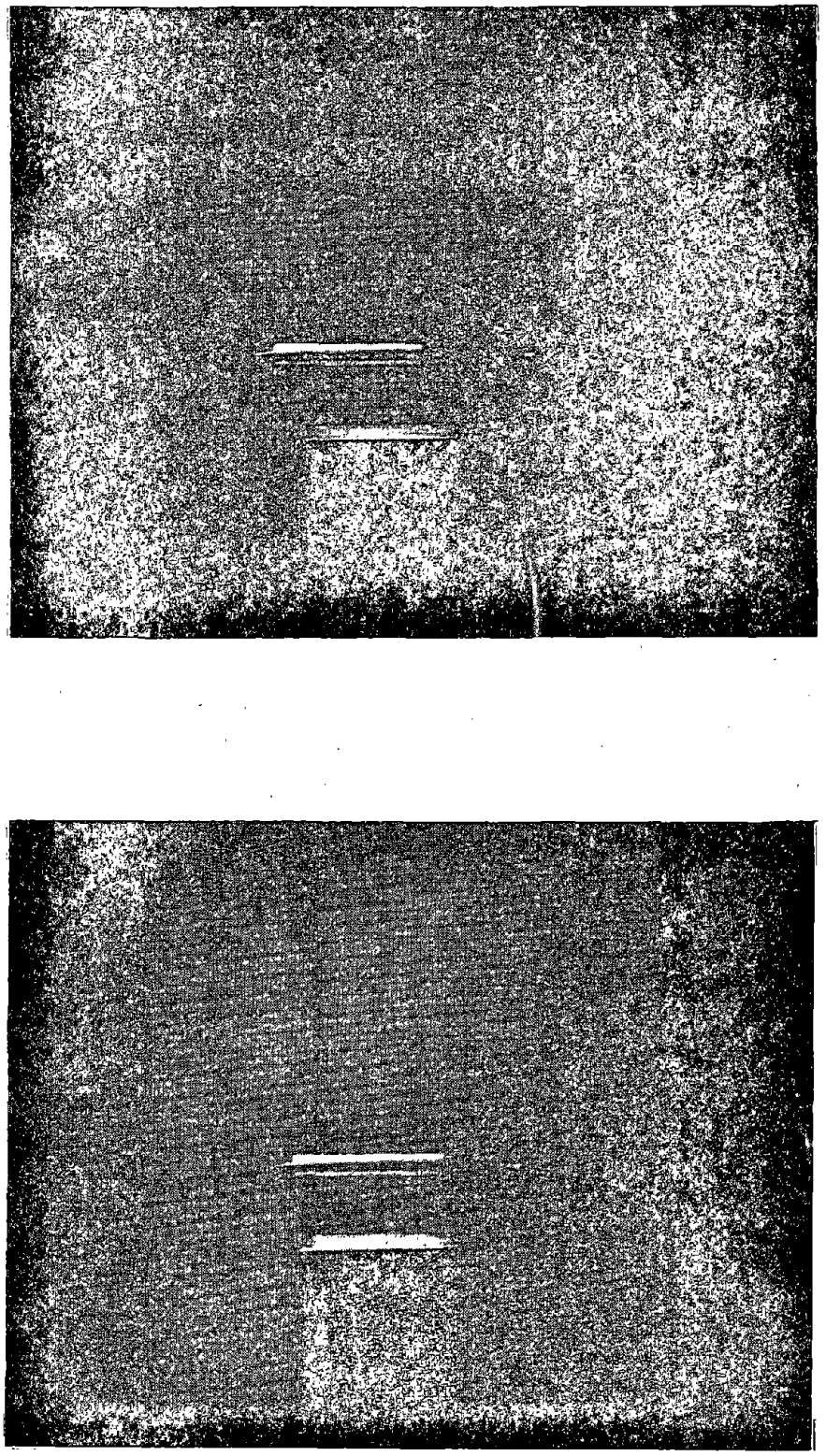

Figure 32. Photographs showing stability of missile with improved carrier design.

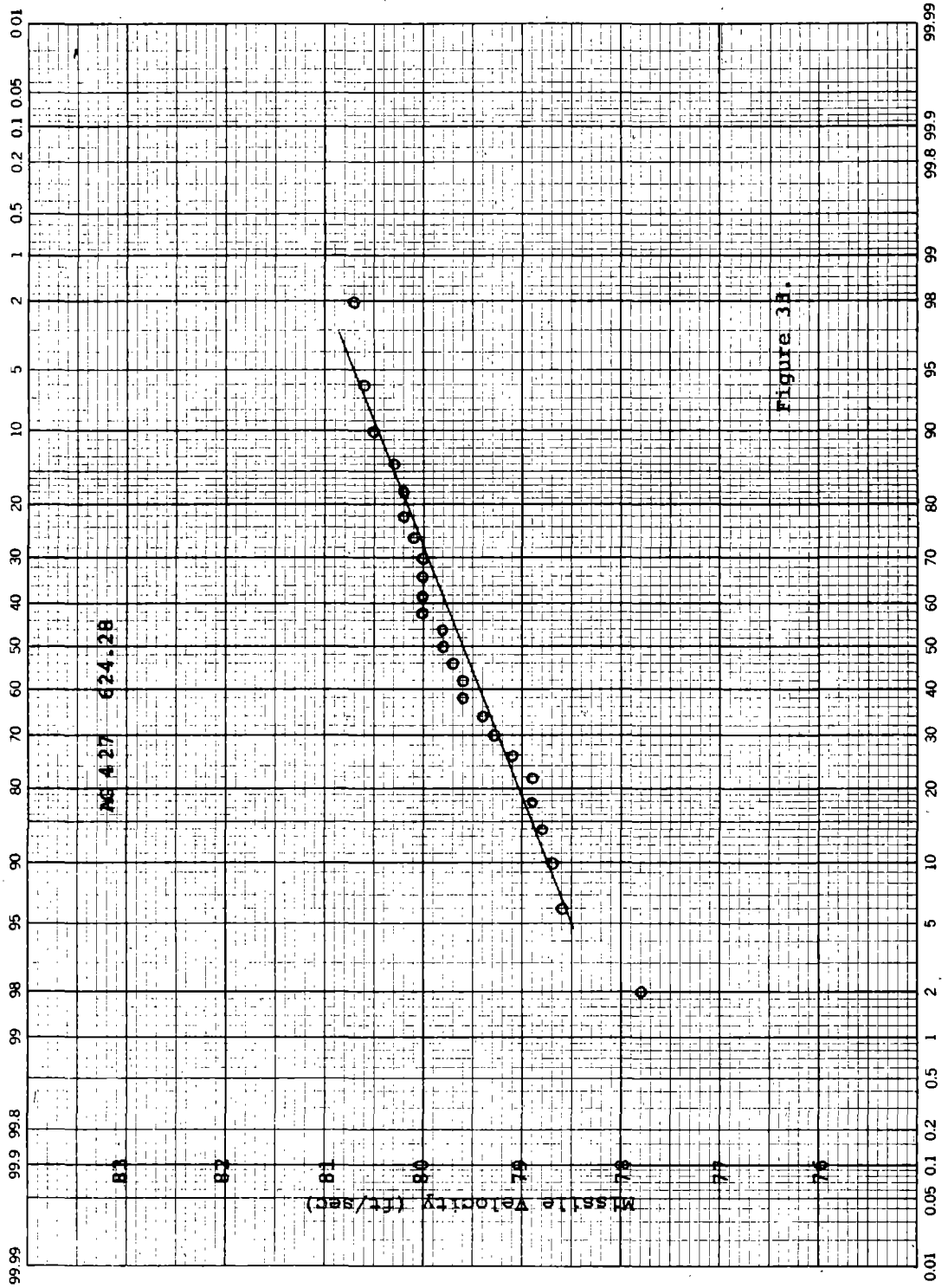

Figure 33. Typical probability paper plot of 25 data points in pressure-velocity calibration experiment

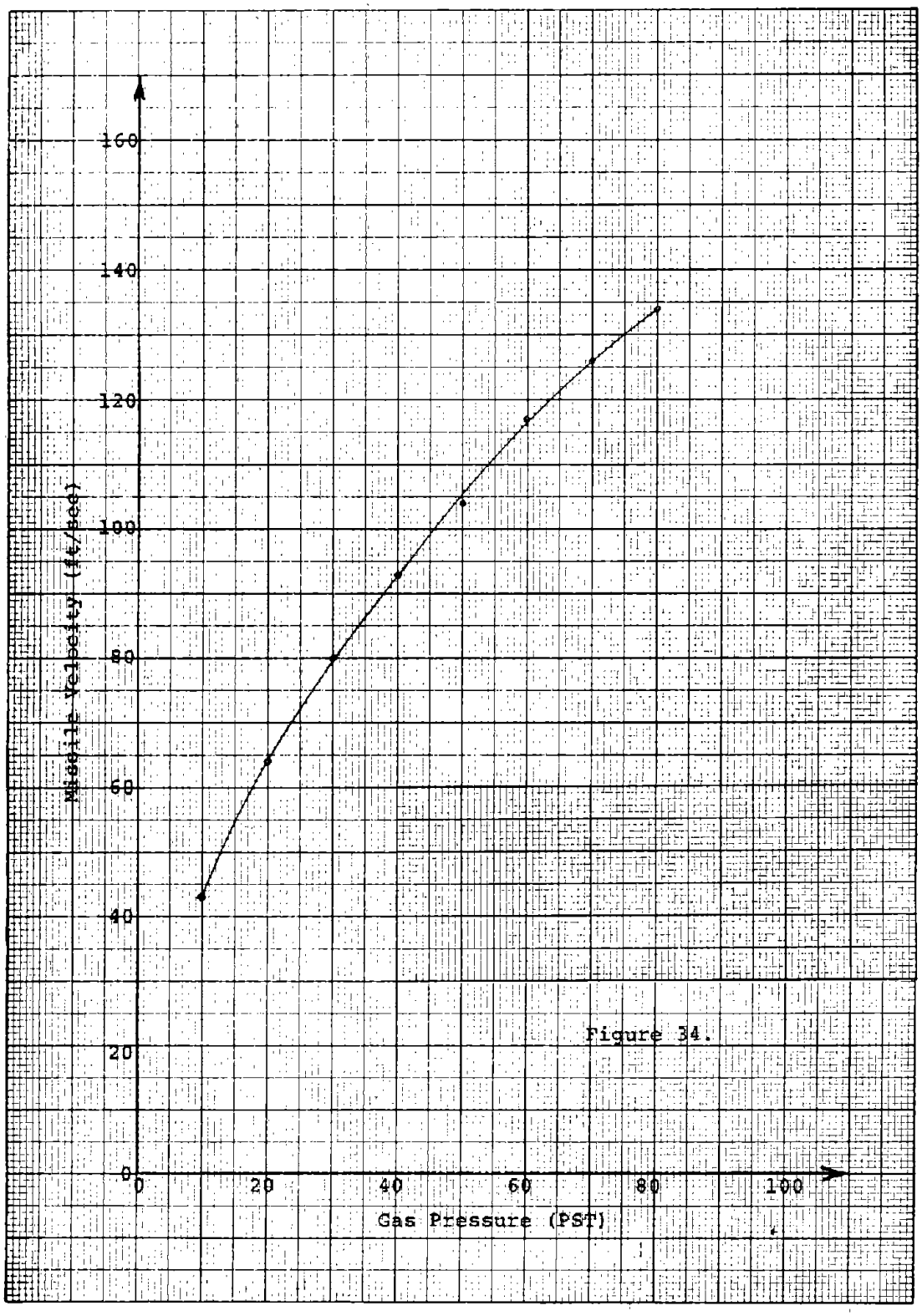

Figure 34.

Figure 34. Pressure-Velocity Calibration
Barrel: 220 VB2
Missile: 200/25/1.5B
Gas: Air

been tested. Figure 35 illustrates one step in the test in which a left eye was in the test position at an impact of sufficient velocity to cause fracture.

In any destructive type of test, such as the impact resistance test, the problem of damage to a specimen by impacts below failure impact level with consequent reduction of impact resistance is a real and constant one. One of the simpler procedures, but one which requires an increased number of specimens and some concept of the expected mean value is known as the Bruceton or staircase technique.

In the procedure the first specimen is hit with an impact presumed to be the mean impact resistance. If the specimen fractures then the second specimen is hit with an impact one increment lower than the first impact. If the first specimen does not fracture then the second is hit with the next higher incremental impact. This up or down increment of impact of the next specimen dependent upon survival or failure of the present specimen is continued until all specimens have been hit but once. The data may be analyzed mathematically by the procedure described in Appendix 1.

Figure 35. Glass safety lens in frame mounted upon anthropomorphic head.

Because of the difference in impact behavior of the three materials, two failure criteria were used. A lens was considered to have failed if either lens material was lost from the ocular surface or if the needle touched a piece of carbon paper taped to the eye surface of the anthropometric head.

The patch that can be observed covering the eyeball is a layer of carbon paper over white paper. Its function is to detect the impact of lens fragments or the needle itself upon the eyeball. Figure 36 is a 1.7X magnification of an AO SAP broken by the 7.06×10^{-3}lb. missile (No. 200/25/C) at 54 ft. sec. velocity (0.32 ft. lb. impact energy). The site of the impact is indicated by the arrow.

Brittle Plastic, CR-39 Resin, Safety Glasses

The greater strain limit and lower tensile strength of CR-39 plastic as compared to glass leads to a different type of failure mechanism. At equivalent impact velocity, 50-60 ft. sec.$^{-1}$, where glass displays quite complete brittle fracture (Figure 36), CR-39 does not behave completely as a brittle material. Figure 37 illustrates the effects of an impact at 58 ft. sec.$^{-1}$, (0.36 ft. lb. energy). Brittle fracture from the front surface at the site of the impact

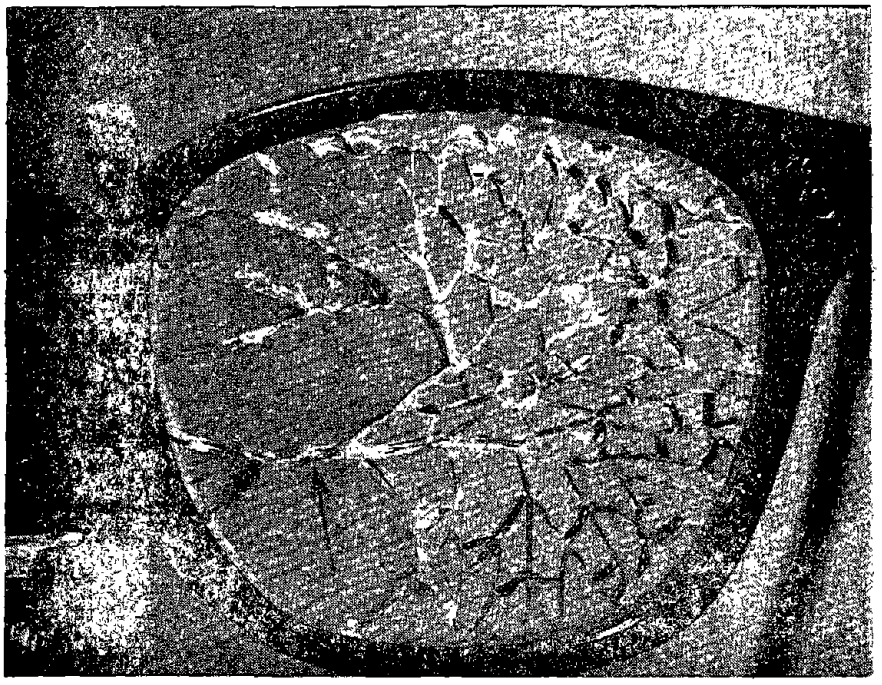

Figure 36. Glass safety lens fractured by 200/25/C needle missile at 54 ft/sec. (0.32 ft.lb. energy). Arrow indicates impact site.

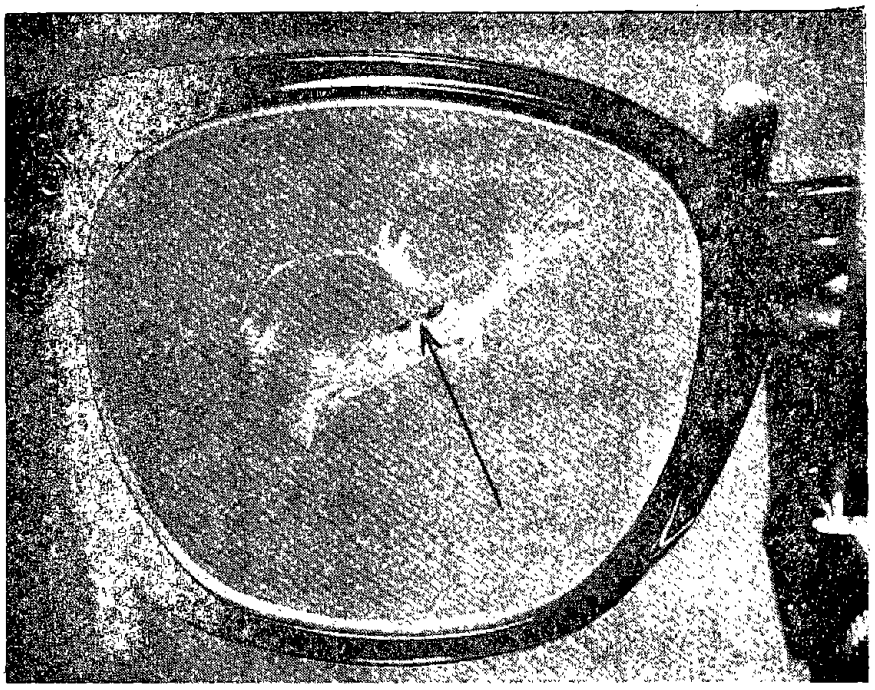

Figure 37. CR-39 plastic safety lens fractured by 200/25/C needle missile at 58 ft./sec. (0.36 ft.lb. energy). Arrow indicates impact site. A fragment was ejected from rear surface.

(arrow) occurred but at that velocity the missile had insufficient energy to dislodge the fragment completely.

Polycarbonate Plastic Lenses (Gentex)

Figure 38 shows a front view of a polycarbonate lens that received two impacts from the 200/25/C missile. Impact number 32, at right, at 191 ft./sec. caused a simple penetration of the needle into puncture but without retention of the needle. Impact number 33, at left, caused puncture and simple brittle fracture. Note that the needle is retained by the lens. Figure 39 is a rear view showing the degree of penetration, about 7 mm. This magnitude of penetration, coupled with the movement of lens and frame upon impact, is sufficient for the needle point to reach the eyeball.

Data Collected

The impact resistance data collected for the three kinds of industrial safety spectacles are given, as probability graphs in Figures 40, 41, and 42.

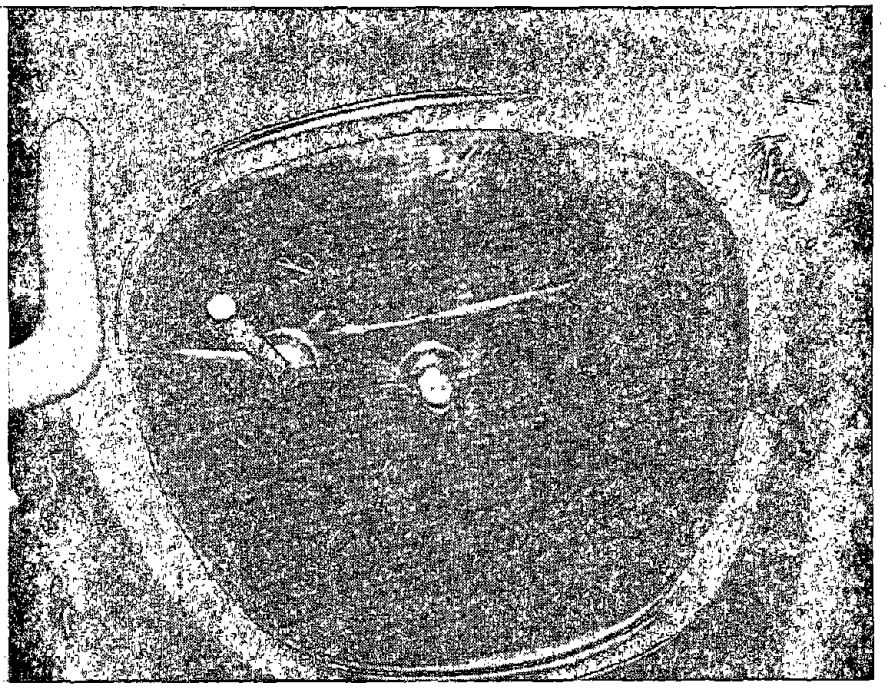

Figure 38. Coated polycarbonate (GENTEX) safety lens illustrating two types of impact behavior with needle missile. Impact No. 32 (191 ft./sec.) at right produced simple puncture without retention of needle. Impact No. 33 (193 ft/sec) produced puncture and brittle cracking.

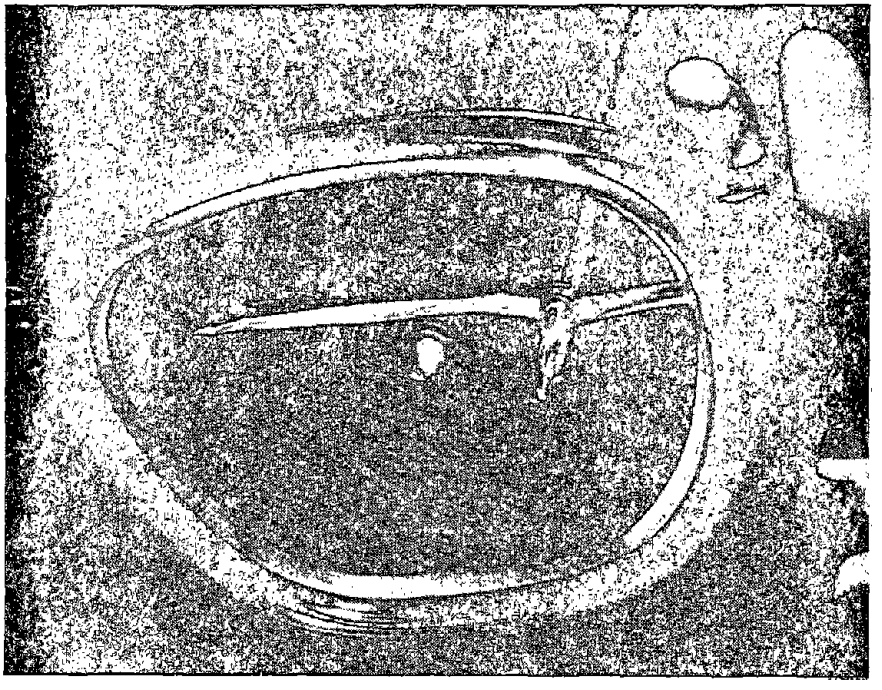

Figure 39. Rear view of the same lens as in Figure 8 showing 7 mm penetration of the needle.

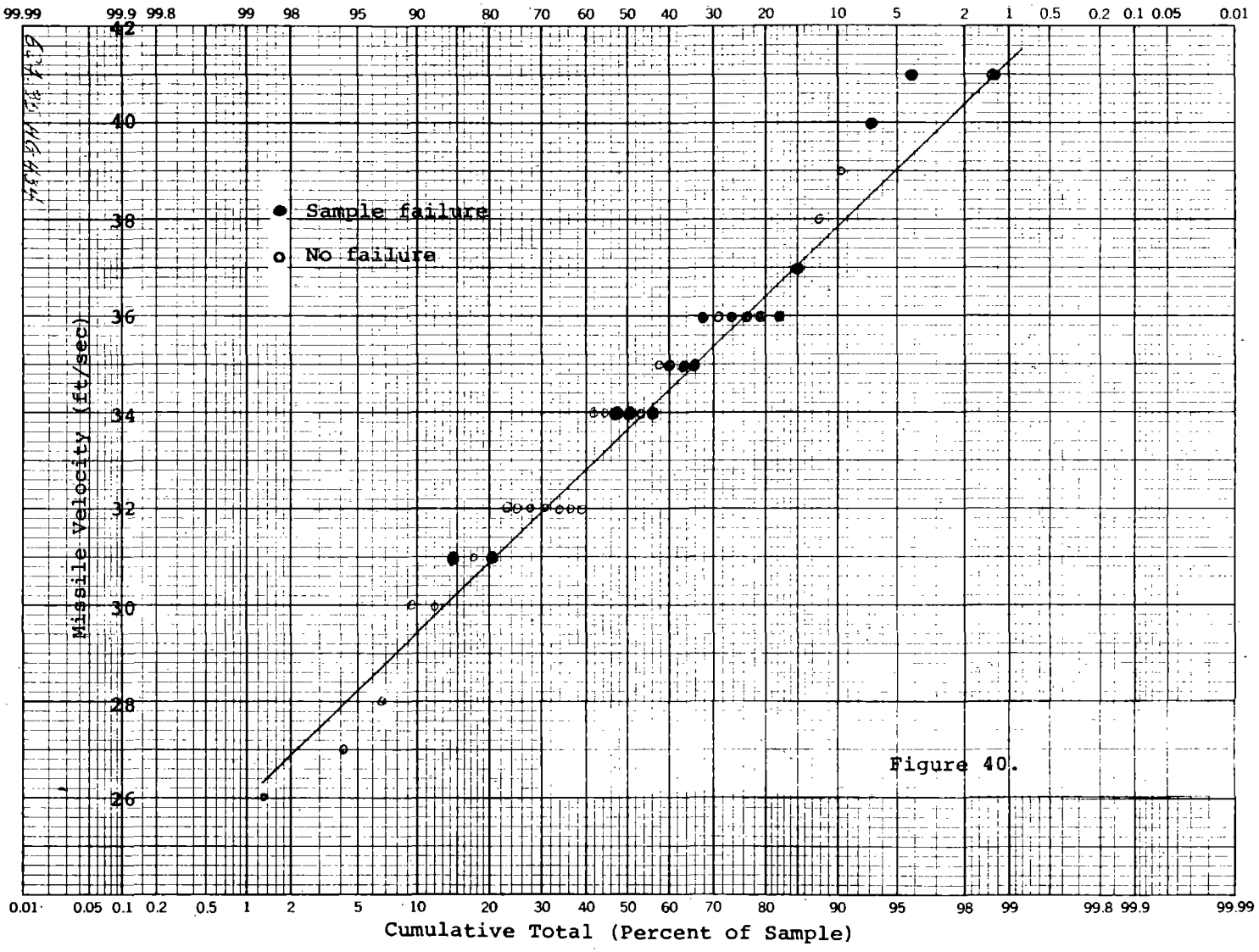

Figure 40.

Figure 40. Impact test data points for industrial safety spectacles with air tempered glass lenses.

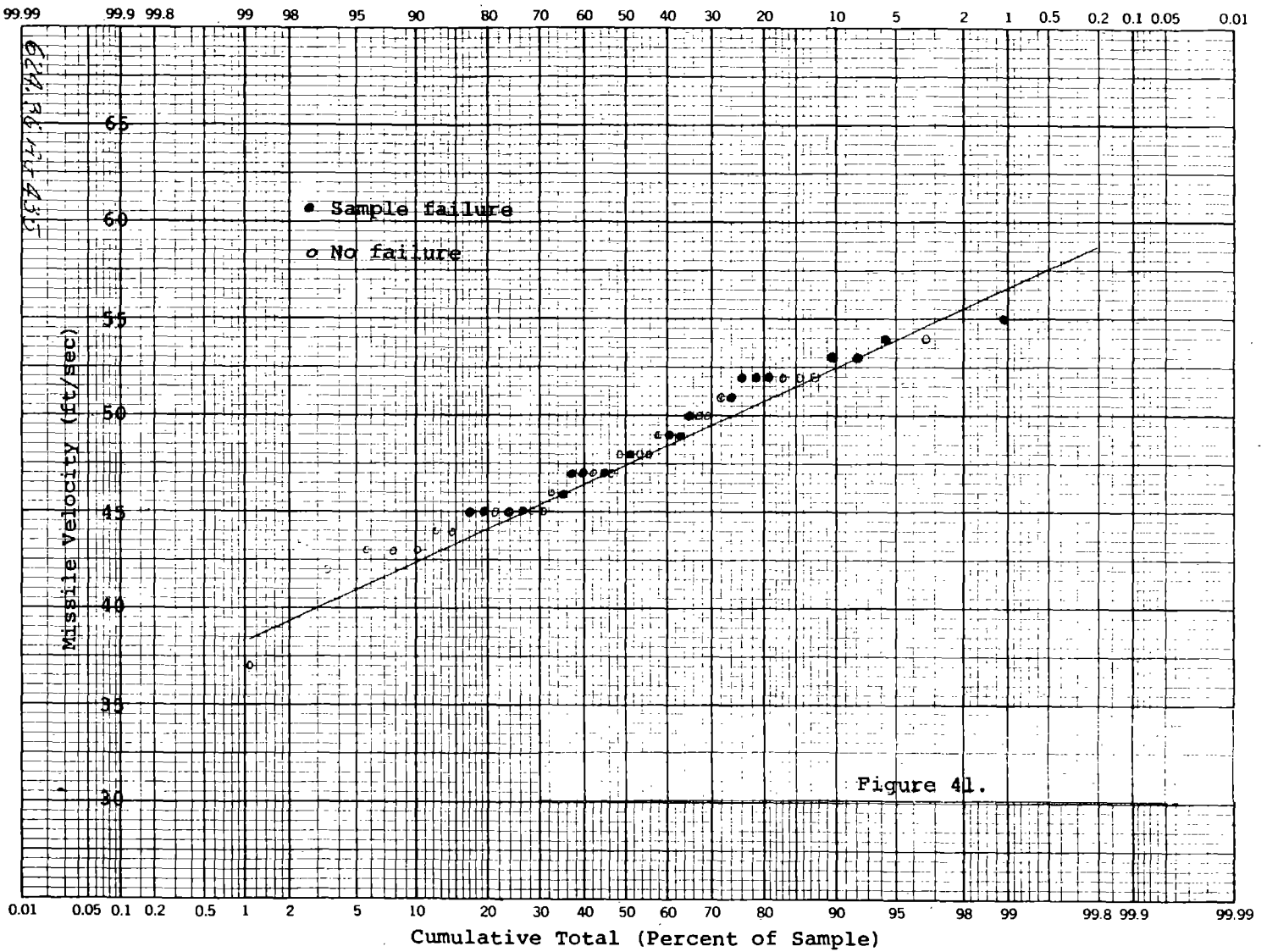

Figure 41.

Figure 41. Impact test data points for industrial safety spectacles with CR-39 plastic lenses.

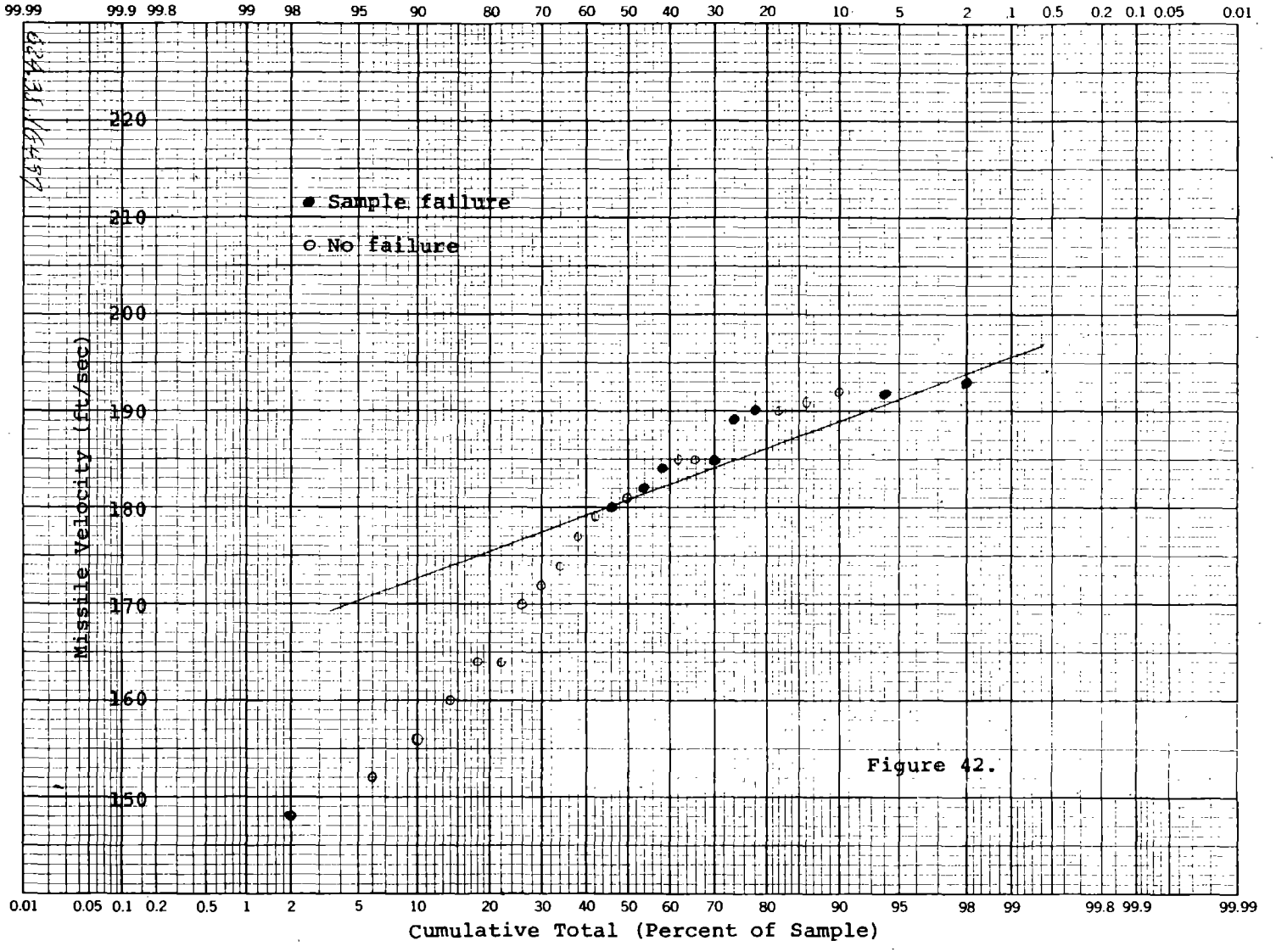

Figure 42.

Figure 42. Impact test data points for industrial safety spectacles with coated polycarbonate (Gentex) lenses.

A comparison of the impact resistance appraisal by the 200/25/C missile with values obtained by two other types of tests is given in Table 17 on the next page.

Some interesting facts are shown by the data in Table 17. To give perspective, it should be noted that the impact velocity of the Z87.1 1-inch ball dropped 50 inches is 16.4 ft./sec. All glass and CR-39 lenses were picked at random from AO regular production - no special selection was made. The coated polycarbonate lenses were purchased on the open market from Gentex, the only manufacturer known to us.

Data for the needle plus carrier show the CR-39 lenses to be more impact-resistant than glass lenses and the Gentex lenses to be far stronger than either. These results were obtained on lenses in AO safety spectacle frames mounted on the headform.

The data for breakage using the Z87.1 drop-ball and the .22 cal. air gun are the same as those shown in Figures 17 and 18; the results are tabulated here all in terms of velocity for convenience. The Gentex lenses were enormously stronger than glass or CR-39 for the 1" ball, but not as strong as the CR-39 lenses, and not greatly stronger than glass, when impacted with the .22 cal. (0.218 inch) steel ball.

This surprising susceptibility of polycarbonate to the .22 cal ball is, we believe, brought about by the abrasion-resistant coating used on the lenses as was mentioned previously. From further work done at AO on other programs, it appears that the impact strength, coating thickness, and abrasion resistance of Gentex lenses have varied considerably over the time the product has been on the market and we venture the following observations:

1. A hard (hence abrasion resistant and brittle) thick coating well-bonded to the polycarbonate appears to degrade impact resistance considerably as compared to uncoated material.

2. Conversely, a comparatively soft (and hence less abrasion resistant and less brittle) coating, or one which delaminates easily under impact conditions, tends to degrade impact resistance less, particularly when thin.

Tests on other proprietary coatings which various firms have offered to AO for use on other substrate plastics qualitatively support the observations above. Since any worthwhile coating must be relatively hard and thick to be abrasion resistant under realistic use conditions, and must not delaminate in use,

TABLE 17. IMPACT RESISTANCE OF INDUSTRIAL SAFETY SPECTACLE LENSES

Material	Tempered Glass	CR-39	Coated Polycarbonate
Needle & Carrier			
v(50)	33.7 ft/sec.	47.3	183
v(16)	30.4	43.4	174
s	3.3	3.9	9
s/v(50)	9.8%	8.2%	4.9%
Z87 1-inch ball			
v(50)	29.8 ft/sec.	23.4	See
v(16)	27.0	21.0	Note
s	2.8	2.4	Below
s/v(50)	9.4%	10.3%	
0.218-inch ball			
v(50)	83.5 ft/sec.	174	123
v(16)	70.0	151	95
s	13.5	23	28
s/v(50)	16.2%	13.2%	23%

NOTE: The coated polycarbonate did not fail at 62 ft/sec., the limit of the test.

v(50) is the velocity at which half the sample failed.
v(16) is the velocity at which 16% of the sample failed.
s is standard deviation, and
s/v(50) is coefficient of variance.

it appears that any worthwhile coating will inevitably degrade polycarbonate's impact resistance somewhat, so one must be careful in making inferences about coated products from data on uncoated samples. Nevertheless, as Table 17 shows, coated polycarbonate lenses offer dramatic improvement over glass lenses in impact resistance for a variety of missiles. Furthermore, glass lenses are the item with which to compare, since CR-39 lenses are rarely used in industry because of their lack of abrasion resistance.

SUBTASKS 3-6: IMPACT TESTING OF OTHER DEVICES

On succeeding pages is presented a photograph of each type of device tested, followed by its generic name as given in Z87.1 and the particular model number and name of the AO product tested as representative of that type of device. The lenses, plates, or windows used in the device are listed with pertinent information. Following this, the mean value of velocity v(50), standard deviation s, and coefficient of variance s/v(50) for the failure distribution are given in a table. Statistical parameters were determined using the calculation methods of Appendix 1. Probability-paper graphs of the failure distributions are also given showing all data points.

The failure criterion consisted of brittle fracture with ejected pieces of the impacted element unless otherwise noted. No attempt was made to test all possible combinations of lenses, plates, and windows with goggles, headgears, and helmets because of the enormous scope of such a project and because we were trying to find large effects in order to assess the value of the high-speed test. AO products were used because they represent the types shown in Fig. 8 of Z87.1, were readily available, and could be obtained at cost so as to conserve project funding.

Figures 43-54 and Tables 18-21 present results for various types of "flexible-mask" or "flexible-fitting" goggles (Subtask 3). Figures 55-69 and Tables 22-26 are for different types of cup goggles (Subtask 4). Figures 70 and 71 and Table 27 are for a typical welding helmet (Subtask 5), while Figures 72-77 and Table 28 are for faceshields (Subtask 6).

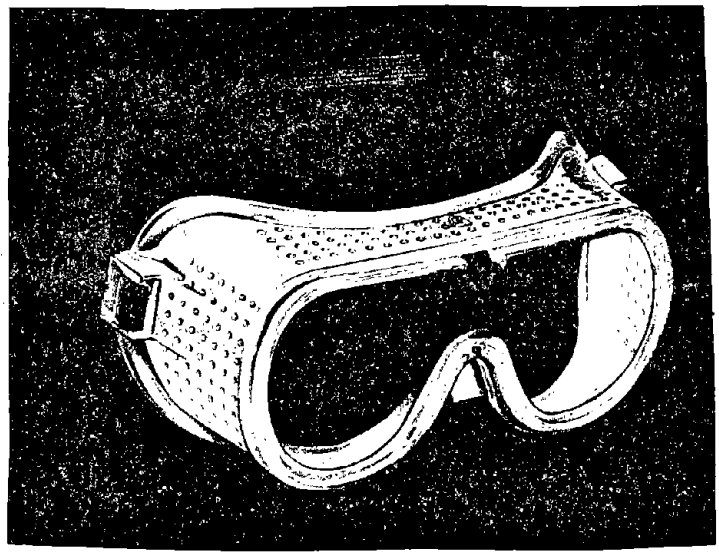

Figure 43

Goggles, Flexible Fitting, Regular Ventilation
(Type 1 in ANSI Z87.1 Fig. 8)
AO 482B Impact Goggle

Tested with #209C clear 0.050 in. thick polycarbonate lens

#209CAF clear 0.050 in. thick polycarbonate lens with anti-fog coating

TABLE 18. FAILURE* VELOCITIES WITH WEIGHTED NEEDLE

	v(50)	s	s/v(50)
482B with 209C lens	186 ft/sec.	4 ft/sec.	2%
with 209CAF lens	190	8	4

* Because of flexibility of the lens and mask, failure on impact was defined as penetration of the lens until the needle point made contact with the "eyeball" of the anthropometric head during the impact event.

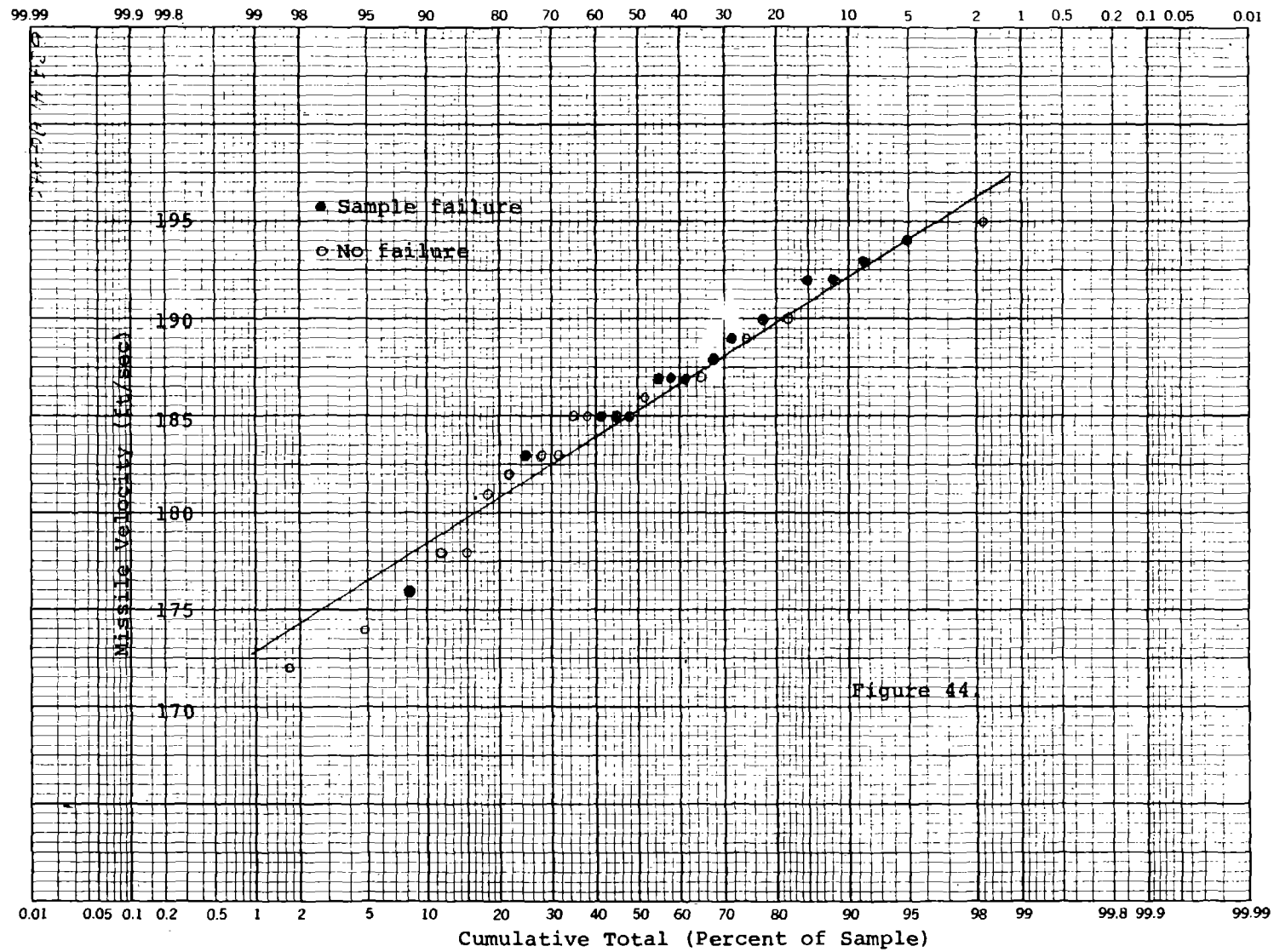

Figure 44. Impact test data points for AO 482B impact goggle (See Fig. 43) with uncoated polycarbonate lens.

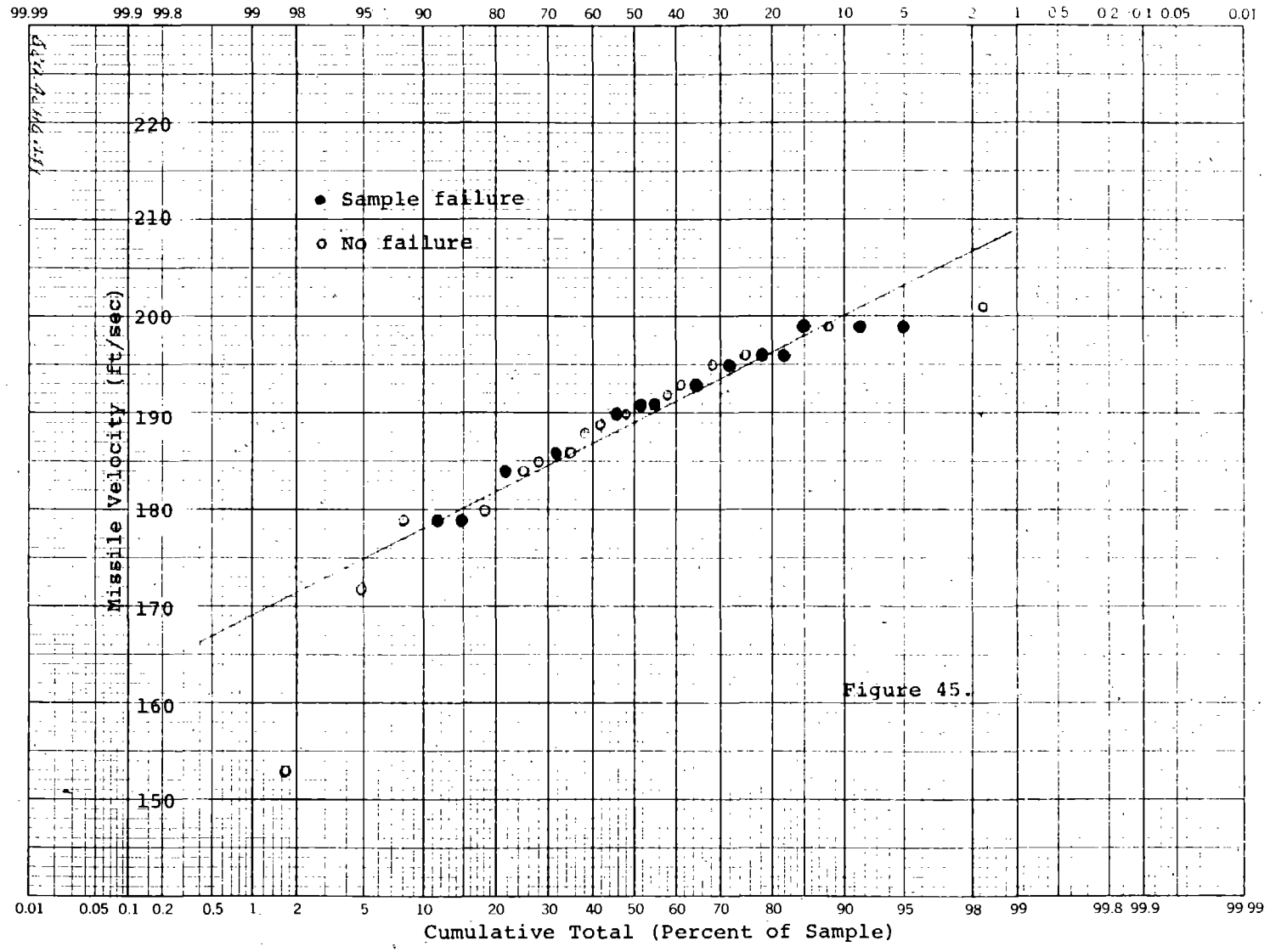

Figure 45.

Figure 45. Impact test data points for AO 482B impact goggle (See Fig. 43) with anti-fog coated polycarbonate lens.

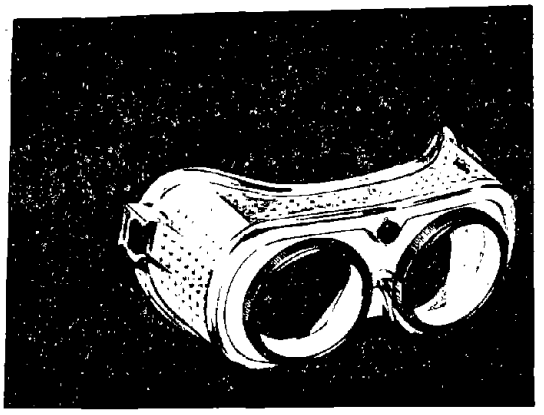

Figure 46

Goggles, Flexible Fitting, Regular Ventilation
(Not specifically shown in Fig. 8 of ANSI Z87.1)
AO 489B Impact Goggle

Tested with #50 clear 50mm round flat impact-resistant glass lenses

#112 shade 1.7 green 50mm round impact-resistant green glass lenses

TABLE 19. FAILURE VELOCITIES WITH WEIGHTED NEEDLE

	v(50)	s	s/v(50)
489B with #50 lens	42 ft/sec.	4 ft/sec.	10%
with #112 lens	55	5	9

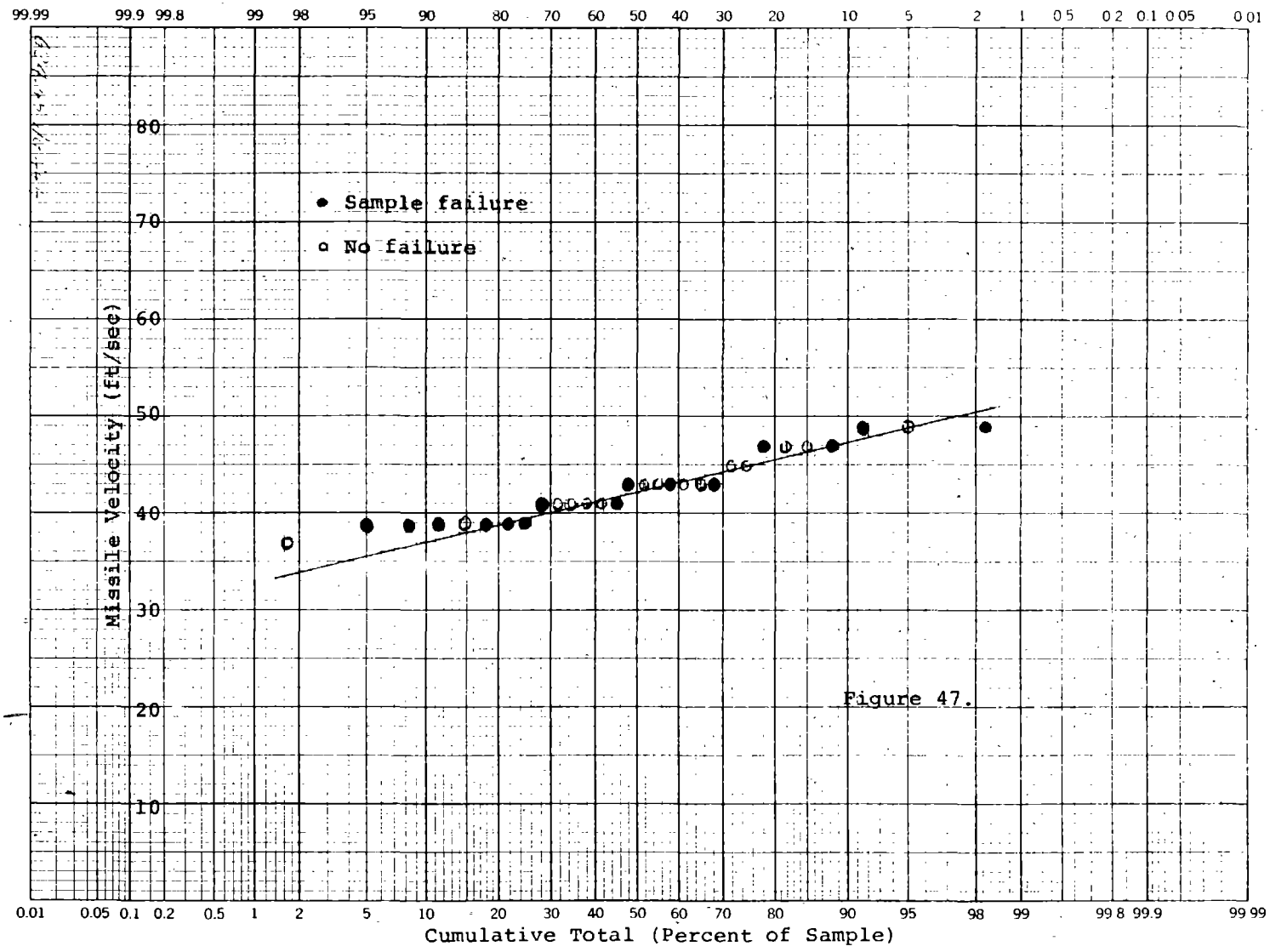

Figure 47. Impact test data points for AO 489B impact goggle with #50 clear glass lenses (See Fig. 46).

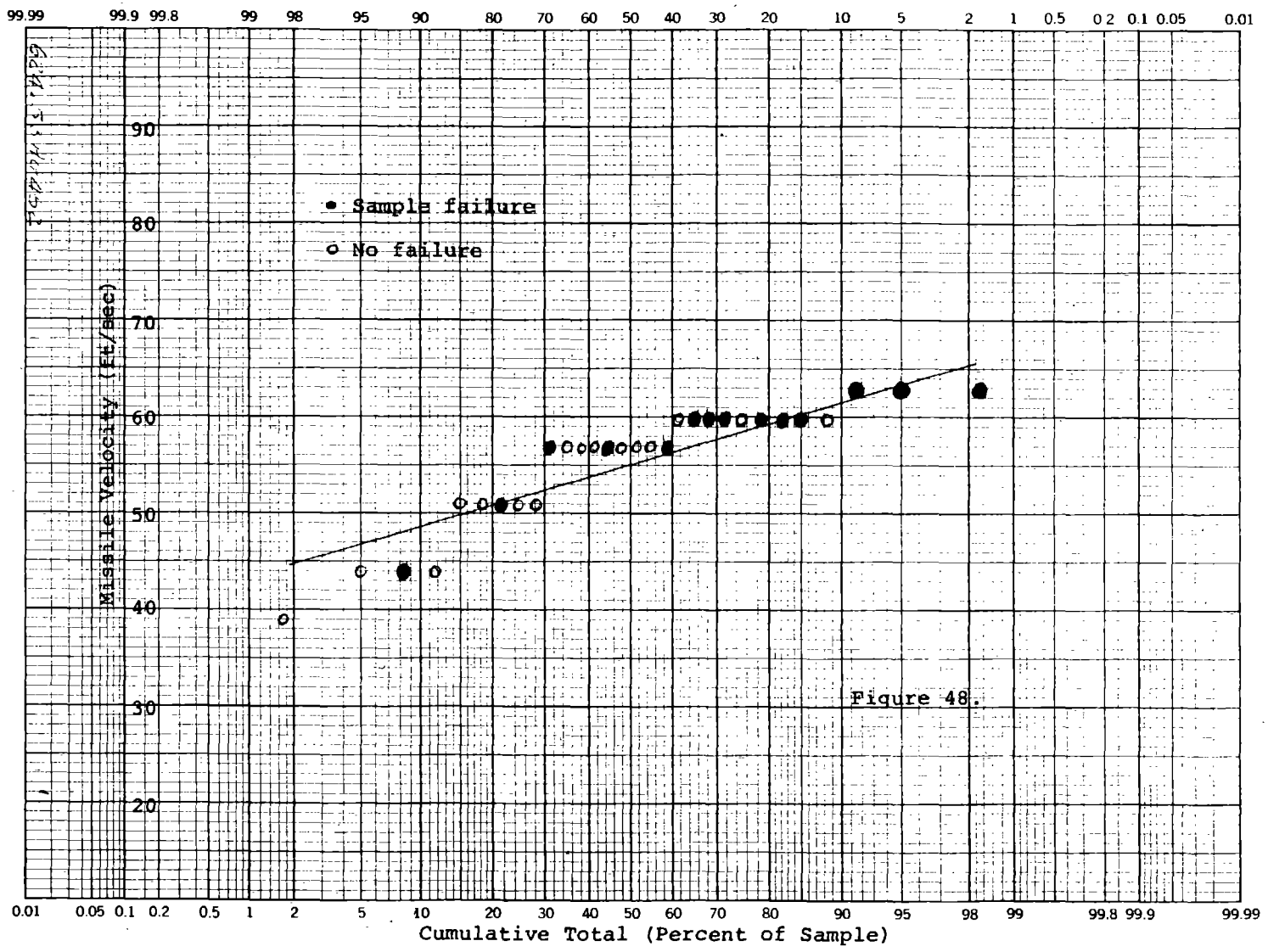

Figure 48. Impact test data points for AO 489B impact goggle with #112 green glass lenses (See Fig. 46).

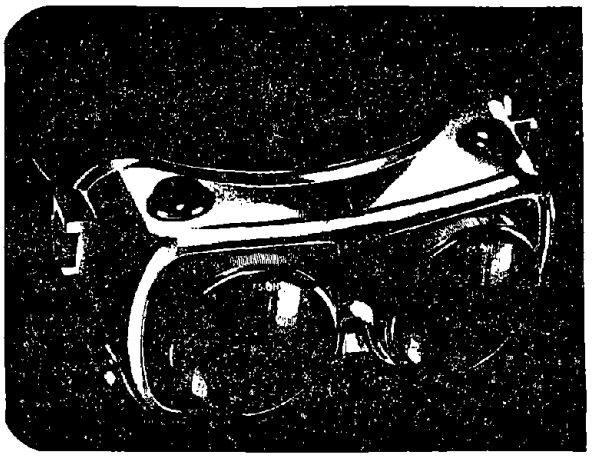

Figure 49

Welding Goggles, Coverspec Type, Tinted Lenses
(A flexible-fitting variant of Type 8 of Fig. 8
of ANSI Z87.1)
AO 486B Welding Goggle

Tested with #75 shade 5 green 50mm round impact-resistant glass lens with #54 clear glass cover lens

Same #75 lens and #185 0.050 in. thick acetate cover lens

Same #75 lens and #189 0.050 in. thick CR-39 cover lens

TABLE 20. FAILURE VELOCITIES WITH WEIGHTED NEEDLE

	v(50)	s	s/v(50)
486B with #75 & #54	41 ft/sec.	7 ft/sec.	17%
with #75 & #185	130	22	17
with #75 & #189	201	19	10

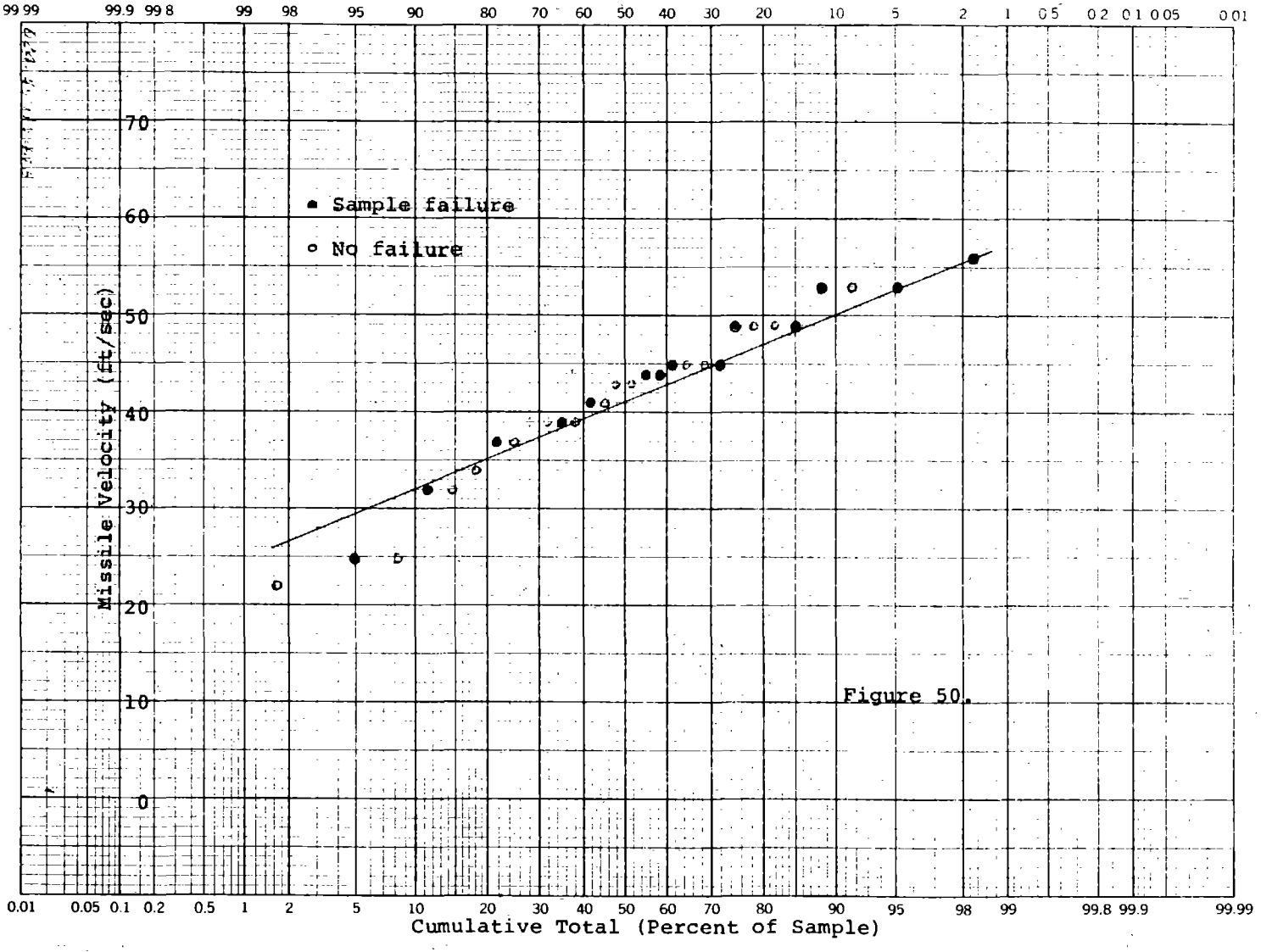

Figure 50. Impact test data points for AO 486B welding goggle with glass lenses and glass cover lenses (See Fig. 49).

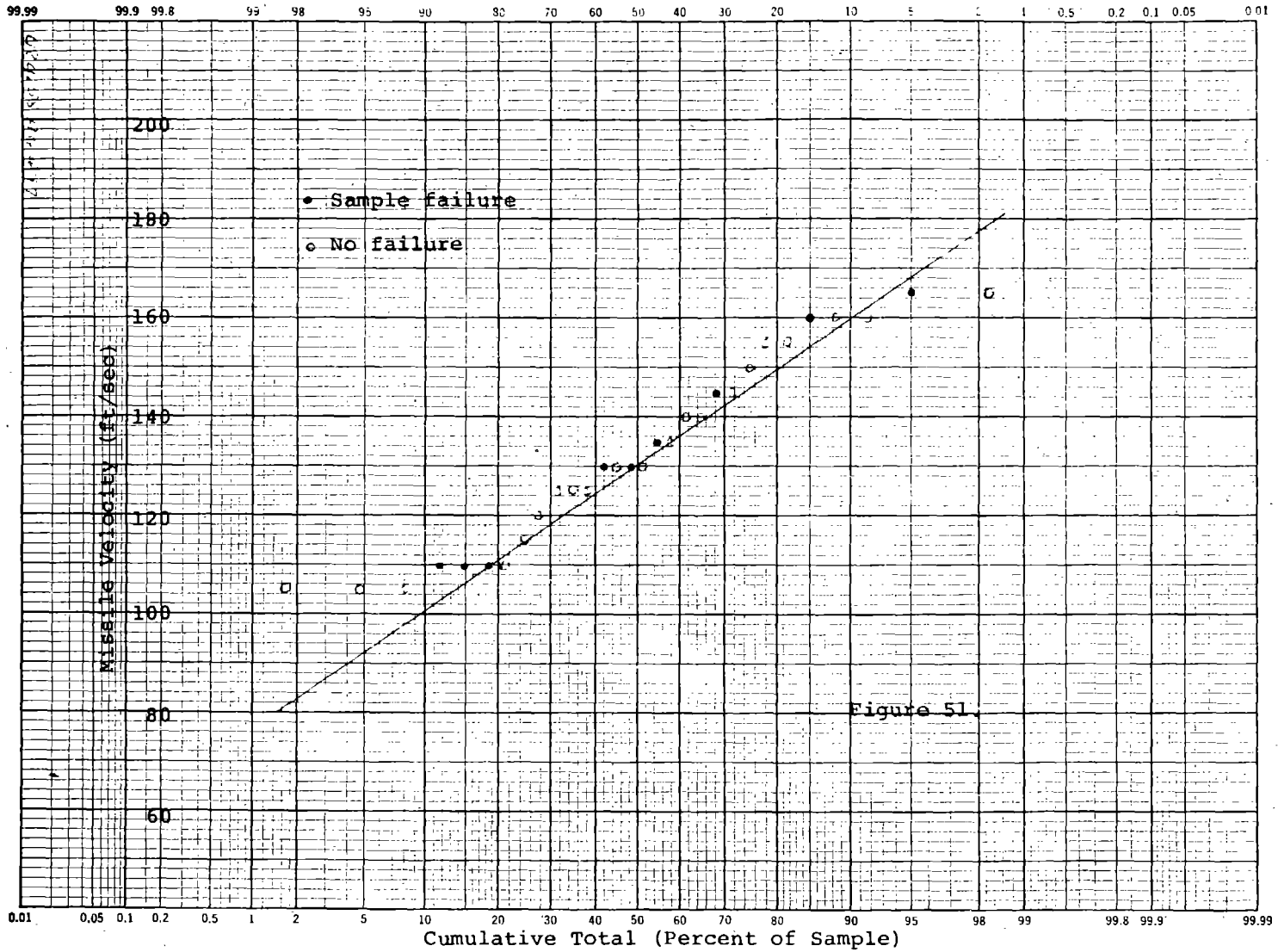

Figure 51.

Figure 51. Impact test data points for AO 486B welding goggle with glass lenses and acetate cover lenses (See Fig. 49).

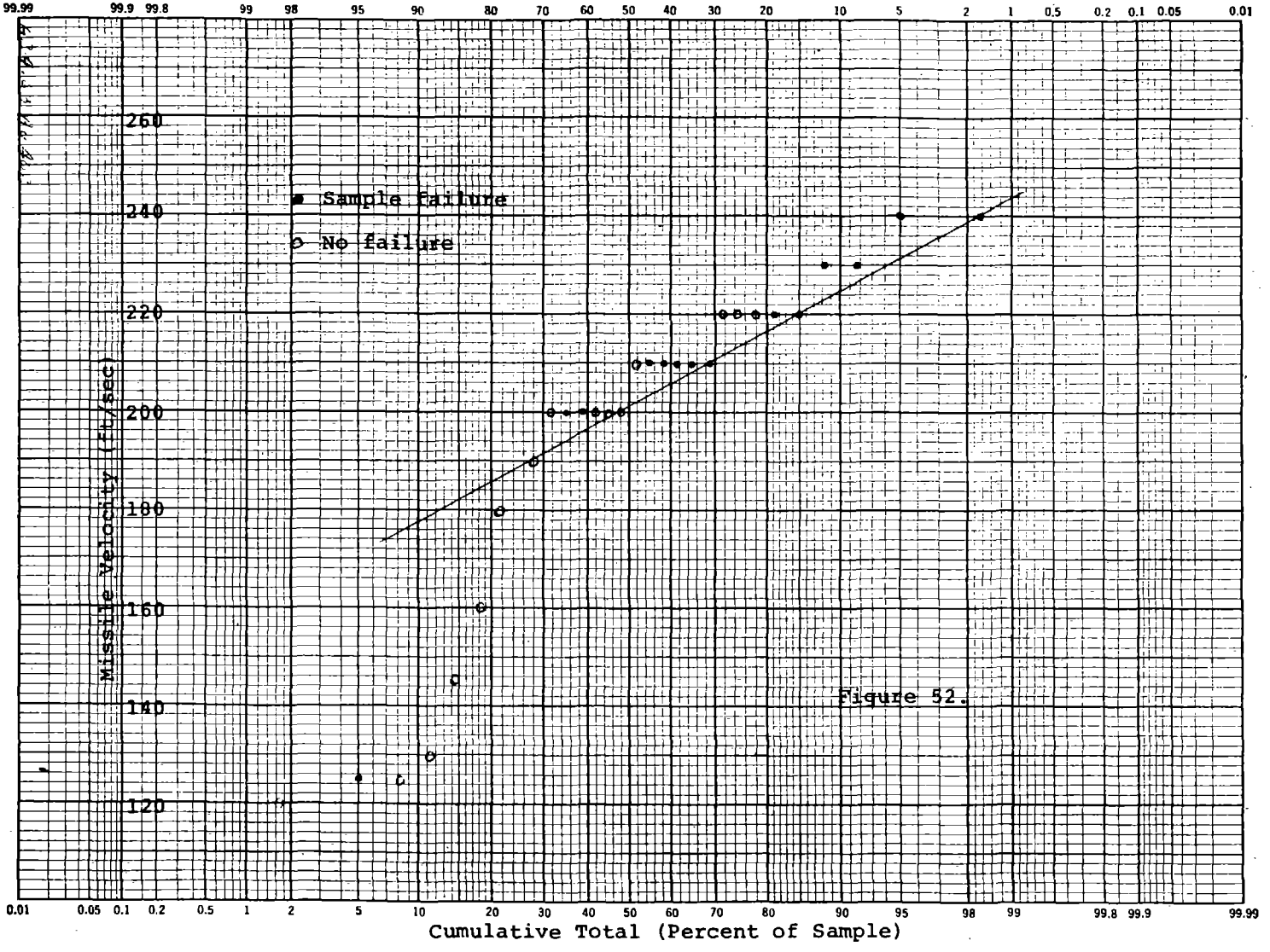

Figure 52. Impact test data points for AO 486B welding goggle with glass lenses and CR-39 cover lenses (See Fig. 49).

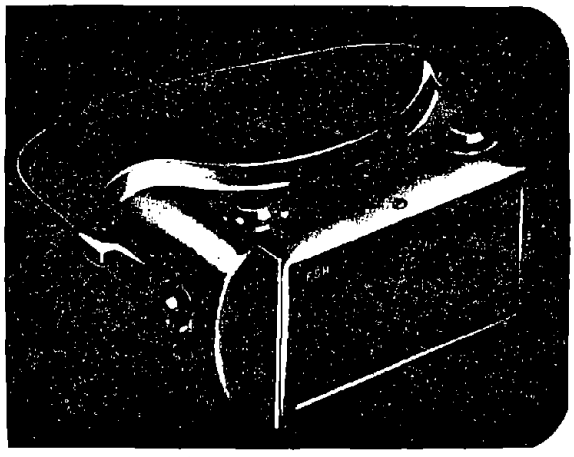

Figure 53

Welding Goggles, Coverspec Type, Tinted Plate Lens
(A flexible mask variant of Type 9 of Fig. 8
of ANSI Z87.1)
AO 488 Wide Vision Welding Goggle

Tested with #80 shade 5 green 2" x 4¼" impact-resistant glass welding plate and #168 clear CR-39 cover plate

TABLE 21. FAILURE VELOCITIES WITH WEIGHTED NEEDLE

	v(50)	s	s/v(50)
488 with #80 & #168 plates	75	8	11

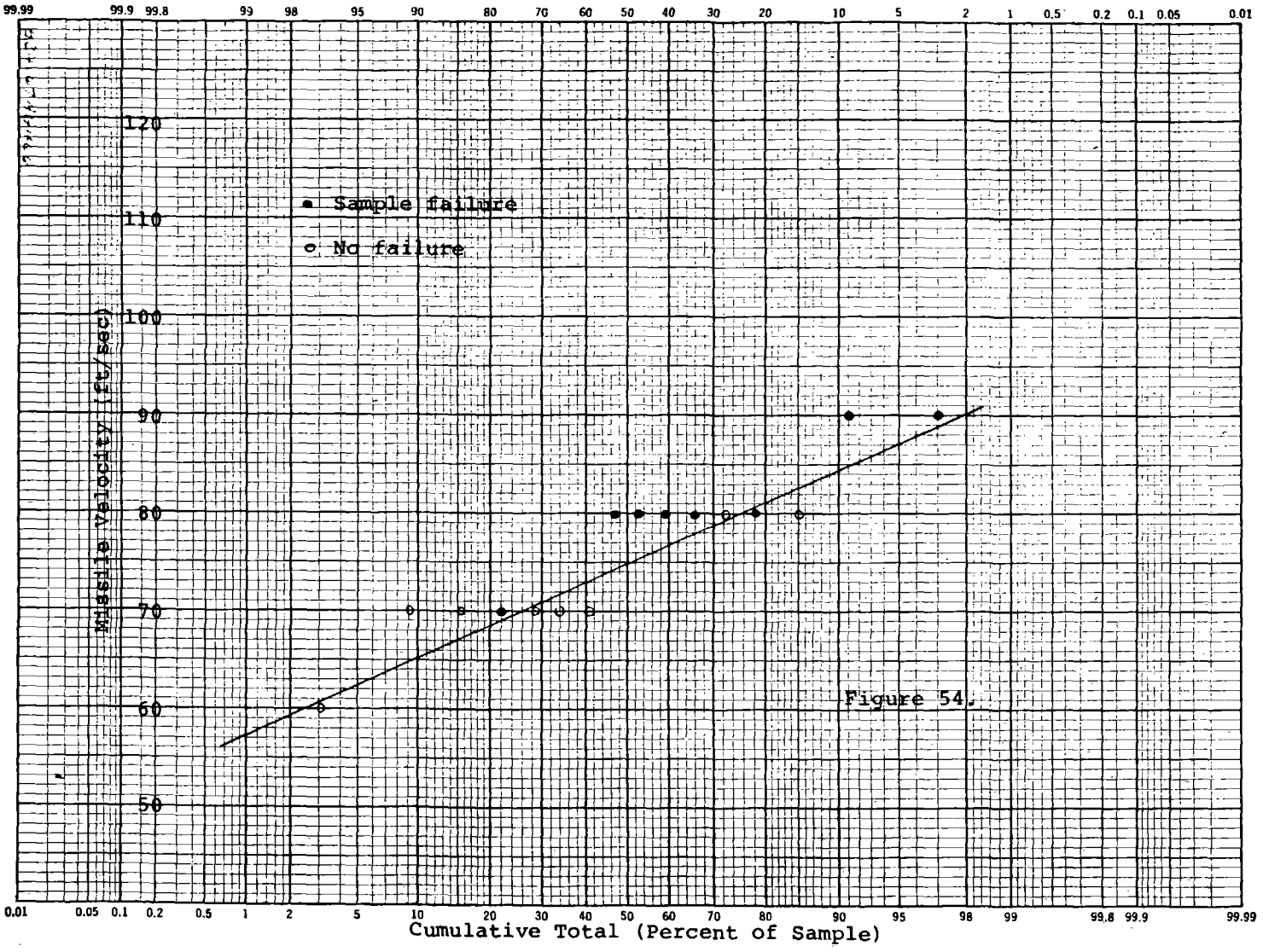

Figure 54.

Figure 54. Impact test data points for AO 488 welding goggle with glass plate and CR-39 cover plate (See Fig. 53).

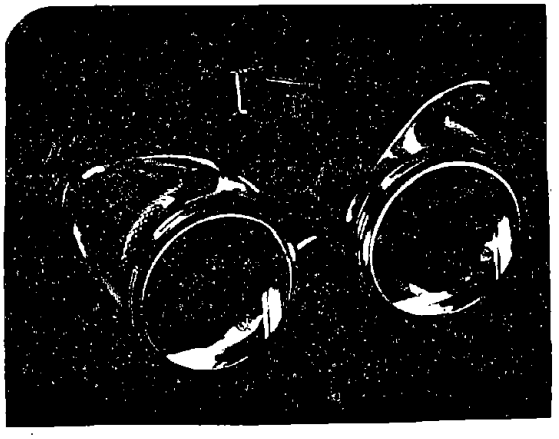

Figure 55

Chipping Goggles, Eyecup Type, Clear Safety Lenses
(Similar to Type 7 of Fig. 8 of ANSI Z87.1)
AO 301A DURALITE® Goggle

Tested with #50 clear 50mm round flat impact-resistant glass lenses

#112 shade 1.7 green 50mm round impact-resistant glass lenses

TABLE 22. FAILURE VELOCITIES WITH WEIGHTED NEEDLE

	v(50)	s	s/v(50)
301A with #50 lens	42 ft/sec.	4 ft/sec.	10 %
with #112 lens	54	9	17

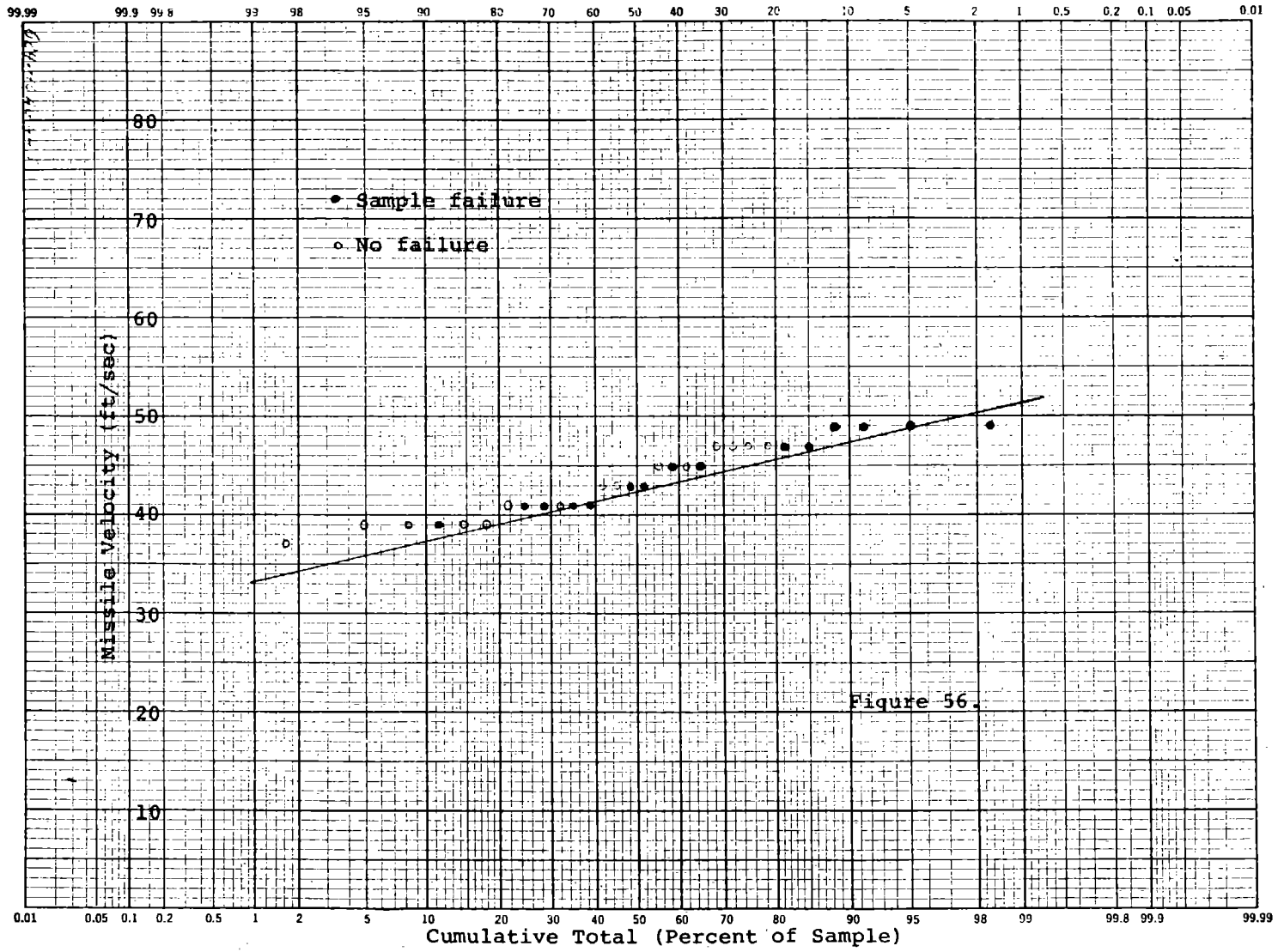

Figure 56. Impact test data points for AO 301A cup goggle with clear glass lenses (See Fig. 55).

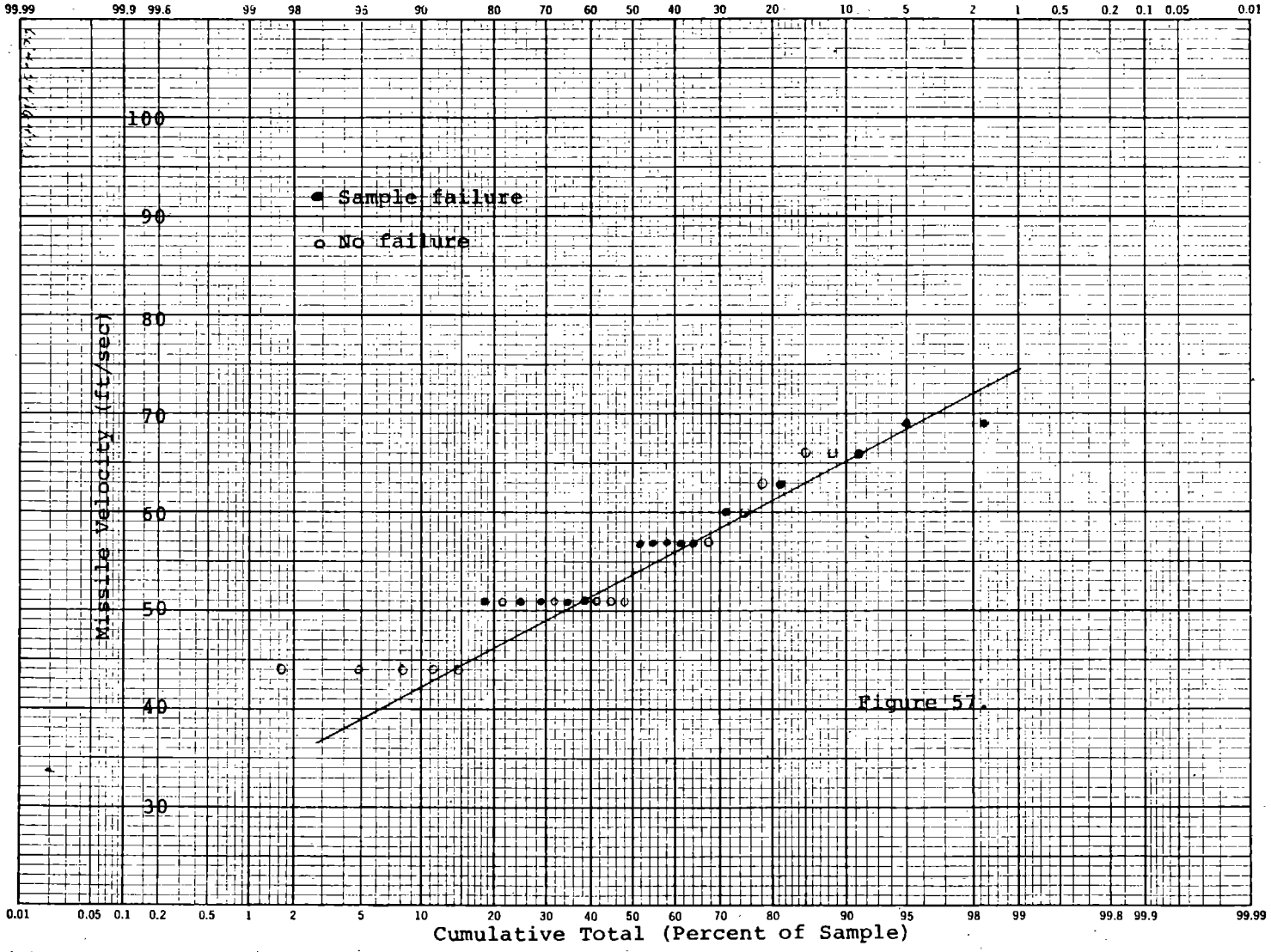

Figure 57. Impact test data points for AO 301A cup goggle with green glass lenses (See Fig. 55).

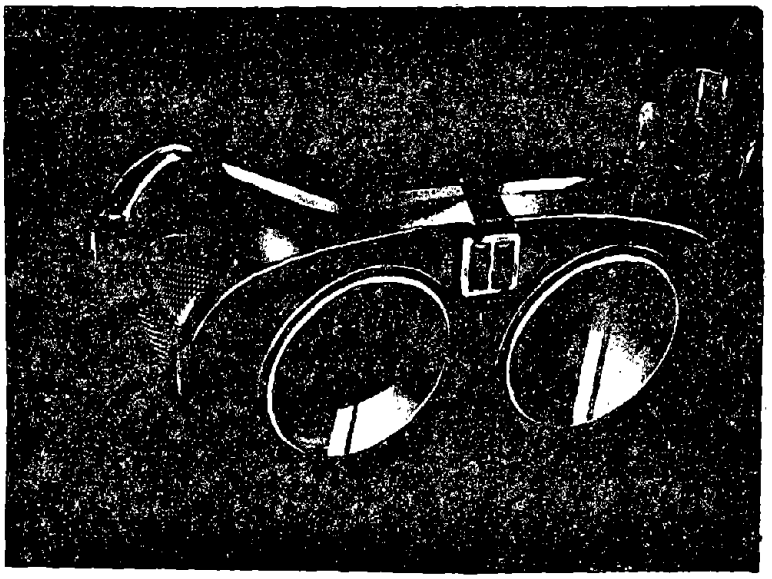

Figure 58

Chipping Goggles, Coverspec Type, Clear Safety Lenses
(A variant of Type 8A of Fig. 8 of ANSI Z87.1
having a rigid bar bridge)
AO 325CB Coverglass Goggle

Tested with #50 clear 50mm round flat impact-resistant glass lenses

#112 shade 1.7 green 50mm round impact-resistant glass lenses

TABLE 23. FAILURE VELOCITIES WITH WEIGHTED NEEDLE

	v(50)	s	s/v(50)
325CB with #50 lens	63 ft/sec.	3 ft/sec.	5 %
with #112 lens	60	9	15

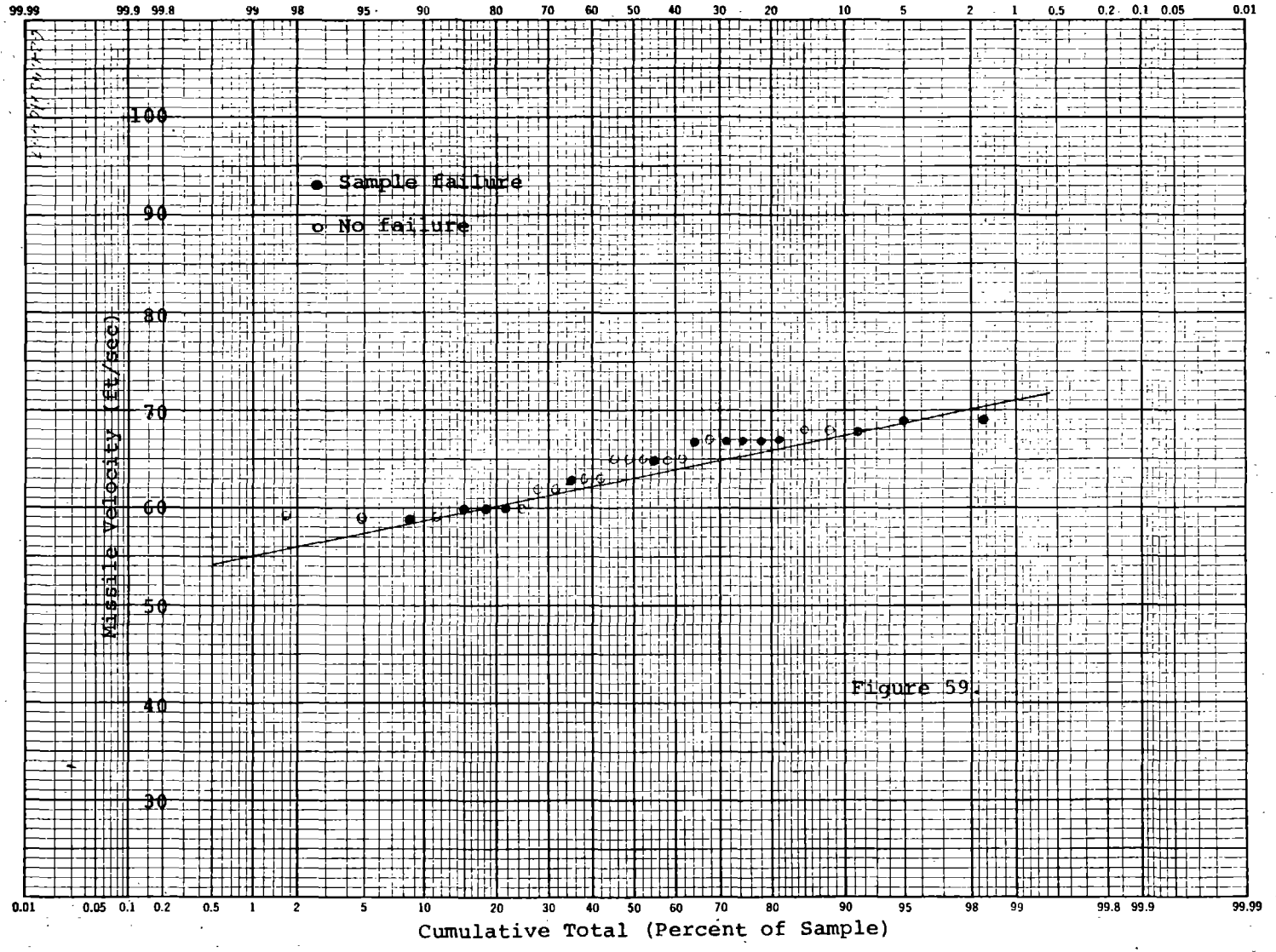

Figure 59. Impact test data points for AO 325CB coverglass goggle with clear glass lenses (See Fig. 58).

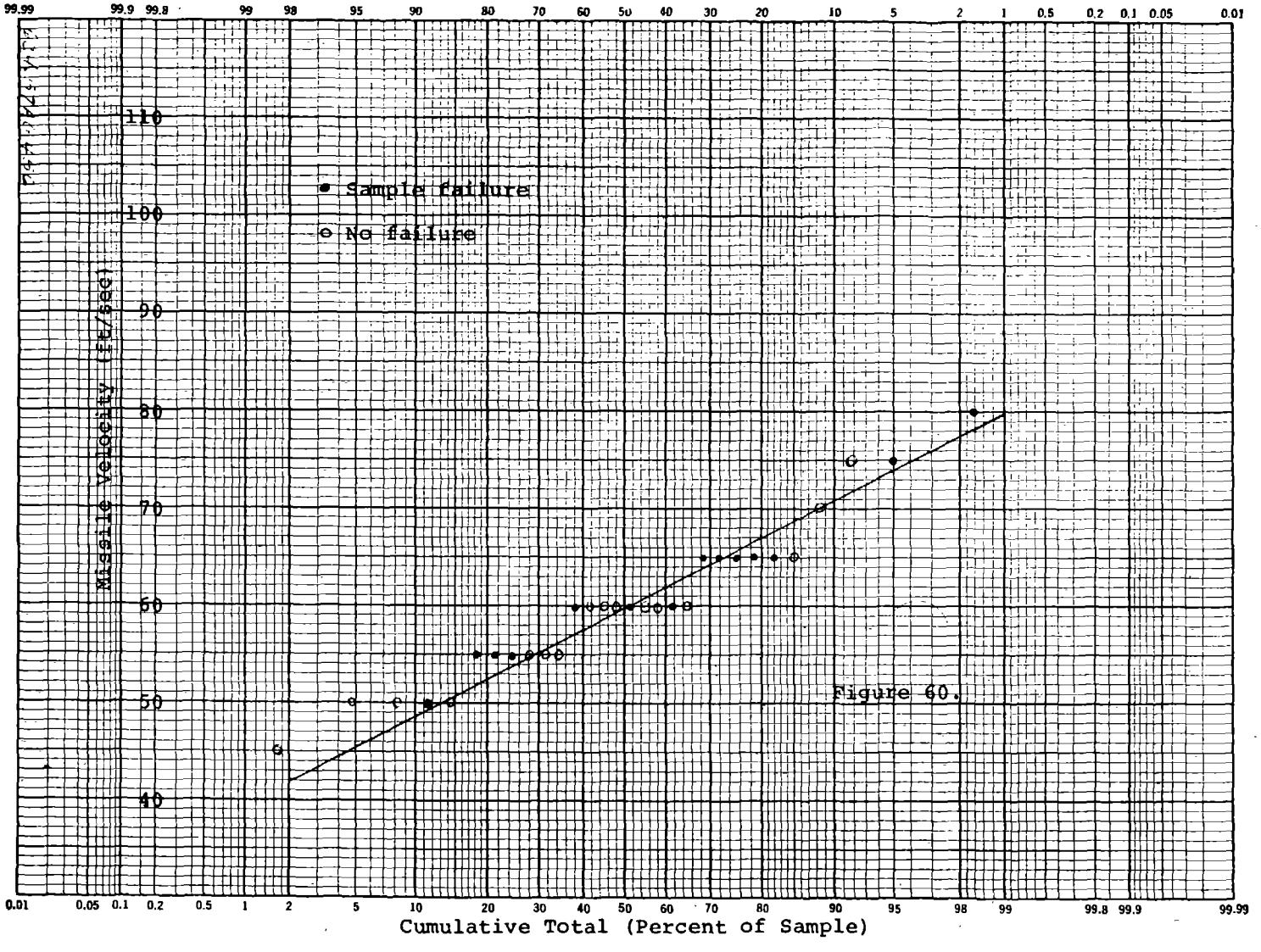

Figure 60.

Figure 60. Impact test data points for AO 325CB coverglass goggle with green glass lenses (See Fig. 58).

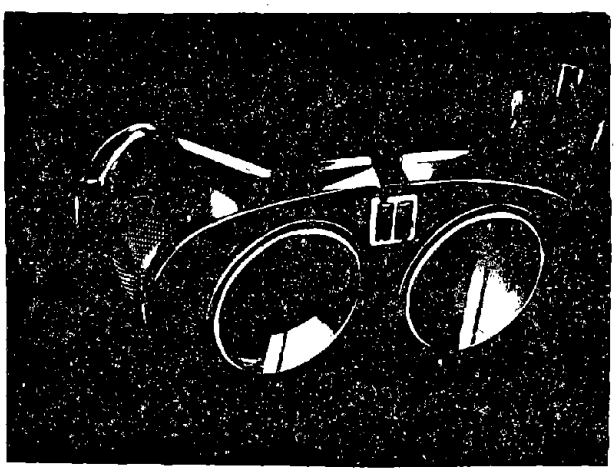

Figure 61

Chipping Goggles, Coverspec Type, Clear Safety Lenses
(A variant of Type 8A of Fig. 8 of ANSI Z87.1
having a flexible leather bridge)
AO 325C Coverglass Goggle

Tested with #112 shade 1.7 green 50mm round impact-resistant glass lenses

#75 shade 5 green 50mm round impact-resistant glass lenses with #54 clear glass cover lens

TABLE 24. FAILURE VELOCITIES WITH WEIGHTED NEEDLE

	v(50)	s	s/v(50)
325C with #112 lens	52 ft/sec.	7 ft/sec.	13%
with #75 & #54 lenses	35	5	14

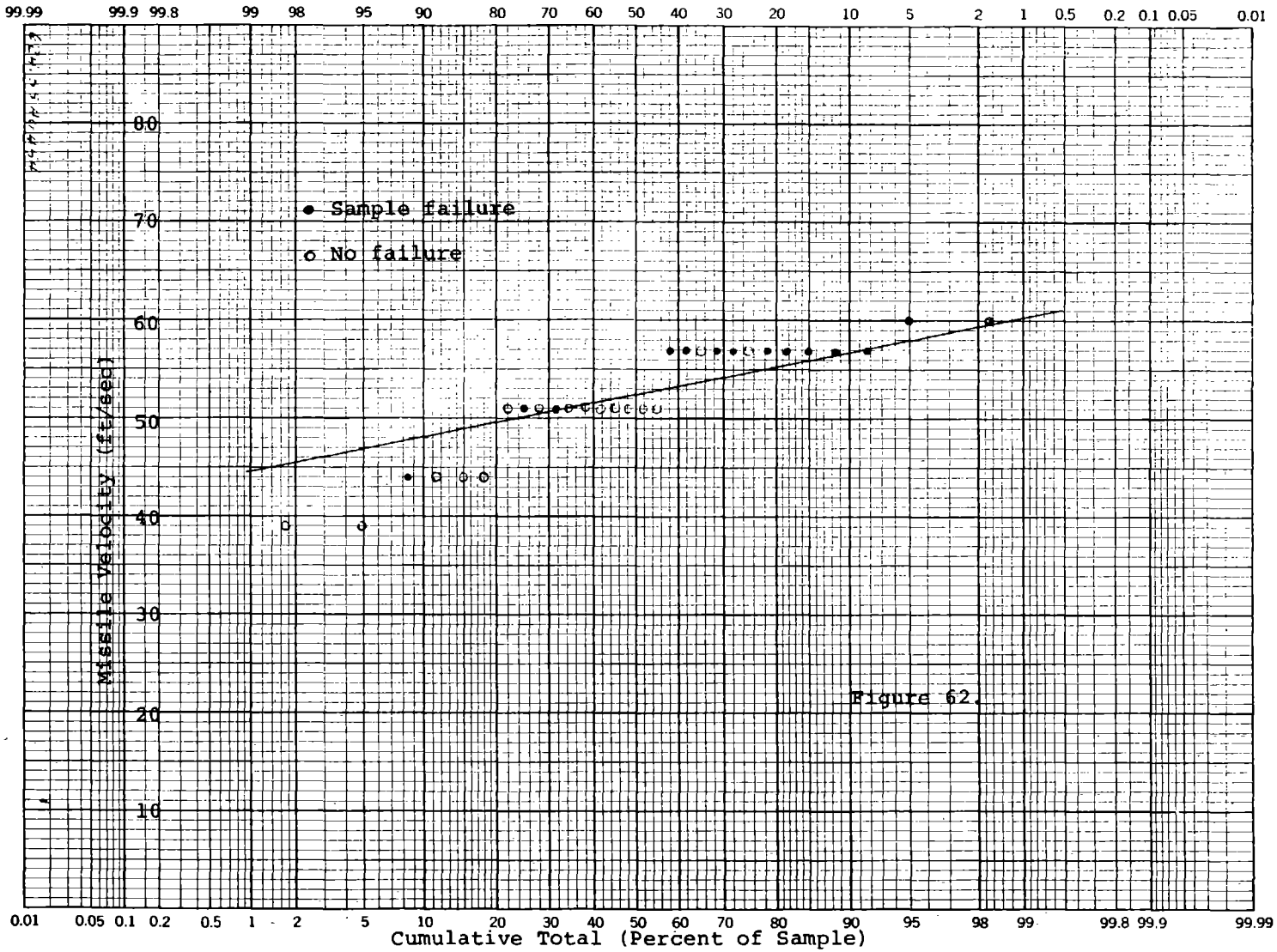

Figure 62. Impact test data points for AO 325C coverglass goggle with green glass lenses (See Fig. 61).

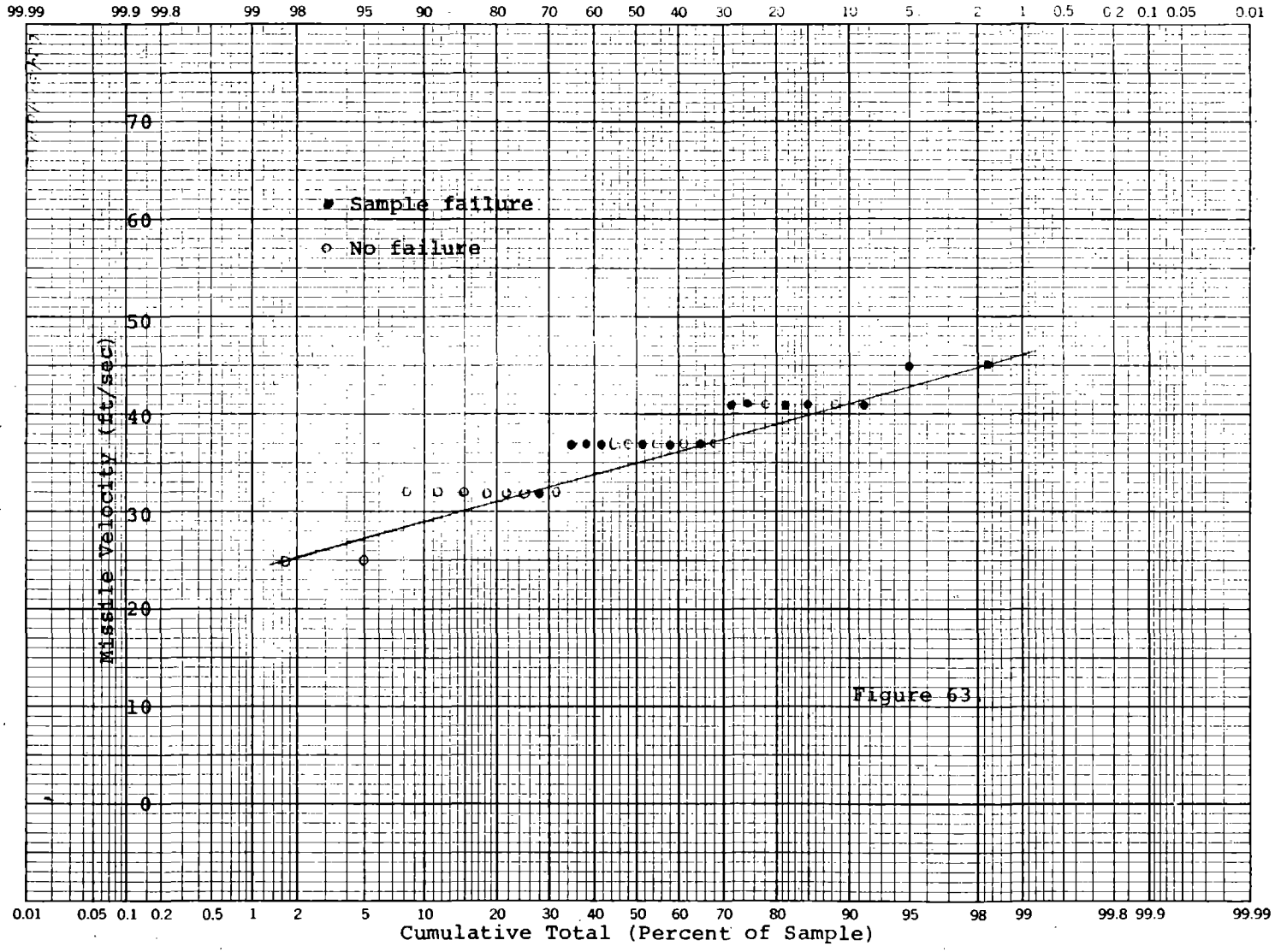

Figure 63. Impact test data points for AO 325C coverglass goggle with green glass lenses and glass cover lenses (See Fig. 61).

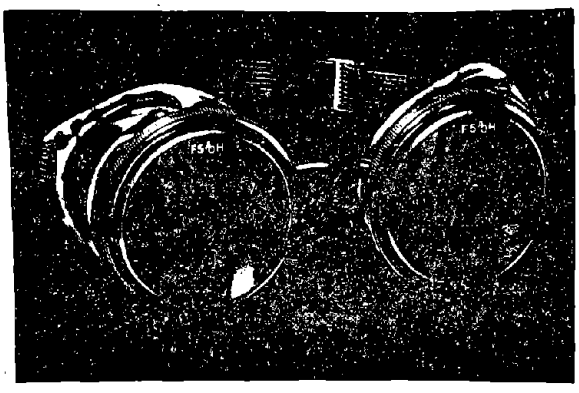

Figure 64

Welding Goggles, Eyecup Type, Tinted Lenses
(Type 7 of Fig. 8 of ANSI Z87.1)
AO 404A DURAWELD™ Goggle

Tested with #75 shade 5 green 50mm round impact-resistant glass lens with #54 clear glass cover lens

Same #75 lens with #185 clear acetate cover lens

TABLE 25. FAILURE VELOCITIES WITH WEIGHTED NEEDLE

	v(50)	s	s/v(50)
404A with #75 & #54	37 ft/sec.	5 ft/sec.	14%
with #75 & #185	143	9	6

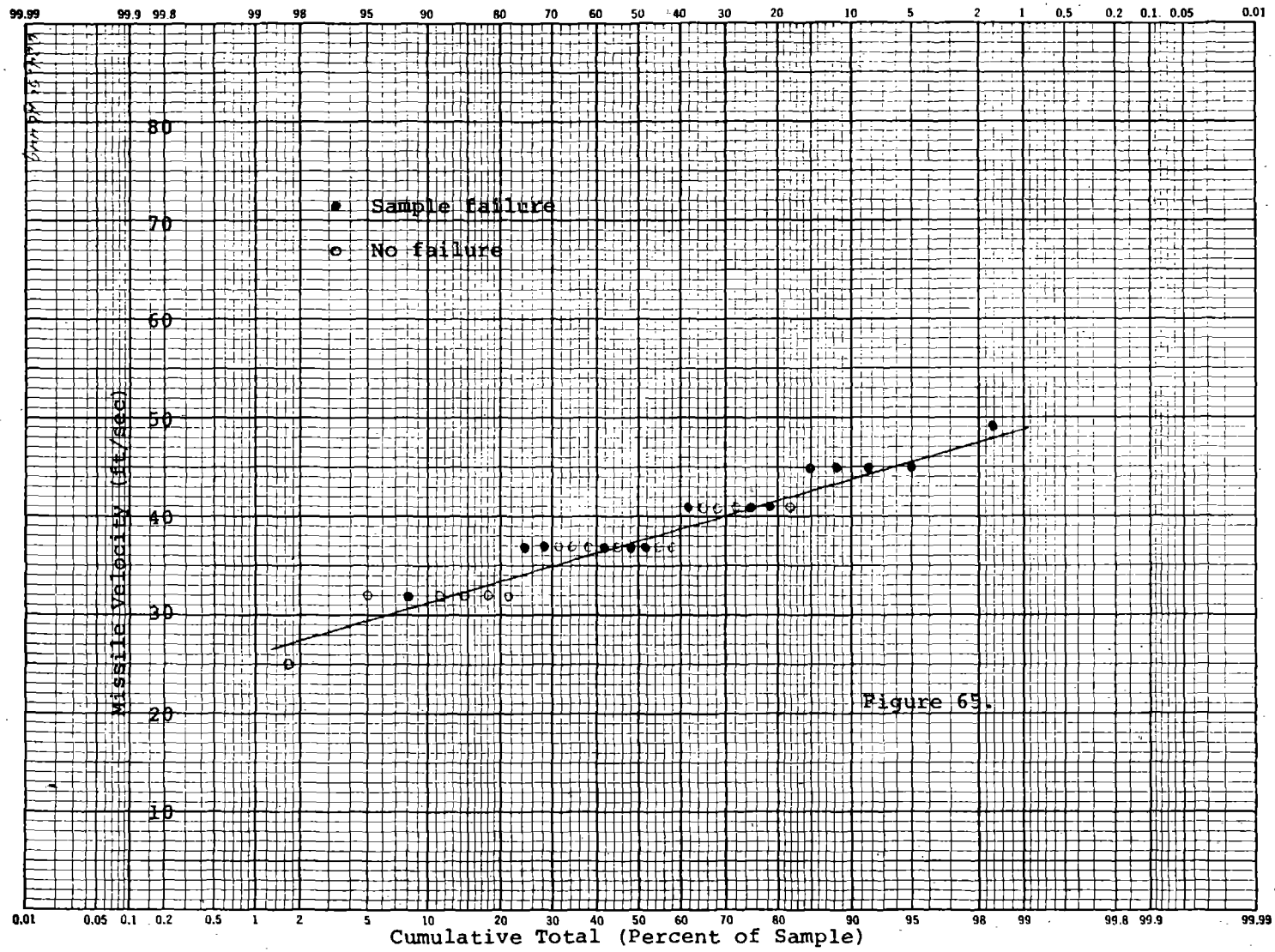

Figure 65.

Figure 65. Impact test data points for AO 404A goggle with green glass lenses and glass cover lenses (See Fig. 64).

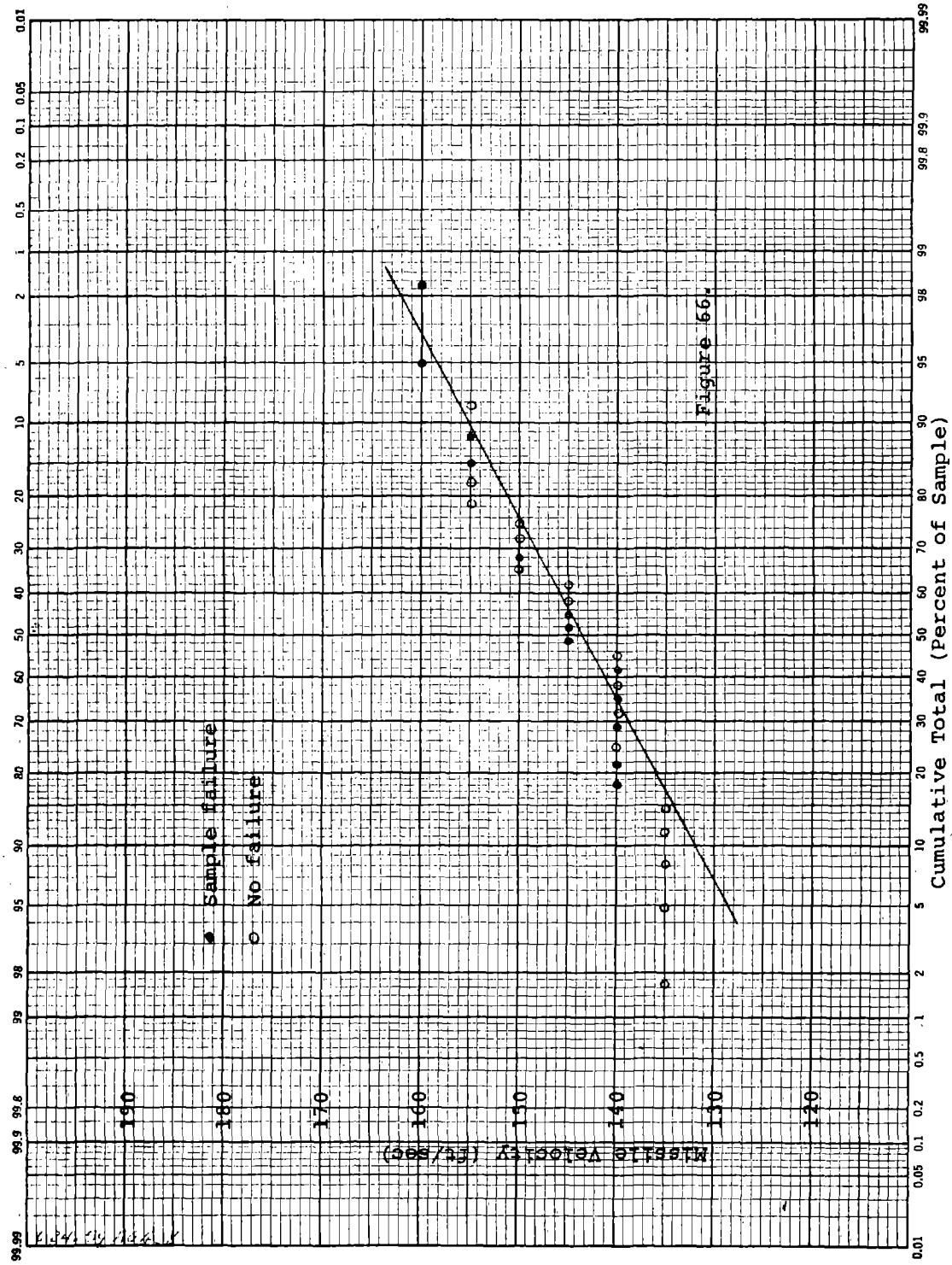

Figure 66. Impact test data points for AO 404A goggle with green glass lenses and acetate cover lenses (See Fig. 64).

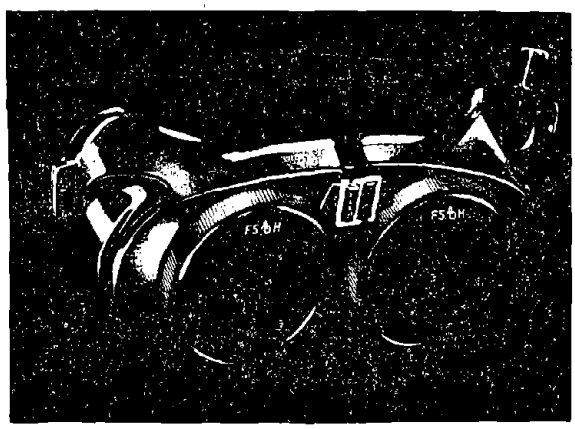

Figure 67 (AO 329C pictured)

Welding Goggles, Coverspec Type, Tinted Lenses
(Type 8 of Fig. 8 of ANSI Z87.1)
AO 329C and 329CB Welder's Coverglass Goggle (similar to AO 325C and 325CB except with opaque sideshields)

Tested with #75 shade 5 green 50mm round impact-resistant glass lens with #185 acetate cover lens

TABLE 26. FAILURE VELOCITIES WITH WEIGHTED NEEDLE

	v(50)	s	s/v(50)
329C with #75 & #185	176 ft/sec.	6 ft/sec.	3%
329CB with #75 & #185	194	8	4

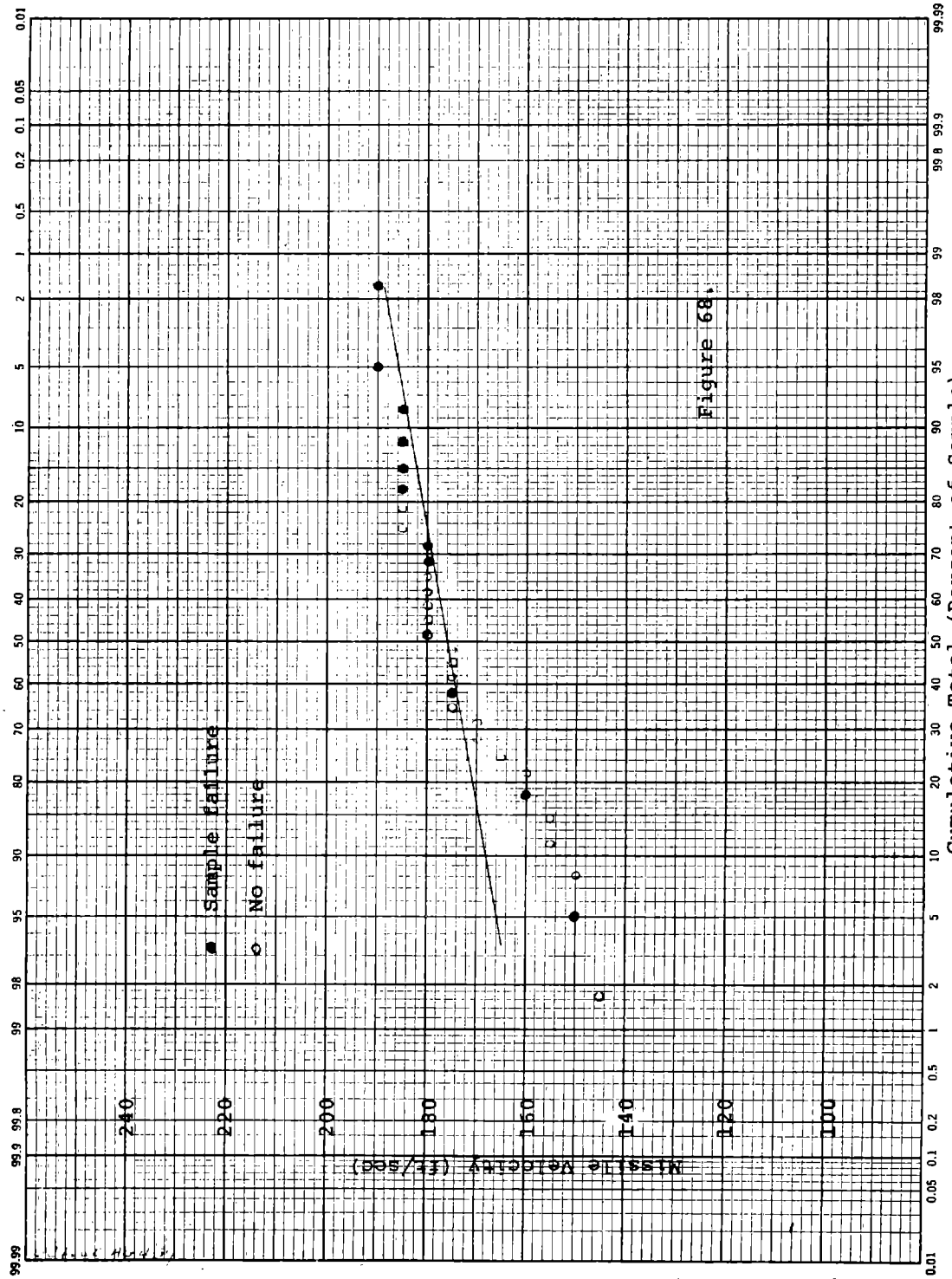

Figure 68. Impact test data points for AO 329C Coverglass goggle with green glass lenses and acetate cover lenses (See Fig. 67).

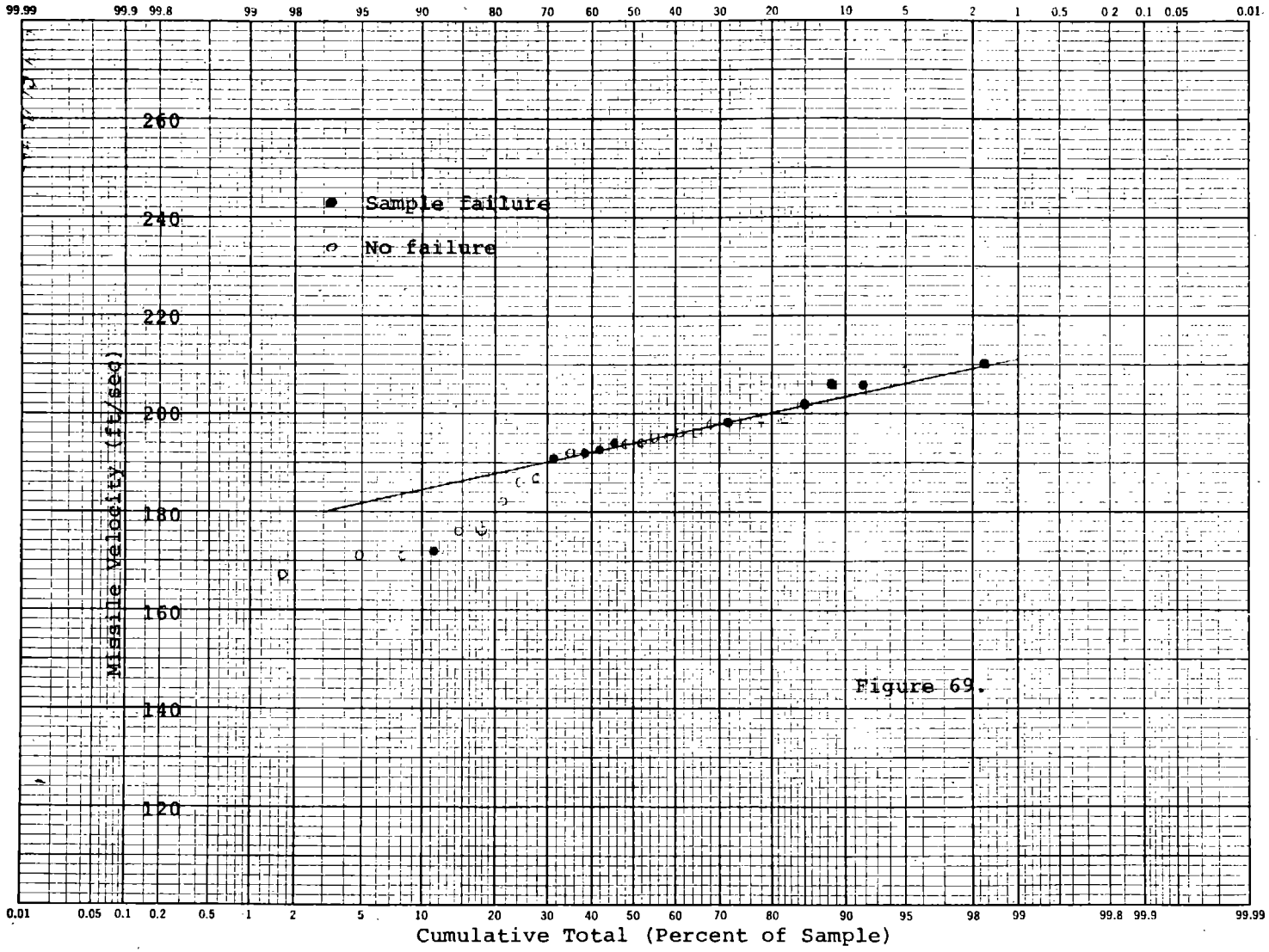

Figure 69. Impact test data points for AO 329CB Coverglass goggle with green glass lenses and acetate cover lenses (See Fig. 67).

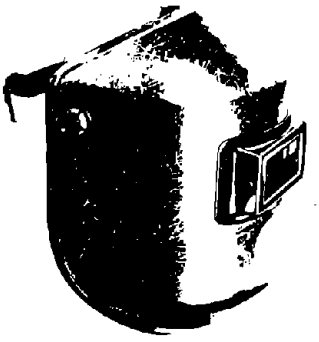

Figure 70

Welding Helmet
(Type 11 of Fig. 8 of ANSI Z87.1)
AO 9702C Curved Chin Fiber Glass Welding Helmet
with Fixed Plateholder

Tested with #80 shade 5 green 2" x 4¼" impact-resistant glass welding plate and #176 clear glass plastic-coated cover plate

TABLE 27. FAILURE VELOCITIES WITH WEIGHTED NEEDLE

	v(50)	s	s/v(50)
9702C + #80 &with #176	70 ft/sec.	10 ft/sec.	14

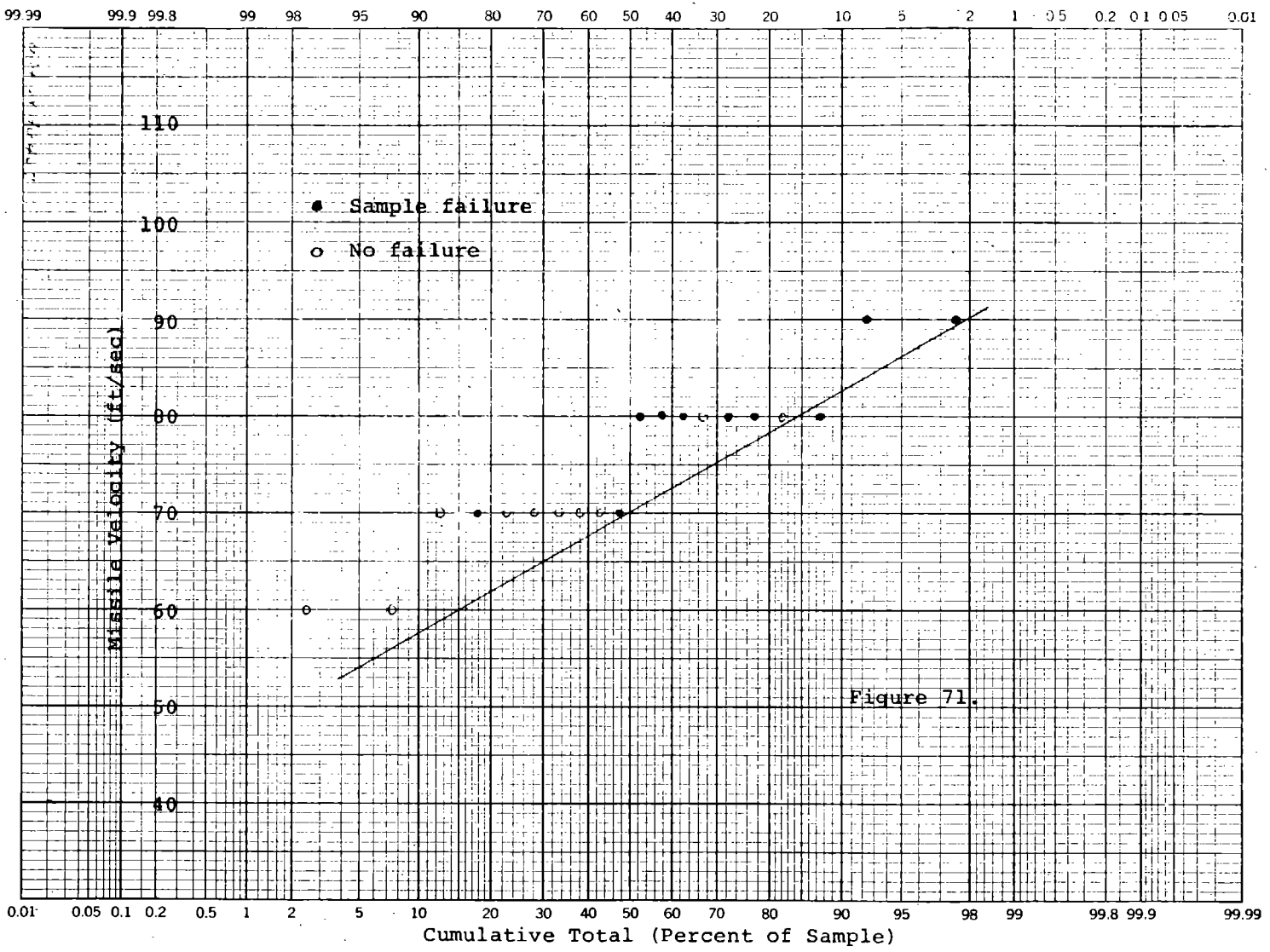

Figure 71. Impact test data points for welding helmet with glass welding plate and plastic-coated glass cover plate (See Fig. 70).

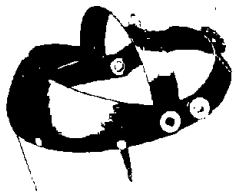

Figure 72

Face Shield with Plastic or Wire Mesh Window
(Type 10 of Fig. 8 of ANSI Z87.1)
AO H3 Headgear

Tested with #10W64 0.040 in. thick acetate window

#W8S wire mesh window

#W66 0.060 in. thick acetate window

#W85 0.050 in. thick propionate window

#WP85 0.050 in. thick polycarbonate window

TABLE 28. FAILURE VELOCITIES WITH WEIGHTED NEEDLE

		v(50)	s	s/v(50)
H3 with	#10W64	148 ft/sec.	18 ft/sec.	12
	#W8S	130	9	7
	#W66	182	9	5
	#W85	160	7	4
	#WP85	AT 260	NO PENETRATION	

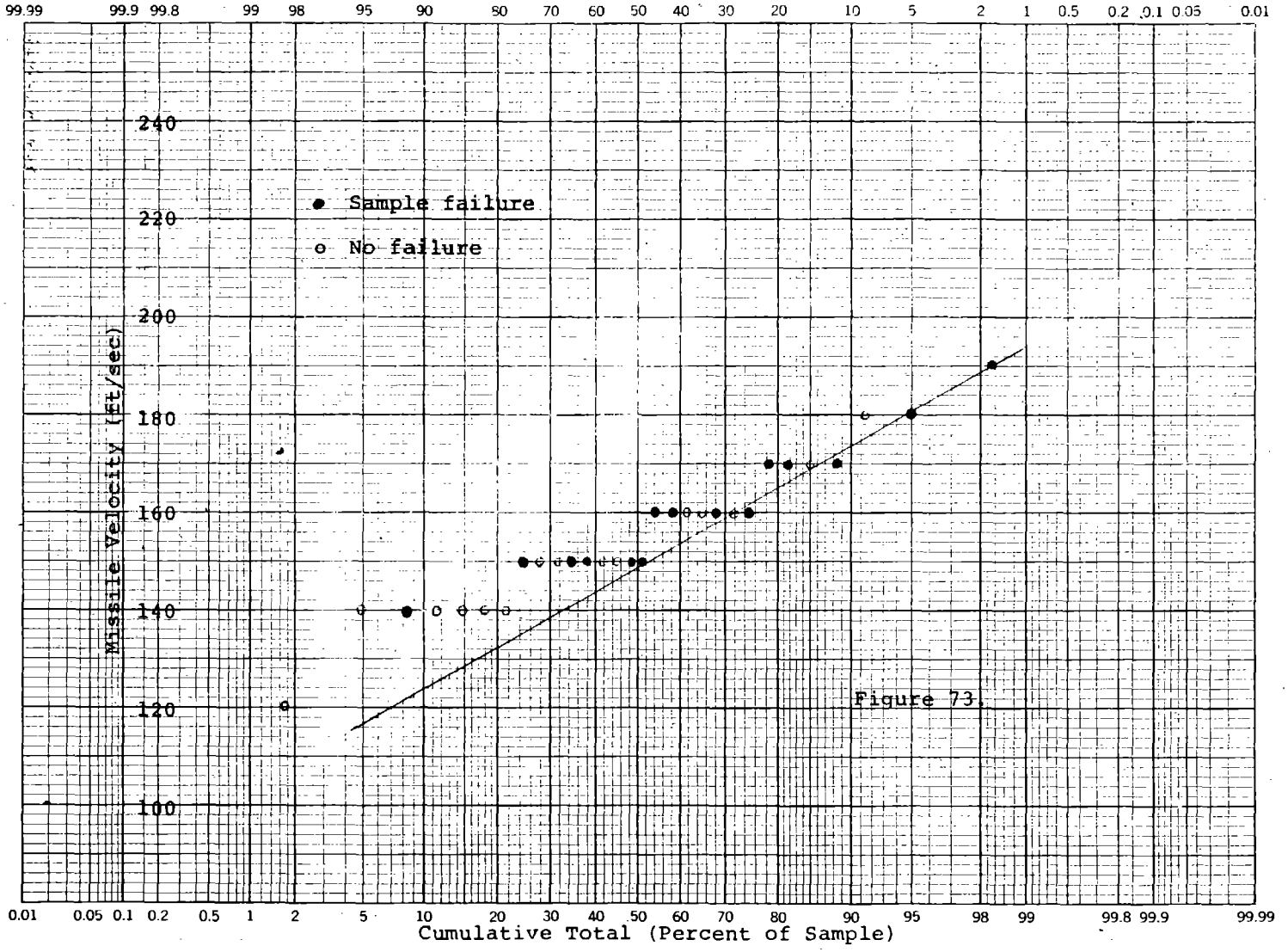

Figure 73. Impact test data points for AO H3 headgear and 0.040" thick acetate window (See Fig. 72).

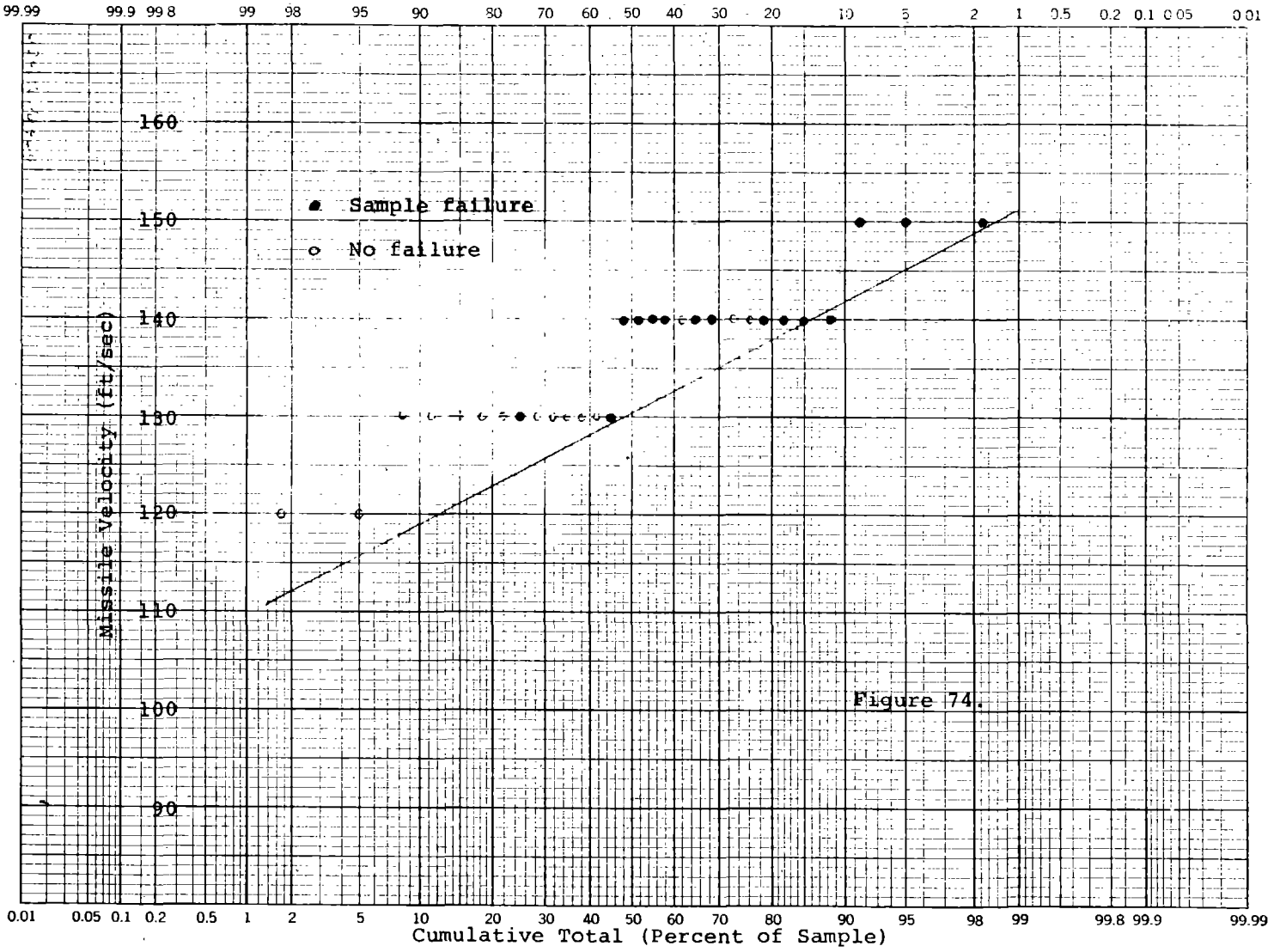

Figure 74. Impact test data points for AO H3 headgear and wire mesh window (See Fig. 72).

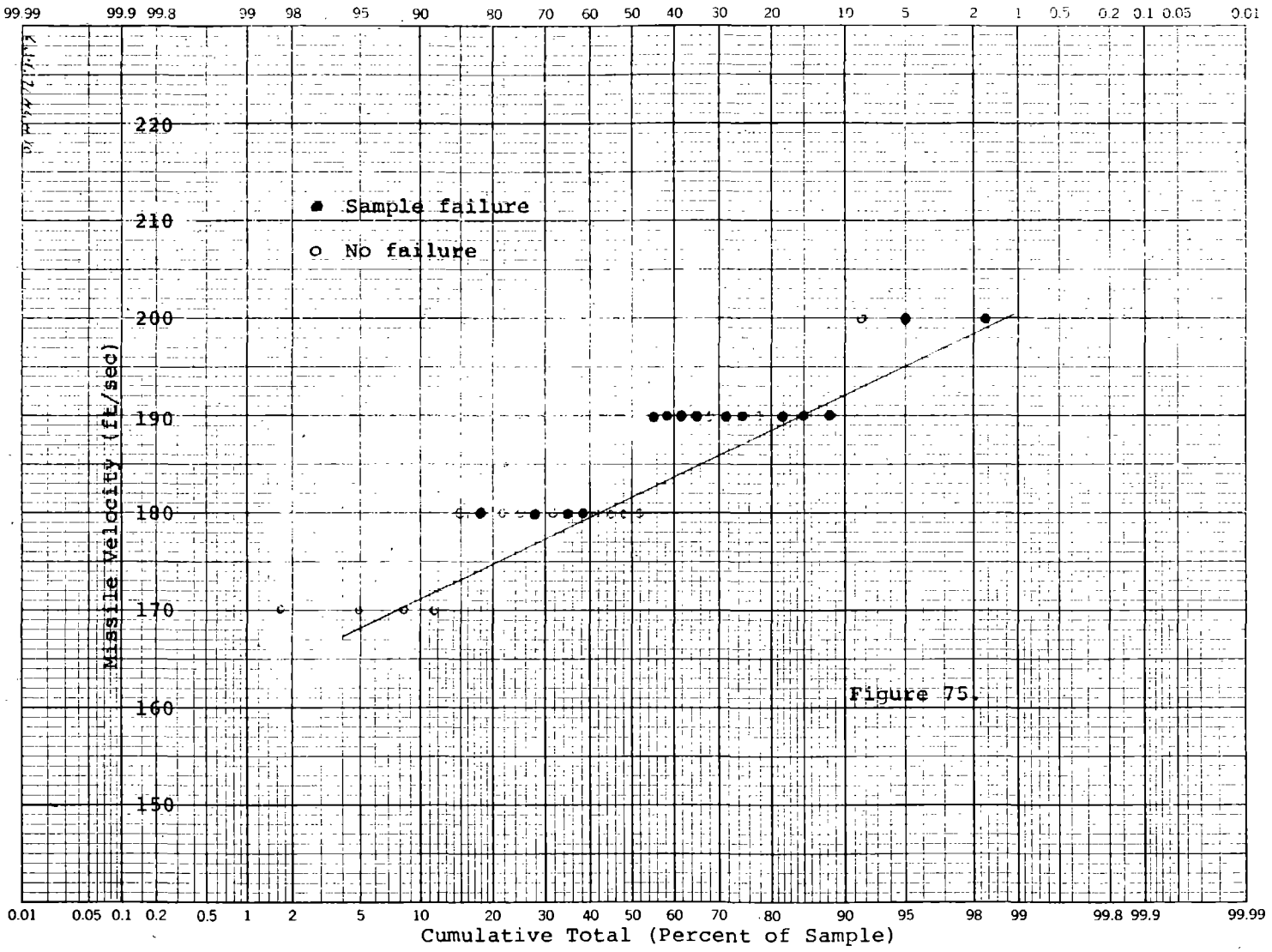

Figure 75. Impact test data points for A0 H3 headgear and 0.060" thick acetate window (See Fig. 72).

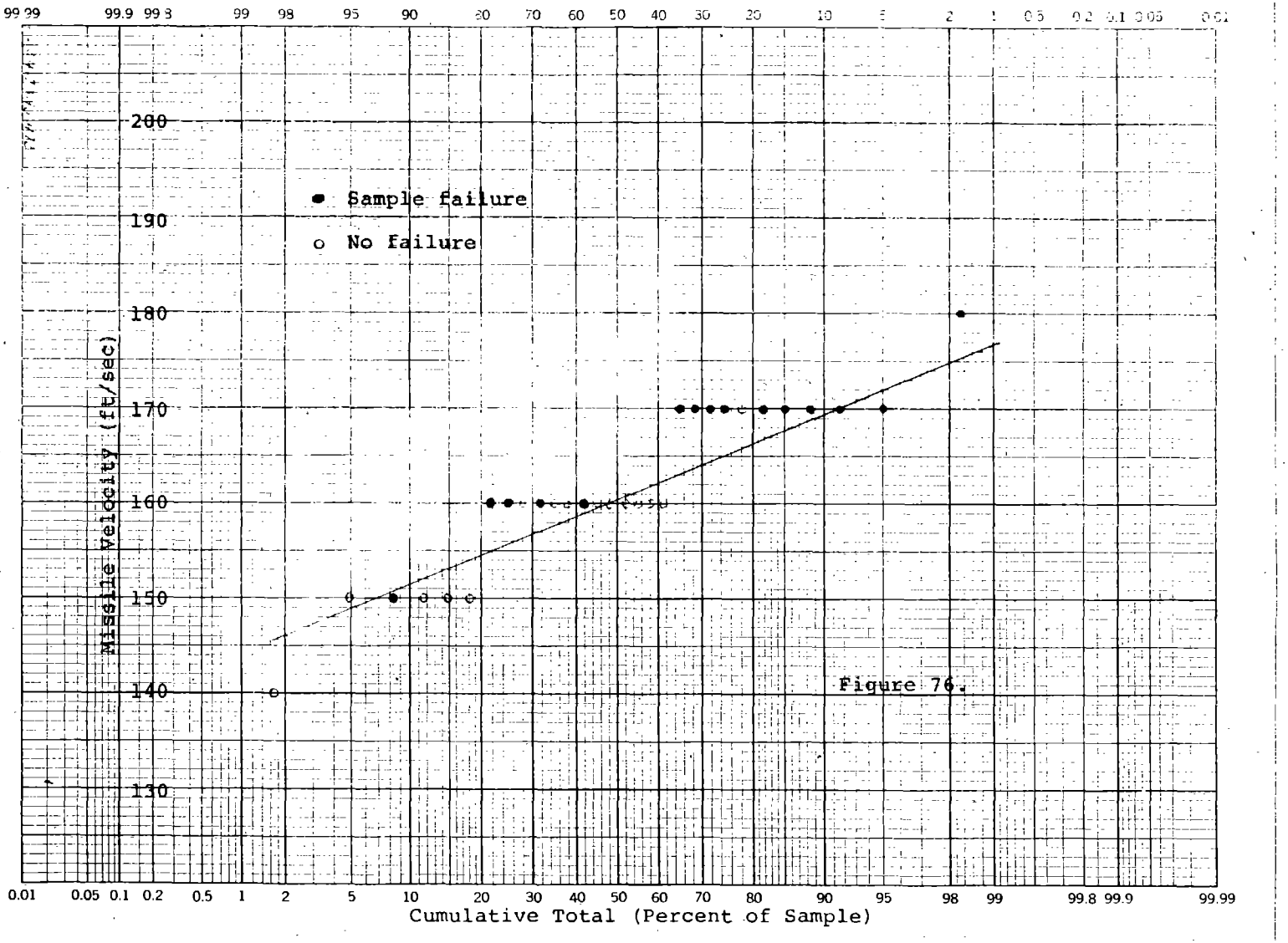

Figure 76. Impact test data points for AO H3 headgear and 0.050" thick propionate window (See Fig. 72).

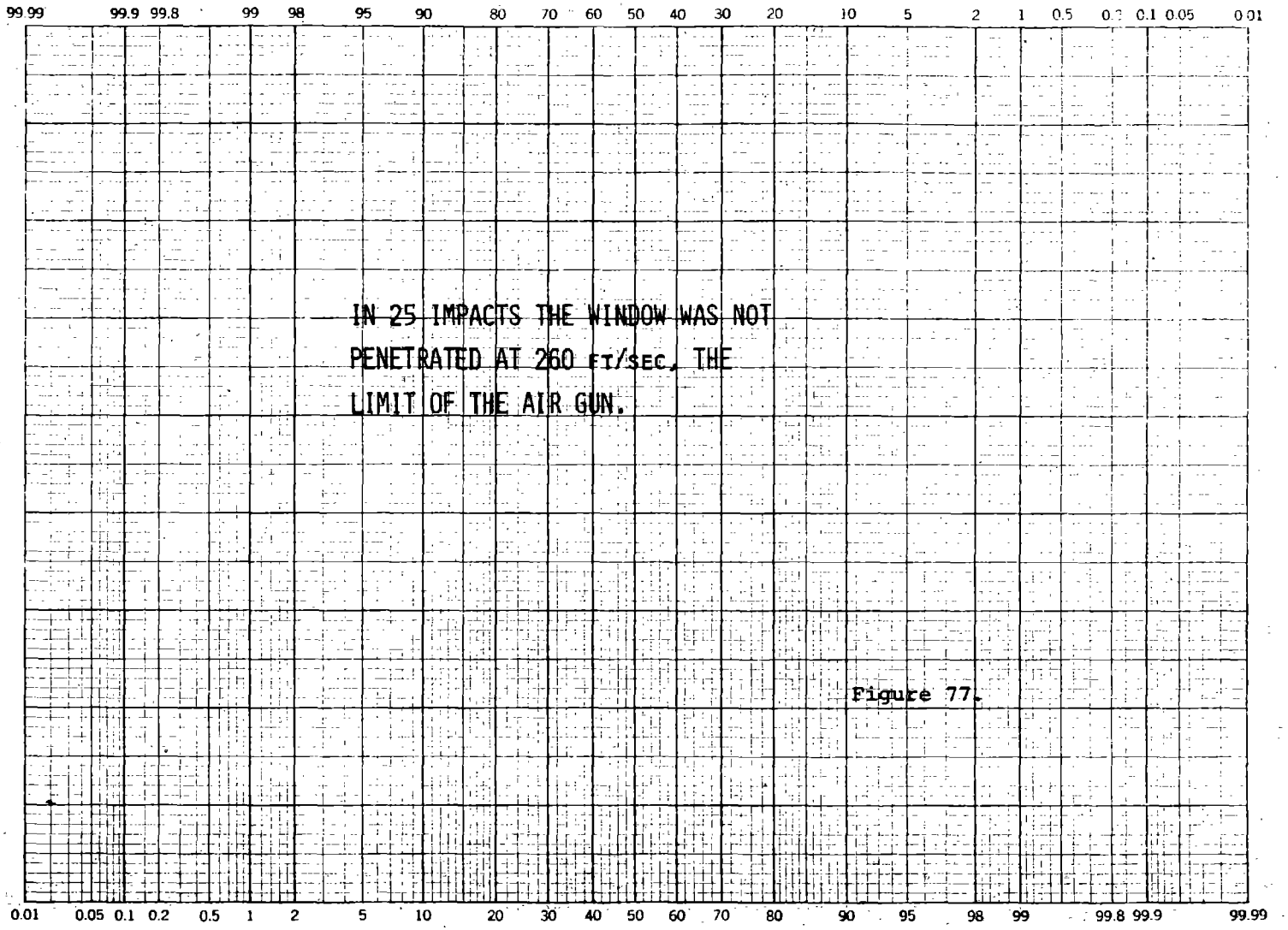

Figure 77. Impact test data for AO H3 headgear with 0.050" thick polycarbonate window (See Fig. 72).

SUBTASK 7: ANALYSIS OF TASK 2 RESULTS

Impact Test Results

It should first be pointed out that all eye and face protection devices or components tested meet the various impact test requirements of Z87.1 such as the drop-ball or low-speed weighted needle as applicable. The tests carried out under this contract are for conditions for which the products were not specifically designed and so an interestingly wide range of results is obtained.

Flexible mask goggles with clear plastic windows (Fig. 43) are by far the most commonly used form of eye protection after safety spectacles, and data in Table 18 show them to be very impact-resistant. No testing of acetate windows was carried out since AO no longer catalogs acetate windows even though they pass Z87.1 requirements. From results for faceshield windows shown in Table 28, it may be inferred that acetate windows would be considerably less impact resistant to the high-speed needle than polycarbonate windows. It should also be pointed out that the coated polycarbonate windows showed no significant difference in impact resistance from the uncoated ones. The AO DURAFON™ coating offers a very worthwhile degree of antifog behavior and abrasion resistance as compared to uncoated polycarbonate but without the brittleness which seems to accompany more highly abrasion-resistant coatings as discussed above.

The next type of product, a flex mask goggle with round flat heat-strengthened glass lenses (Fig. 46) shows noticeably more impact resistance than do plano 6-curve safety spectacle with glass lenses as seen by comparison of Table 19 and Table 17, but substantially less than the goggles of Fig. 43. It turns out that this type of goggle was designed primarily for use in atmospheres which cause etching of plastic lenses. It would appear, however, that use of a CR-39 cover lens over the glass lens would greatly improve the performance of this impact goggle; this may be inferred from data in Table 20 for an essentially similar goggle-lens combination with an additional CR-39 cover lens. CR-39 is much more resistant to chemical attack than softer plastics.

Comparison of data in Tables 19 and 20 would indicate that a clear glass cover lens doesn't afford much impact-resistance improvement when used over a new heat-treated 50mm round flat lens, but that plastic cover lenses do. We emphasize that this conclusion is for new lenses and coverplates; even a glass coverplate tends to protect the surface of the heat-strengthened glass inner lens from pitting and scratching which weakens it substantially.

The flex-mask goggle using a 2" x 4¼" glass welding plate (Fig. 53) and a CR-39 cover plate has significantly more strength than glass safety spectacle lenses but not the high impact strength obtained with 50mm round lenses used with a CR-39 cover plate (Table 20). This is presumably because the greater area of the 2" x 4¼" plate makes it easier for the missile to deflect the plates causing tension on the ocular side which would assist in breakage.

Turning now to cup goggles of various types, the similarity of results shown in Tables 19 and 22 would tend to indicate that, for the light-weight projectile involved in these tests, the difference in flexibility of the goggle body has relatively little effect on impact strength. Tables 22, 23, 24 and 25 indicate that goggles with heat-strengthened lenses alone or in combination with glass cover lenses are approximately as strong as safety glasses with glass lenses, whereas data in Tables 25 and 26 again illustrate the large gain in strength resulting from use of plastic cover lenses.

The single welding helmet plate combination tested (Table 27) showed impact strength greater than that of glass safety spectacles - see Table 17.

Face shields (Table 28) showed high impact resistance as a class, with the cellulosic plastics acetate and propionate behaving roughly similarly in thicknesses of 0.040, 0.050, and 0.060 inch. Fracture of the cellulosic faceshields was brittle, with cracking and ejected fragments. The wire mesh window, while not as strong, has unique advantages for some applications but obviously should usually be worn over safety spectacles. The polycarbonate window was impregnable at the test limit of 260 ft/sec., again illustrating the remarkable safety performance of this material.

Assessment of the Test Method

The needle, which can be used for only one shot, is inexpensive and readily obtainable. The reusable needle carrier is easy to make, as is the modified barrel to fit the airgun which AO, NIOSH, and several other firms in the safety industry already own. Missile stability over the necessary barrel muzzle to target distance of a few inches is satisfactory as can be judged both by the high-speed photographs of Fig. 32 and by the consistent attitude with which needles stick into polycarbonate test objects. The coefficient of variance of missile velocity distribution (Table 16) is sufficiently small (0.7% to 1.0% depending on velocity) so as not to affect perceptibly the accuracy of data obtained on test objects where coefficients of variance for failure speeds are 2% or larger as shown in Tables 18-28.

Drawings of the Singer needle, its aluminum carrier, and the modified Crosman airgun barrel are shown in Figures 28-30. Missile speeds of approximately 150 ft/sec. can be obtained with air at 200 psi as propellent; use of helium at 200 psi increases the attainable speed to 260 ft/sec., high enough to cause failure of all objects tested except the polycarbonate faceshield. As reported above, use of a lighter needle-pointed missile was found unsatisfactory simply because it tended to bounce off glass lenses without inflicting damage other than minor pitting at velocities readily obtainable with an airgun. In addition, complaint experience accumulated over the years at AO with industrial eye and face protectors indicates that on the relatively rare occasions when failure resulting in eye injury occurs, if it is caused by a pointed or sharp missile then that missile is relatively massive.

One obvious improvement should be made to the test method, and that is to increase the attainable missile velocity since Table 28 shows that it was not possible to penetrate a polycarbonate faceshield. The barrel shown in Fig. 30 has an accelerating section about 9 inches long. From experience gained (since the experimental work for this contract was finished) in setting up an air gun to give 190 meters/sec velocity to a 6 mm steel ball for an ISO test, it appears that missile velocity increases approximately as the square root of the accelerating length. Hence we would recommend a barrel length increase of from 21½" (Fig. 30) to 48", which would quadruple the accelerating length to 36"; this should make speeds of 250-300 ft/s available with air and 400-500 ft/s with helium.

Future Impact Performance Standards

We present here some thoughts which seem pertinent to impact performance tests which might be desired in future standards, particularly with regard to the high-speed weighted needle test discussed above. This information is not required by the contract and is presented here in the event it might be helpful. For convenience in discussion, we coin the word "speedle" (from "speedy needle") for the high-speed weighted needle.

1. The speedle test seems to us to be a very useful one that is complementary to the drop-ball test. The speedle obviously tests impact resistance to sharp objects but results are relatively insensitive to lens mounting, whereas the drop-ball tends to test by flexing the target until tension is created on the opposite surface sufficient to initiate breakage. The drop-ball when applied to products mounted on an anthropomorphic head appears to be a good test for aspects such as lens retention, mechanical strength of lens mounting systems, and deformability of the protector to the point where parts of it contact the eye, in a word, robustness; the

speedle is a relatively poor test in this respect.

It is our opinion, then, that both the drop-ball and the speedle tests should be employed in future performance tests for eye and face protective products. It should be mentioned that some standards employ a high-speed steel ball of 0.20 to 0.25 in. diameter as a test missile. In our experience this test is not in general as much a departure from the drop-ball as is the speedle and so does not complement the drop-ball as well if only two tests are to be employed.

2. We feel that future standard impact performance tests should be carried out with the protectors mounted on the anthropomorphic headform. While this would require re-definition of drop-ball height and hence velocity (or possibly size) it would lead to much more realistic assessment of protective properties.

3. Impact testing should be carried out in ways other than by a missile striking the protector frontally at the eye position. For example, the speedle shot into the flexible mask portion of the protector shown in Fig. 43 from a direction 90° from frontal penetrates the mask and reaches the eye more easily than when impinging on the polycarbonate lens. As a start, use of one impact from the side by both drop-ball and speedle appears worth investigating.

4. As a generalization, speedle test results reported above tend to classify products into two categories with regard to impact resistance;

spectacles with glass or CR-39 lenses or goggles and helmets with glass lenses and glass cover lenses.

protectors with polycarbonate lenses or with glass lenses behind plastic cover plates.

This would appear to point out two possible directions which could be taken by future standards. The first is to divide protectors into two classes with different impact requirements, an approach used in many European standards, while the second is to embark on a program of raising the impact requirements in steps until all products fall in the higher category. Our experience indicates that while industrial eye injuries are relatively rare, they do tend to occur primarily with products which fall in the lower category of speedle impact resistance. (This observation may be biased by the fact that glass safety spectacles are the most widely-deployed type of protector and data available to NIOSH may suggest otherwise.) This observation, coupled with the clear feasibility of increasing impact strength without losing comfort or causing major cost consequences to the user provided the program is

timed sensibly, would cause us to favor the approach of upgrading all products in steps to the higher performance level.

SUMMARY OF TASK 2

The high-speed weighted needle test developed in this task appears to be a sufficiently easy, economical, reproducible and realistic simulation of a rapidly-moving sharp missile which is more representative of many missiles encountered in a typical machine shop than is the drop-ball. While much work would need to be done by NIOSH and others to set performance levels for future standards, this test method appears to be a satisfactory basis upon which to build performance requirements; a better quantitative knowledge of hazards would also be very helpful in setting new performance requirements.

TASK 3

Task 3 consists of three subtasks:

SUBTASK 1. OPTICAL REQUIREMENTS - Identification of the optical and mechanical attributes of eye and face protective devices which are critical to the protection, usage, and comfort of the wearer, for testing and evaluating the problems of distortion and prism effects - more broadly, optical imperfections - in terms of their influence on the optical properties, and for recommending tolerance limits on optical attributes,

SUBTASK 2. TEST METHODS - Testing and evaluating the existing definitions and test methods for refractive power, prismatic power, and definition in Z87.1 and development and recommendation of improved definitions and test methods as deemed necessary - objective test methods, such as modulation transfer function techniques (MTF) being particularly emphasized, and

SUBTASK 3. DEFECTS - Development of criteria for physical defects (such as trapped bubbles) and mechanical defects (such as rough edges) and classification of these defects in the usual categories of Critical, Major A, Major B, and Minor.

SUBTASK 1

Introduction

The basic approach chosen has been to first examine the optical requirements of the eye for good visual acuity - "sharp vision" - and for comfortable functional vision, and the work reported below deals only with these requirements. Only after determination of these requirements is it possible to draw up rational recommendations for optical requirements for eye and face protectors.

Optical Attributes and Aberrations

Lenses in general possess the following attributes:

1. Vertex Power
2. Axial astigmatism
3. Oblique or off-axis astigmatism

4. Magnification and distortion
5. Prism
6. Resolving power
7. Spherical aberration
8. Coma
9. Chromatic aberration

For ophthalmic lenses in general, items 7 and 8 are of little consequence. Spherical aberration and coma both depend on the diameter of the bundle of light which passes through a lens. Since the eye's pupil is the system limiting aperture, only about 2-7 mm diameter of the spectacle lens is used at any one time, which reduces these aberrations to insignificance. Chromatic aberration is a function of the lens power and lens material and for zero power lenses with today's lens materials is inconsequential. So we turn to a more detailed examination of the first 6 attributes above.

1. Vertex Power -- The lens shown in Figure 78 has an optical axis which is defined as the straight line joining the centers of curvature of the two spherical surfaces.

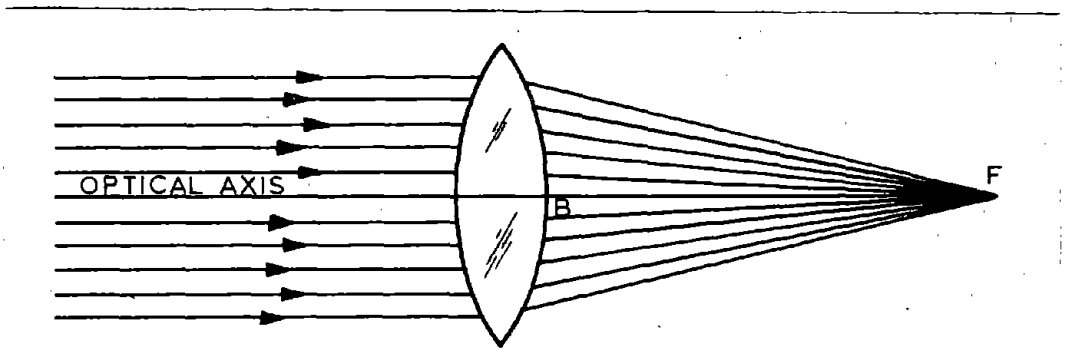

Figure 78. Diagram showing determination of vertex power

A cylindrical bundle of parallel light rays traveling parallel to the optical axis is incident on the lens which focuses the light to point F, the focal point. The distance from the vertex B to the focus F is called the vertex focal length,BF. In the ophthalmic industry it is customary to specify a lens by a quantity called the rear vertex power, or simply power, measured in diopters. Power in diopters (D) is defined as the reciprocal of the vertex focal length in meters, where it is understood that the reference vertex is the "back" vertex or vertex of the surface closest to the eye, the ocular surface. For a perfect zero-power lens, BF is infinite.

2. Axial Astigmatism -- If a bundle of rays parallel to the optic axis is focused into two relatively sharp lines

as shown in Figure 79, the lens is said to have axial astigmatism. The lens has different vertex focal lengths, and hence different powers, in different meridians. We can find the meridian of maximum power, AB in Figure 79, and of minimum power, CD; these are called the principal meridians. The axial astigmatism is the difference in power between these principal meridians, in diopters.

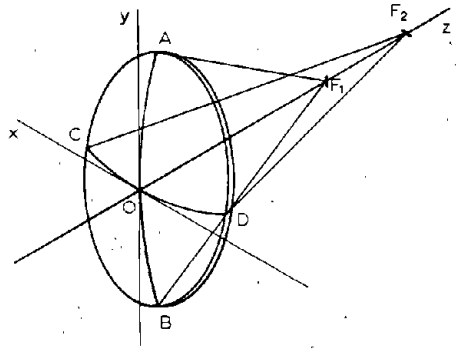

Figure 79. Lens having axial astigmatism

3. Oblique Astigmatism -- Figure 80 shows a bundle of parallel light, not parallel to the optic axis, which is incident on a lens. When we examine the focusing properties of the lens it is found that there are two lines of sharp focus even if the lens has two perfectly-spherical surfaces and hence shows no axial astigmatism. Oblique astigmatism is an inherent optical defect or aberration which is present to some degree in all lenses. Light which lies in the meridian AB and sections parallel to AB focuses in the line T called the tangential focus. This term arises from the fact that the focal line is tangent to a circle centered on the optical axis. Light in the other principal meridian CD focuses in a line S which is at right angles to line T. S is called the sagittal (or sometimes secondary) focus. The difference between the powers corresponding to the T and S focal lengths is the oblique astigmatism, expressed in diopters.

Figure 81 shows a lens cross-sectioned in the AB principal meridian. Point F is the focal point for light parallel to the optic axis and OF is the back vertex focal length. The focal plane is defined as a plane perpendicular to the optic axis through the point F. JK is an off-axis ray which lies in the yz plane and makes an angle θ with the optic axis. T is the

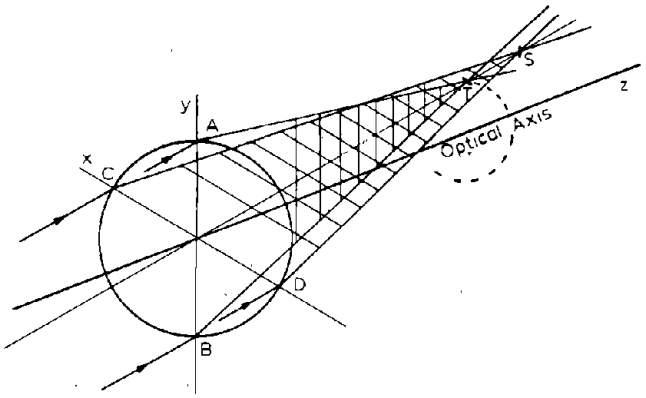

Figure 80. Lens showing oblique astigmatism

focal point associated with a bundle of rays parallel to JK and in the principal meridian AB. The distance ΔT corresponds to the tangential power error. Rays which lie in the CD meridian of Figure 80, and are in and out of the paper in Figure 81, intersect at S, the sagittal focus. ΔS corresponds to the sagittal power error. The actual powers are given by

$$\text{Tangential power (diopters)} = \frac{1}{\text{OT (meters)}} = D_T$$

$$\text{Sagittal power (diopters)} = \frac{1}{\text{OS (meters)}} = D_S$$

$$\text{Power (vertex power, diopters)} = \frac{1}{\text{OF (meters)}} = D_V$$

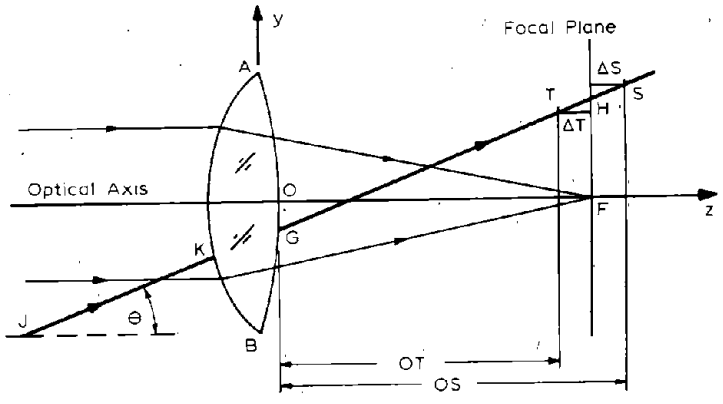

Figure 81. Cross section in the AB meridian of lens with oblique astigmatism

The so-called "T power error" is $D_T - D_V$ and the "S power error" is $D_S - D_V$. The oblique astigmatism is $D_T - D_S$ = T power error - S power error.

When we consider another bundle of rays incident at a different value of θ, the T and S power errors are different, increasing as θ^2. Angle θ can be considered as the angle of view or gaze for ophthalmic lenses. The magnitudes of the T and S errors are also dependent on the lens shape; if lenses of the same power are made using different combinations of radii for the surfaces, the T and S errors will change. Before exploring this point further we must discuss some of the simpler terminology and formulas of ophthalmic optics.

Ophthalmic Power Terminology and Formulas

Figure 82 shows a typical meniscus-shaped ophthalmic lens with appropriate labeling. The lens is described by the radii of its spherical surfaces, R_1 and R_2, the axial thickness t, and the index of refraction n of its material.

The true refractive power of a lens surface is defined as

$$P \equiv \frac{n-n'}{R}, \quad \begin{matrix} P \text{ in diopters} \\ R \text{ in meters} \end{matrix} \qquad (89)$$

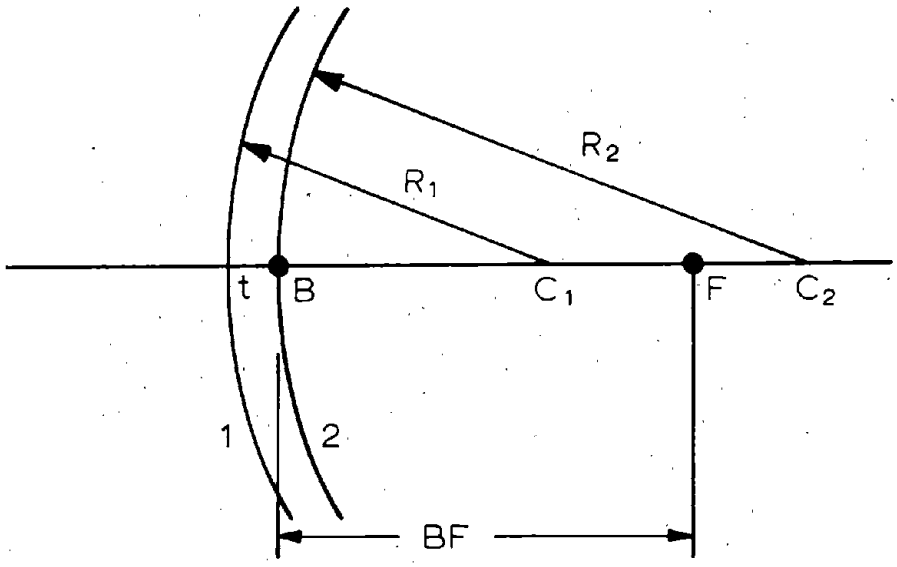

Figure 82. Typical lens shape with appropriate labeling

where R is the radius of the surface, n' the index of the medium preceding the surface, and n the index of the medium following the surface. R is positive if the center of curvature C lies to the right of the lens surface and negative if to the left. As shown in Figure 82, R_1 and R_2 are both positive for the normal ophthalmic lens.

The plano glass safety spectacle lens is made of spectacle crown of index 1.5232 (at the sodium D line, λ = 589.3 nm) and the index of air is 1. Design radii for the AO plano safety lens are R_1 = 89.50 mm, R_2 = 88.333 mm. Hence, the true surface powers are

$$P_1 = \frac{1.5232-1}{0.0895m} = 5.846D \qquad (90)$$

$$P_2 = \frac{1-1.5232}{0.088333m} = -5.923D$$

Now there is a convention of nomenclature in the ophthalmic industry for the description of lens surfaces and lens tools. Lens curves are not usually described by their radii or true surface powers, nor are lens-making tools usually described by their radii or the true surface powers they produce. Instead, the convention is that surfaces and tools are named for the surface power they would have or would produce if the lens material had index 1.53. These quantities are called "1.53 powers" and "1.53 tools." So it is frequently necessary to convert from 1.53 powers to true powers or vice versa. The conventional 1.53 powers for the AO safety lens are then

$$P_1\ (1.53) = \frac{1.530-1}{0.0895m} = 5.922D \qquad (91)$$

$$P_2\ (1.53) = \frac{1-1.530}{0.088333m} = -6.000D$$

and hence the name "6-curve" lens.

The formula commonly used to calculate the back vertex power D_V of a lens is

$$D_V = \frac{P_1}{1 - \frac{t}{n} P_1} + P_2 \qquad (92)$$

where

P_1 and P_2 are the true surface powers in diopters

t is the lens thickness in meters

Using the true surface powers from Eq. (90) and the design center thickness t = 3.4 mm for AO lenses, we find

$$D_V = \frac{5.846}{1 - \frac{0.0034}{1.5232}(5.846)} - 5.923 \qquad (93)$$

$$= 0.000D.$$

It is important to note that a zero-power lens does not have "parallel" surfaces (surfaces of the same radii) unless the surfaces are flat.

One further ophthalmic term needs definition. For reasons we will not elucidate, the 1.53 power of the ocular surface of some (but not all) lenses, with the sign changed, is called the "base curve". So our plano safety lens, from Eq. (91), is called a "6-base" lens. Now let us return to the discussion of oblique astigmatism.

Before the digression on terminology and formulas, we mentioned the fact that the T and S power errors and oblique astigmatism change if the base curve changes even though the lens power remains constant. Figure 83 shows this dependence for a plano lens used at an angle of view of 30° for viewing a distant object. It is interesting to note the decrease in T and S power errors and their difference, oblique astigmatism, for flatter base curves. Under the conditions given, the oblique astigmatism is 0.038D for a perfect 6-base lens, more than half of the Z87.1 tolerance (1/16D) for axial astigmatism, and the power errors are also a substantial fraction of the Z87.1 tolerance (± 1/16D) for vertex power.

4. Magnification and Distortion -- The magnification of a lens is defined as the ratio of image size to object size. When a single number is given for magnification it is the axial magnification, calculated from the ratio of the sizes for a small object and its image located near the optic axis. For a real lens imaging an extended object it is generally found that the magnification varies with the angle θ which the rays from the object point make with the optic axis. This variation of magnification with angle is called distortion. All lenses of positive power, plus lenses, produce "pin-cushion" distortion when imaging a square object,

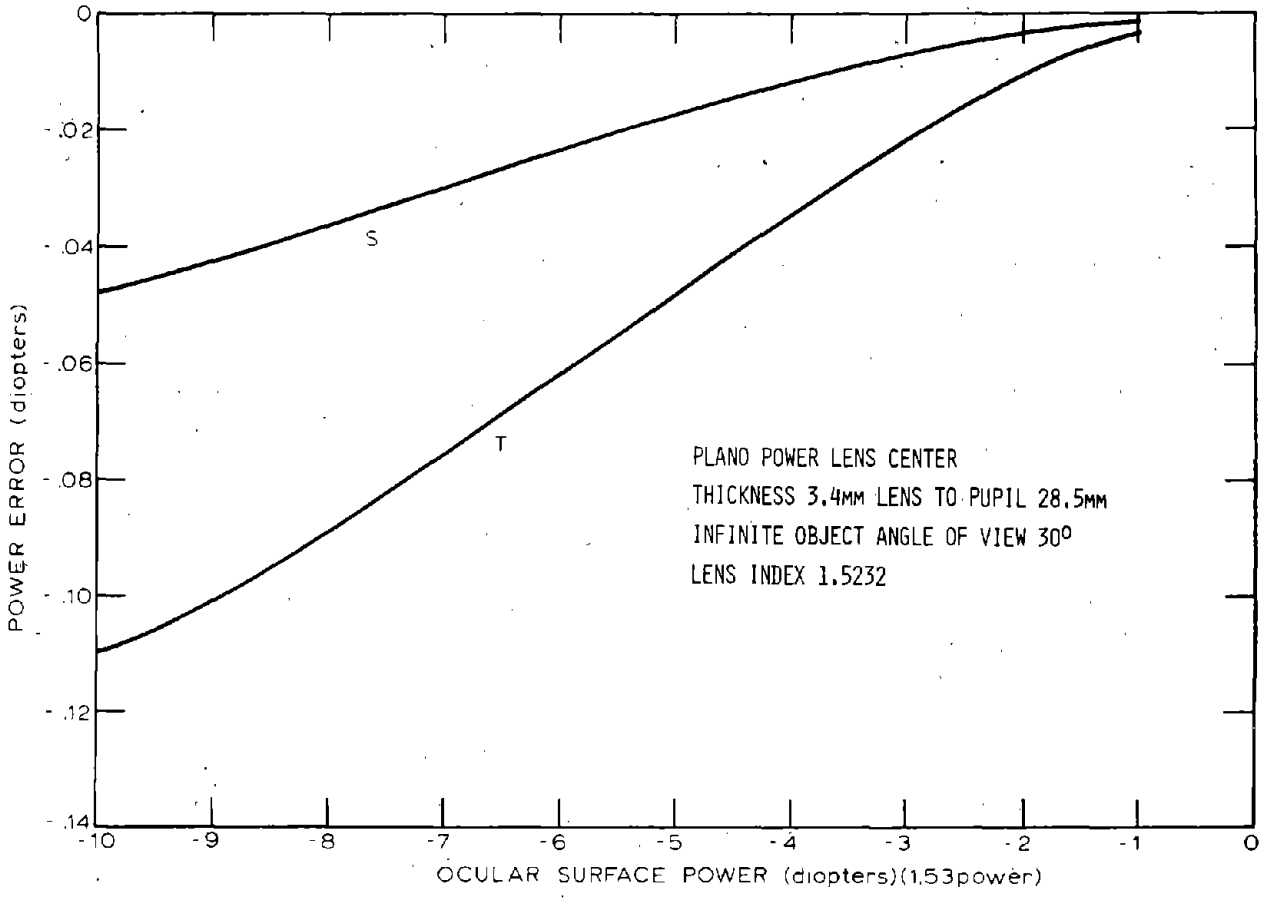

Figure 83. S and T power errors at an angle of view of 30°

while lenses of negative power, minus lenses, produce "barrel" distortion. These effects are shown in Figure 84.

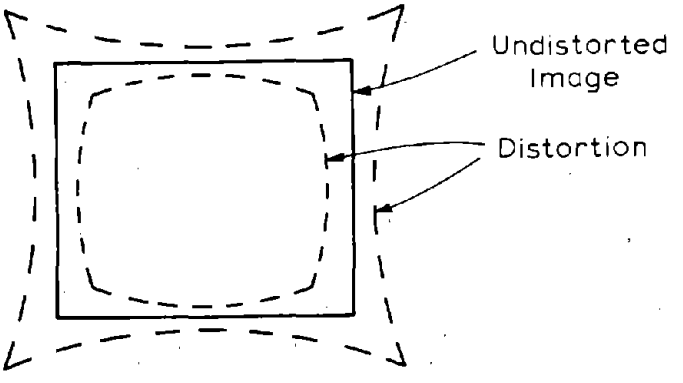

Figure 84. Diagram showing "pin cushion" and "barrel" distortion

Bechtold[16] has computed the distortion for several lens powers as a function of base curve and he showed that all plano lenses have an insignificant amount of distortion in the technical sense defined above. Occasional complaints of distortion in safety lenses must stem from other causes such as local variations in surface curvature. In the rest of this discussion, then, we will call axial magnification simply magnification.

The effects of magnification imbalance can sometimes be significant for spectacle lenses because they are used for binocular vision. If the two lenses in a pair of glasses form images of unequal size and if the eye and brain are not able to accommodate this disparity in size, a condition known as aniseikonia can result. This condition need not arise solely from unequal retinal image sizes, but can be caused by the cortical processes involved in the formation of the "image" in the brain. It is possible to induce aniseikonia by rendering the retinal images unequal in size by the use of lenses placed before the eyes; conversely, aniseikonia is sometimes corrected by wearing specially-designed spectacle lenses which give a compensating magnification difference or imbalance.

The magnification of spectacle lenses can be expressed approximately (Morgan[17], page 88) as the product of a shape factor M_S and a power factor M_P:

$$M = M_S M_P$$

$$= \frac{1}{1 - \frac{t}{n} P_1} \cdot \frac{1}{1 - z\, D_V} \qquad (94)$$

where z is the distance from the lens ocular vertex to the entrance pupil of the eye, approximately 20 mm. The shape factor gets its name because the first term in Eq. (94) depends on the front surface curvature through P_1 and the thickness t, while the power factor involves the lens power.

Let us calculate the maximum magnification imbalance which could occur for two lenses which meet the Z87.1 power and thickness tolerances. Suppose one lens has a power of + 1/16D caused by a front surface power P_1 which is 1/16D greater than nominal (it is assumed that P_2 adjusts so that $D_V = + 1/16D$). Since the nominal power of the first surface is 5.846D, (see Eq. 90), $P_1 = 5.846 + 0.062 = 5.908D$. We also assume the lens has the maximum thickness of 3.8 mm allowed by Z87.1. Then

$$M_1 = \frac{1}{1 - \frac{0.0038}{1.5232}(5.908)} \cdot \frac{1}{1 - 0.020\ (0.062)} \qquad (95)$$

$$= (1.014959)(1.001242) = 1.016218$$

Using a similar argument for a lens of - 1/16D power and 3.0 mm thick, we find

$$M_2 = \frac{1}{1 - \frac{0.0030}{1.5232}(5.784)} \cdot \frac{1}{1 - 0.020\ (-0.062)} \qquad (96)$$

$$= (1.011523)(0.998762) = 1.010271$$

The magnification imbalance is given by

$$M_1 - M_2 = 0.0059 = 0.59\% \qquad (97)$$

which is a small amount, as will be discussed later.

5. Prism -- A block of optical material which has two intersecting planes as shown in Figure 85 is a prism. After a ray of light has been refracted at the two prism surfaces, the angle ε between its initial and final directions, the ray's deviation, is given by

$$\varepsilon = (n-1)\alpha \qquad (98)$$

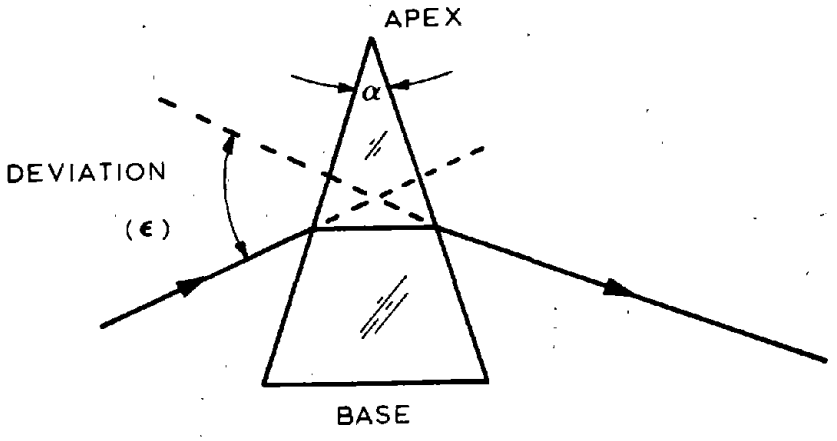

Figure 85. Ray of light passing through a prism

when the prism angle α is small. For ophthalmic work that deviation is given in units of prism diopters (Δ), which is an angle corresponding to a deviation of a ray by one centimeter at a distance of one meter. Hence,

$$\text{Prism } (\Delta) = 100 \tan \varepsilon. \tag{99}$$

The Z87.1 tolerance of $1/16\Delta$ for prism corresponds to an angle α between the flat faces of, say, a welding plate found from (99) and (98) as follows: Since α is a small angle,

$$\tan \varepsilon \approx \varepsilon = \frac{\frac{1}{16}\Delta}{100} = \frac{1}{1600} \text{ radian}$$

$$= 0.625 \text{ mr} = 2.15 \text{ min.} \tag{100}$$

so

$$\alpha = \frac{\varepsilon}{n-1} = \frac{\varepsilon}{0.523} = 4.1 \text{ min.}$$

When a 6-base plano safety lens has $1/16\Delta$ of prism it means that planes tangent to the surfaces at the design optical center of the lens are not parallel but have an included angle of 4.1 min. The subject of proper measurement of prism in 6-curve plano lenses will be discussed under Subtask 2.

6. Resolving Power -- The resolving power of an optical system is the angle between two neighboring point sources when their images can just be distinguished as two rather than one. Under the very best of conditions the eye can resolve the images of two point objects which subtend an angle of 0.4 minutes of arc at the eye. The most common criterion for normal vision is the ability of the eye to resolve objects separated by one minute of arc.

In ophthalmic work the resolving power of the eye is called visual acuity (VA). One of the most common test charts used to measure visual acuity consists of rows of letters of different sizes. Letters in the row corresponding to normal vision subtend 5 minutes at an eye 20 feet away, and the width of the lines subtend 1 minute of arc. Other rows contain larger or smaller letters of known sizes. Visual acuity by this test method is expressed as the Snellen fraction:

$$\text{Visual Acuity} = \frac{\text{Distance at which test is made}}{\text{Distance at which smallest letters read subtend an angle of 5 minutes}} \tag{101}$$

So, for example, a person with normal acuity has "20/20 vision" while a person whose VA is 20/40 can read letters only as small as 10 minutes at 20 feet.

Now Z87.1 uses a third way to express resolving power; safety lenses must exceed a minimum "definition", or ability not to degrade excessively the image of a standard test chart when placed in front of a specified test telescope. The relationships between resolving power, definition, and visual acuity will be explored later in this report.

Wearer Visual Requirements

The material discussed above will now be related to the needs of the wearer of plano eye protection. An emmetrope is defined as a person with physiologically normal eyes and visual acuity of 20/20 or better. Our basic approach is to deal with the problem of recommending lens tolerances and test methods so as not to degrade an emmetrope's acuity noticeably under occupational conditions. There are, of course, many wearers of plano eye protection whose acuity is less than 20/20 but not so bad that they feel the need for corrective lenses. Conversely, (see Borish,[18] Chap. 10) many wearers of planos have vision better than 20/20.

If nominally plano lenses have some plus power the emmetrope can do nothing to accommodate for the fact that images of distant objects will fall just short of the retina, causing a very slightly blurred image, Fig. 86. If the lens had minus power, which causes light to act as though it were focused behind the retina, the image is again blurred, see Fig. 86. In this case the person can exert accommodation, i.e., strengthen the power of the crystalline lens of the eye, and bring the light to focus on the retina. Peters[19] found that plus power of up to +0.25D would not reduce the acuity below 20/25, but that as much as -1.0D of power could be present before acuity fell to 20/25. Thus, for an infinite object distance the wearer of such a lens could accommodate by 1.0D and produce a clear image. Experience has shown that a pair of eyes can use only about half of the total amplitude of accommodation for long periods of time without discomfort. Any accommodation used to compensate for the minus lens would not be available for near work, and this would become a problem for people as they became older (see Stimson,[20] page 194). So anything approaching -1.0D would be unsuitable, but perhaps as much as -0.25D could be tolerated.

However, there are two other factors which preclude having as much as -0.25D present in a plano lens. When eyes accommodate they do so nearly in unison, that is, if the left eye accommodates by 2.0D to view an object 0.5m away, then the right eye accommodates nearly the same amount. Stoddard and Morgan[21]

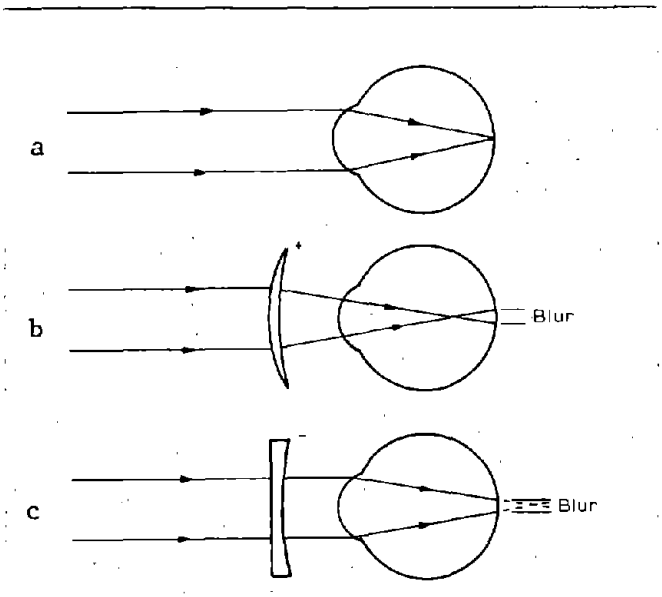

Figure 86. Blur caused by lenses with plus and minus power when used by an emmetrope

presented data indicating that a difference in accommodation between eyes is possible, the average value of the maximum difference being approximately 0.12D. This amount happens to coincide with the 1/8D mismatch which is the worst that can occur for axial viewing between plano spectacle lenses meeting Z87.1 requirements. While such a mismatch would occur relatively infrequently, safety lenses are glazed into spectacles without matching for power provided they meet Z87.1.

The second reason why a relatively large negative power error like -0.25D would be undesirable is an additive effect which could occur with oblique T and S power errors. Davis,[22] in a paper on the optics of plano lenses computed the aberrations present in plano lenses. For near objects and 30^{o} off-axis viewing, the sphere power errors become as large as -0.2D with -0.1D of astigmatism and 0.1D of power imbalance. These off-axis errors occur even with lenses having truly zero axial power, and they are already approaching the limit suggested by Stoddard and Morgan's work. In addition, while the eyes have some capability to accommodate for power errors or imbalance as stated above, they have essentially none to accommodate for astigmatism, so it is our present opinion that axial astigmatism tolerances should be kept as small as reasonably possible.

In the section above on magnification and distortion it was calculated that the worst magnification imbalance which would occur in a pair of plano safety glasses whose lenses met Z87.1 tolerances was 0.59%. Emmetropes can sometimes distinguish

0.25% magnification imbalance, but magnification imbalance is not considered to be clinically significant until it is 0.75% or more and accompanied by symptoms such as headaches and nausea. Borish,[18] Chapter 8, gives a considerable amount of data on the magnitude and frequency of aniseikonia, and it is clear that most spectacle wearers can tolerate considerably more than 1% magnification imbalance, so the 0.59% above represents no problem, particularly since the chance of two lenses being paired of such mismatched curves, thicknesses, and powers necessary to give the 0.59% is extremely small.

Consider now the problem of prism imbalance. Prism imbalance between the two eyes can cause muscular strain and resulting discomfort. A person can tolerate readily about 0.5Δ of horizontal imbalance or about 0.25Δ of vertical imbalance but further amounts are undesirable - see the requirements for first quality prescription ophthalmic lenses given in Z80.1-1972[23] for allowable prism imbalance between lens optical centers: The Z87.1 tolerance of 1/16Δ implies a maximum allowable mismatch of 1/8Δ within a pair of spectacles although this would be a rare occurrence. Prism imbalances which can arise for off-axis near viewing, Figure 9, can amount to 0.3Δ to 0.4Δ as Davis[22] has shown even though there is no imbalance on axis.

The wearer requirement for Z87.1 definition, i.e., lens resolving power, is more difficult to determine directly and requires a certain amount of analysis to infer; hence this discussion will occur later. Definition or resolving power is aperture-limited but is not affected by small amounts of lens power or prism for which compensation or accommodation can be made. Definition is affected by axial astigmatism since a compromise focus is not as sharp as the image at focus for a spherical lens. Definition is adversely affected by irregularity of lens surfaces (irregular departures from perfect sphericity), inhomogeneous optical materials (refractive index n not constant), and haze in the lens. Inhomogeneous optical materials are not a problem with today's technology in eye protection, and the effects of varying refractive index n and surface irregularities are lumped together for practical purposes anyway since they both cause minute variations in optical path nt through a lens, where t is lens thickness. Haze is an independent parameter.

While haze is not normally a problem with glass lenses, small amounts of it can occur in plastic lenses. We were not able to find any published material on the effects of haze in spectacles or other eye and face protectors. There has been considerable work done to study meteorological visibility as affected by atmospheric conditions, and other studies done to determine the effect of dirty or hazy windshields on acuity. It does not appear that these could yield a direct answer to

the effects of haze occurring only in a thin layer placed immediately before the eye. In one experiment carried out at AO under other programs, it was determined that many people would object to their glasses when the effects of scratching became so pronounced as to yield a haze of about 4% when measured by the Z87.1 method; the haze effect of scratching on acuity may not be the same, however, as that caused by a number of small scattering centers.

With regard to the effect of haze on definition a preliminary experiment was carried out. Two observers with normal vision had their visual acuity measured with a Snellen "E" chart with and without haze samples placed in front of their eyes. The haze samples utilized were the calibrated standards of glass and plastic from a Gardner Hazemeter, and hence correspond closely to the percent haze which would be measured using the method called out in Z87.1.

No measurable decrease in acuity was found until the haze was in the neighborhood of 20%, although the haze became unpleasant before that value was reached. From other work at AO we know that haze is undesirable in critical viewing situations, and the experiment above tells us that in order to quantify the relationship between haze and acuity loss it would be necessary to set up a carefully-controlled measurement of acuity under different conditions. These conditions would involve measurement of acuity for a dimly-lighted target immediately adjacent to a glare source or bright object. A welder, for instance, is trying to see the work piece by looking past the bright fireball of the arc at the relatively dim work area. Another example where the effect of haze would be pronounced is in viewing objects near light fixtures, particularly incandescent bulbs.

To set up and carry out the acuity measurements required in a reproducible manner would take a more substantial experimental effort than could be carried out under this contract, so further testing was not done. Two factors should be considered, however. First, we can say with considerable certainty from AO experience that there is no requirement for eye protection which cannot be met today with haze less than 3%. Second, there are at most only a few products where haze might occasionally exceed 3%, and there exist viable low-haze alternatives for these products. With these factors in mind, we would recommend a 3% haze limit rather than the 6% presently allowed by Z87.1. The 6% limit, incidentally, stems from the days when plastic materials were much less developed than today; glasses used for eye protection, except for a few used for laser eye protection, are very low in haze.

Following study of the relationship between visual acuity and Z87.1 definition in Subtask 2 a complete set of recommended

optical tolerances will be listed.

SUBTASK 2A: NON-MTF TEST METHODS

Present Test Method

Description--
The present test is shown in Figure 87. An eight power telescope with 0.75 inch (19 mm) aperture is used to view chart pattern 20 described in NBS circular C533 at a distance of 35 ft. Pattern 20 is a high contrast line target with a spatial frequency of 0.80 line pairs/mm. The exit pupil of the telescope is 2.4 mm (19 mm entrance pupil/8X).

Operation--
The telescope eyepiece is moved with respect to the reticle until the reticle is in sharp focus. The eyepiece plus reticle are then moved as a unit until the image of the target viewed through the telescope without the safety lens is in focus at the same time as the reticle. This position of the eyepiece corresponds to zero power. The telescope is aligned so that the image of pattern 20 is centered with respect to the reticle pattern. A +0.063D lens and a -0.063D lens are placed in turn in front of the telescope to calibrate the position of the eyepiece plus reticle assembly. The safety lens to be tested is then placed in front of the telescope, and the powers of the horizontal and vertical meridians are measured. Z87.1 requires that the difference between any two meridians (astigmatism) shall not exceed 0.063D, and that the power in any meridian shall not exceed $\pm$ 0.063D.

The lateral displacement of the target image is used to measure the prism which shall be less than 0.063 prism diopters.

The radius of the circle used for prism measurement on the NBS target is 0.25 inch. 0.25 inches subtends 59.5 milliradians or 2.05 minutes at 35 ft. 1/16 prism diopters equals 62.5 milliradians therefore the target circle is approximately 5% too small. The radius of the target circle subtends 16.4 minutes at the eyepiece of the 8X telescope.

Definition is measured by adjusting the telescope for best focus and judging whether pattern 20 is "clearly resolved." Each line pair of pattern 20 subtends an angle of 0.40 minutes at 35 ft. with the unaided eye. The pattern subtends 3.2 minutes of arc at the eyepiece of the 8X telescope (18.8 line pair/deg.). A person with normal vision should be able to resolve 1 minute (60 line pair/deg.).

Before discussing advantages and disadvantages of these Z87.1 test methods it is worthwhile to consider some of the fundamental limitations to measurement accuracy.

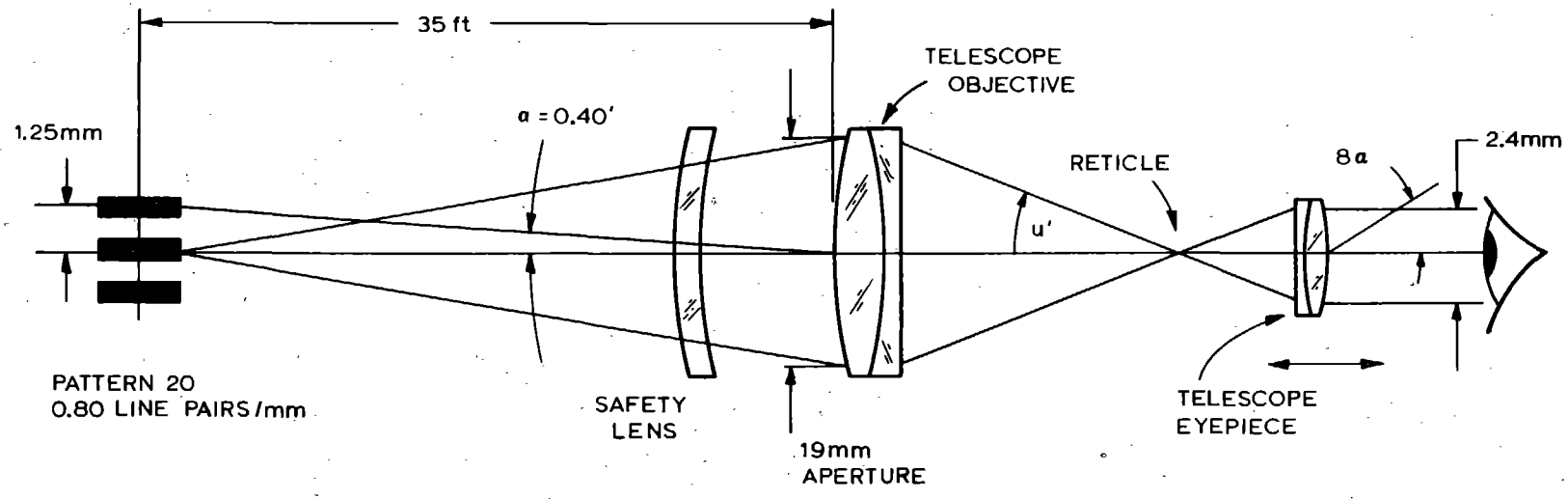

Figure 87. Z87.1 test telescope viewing bar pattern on resolution chart used for definition test.

Physical Limitations of Optical Tests

Diffraction--

The image of a point source formed by a perfect optical system will not be a point but a finite size disc with a series of bright and dark rings surrounding the disc. This image is called the diffraction pattern or the Airy disc. The diffraction pattern resulting from the finite aperture of an optical system places a limit on the maximum resolution obtainable from the optical system. See Ref. 24, pp. 135-141 and pp. 290-325 for an excellent discussion of the physical limitations of optical systems and image evaluation.

In the next two sections we evaluate for the Z87 case the limits to "depth of focus" and "image sharpness" caused by diffraction.

Depth of Focus, Longitudinal Resolution--

Figure 88 shows the Z87 test telescope testing a nominally plano lens which in the drawing actually has a slight negative power, resulting in an image shift ΔL. How small a value of ΔL can we reasonably expect to be able to measure? We designate by ΔL_m this minimum detectable image shift. The Rayleigh Limit indicates that the minimum amount of image shift or defocus ΔL_m detectable by a trained observer is, for lenses in air, given by (see reference 24)

$$\Delta L_m = \pm \lambda/2 \sin^2 u' \qquad (102)$$

For small u', sin u' = tan u' = A/2i, hence

$$\Delta L_m = \pm 2\lambda \left(\frac{i}{A}\right)^2 \qquad (103)$$

For a typical Z87 test telescope A would be 19 mm and i might be 200 mm. Then for λ = 0.55 μm, the "depth of focus" is

$$\Delta L_m = \pm 0.12 \text{ mm} \qquad (104)$$

We can also calculate the minimum detectable lens power of a nominally plano lens, which we call P_m. P_m is simply that power of a lens being tested which would result in an image shift ΔL_m given above. If we let P_o be the power of the telescope objective, P_c the combined power of the nominally plano lens and objective and assume the Z87.1 target is infinitely distant (because doing so simplifies the equations but doesn't change the results) we can write:

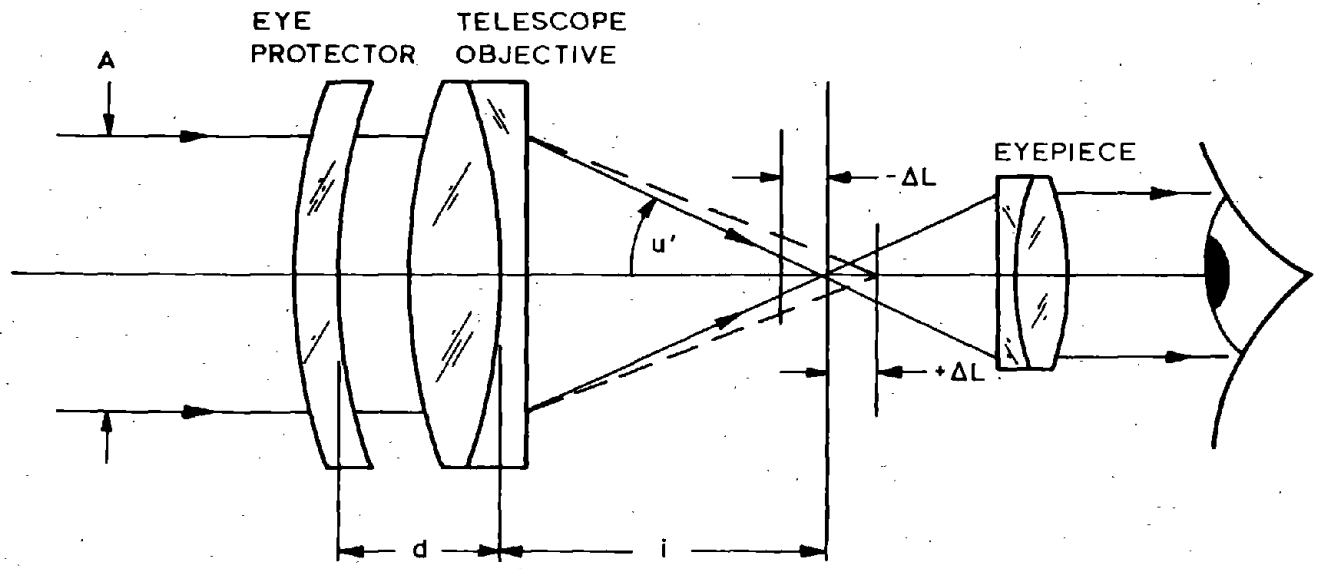

Figure 88. Longitudinal resolution for Z87.1 test telescope.

$$P_o = \frac{1}{i}, \qquad P_c = \frac{1}{i + \Delta L_m} \tag{105}$$

Hence

$$\Delta P = P_c - P_o = \frac{1}{i + \Delta L_m} - \frac{1}{i} \tag{106}$$

$$= \frac{i - (i + \Delta L_m)}{(i + \Delta L_m) i}$$

But since $\Delta L_m << i$,

$$\Delta P = P_m \approx \frac{\Delta L_m}{i^2} = \pm \frac{2\lambda}{A^2} \tag{107}$$

(It was sufficiently accurate for our purposes here to assume that the telescope objective and safety lens are "thin" lenses and that the safety lens is placed close to the objective.)

So, for example, if

$$A = 19 \text{ mm} = 0.019 \text{ m}$$

$$\lambda = 0.55 \ \mu\text{m} = 0.55 \times 10^{-6} \text{ m}$$

then

$$P_m = \pm 0.003D \tag{108}$$

For comparison, the value of P_m corresponding to a depth of focus ΔL_m for a 2.4 mm pupil would be $\pm$ 0.19D and for a 5 mm pupil would be $\pm$ 0.044D.

It is not difficult to show that, for the conditions of testing near-plano lenses, P_m is also the accuracy limit to measurement of the lens power. Eq. (107) quantifies a basic trade-off in testing for power (and astigmatism); a large aperture must be utilized for accuracy, and this causes power variations of local zones of the safety lens to be averaged in the measurement.

Definition, Lateral Resolution--
The Raleigh Criterion and diffraction theory give for the separation h of two lines which are just resolved after being imaged by a lens system in air (see Fig. 89 and Ref. 24)

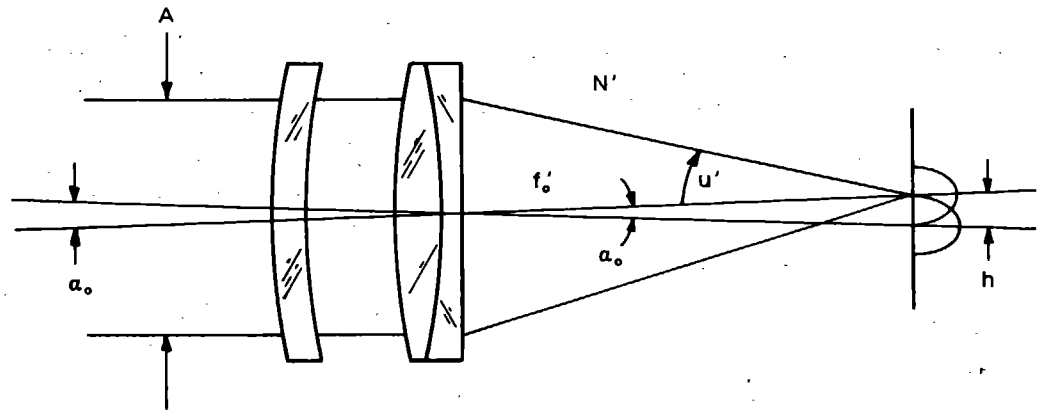

Figure 89. Lateral resolution for Z87.1 test telescope.

$$h = 0.50\lambda/\sin u' \tag{109}$$

As before, $\sin u' = \tan u' = A/2f_o'$, for small u',

so $$h = \frac{\lambda f_o'}{A} \tag{110}$$

This linear resolution h corresponds to an angular resolution α_o of

$$\alpha_o = h/f_o'. \tag{111}$$

Hence

$$\alpha_o = \lambda/A \tag{112}$$

for $\lambda = 0.55 \times 10^{-6}$ m

$A = 19 \times 10^{-3}$ m

$$\alpha_o = 0.029 \text{ milliradians} = 0.10 \text{ minutes} \tag{113}$$

For comparison the angular resolution of a 2.4 mm pupil for two lines gives 0.23 milliradians or 0.78 minutes.

As discussed above, the width of a line pair in Chart Pattern 20 subtends an angle of 0.40 minutes at the Z87 telescope, and hence, from (113), an angle 4 times the diffraction limit for a 19 mm aperture or approximately the diffraction limit for a 5 mm aperture.

To summarize this discussion of basic physical limitations of optical test methods, both the "longitudinal resolution" ΔL_m of eq. (103) and the "lateral resolution" h of (110) or α_o of (112) are determined basically by aperture diameter A since for practical reasons the wavelength λ cannot be varied greatly. Both types of resolution become better as aperture increases; "fast" lenses - those with large aperture - allow more accurate measurements to be made, with a resulting averaging of lens behavior over the aperture. We will consider the optimum aperture for testing in future work after taking into account the MTF (Modulation Transfer Function) characteristics of the eye and other factors.

Advantages of Present Telescope Test (Z87.1)

1. Low cost of instrumentation.

2. Measurements relatively easy to make.

3. Human visual system is used to evaluate effects of protective eyewear on visual resolution or definition.

Disadvantages of Present Telescope Test (Z87.1)

1. Measurements are subjective among various observers.

2. The phrase "clearly resolved" in the definition tests is not objectively or even subjectively defined.

3. 19 mm of the safety lens is being used whereas the maximum diameter of the pupil of the eye is 8 mm in dim light, 3 to 4 mm in bright light and 2 mm in sunlight.

4. Spectral distribution and intensity level of the target are not defined. These parameters affect the definition measurement. Sufficient intensity is not available to allow measurements on lenses or plates of high shade number.

5. The minimum optical quality of the telescope and observer's eye are not defined. There should be a specification on the target pattern that must be resolved by the observer when viewing through the telescope alone before testing any product.

6. The mounting of eye protector relative to the telescope (tilt and centration) is not defined. Decentration and/or tilt will have a significant effect on the prism measurement.

7. Power, astigmatism, prism and definition are not measured after the lenses are mounted in frames. Any optical effects introduced by stress or mounting geometry are thus not measured. For instance, the prism imbalance presented to the two eyes by the eye protector is not measured.

8. Calibration lenses are not available; calibration must be done indirectly although the method is very accurate.

9. The correct amount of astigmatism in an eye protector will only be obtained when the cylinder axis is parallel to the horizontal or vertical target lines unless the observer uses a different target or rotates the target or lens under test.

To elaborate on this point, the amount of power in an arbitrary meridian of a lens with astigmatism is given by

$$P_\theta = P_1 + (P_2 - P_1) \sin^2 \theta \qquad (114)$$

where P_1 is the meridian with the least power and P_2 is the meridian with the most power (90^o from P_1) and θ is the angle of the meridian measured from P_1 ($0 \leq \theta \leq 90^o$). See Figure 90.

Let $P_2 - P_1 = C$ (astigmatism) (115)

Then $P_\theta = P_1 + C \sin^2 \theta$

If the astigmatism axis makes an angle θ with the lines of the target, the measured astigmatism will be $P_2' - P_1' = C'$, where

$$P_1' = P_1 + C \sin^2 \theta$$

$$P_2' = P_1 + C \sin^2 (90-\theta) = P_1 + C \cos^2 \theta$$

$$P_2' = P_1 + C(1 - \sin^2 \theta)$$

$$C' = P_2' - P_1' = C(1 - \sin^2 \theta) - C \sin^2 \theta$$

Hence $C' = C \left[1 - 2 \sin^2 \theta\right]$ (116)

Thus if $\theta = 45^o$, $C' = 0$ and no astigmatism will be detected.

Improvements to Present Telescope Test

One practical disadvantage of the present telescope test is the 35 ft. distance between the target and telescope. This lack of compactness could be overcome by utilizing a target at the focal plane of a collimator in front of the telescope. The target would have a line spacing so that the angle subtended by one cycle of the target at the telescope objective would be the same as that of the present target viewed from 35 ft. Figure 91 shows such a set-up.

The optical quality of the telescope and observer's eye with regard to definition or acuity and astigmatism should be defined. The minimum acceptable definition and maximum acceptable astigmatism measured by the observer when viewing the target through the telescope without an eye protector in front of the telescope could be defined.

A different frequency target should be selected so that the definition test is a "go - no go" test (resolved or not resolved rather than "clearly resolved"). Line targets should be arranged every 22.5^o so that the maximum angle the cylinder

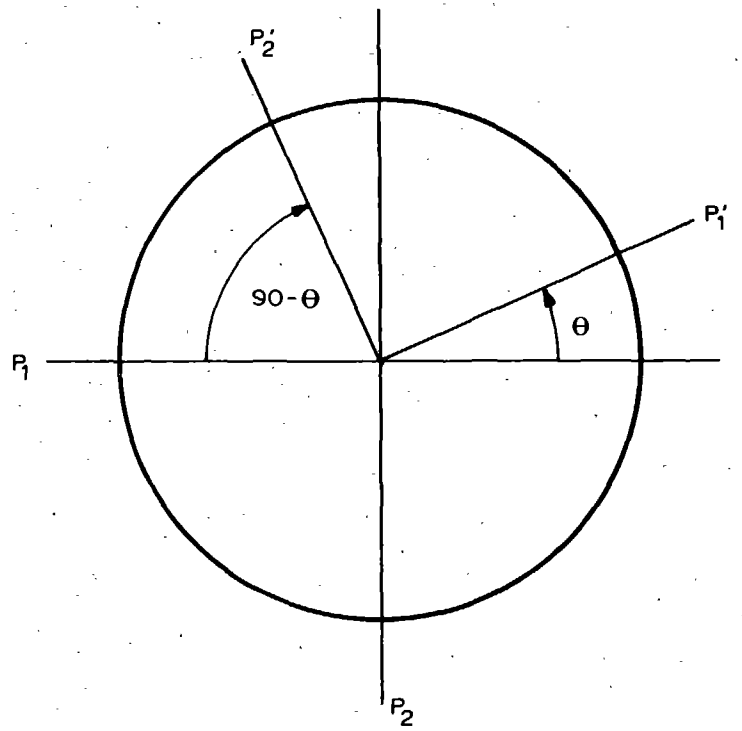

Figure 90. Diagram illustrating relationship between actual astigmatic axes P_1 and P_2 and the axes P_1' and P_2' of measured astigmatism.

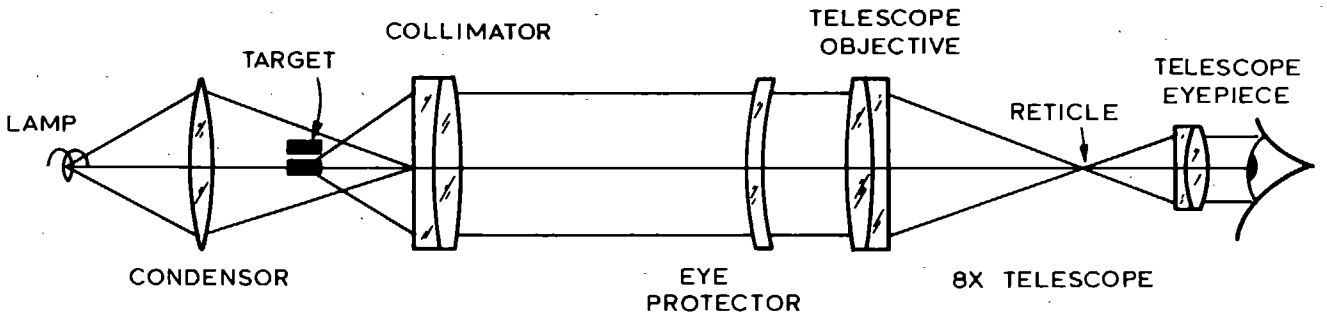

Figure 91. Optical schematic showing replacement of the present Z87.1 distant target by a target in the focal plane of a collimator.

axis can make with a target is 12.25°. Since the measured astigmatism is given by $(1-2 \sin^2 \theta)C$ and the maximum θ is 12.25°, the measured astigmatism will be at least 91% of the true value. A possible target is shown in Figure 92.

In addition, it should be specified that the observer measure definition at the best average or compromise focus between the two astigmatic foci.

It would be helpful to define illumination of the target in terms of intensity and spectral distribution.

Some testing of finished protectors should be carried out. As a start, we would suggest the measurement of the prism imbalance presented to the eyes of a user by the eye protector. A possible test is that based on the German standard DIN 4646, June 1974, but modified to use a He-Ne laser light source. Figure 93 shows the test set-up. A light beam 6 mm in diameter is divided into two parallel beams separated by the average interpupillary distance. The two beams pass through the eye protector and are brought to a common focus on the optical axis of the lens if there are no prism effects in the eye protector. If prism is present, one or both spots on the screen will be displaced from the center of the screen. An area is defined on the screen corresponding to the prism imbalance tolerance. Both spots must lie within the area for the eye protector to pass the test.

If the eye protector deviates a beam by an angle ε, then the displacement h in the focal plane is given by

$$h = \varepsilon f \tag{117}$$

Now prism power in diopters is 100ε - see eq. (99) - so if f = 1m, power of 1/16 prism diopter corresponds to a value of h = 0.625 mm. The diffraction-limited spot diameter d of a circular aperture is

$$d = 1.22\frac{f\lambda}{A}, \tag{118}$$

so for A = 6 mm, λ = 0.633 μm, (He-Ne laser)

$$d = 0.129 \text{ mm} \tag{119}$$

which is adequately small to allow measurement of h.

If we oversimplify, it might be said that the maximum allowable value of prism imbalance arising from two safety lenses should be 1/8Δ, since individual prism tolerances are 1/16Δ. But effects of inter-pupillary distance (PD),

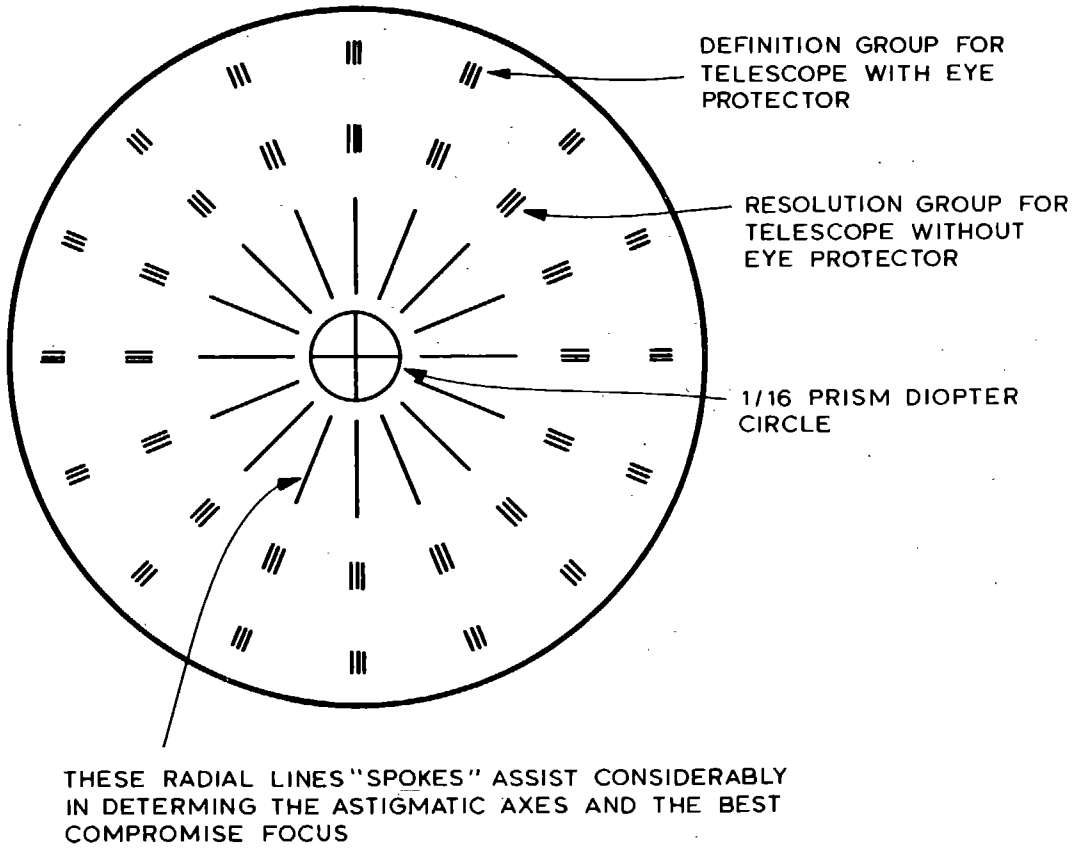

Figure 92. A target for performing Z87.1 telescope tests which might make the operator's job easier.

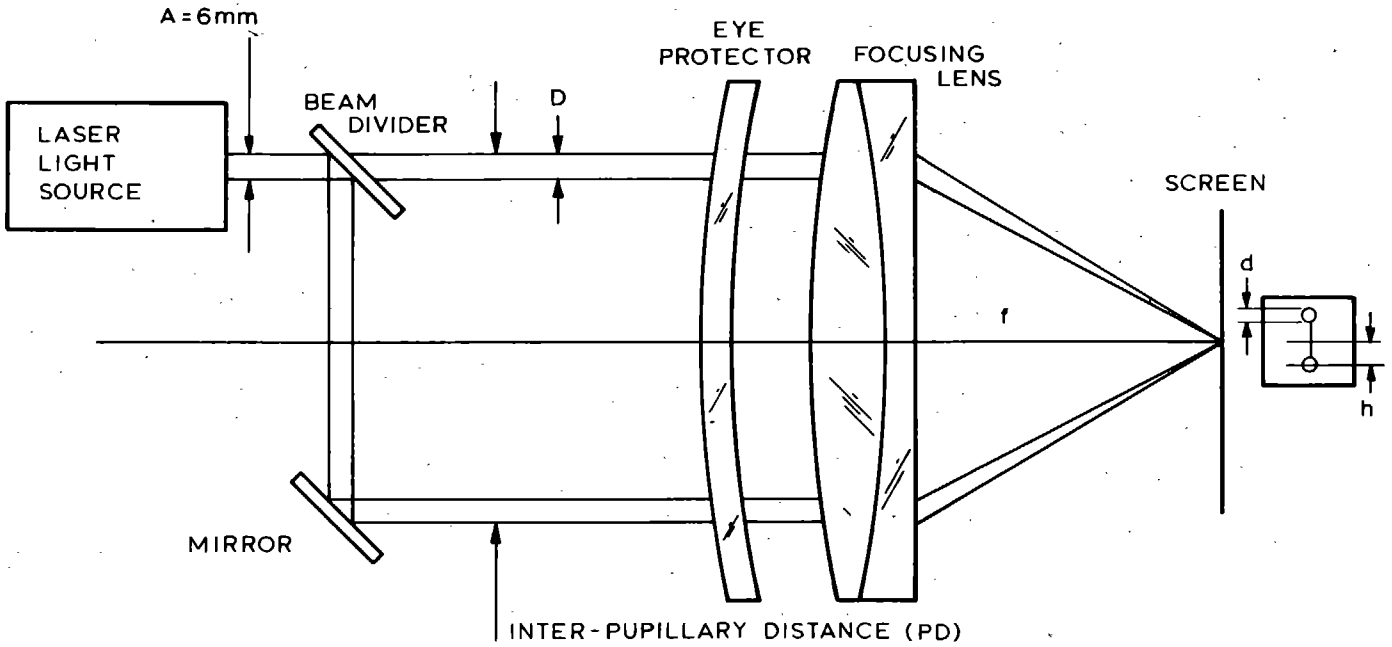

Figure 93. Optical schematic for prism-imbalance testing device with suggested modifications from the test of DIN 4646.

frame face-form, and pantoscopic tilt may cause the imbalance to vary, as may the curvature of items such as face shields or some goggle windows.

The use of a beam-splitting arrangement with a gas laser source instead of a more conventional light source as employed in DIN 4646-1974 is to avoid wasting light so that shade numbers as high as possible may be measured. The suggested imbalance set-up of Fig. 93 can, of course, measure prism as well as prism imbalance, and so might do this well for welding plates.

We recommend that the device shown in Fig. 93 be breadboarded and that a wide variety of eye protective devices be measured to establish the exact capability of the device and to provide information useful for establishing a future prism imbalance tolerance. It should be remembered that many eye protectors are worn over prescription glasses, which may also have prism imbalance - see ANSI Z80.1 - 1972, Requirements for First Quality Prescription Ophthalmic Lenses. Any future imbalance limit may need to account for this case.

Conclusions

While these recommended changes would improve the present telescope test (Z87.1) the measurements, especially for definition, would still be subjective. An objective test method is therefore very desirable if practical.

Survey of Non-MTF Test Methods

There are a number of non-MTF test methods that are well known and in common use. We have considered the following methods for which we will give a brief description, the advantages and disadvantages, and a reference. Personnel working on this contract have "hands-on" experience with all these methods except the Hartmann test which is used primarily on large astronomical objective lenses or mirrors.

Star or Pinhole Test--
This consists of a visual examination of the image of a point source (Ref. 25).

Advantages--
1. Low cost.

Disadvantages--
1. Requires skilled observers.
2. Very subjective (especially definition).
3. Difficult and costly to automate.

Resolving Power Test--
This consists of the visual examination of the image of line targets. (Ref. 26) The present Z87 telescope test is an example of this type of test. Its advantages and disadvantages have been discussed above.

Ronchi Test--
The image of a grid formed by the optical system under test is allowed to fall onto a second grid (or reimaged onto the object grid). The resulting moire pattern is analyzed. (Ref. 27)

Advantages--
1. Low cost.

Disadvantages--
1. Requires skilled observers.
2. Definition not measured.
3. Analysis complex - the fringes seen correspond to the derivative of the wave front.
4. Difficult and costly to automate.

Foucault or Knife Edge Test--
The image of a pinhole or slit is cut with an edge and the resulting illumination of the system aperture observed. (Ref. 28)

Advantages--
1. Low cost.

Disadvantages--
1. Requires skilled observers.
2. Analysis complex.
3. Definition not obtained.
4. Costly to automate.

Twyman-Green Interferometer--
The eye protector is placed in the test arm of the interferometer and the resulting fringe pattern is analyzed (Ref. 29)

Advantages--
1. Effects of various parts of aperture can be obtained with one measurement.

Disadvantages--
1. Analysis complex and relatively long.
2. Basic instrument costly.
3. Sensitive to misalignment and vibration.
4. Automation complex and very costly.

Shearing Interferometer--
Part of the wavefront transmitted by the eye protector is shifted laterally (sheared) and allowed to interfere with the

non-shifted part of the wavefront. The resulting interference pattern is analyzed. The interference pattern corresponds to the derivative of the wavefront. (Ref. 30)

Advantages--
1. Effects of various parts of the aperture can be obtained with one measurement.

Disadvantages--
1. Analysis complex and relatively long.
2. Automation complex and very costly.

Hartmann Test--
This method is similar to theoretical ray tracing. A set of small diameter beams are distributed over the aperture of the optical system under test. The deviations of the beams are measured and analyzed. (Ref. 31).

Advantages--
1. Low cost if a non-automatic system is used.

Disadvantages--
1. Definition not measured.
2. Costly to automate.
3. Analysis of ray deviations complex.

Optical Bench Tests--
The lens is placed on a lens bench in front of a collimator and physical measurements are made from the surfaces of the optical system to the image. (Ref. 32)

Advantages--
1. Medium cost.

Disadvantages--
1. Skilled observers required.
2. Time consuming.
3. Definition subjective (bar target).
4. Costly to automate.

Point, Line, Edge Spread Function--
The image of a point or a line is cut by an edge, or scanned by a pinhole or slit. The change in energy with position of the edge or aperture is measured. (Ref. 33)

Advantages--
1. Medium cost.

Disadvantages--
1. Requires skilled technicians for manual operation.
2. Time consuming.
3. Costly to automate.

4. Becomes complicated when axial astigmatism is present, since measurements must be made in the two principal meridians which must first be located.

Encircled Energy--
An image of a point source formed by an optical system is sampled by a small aperture. The position of the aperture for maximum energy and the amount of the maximum energy are analyzed. (Ref. 24)

Advantages--
1. Medium cost.
2. Easily automated.
3. Analysis relatively simple.
4. Non-subjective.
5. Measuring time is fast.

Disadvantages--
1. Lens properties measured are the average values for the aperture diameter of the lens actually employed in the test. If it is desired to test an entire 50 mm diameter lens using, say, a 5 mm aperture so as to explore zonal variations then approximately 100 measurements must be made. Alternatively, a smaller number of sites may be checked - a sampling method is employed - or some form of automatic scanning method may be used.

2. The amount of encircled energy will correlate with bar-chart resolution (Z87 "definition") but not in a simple one-to-one manner.

A need at AO for accurate objective determination of optical properties of plano lenses caused a device for measurement of encircled energy to be breadboarded for that purpose. That work was in progress before issuance of the NIOSH Request for Proposal which resulted in this contract, so the work reported here was not carried out under this contract. Nevertheless, we feel that knowledge of this work is of advantage to NIOSH since it allows consideration of a breadboarded system which worked rather than a system concept which has never been tried. The system as breadboarded is shown in Figure 94 and will now be described.

A collimated 1 mm beam from a helium-neon gas laser is expanded to a 19 mm diameter beam by lenses L1 and L2. The expanded beam passes through the beamsplitter and eye protector and is brought to a focus on the surface of the semi-transparent mirror M1 by a focusing lens L3. Part of the light is transmitted by mirror M1 and part is reflected back through the focusing lens L3 and eye protector to the beam divider. Part

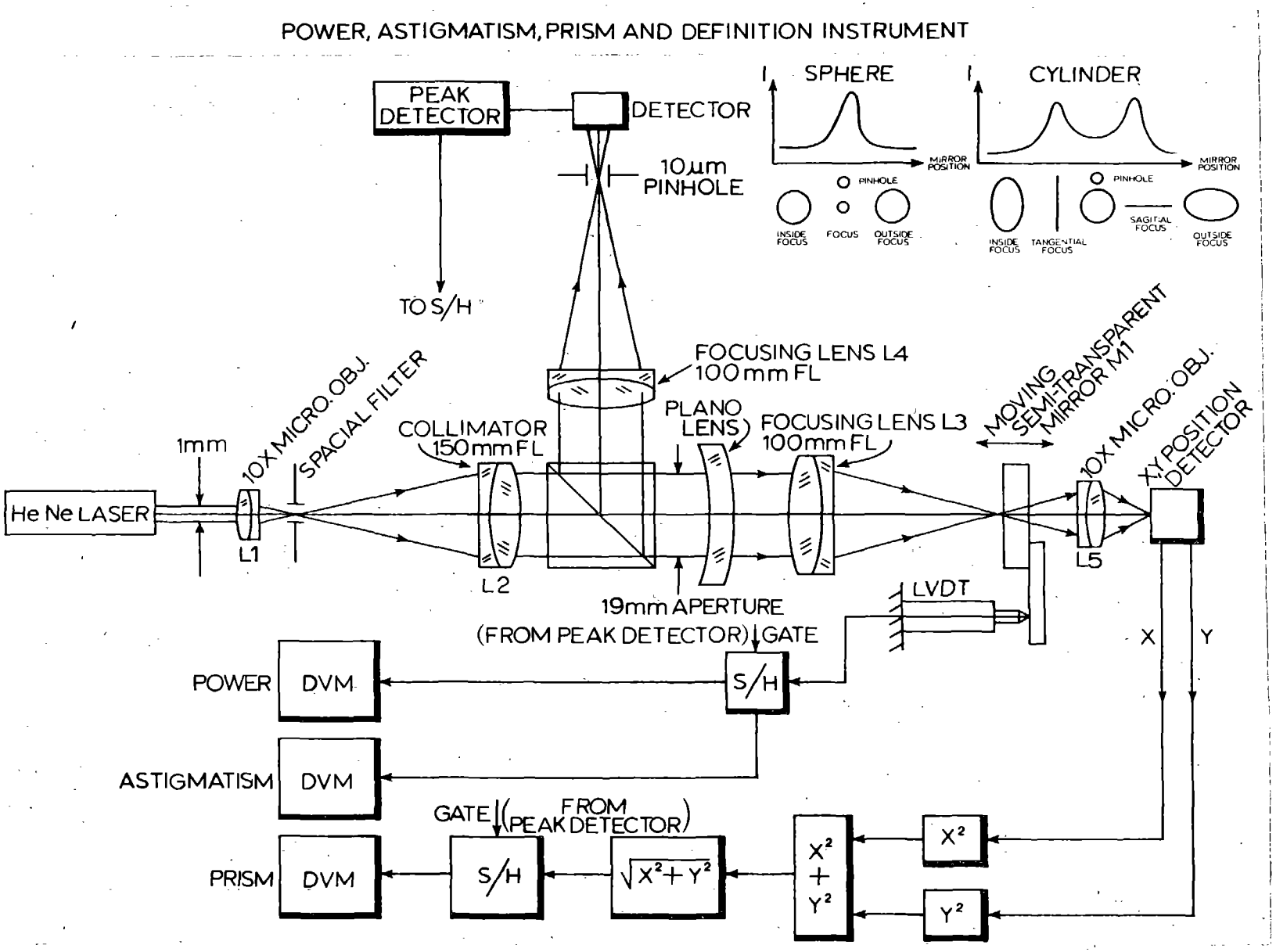

Figure 94. Schematic for possible objective test device for power, astigmatism, prism and definition by encircled energy.

of this return beam is reflected to focusing lens L4 which brings the beam to a focus on the pinhole. Mirror M1 is driven back and forth and its position is monitored by a linear variable displacement transducer (LVDT).

If the eye protector has no astigmatism, the size of the image at the pinhole will be smallest when mirror M1 is at the focus of lens L3. Hence the energy measured by the detector will be a maximum. The output of the LVDT at this point can be made to give the power of the plano lens. A peak detector circuit and sample and hold (S/H) will drive a digital voltmeter (DVM) calibrated to read directly in lens power.

If the eye protector has astigmatism, the image at the pinhole will start out as a large ellipse, come to a line focus, go to a large circle, come to a line focus at right angles to the first line focus and then go to a large ellipse. Since the pinhole diameter is selected to be less than the image line width, the detector will give two peaks. The difference between the two corresponding lens power values equals the astigmatism, and the average of the two values gives the lens equivalent sphere power.

If the definition of the lens is poor the size of the diffraction pattern will be increased and the peak energy passing through the pinhole (encircled energy) will be reduced. Encircled energy is a standard measure of lens quality and can be correlated to resolution and MTF.

If the eye protector has prism the position of the image on the surface of mirror M1 will be displaced. Lens L5 and mirrors M2 and M3 relay this image onto the surface of an X,Y position detector which gives the prism magnitude.

Performance of the breadboard was as follows:

Attribute	Accuracy	Range
Power	$\pm$ 0.003D	$\pm$ 0.125D
Astigmatism	0.003D when greater than 0.03D	0-0.125D
Prism	$\pm$ 0.005Δ	0-0.1Δ

No effort was made to correlate numerically the amount of encircled energy with Z87.1 definition although it was observed that lenses with good definition gave high encircled energy and vice versa as would be expected.

Several important features of the optical system shown in Fig. 94 should be noted:

1. The system of plano lens under test, lens L3, and moving mirror M1 is retroreflective when M1 is at the focal plane of the combination if the plano lens has sphere power or for each focal line when the plano lens has astigmatism. Hence the focused light reaching the 10 μm pinhole is always on the pinhole axis. This means that it is not necessary to move the pinhole either back and forth along the optical axis or in directions transverse to the optical axis to be sure of reading the maximum amount of encircled energy (plano with sphere power) or the two maxima (plano with astigmatism).

2. The system has azimuthal symmetry and it is not necessary to know the principal meridians of astigmatism in order to determine the amount of astigmatism.

3. When the tangential and sagittal foci are too close together the signal peaks from the encircled energy detector merge and it is not possible to measure astigmatism, particularly if lens definition or resolution is poor so that the peaks are broadened for this reason. It was possible in the breadboard to measure astigmatism of less than half the Z87.1 tolerance as shown in the performance listing above. Optimization of pinhole diameter might decrease the minimum astigmatism measurable since 10 μm is about 2½ times the diffraction-limited spot diameter for the 100 mm focal length, 19 mm beam diameter, and 633 nm He-Ne laser of Fig. 94 (see Eq. 118).

SUBTASK 2B: MTF TEST METHODS

Introduction

The image formed by a lens or optical system of an object with a sinusoidal intensity distribution will also have a sinusoidal intensity distribution. The image will have the same contrast as the object at low spatial frequencies (large patterns). The contrast will go to zero as the spatial frequency approaches the diffraction-limited resolution.

The modulation is defined as the ratio of the maximum intensity minus the minimum intensity to the maximum intensity plus the minimum intensity:

$$\text{Modulation} = \frac{I_{MAX} - I_{MIN}}{I_{MAX} + I_{MIN}} \qquad (120)$$

The modulation transfer function of the lens or system is defined as the modulation of the image M_i divided by the modulation of the object M_o.

$$\text{Thus} \quad MTF(\nu) = \frac{M_i}{M_o} \equiv M(\nu) \qquad (121)$$

where ν is the spatial frequency of the sinusoidal test pattern. If a high contrast object is used, then $I_{MAX} >> I_{MIN}$, $M_o = 1$, and the MTF is given by M_i.

Quoting W. Smith: "A plot of MTF vs. frequency is an almost universally applicable measure of the performance of an image-forming system, and can be applied not only to lenses, but to films, phosphors, image tubes, the eye and complete systems. One particular advantage of MTF is that it can be cascaded by simply multiplying the MTF's of components which are not directly connected (lenses that are separated by a diffuser of some sort since the aberrations of one component may compensate for aberrations in another) to obtain the MTF of the system." Smith's book, (Ref. 24, pages 308 - 324) contains a good brief introduction to MTF ideas.

MTF at a single frequency is being used by Kodak and Polaroid to measure the definition of multi-element camera lenses on the production line (Ref. 35). It is also a universally accepted technique for measuring image quality in the precision optics industry. MTF methods have been used at AO on multi-element camera lenses with good correlation to photographic and visual image quality.

Before studying suitable MTF test methods for plano eye protectors, it is necessary to consider the requirements of the human eye for good vision in terms of MTF concepts.

MTF of the Eye

The MTF of the human eye is discussed very thoroughly by van Meeteren (Ref. 36). The human eye is diffraction limited when the pupil is less than 1 mm in diameter. Longitudinal chromatic aberration is the dominant aberration in white light and reduces the diffraction-limited MTF considerably when the pupil is greater than 2 mm. The effect of spherical aberration, coma, and astigmatism is negligible for pupils less than 3 mm and always moderate compared to longitudinal chromatic aberration.

In order to help in selecting appropriate MTF test parameters, we will consider the case where the eye protector degrades the MTF by the same amount that 1/4 wave defocus (the Rayleigh Criterion) degrades the MTF of a perfect lens whose aperture and focal length are the same as the eye. In addition, we will make the calculation for a spatial frequency corresponding to 20/20 Snellen acuity, since that value is normally considered to signify good vision.

The pupil of the eye can range from 8 mm in very dim light to less than 2 mm under very bright conditions. We shall

choose a 3 mm pupil since it represents a bright light condition typical for well-lighted indoor conditions.

The unaccommodated theoretical eye has a focal length f of 16.7 mm (Ref. 37) in vitreous humor of refractive index $\eta = 1.336$. A diffraction-limited lens has a spatial frequency ν_o corresponding to its limiting resolution ("cut-off frequency") given by (Ref. 24, p. 319)

$$\nu_o = \frac{\eta A}{f\lambda} . \tag{122}$$

Hence for the 3 mm pupil chosen,

$$\nu_o = \frac{1.336\ (3\ \text{mm})}{16.7\ \text{mm}\ (0.55 \times 10^{-3}\ \text{mm})}$$

$$= 436\ \text{cycles/mm at the retina} \tag{123}$$

for a sinusoidal object pattern of high contrast. This corresponds to a linear image size of 1/436 = 2.29 μm/cycle on the retina, and to an angular image size of

$$2.29\ \mu\text{m}/16.7\ \text{mm} = 1.37 \times 10^{-4}\ \text{radian/cycle}$$

$$= 0.47\ \text{minutes/cycle.}$$

Now 20/20 Snellen acuity corresponds approximately to resolving an angular frequency of 2.0 minutes/cycle since the distance between bars on the Snellen "E" subtends 2.0 minutes at the test distance. Hence the spatial frequency corresponding to 20/20 is 0.47/2.0 = 0.24 of the limiting spatial frequency ν_o.

It is necessary to take into account the fact that the Snellen "E" is approximately a bar chart with square-wave intensity modulation rather than a sinusoidal pattern. If the MTF for a square wave is designated by $S(\nu)$, then(Ref. 24, p. 318)

$$S(\nu) = \frac{4}{\pi}\left[M(\nu) - \frac{M(3\nu)}{3} + \frac{M(5\nu)}{5} - \ldots\right] \tag{124}$$

For a diffraction-limited aperture where $\nu = 0.24\ \nu_o$, from Fig. 11.15 of Ref. 24 or Table 69 of Ref. 38

$$M(\nu) = 0.71$$
$$M(3\nu) = 0.17$$
$$M(5\nu) = 0, \text{ etc.}$$

So

$$S(0.24\ \nu_o) = \frac{4}{\pi}\left(0.71 - \frac{0.17}{3} + 0\ \ldots\right)$$

$$= 0.83 \qquad (125)$$

The decrease in $M(0.24\ \nu_o)$ for 1/4 wave defocus is from 0.71 to 0.59, and for $S(0.24\ \nu_o)$ from 0.83 to 0.69.

If we were to adopt the Rayleigh Criterion (1/4 wave defocus) for the maximum image degradation caused by the eye protector, then $M(0.24\ \nu_o)$ for the eye protector at the spatial frequency corresponding to 20/20 Snellen acuity would have to be 0.59/0.71 (or 0.69/0.83) and hence equal to 0.83 of the value with no lens in the system when a 3 mm aperture is used to simulate the effect of a 3 mm pupil for the eye.

DEFINITION AND MTF OF A SAFETY LENS

In the material immediately above we have determined the degradation in MTF which would correspond to the Rayleigh Criterion ("sensibly perfect" imaging for a skilled observer) and found that the MTF of a safety lens would have to be 0.83 in a 3 mm pupil at the spatial frequency corresponding to 20/20 Snellen acuity. We need now to consider the change in MTF which is caused by a just-acceptable safety lens; i.e., a lens which causes pattern 20 of the NBS chart to be "just resolvable".

First, Z87.1 requires that pattern 20 be "clearly resolved" but that is a very difficult requirement to quantize. The tendency of operators is to judge between "resolved" or "not resolved" and we expect that most safety spectacle lenses are accepted or rejected on this basis. In addition, the physiological data which are needed to quantify the results of this test are in terms of ability to resolve or not to resolve, so the work below will be on the basis of "resolvable" rather than "clearly resolvable".

The limiting spatial frequency ν_o is (eq. 122)

$$\nu_o = \frac{\eta A}{f\lambda} \qquad (126)$$

in line pairs per unit of length in the focal plane of the lens when A, f, λ are in the same units. Rather than work with line pairs/mm or cycles/mm it is convenient in many cases to work in terms of line pairs/degree, particularly for a zero-power lens or optical system. An angular subtense of θ for a very distant object corresponds to a lateral

distance $f\theta$ in the focal plane of a lens, so the number of cycles/radian ν_1 equals the number of cycles/mm, ν_0, times the number of mm/radian in the focal plane, f;

$$\nu_1 = \nu_0 f = \frac{\eta A}{\lambda} \tag{127}$$

and since we are interested in cycles/degree in air where $\eta = 1$, the limiting frequency ν_2 in cycles/degree is

$$\nu_2 = \frac{1}{57.3} \frac{A}{\lambda} \tag{128}$$

Let us now consider the Z87.1 telescope test for definition. Each line pair of pattern 20 subtends 0.40' at the unaided eye at 35 ft. Through an 8X telescope each line pair subtends 8(0.40') = 3.2'. It is our experience that most observers can resolve pattern 48 using the 8X telescope and well-illuminated NBS chart when no safety lens is placed before the telescope. This corresponds to an angular subtense of

$$\frac{20}{48} (3.2') = 1.33' \text{ per cycle.}$$

Since the 8X telescope has a 19 mm entrance pupil its exit pupil is 19/8 = 2.4 mm which becomes the effective pupil diameter for the eye under lab lighting conditions.

Now 3.2'/cycle corresponds to 0.31 cycles/minute or 18.8 cycles/degree, while 1.33'/cycle corresponds to 0.75 cycles/minute or 45 cycles/degree. As shown by Fig. 95 below, a contrast of approximately 0.060 is required to resolve a square-wave bar-chart of 0.31 cycles/minute and a contrast of approximately 1 is required for 0.75 cycles/minute. These contrast values correspond to square-wave modulation values, $S(\nu_2)$, of 0.031 and 1 respectively. Now the limiting frequency ν_2 for a 2.4 mm aperture is, from (128),

$$\begin{aligned} \nu_2(2.4) = \frac{1}{57.3} \frac{2.4 \text{ mm}}{550 \text{ nm}} &= 76 \text{ cycles/degree} \\ &= 1.27 \text{ cycles/minute} \end{aligned} \tag{129}$$

To change from square-wave modulation $S(\nu_2)$ to sine-wave $M(\nu_2)$ we utilize the fact that, for pattern 20, 18.8 cycles/degree is approximately 25% of the limiting frequency given by (129), so we may neglect higher-order terms in eq. 124 and infer that

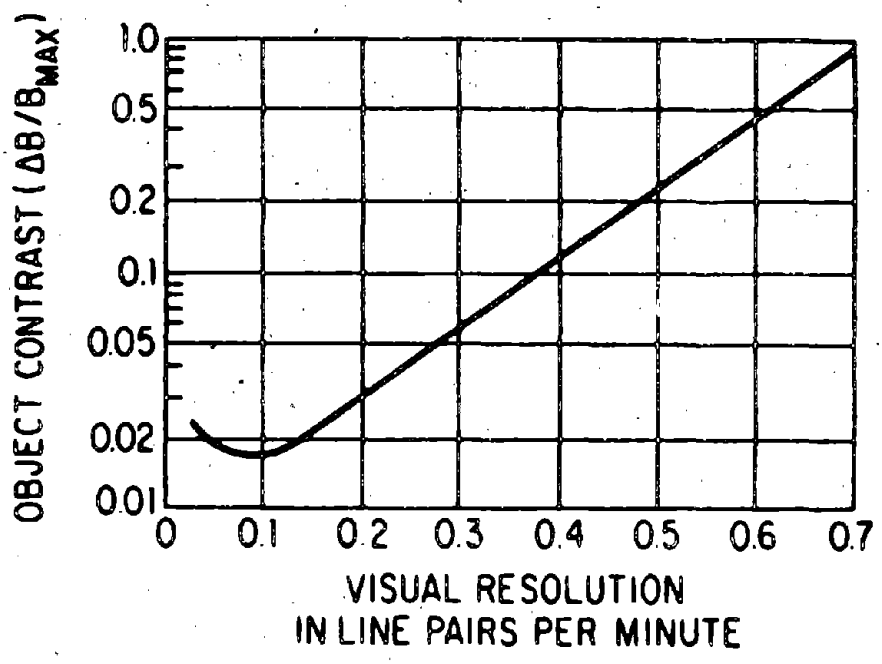

Figure 95. The object contrast ($\Delta B/B_{max}$) necessary for the eye to resolve a pattern of alternating bright and dark bars of equal width. (From. Ref. 24, p. 106)

$$M(18.8 \text{ cycles/degree}) = \frac{\pi}{4} S(18.8 \text{ cycles/degree})$$

$$= \frac{\pi}{4} (0.03) \approx 0.02. \qquad (130)$$

At the same time we know that $M(\nu_2) = 1$ when $S(\nu_2) = 1$ (Eq. 124).

In the paragraphs above we have calculated that image modulation values of ≈ 1 and 0.02 are required for the eye to just resolve patterns 48 and 20 of the NBS chart through the telescope with no safety lens or when a just-acceptable lens is placed in front of the 19 mm telescope aperture. We would now like to calculate the MTF of the safety lens responsible for causing pattern 20 to be "just resolvable".

In order to ascribe an MTF to the safety lens by itself we must assume that the optical effect of the lens across the 19 mm aperture is to introduce random errors in the wavefront of the telescope - see Ref. 24, pages 311-312. This means that any power error component has been nullified by refocusing before the definition is measured. It also means that the telescope must be quite well-corrected, which it evidently is because we have shown above that high image modulation (≈ 1) is required to resolve pattern 48 with no lens in the system.

With this assumption, we have, from Eq. 121, since in general

$$M_i = MTF(\nu)\ M_o, \tag{131}$$

then

$$M_i = \left[MTF_{eye}\ (18.8)\right]\left[MTF_{lens}\ (18.8)\right]\ M_o \tag{132}$$

Figure 96, from van Meeteren (Ref. 36) shows that the MTF of the eye at 18.8 cycles/degree (line pairs per degree - ppd in Fig.96) is 0.50 for a 2.4 mm pupil. The modulation M_o of the NBS high contrast target is approximately 1, so (132) becomes

$$0.02 = 0.50\left[MTF_{lens}\ (18.8)\right] 1$$

$$\therefore\ MTF_{lens}\ (18.8\ ppd) = 0.04 \tag{133}$$

for a "just-acceptable" lens which introduces random error in the wavefront. To give some idea of the magnitude of this effect, since 18.8 ppd is 25% of the limiting spatial frequency ν_2(eq. 129) for a 2.4 mm pupil, the effect on resolution of pattern 20 corresponds very roughly to that of a defocus of 3 Rayleigh Limits, as may be seen by examining Fig. 11.16 in Ref. 24. From the argument leading to Eq. 108, 3 Rayleigh Limits corresponds to a defocus condition of approximately 0.01 D, or about 1/12th of the range of + 1/16 D allowed for safety lens power. In our experience, 0.01 D is about 3 times the standard deviation of a trained observer, so the analysis above and experience seem to be in satisfactory agreement.

It should be pointed out that the numerical analysis carried out above in this section is very approximate in nature. The basic purpose of the analysis was to find out whether a safety lens which is just-acceptable for definition by the Z87.1 telescope test would cause a sufficiently large drop in MTF as compared to a perfect lens so that an MTF test could be suitable as a replacement for the definition test of Z87.1.

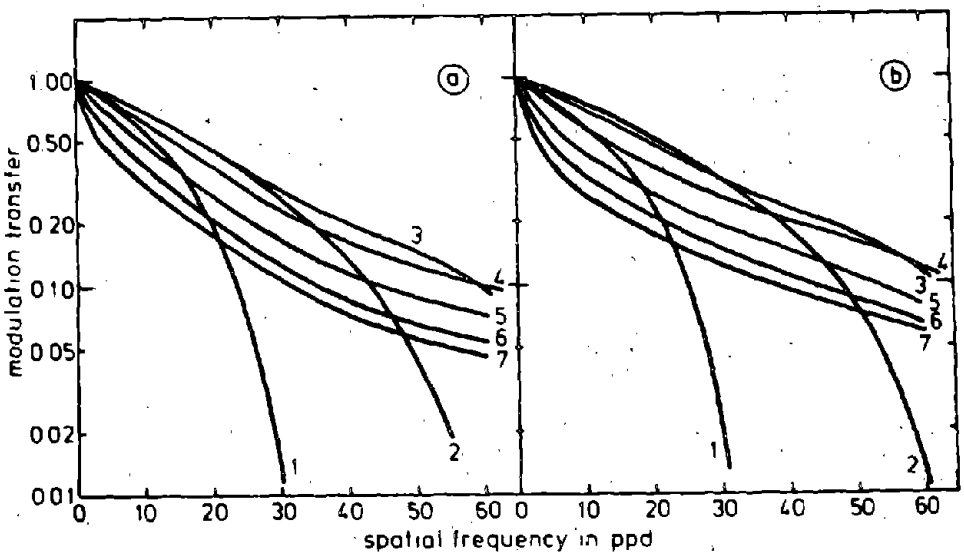

Figure 96. Foveal modulation transfer functions for different pupil sizes. (a) refers to vertical sine wave gratings, (b) to horizontal sine wave gratings. The latter is not affected by the foveal chromatic magnification error.

The MTF of a perfect (diffraction-limited) lens at a spatial frequency of 25% of its limiting frequency is 0.70 - see Fig. 11.15 of Ref. 24, and eq. (133) shows a decrease of MTF to 0.04 for a just-acceptable lens, so there is a readily-measurable decrease. In the next section we will comment on the implications of the approximate nature of the calculations above.

CHOICE OF A PRACTICAL MTF TEST

The approximate analysis of the previous section has shown that an MTF measurement for plano safety lenses may be a good objective test, but the analysis is not sufficiently exact to determine optimum test conditions. Observers vary, telescopes vary, the nature of wavefront errors introduced by the safety lens (after re-focusing to eliminate power contribution) will vary from lens to lens, and hence the shape of the MTF curve versus spatial frequency will vary from lens to lens. How, then,

would one go about determining whether a lens has suitably good resolution or Z87.1 definition?

It is, of course, possible to measure the complete MTF curve for a lens, choosing one aperture size of interest. This is a costly measurement to make, however, and those companies mentioned earlier who employ MTF measurement of lenses routinely do so at a single frequency which has been determined previously to best correlate with necessary performance attributes of the lenses. This simplifies and speeds measurement greatly and it is our contention that any worthwhile test should be economically reasonable to apply to 100% of production lenses so as to weed out all lenses whose resolution is unsatisfactory.

If one chooses to test at a single frequency, the question then arises as to choice of frequency. When one examines the MTF curves shown in Section 11.10 of Smith's book (Ref. 24), one is impressed by the variation in MTF at high frequencies caused by different types of aberration. For all types, however, the rate of change of MTF with frequency is monotonic and roughly proportional to the magnitude of the wavefront error for optical path differences of up to about one wavelength (4 times the Raleigh limit) when spatial frequencies are in the neighborhood of 5% to 20% of the limiting frequency given by Eq. (126). Such a range of spatial frequencies should be involved in any single-frequency test method for lenses having the degree of wavefront errors discussed above.

In addition, it is necessary to choose the area or areas of the safety lens to be tested. Z87.1 chooses the central 19 mm aperture. The pupil of the eye utilizes at any one time only a 2-8 mm diameter zone of the lens, and really only a 2-4 mm zone for high acuity vision, so the argument might be made that a lens should be scanned utilizing a small aperture and MTF or perhaps power variation plotted as a function of position. The ISO has proposed such a method in their Draft Proposal ISO/DP 4854, April 1976, for Draft Eye Protection Standard ISO/TC 94/SC 6 as an alternative to the telescope test. The method, while very sensitive, does not appear to the writer to be a practical one for testing any sizable fraction of the approximately 10^7 pairs of plano safety lenses produced per year in this country.

Proceeding pragmatically, our experience has been that users experience scarcely any problems from poor definition when lenses are substantially better than the requirements of Z87.1 - say pattern 28 or better - but that the subjectivity of the go/no-go decision which must be made relative to pattern 20 would allow lenses to reach the market which would cause complaints by some people. One can only pity the telescope operator who must make hundreds of decisions per shift!

On this basis, we would recommend that as an initial step a thorough measurement program be carried out on a large number of safety lenses, utilizing the present 19 mm aperture, to determine correlations between

1) definition as measured by the Z87.1 test.

2) MTF at one frequency after a preliminary experiment to determine an approximately optimal frequency in the range of roughly 5% to 20% of the limiting frequency.

3) percent of encircled energy as measured by the method discussed earlier.

Reasons for recommendation of the use of a 19 mm zone are to be able to correlate with the historical benchmark of the Z87.1 definition test and that this is the zone most used by the eye for critical vision. Results from this measurement program should lead to minimum acceptable levels of encircled energy and MTF which could be used in a new standard.

SUGGESTED MEASUREMENT EQUIPMENT

Earlier in this report a system (Fig. 94) was described which will measure sphere power, astigmatism, prism, and encircled energy for plano lenses. In that discussion we pointed out that encircled energy is a useful figure of merit for lens definition. We will proceed below to describe an additional modification of the system which will allow it to make the most meaningful single-frequency MTF measurement of a lens at the same time the other parameters are measured; this technique should allow a practical correlation to be obtained between MTF and encircled energy.

The modification (see system schematic diagram, Fig. 94) is to add elements so as to allow MTF measurement. A 45^{o} beam-splitter is placed between the beamsplitting cube (in the center of Fig. 94) and lens L4. A fraction of the beam is then diverted to the MTF measuring system shown in Fig. 97 below.

Before proceeding to describe operation of the modified system we should describe the consequences of lens astigmatism when making MTF measurements. Orientation of the cylinder axis of astigmatism makes no difference to the amount of encircled energy measured at best compromise focus through a round pin-hole, although magnitude of the astigmatism does. MTF, however, will very greatly depend on the alignment of the cylinder axis with the axis of the sinusoidally-modulated straight "lines" and on whether the focus position chosen corresponds to best focus for one axis. When we consider the

wearer of safety lenses, he or she has little choice of either the axis of cylinder or the orientation of objects which constitute the visual task at work. It is our opinion, then, that the measurement of MTF, amount of encircled energy, or Z87.1 definition should be made at the best compromise focus between the two axial astigmatic foci, since that represents the best average condition for the wearer with normal vision.

Conceptually, measurement of MTF at one spatial frequency involves imaging a sinusoidally-modulated grating with a lens to be tested and measuring the modulation of the image of the grating by scanning the image with a narrow slit and detecting the amount of energy transmitted by the slit as it traverses the image. Because of the reversibility of passive optical systems, equivalent results may be obtained by using a narrow slit as object, and traversing a sinusoidal grating across the slit image - the slit image being the line spread function of the lens under test. It is more convenient for our use, however, to scan the point spread function of the lens with the sinusoidal grating since the source for all the other measurements is the spatial filter pinhole. This is a proper measurement of MTF since the line spread function of an optical system is simply the summation of many point spread functions and is appropriate because of our choice of making the measurement of MTF at the best compromise focus.

The system of Figure 97 will allow measurement of MTF of the plano eye protector at one spatial frequency and one wavelength. An experiment will need to be performed to determine an optimum frequency to be used, as discussed above, and provisions for easy interchange of different gratings should be made. Since eye protectors are singlet lenses, MTF at any one wavelength is adequate to determine their performance at other wavelengths. The grating position should be adjusted so that the grating is optically conjugate to the aperture used for encircled energy measurement. Control logic should be such that when the moving mirror is at the best compromise focus so that encircled energy is maximized (sphere power) or at the compromise focus (astigmatism), then MTF is measured.

From Eq. 126, the limiting spatial frequency ν_o for a 19 mm aperture and a lens of 100 mm focal length in air (L6 in Fig. 3) at the HeNe laser wavelength of 633 nm is

$$\nu_o = \frac{19}{100 \times 633 \times 10^{-6}} = 300 \text{ cycles/mm.}$$

So recommended trial frequencies of 0.05 ν_o to 0.20 ν_o would require gratings of 15 to 60 cycles/mm.

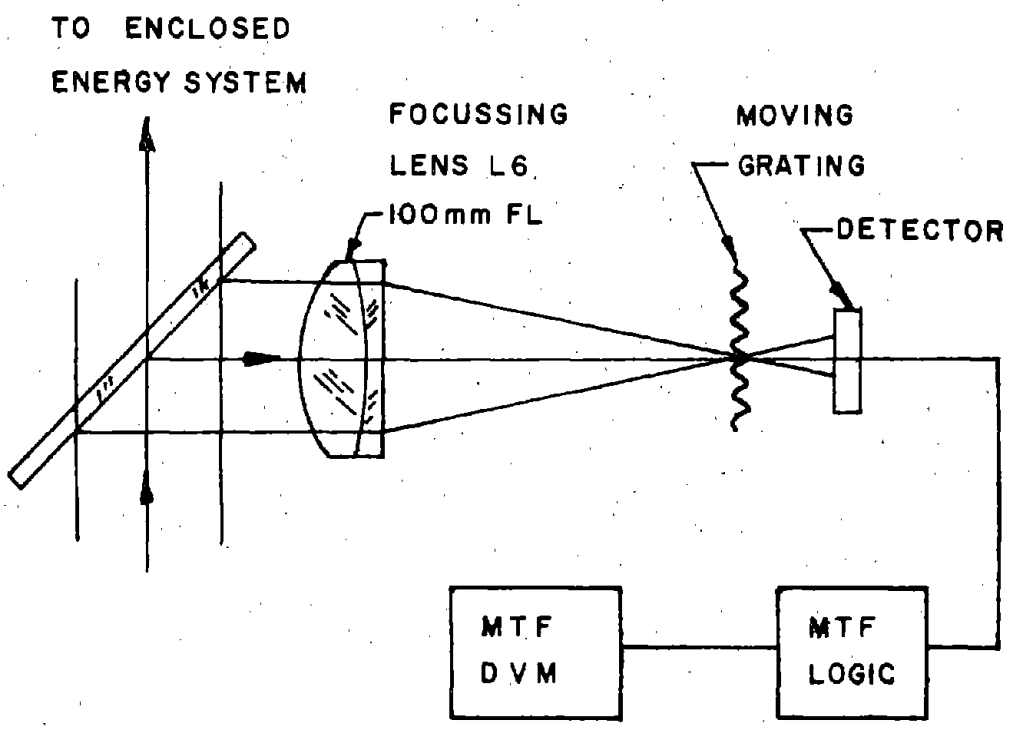

Figure 97. Additional optical arm for measurement of MTF of plano safety lens.

Addition of the elements of Fig. 97 to the system of Fig. 94, should allow the combined system to measure power, astigmatism, prism, encircled energy, and MTF objectively and provide data for correlation with results obtained by present Z87.1 methods.

SUMMARY AND RECOMMENDATIONS FOR SUBTASKS 1 & 2

We have studied the optical requirements for plano eyewear from the point of view of maintaining high visual acuity for the large fraction (approximately 50%) of the industrial population whose acuity is 20/20 or better. The conclusion reached was that the present tolerances for sphere power (± 1/16D), axial astigmatism (1/16D), and prism (1/16Δ) in a single lens given in Z87.1 are adequate.

It may be asked whether the tolerances are sensible. Broadly speaking, three general types of recommendations can be made about these three optical tolerances; loosen them, tighten them, or leave them alone.

If the tolerances were loosened, say, to ± 1/8D, 1/8D, and 1/8Δ for power, astigmatism, and prism instead of the present ± 1/16D, 1/16D, 1/16Δ of Z87.1, what would the consequence be? The maximum allowable mismatch for a pair of lenses would then exceed the comfortable power imbalance, the oblique power and astigmatism errors could become undesirably large, and the maximum magnification imbalance can be calculated to be approximately 0.9% which still would not be bothersome to any significant fraction of the population. Maximum axial prism imbalances could become 0.25Δ which seems undesirably large for an emmetrope. Since lenses meeting Z87.1 requirements are low in cost there does not seem to be any compelling reason from this direction for loosening tolerances. In addition, since the study under this contract of optical tolerances for plano eye protectors was completed, the writer (Mr. LaMarre) attended in May 1977 a session of Working Group 5 of the Sub-Committee ISO/TC 94/SC 6 during which experts from the United Kingdom, France, Germany, Italy, Czechoslovakia, Denmark and the U.S.A. discussed in detail the physiological limits on which the tolerances for plano optics should be based in order to maintain good acuity. Agreement was not reached on all points, but it is clear to the writer that doubling the Z87.1 tolerances would result in power imbalances, astigmatism, and prism imbalances equal to or in excess of the physiological limit guidelines which are being formulated by this ISO Working Group.

For reasons discussed in this report and again from evaluation of the expert opinions at the May 1977 ISO meeting, the three Z87.1 tolerances seem adequately tight for unmounted spectacle lenses which are glazed (inserted in frames) without matching. There is, then, no good reason to tighten them without a great deal of basic study about optical errors which occur for off-axis viewing purely as a consequence of eye protector design factors such as lens base curve, pantoscopic tilt, and faceform angle for spectacles, curvature of "wrap-around" protectors such as flexible-fitting goggles and faceshields, etc. For example, the information shown in Fig. 83 might suggest that a flatter base curve than a 6-base would improve lens performance off-axis, but no such conclusion can be reached because of numerous other performance factors which must be considered. It should be clear, then, that tolerances and lens design are interwoven and should ideally be based on binocular vision considerations. To study the problem thoroughly from that basis was beyond the scope of this contract but should be the direction of future work if any is needed. As a beginning, we have recommended that data begin to be accumulated on the magnitude of prism imbalance which wearers are currently tolerating. In order to study the magnitude of this imbalance we have recommended a simple experimental set up and measurements to permit a future requirement for prism imbalance to be selected, and also to serve as a first step in a desirable

program of changing all optical testing over to the basis of the protector as worn.

With regard to haze, we have recommended a reduction in maximum allowable haze of all optical materials, glass or plastic, to 3% from the present Z87.1 value of 6% which applies only to plastic lenses.

In the case of lens definition (resolution) we have concluded that the present requirement of Z87.1 may or may not be adequately stringent: the present subjective test method is so operator-dependent and judgmental as to make it difficult to determine whether resolution of pattern 20 is an adequate requirement or whether a tighter specification is desirable. For this reason we have recommended a correlation of results from the Z87.1 definition test with those obtained by two objective methods, encircled energy and a simplified single-frequency MTF method.

We have evaluated existing optical test methods in Z87.1 and recommended clarifications in definitions and improvements in test methods within the framework of subjective testing. We have then taken advantage of a large amount of prior research to recommend a test device for objective evaluation of power, astigmatism, prism, and resolution by encircled energy and MTF techniques. It was possible to perform analysis showing that a simplified form of MTF testing holds promise as a resolution test for safety lenses, but the construction of such a device, and subsequent implementation of an extensive program of testing safety products with the device, were clearly outside the scale of effort afforded by this contract.

SUBTASK 3: PHYSICAL DEFECTS

Physical defects which can occur in a lens other than the optical ones which have been discussed previously may be categorized as:

1. dimensional
2. improper transmittance, excessive haze, or incorrect color
3. cosmetic

The contract calls for classification of defects of the cosmetic type into categories commonly used for quality assurance - see for example MIL STD 105D. These categories are Critical, Major A, Major B, and Minor, and are defined in the contract as follows:

1. Critical -- A defect that is likely to result in a condition immediately hazardous to the safety and health of an individual using the protective device.

2. Major A -- A defect, other than Critical, that is likely to result in failure to the degree that the device does not provide any protection or a defect that reduces protection and is not detectable by the user.

3. Major B -- A defect, other than Major A or Critical, that is likely to result in reduced protection and is detectable by the user.

4. Minor -- A defect that is not likely to materially reduce the usability of the device for its intended purpose, or a defect that is a departure from established standards and has little bearing on the effective use of the device.

The ophthalmic industry has tended to group the following types of physical defects under the heading "cosmetic defects":

1. scratches
2. pits (digs)
3. fractures (cracks)
4. holes
5. bubbles
6. gray - incompletely polished areas
7. generating marks - a partially polished scratch
8. striae - irregular variation of refractive index resulting in waviness in images
9. inclusions
10. edge chips
11. weld lines (knit lines) - features peculiar to injection-molded lenses caused by uneven filling of the mold resulting in localized striae.

All lenses made exhibit some of these defects if examined with sufficient determination and the aid of microscopes, powerful light sources, dark-field illumination, Schlieren techniques, etc. The question becomes that of deciding at which level of magnitude each defect becomes unacceptable and further whether the nature and the potential consequences of the defect are such as to require classification as Critical, Major A, etc. The defects may affect visual performance noticeably if sufficiently severe and all in principle affect the protective performance since surface or interior flaws serve as stress concentrators which initiate fracture when a sufficiently great local tension is caused by an impact. Ideally, then, if we knew the effect on lens impact resistance for each type of defect versus the size, width, depth, radius... of the defect we could make judgments about acceptable magnitude and frequency of the defects; unfortunately, we do not know these things nor does anyone else, to our knowledge. The reasons are multiple for this lack of quantitative knowledge.

1. Any generated, ground, and polished optical surface contains a multiplicity of invisible flaws extending below the surface. While it is possible to render these flaws visible by laboratory techniques, the techniques themselves change the nature of the flaws and lens material in such a way that impact testing does not yield meaningful results relative to any individual visible defect selected to be tested.

2. Defects of the same type, e.g., scratches, differ in many respects among themselves.

3. Impacts of many different types actually occur to lenses when worn, and the relative importance of various types of defects presumably changes with the type of impact.

4. There is no really good test for impact resistance if we require that a good test stresses a surface uniformly. As an example, the AO proposal prior to this contract stated the following:

"Z87.1 impact resistance studies, where impact velocity is raised beyond the 16.3 fps of the 50 inch drop-ball test until breakage occurs, appear to indicate a three-fold stress system that "finds a weak link" in one of the surfaces, either: (a) elastic denting of the front surface only (bearing stress); (b) flexing of the central region of the lens causing flexural tension of the rear surface; and (c) flattening the lens to cause tangential rim tension. These stresses appear to have an approximate ratio of 10:3:1. In a circular lens, the areas probed are in the realm of 0.1%, 1% and 100% of the areas of the front, back and edge surfaces.

High speed cinematographic and strobe flash photos indicate a somewhat different fracture mechanism in the "high velocity" (in excess of 50 ft/sec) rupture of safety lenses: (a) elastic denting of front surface (as at lower velocity) dominates the system; (b) tension in the minus surface during reflection of the elastic wave provokes fracture when the region of the front surface was strong enough to resist fracture; and (c) edge fracture origin by an internally reflected elastic wave to the region of a Griffith flaw in the ground edge surface."

5. It is very difficult to produce in the laboratory defects such as scratches or digs which are reproducible in behavior in static strength or impact tests and it becomes more difficult to correlate these controlled defects with those which occur normally during production of lenses.

For these reasons, given the multiplicity of defect types, it has not been worthwhile to perform the extremely lengthy and expensive experimental program which would be required to provide useful data. The reader should be aware that AO has spent hundreds of thousands of dollars over a period of years in studying these phenomena and has barely scratched the surface. But there is another important reason which is hinted at by the use of the term "cosmetic defects"; customers will not on the average accept lenses with large defects and this marketplace pressure has resulted in fairly general agreement on defect magnitude and frequency limits at levels which do not appear in practice to be significant contributors to breakage of lenses worn in industry.

We can make the underlined statement above with considerable confidence for the following reason. We have examined over the course of some years hundreds of broken safety lenses. A large proportion of these were involved in impact incidents when worn, although some were broken after being dropped several feet onto concrete floors or other hard surfaces. More than 99% of these lenses were in very poor condition since they showed many heavy scratches, pits, and chips caused by user exposure to grinding, chipping, weld spatter, etc., and these defects were of much greater severity than any manufacturer allows in new lenses. Conversations we have had with personnel of other firms on the subject of breakage of ophthalmic and safety lenses show experience which agrees qualitatively with the AO experience cited above. It is evident that a significant amount of safety lens breakage could be avoided if the manufacturers' warning that "scratched or pitted lenses seriously reduce protection and should be replaced immediately" were heeded more widely.

Given the lack of detailed knowledge about the effects of small defects on impact strength and the fact that lens breakage

in the field occurs almost entirely with severely abused lenses, the only realistic contribution which we can make is to recommend a test method and a set of rejection criteria which experience shows result in very few breakage problems with new or well-cared-for lenses.

The test method which we will recommend is a subjective one. Despite our desire to recommend objective test methods, we cannot do so in this case. Millions of dollars have been spent in the optical industry in the development of objective testing for cosmetic defects, and success has been very limited. Expensive systems are available which can test small areas slowly for certain critical applications in military or astrophysical optical systems, but they are totally impractical for the volume of lenses used in safety. We are aware that work is continuing on improved systems for high volume application but at lower quality levels than we will recommend below.

The test method consists of visual inspection. The inspector sits in a dimly-lighted area in front of a dark hooded booth whose interior is finished in flat black. At the back of the booth is a "light box", a black rectangular box containing a 25 watt frosted incandescent lamp about 8 inches from a rectangular plastic diffusing plate in the front of the box facing the inspector. The box is light-tight. The observer inspects a lens by holding it about 12 inches from the box and 13-16 inches from the eyes. First the lens is viewed against the bright plastic plate where defects such as holes, bubbles, inclusions, gray, and edge chips are detected. The observer then moves the lens downward across the dividing line between bright field and dark field since scratches, pits, fractures, generating marks, striae, and weld lines are more visible at the boundary between fields. Linear defects are more visible when parallel to the edge between fields. The observer then repeats the process above after rotating the lens 90°. It is observed that slight scratches will, in trade terminology, "turn out", that is will not be visible when they are perpendicular to the edge between bright and dark fields, while heavier scratches will remain visible.

Recommended rejection criteria are:

1. A scratch or dig anywhere on the lens surface which does not "turn out".

2. Any visible fracture, hole, bubble, gray, generating mark, striae, inclusion, or weld line.

3. Edge flakes

Convex side -- more than two flakes, or two flakes closer than 1 inch apart measured on the lens periphery, allowed maximum size for flakes being 1/4 x 1/4 mm.

Concave side -- same as convex side except maximum size 1/2 x 1/2 mm.

We would classify all these defects except fractures in the Major A category since they tend to reduce protection and are not detectable by the average user under normal lighting conditions. From the experience cited above about condition of lenses which we have observed that have actually broken in the field, we feel that only fractures reduce impact resistance enough to be classified as critical.

As a final point, we should note that if it is desired to implement a government-regulated inspection system for the defects described above, at least two requirements are evident. First, the inspection system should be defined more exactly than is done above. Second, sets of standard lenses containing just-acceptable defects should be made up and should be available to all interested parties as an aid to standardizing inspection procedures and capability of inspectors. A similar procedure has been widely used in the past by Frankford Arsenal for scratch and dig tolerances for ordnance optics.

REFERENCES

1. American National Standard, Practice for Occupational and Educational Eye and Face Protection, ANSI Z87.1-1968.

2. Sliney, D. H., and B. C. Freasier, Evaluation of optical radiation hazards, Appl. Optics, 12 (1): 1-24, Jan. 1973.

3. Pitts, D. G., The Human ultraviolet action spectrum, Am. J. Optom., 51 (12): 946-960, Dec. 1974.

4. Threshold Limit Values for Chemical Substances and Physical Agents in the Workroom Environment with Intended Changes for 1976, American Conference of Government Industrial Hygienists, Cincinnati, Ohio, 1976.

5. American National Standard for the Safe Use of Lasers, ANSI Z136.1-1976.

6. Judd, Deane B., and Wyszecki, Gunter, Color in Business, Science, and Industry, 3rd ed., Wiley, New York, 1975.

7. Colorimetry, International Commission on Illumination (CIE), Publication CIE No. 15 (E-1.3.1.) 1971, Bureau Central De La CIE, Paris, France.

8. Sutter, E., Hubner, H. J., Krause, E., Ruge, J. Strahlungmessungen an vershiedemen Lichtbogen - Schweissverfahren, Physikalish-Technische Bundesanstalt, Braunschweig, W. Germany, April 1972.

9. Landry, R. J., Eye Protection for Welders, American Optical Corporation Research Report No. 73-14, April, 1973.

10. Kamin, J. I., unpublished communication, August, 1975.

11. Van Someren, E., and Rollason, E. C., Radiation from a welding arc, Welding Journal, 27, p. 448, 1948.

12. Van Someren, E., and Rollason, E. C., Comparison of radiation from argon arc welding with that of metallic arc welding. Welding Journal, 29, p. 566, 1949.

13. Clark, B. A. J., Infra-red transmission limits for welding filters, Australian Journal of Optometry, 50(4): 154-161, June, 1967.

14. Clark, B. A. J., Welding filters and thermal damage to the retina, Australian Journal of Optometry, 51(4): 91-98, Apr. 1968.

15. Clark, B. A. J., Spectral-transmissive requirements for welding filters, Journal of the Institution of Engineers, Australia, 41: 18-20, Jan.- Feb. 1969.

16. Bechtold, E. W., The aberrations of ophthalmic lenses, Am. J. Optom., 35 (1): 10-24, 1958.

17. Morgan, Meredith, Jr., and Henry B. Peters, The optics of ophthalmic lenses, The Associated Student Store, University of California, Berkeley, California, 1948.

18. Borish, Irvin M., Clinical Refraction, Third Edition, Professional Press, Chicago, Illinois,1970.

19. Peters, Henry B., The relationship between refractive error and visual acuity at three age levels, Am. J. Optom. 38 (4): 194-198, 1961.

20. Stimson, Russell L., Ophthalmic Dispensing, (Second Edition), C. C. Thomas, Springfield, Illinois, 1971.

21. Stoddard, K. B., and Morgan, M. W., Monocular Accommodation, Arch. Am. Acad. Optom. 19 (11): 1942.

22. Davis, John K., The optics of plano lenses, Am. J. Optom. 34 (10): 540-556, 1957.

23. American National Standard, Requirements for first-quality prescription ophthalmic lenses, ANSI Z80.1-1972.

24. Smith, Warren J., Modern Optical Engineering, McGraw-Hill, New York, 1966.

25. MIL HDBK-141, Military Standardization Handbook, Optical Design, 5 Oct. 1962, pp. 25-29 to 25-36.

26. Ibid, pp. 26-1 to 26-8.

27. Ibid, pp. 25-20 to 25-24.

28. Ibid, pp. 25-24 to 25-29.

29. Ibid, pp. 25-14 to 25-19.

30. Strong, J., Concepts of Classical Optics, W. H. Freeman & Co., San Francisco, 1958.

31. Ref. 25, pp. 25-3 & 25-4.

32. MIL-STD-150A, Military Standard Photographic Lenses, 28 Jan. 1963, Section 5.

REFERENCES

33. Ref. 24, Chap. 11.

34. Ref. 24, pp. 324-325.

35. Proceedings of the Society of Photo-Optical Instrumentation Engineers, 46: Image assessment and specification, May 20-24, 1974.

36. van Meeteren, A., Calculations on the optical modulation transfer function of the human eye for white light, Optica Acta 21(5): pp. 395-412, 1974.

37. Wyszecki, G., and Stiles, W., Color Science, John Wiley & Sons, Inc., New York, 1967, Table 2.3.

38. Levi, L., Applied Optics, John Wiley & Sons, Inc., New York, 1968.

APPENDIX I

TREATMENT OF DATA

It has been the practice in the investigation of impact resistance at AO to analyze data graphically by use of probability graph paper. The approach was quite simple and straightforward because our impacts with spherical missiles cause no appreciable damage to the specimen and repeated incremented impact could be made until failure resulted. If the data plot to a respectable straight line, then their distribution is Normal or Gaussian and all the mathematical formulas useful in analysis of such distributions can be applied, if so desired.

It happens, however, that two of the more popular data analysis parameters, mean and standard deviation, can be obtained with reasonable precision and accuracy directly from the graphs

mean = $\bar{x} = x_{50}$ = the ordinate at which the graph crosses the 50% abscissa

standard deviation = $S_x = (x_{84} - x_{50})$ or $(x_{50} - x_{16})$ the difference between the 50% ordinate and either the 84% or 16% ordinate

Plotting technique

1. Arrange the data in ascending value from smallest to largest $x_1 \ldots . x_i \ldots . x_n$
2. Determine the bandwidth, W, occupied by each x_i on the abscissa scale by dividing 100%/N where N is the number of data points to be plotted.
3. Locate x_1 on the W/2 abscissa, the center of the first bandwidth and its ordinate.
4. Locate x_2, x_3 ... x_n succeeding bandwidths up scale from x , so that each x_i is plotted at the center of its bandwidth, W.

5. In most cases a visually-determined straight line through the points yield a mean and standard deviation that agree remarkably well with values obtained by mathematical analysis.

   However, if the impact increments have been large enough to yield several points having the same ordinate the line must pass through the right extreme of each group rather than the center. Specimens break only at impact levels higher than their impact resistance level rather than at lower levels. This of course applies for multiple-impact testing only, where all samples are broken.

Bruceton technique data

Failures in the Bruceton data represent impacts that were in excess of the true impact resistance by some unknown number of increments whereas in the multiple-impact procedure a failure is at only some fraction of an increment above the true impact resistance.

Survivals represent an impact lower than the true impact resistance by some unknown number of increments whereas there are no survivals in the multiple-impact system.

Bruceton probability plots

The procedure employed in the treatment of the data in this project was to disregard the "Failure", "Survival" identity of the data and place them all in a single smallest-to-largest rank. Our plotting procedure then continued unchanged from that used with repeated incremented impact data except that each point was properly identified upon the graph. Figure 44 is an illustration of this approach.

During the analysis of the data a second approach occurred to us. This involves plotting the Failures and the Survivals as two separate samples on the same graph paper as illustrated in Figure 98. The straight lines through the two sets of points may be positioned "by eyeball" or from calculated mean and standard deviation. The central line between the Failure line and the Survival line, graphically located to be midway between them is remarkably similar to the "eyeball" line of Figure 44.

Multiple points at a given ordinate

A third problem arose from the occurrence of more than one data point on the same ordinate. This occurs in multiple-impact tests when a large increment is taken. As described

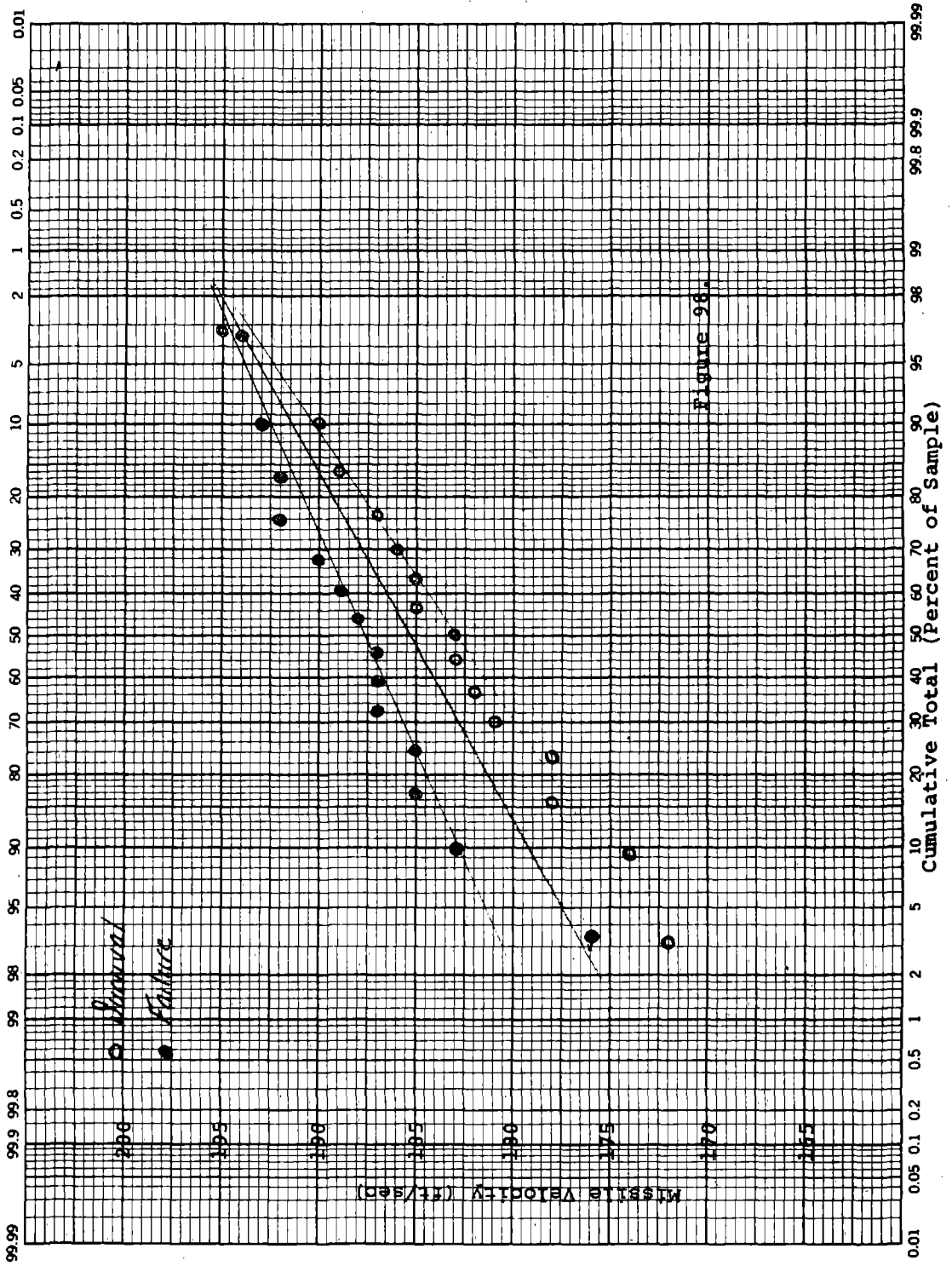

Figure 98. Data points of Figure 44 plotted in separate categories

earlier we have handled this problem by eyeballing the line through or near the right end of the group.

In ranking data it has been our habit to rank from first toward last data created in assigning rank number to data points of the same ordinate. This procedure was used in treating the Bruceton data of this report. In retrospect, we recognize that it could be argued that Failures should lie at the left and Survivals at the right end of the distribution. Then ideally the line would run through or near the right ends of the Failure groups and the left ends of the Survival groups. Such procedure would, in general, raise mean values and reduce standard deviations by small amounts. It would not alter the relative ranking of the impact resistances of the products used as illustrative examples and experimental targets in this study, nor would it alter the discussion and recommendations at the end of Task 2.

Mathematical analysis of Bruceton technique data

An excellent presentation, in general terms and procedural detail, of the analysis of Bruceton or "staircase" data is given in NBS Handbook 91, Aug. 1, 1963, pp. 10-22 to 10-24 (U.S. Gov. Printing Office Stock No. 003-003-00135-0, Cat. No. C13.11.91) by M. G. Natrella.

When application of the analysis technique of page 10-23 of Natrella is made to the data of Fig. 44, a typical impact resistance test of this project, the calculated mean agrees quite well with that obtained by "eyeball" graphical analysis with probability graph paper. The calculation is shown in Table 29. However, the standard deviation given by the method of p. 10-24 is much larger than that obtained from the "eyeball" line of Fig. 44; this calculation is in Table 29 also.

The reason for this difference is illustrated in Tables 29 and 30. In Table 29 exact measured velocities were used and the data were analyzed as though the equally-spaced test levels were 1 ft/s apart. This violates the condition given on p. 10-22 of Natrella for the validity of the calculated method used, that condition being that the spacing between test levels be between half and twice the true standard deviation of the distribution. In this case, from the "eyeball" line of Fig. 44 the standard deviation must be in the vicinity of 5 ft/s. Table 30 shows the analysis when the data points are grouped as though the test levels were 4 ft/s apart as suggested on p. 10-24 of Natrella; agreement is then quite good with the semi-intuitive eyeball line.

There is probably a correct statistical method for handling these data when exact velocities are used, but we are not

Table 29. Calculation of mean impact resistance of data of Fig. 44 by method given on page 10-23 of Natrella (NBS Handbook 91)

y	r	j	j^2	rj	rj^2	
195						
194	1	18	324	18	324	
193	1	17	289	17	289	
192	2	16	256	32	512	
191	0	15				
190	1	14	196	14	196	
189	1	13	169	13	169	
188	1	12	144	12	144	
187	3	11	121	33	363	
186	0	10				
185	2	9	81	18	162	
184	0	8				
183	1	7	49	7	49	
182	0	6				
181	0	5				
180	0	4				
179	0	3				
178	0	2				
177	0	1				
176	1	0	0	0	0	
176	14			164	2208	1
y_o	R			A	B	d

$R \leq N/2$, since $N = 29$

$$\bar{v} = m = y_o + d\left(\frac{A}{R} - \frac{1}{2}\right)$$

$$= 176 + \left(\frac{164}{14} - \frac{1}{2}\right)$$

$$= 176 + \frac{164-7}{14}$$

$$= 176 + 11.2$$

= 187.2 vs. 185 shown on Fig. 44 where line was placed by "eyeball" method.

Table 29. Continued

$$S_x = 1.620d \left(\frac{RB - A^2}{R^2} + .029 \right)$$

$$RB = (14)\ (2208)$$

$$R^2 = (14)^2$$

$$= 1.620d \left(\frac{(14 \times 2208) - 164^2)}{(14^2)} + .029 \right)$$

S_x = 33.2 vs. 5 via "eyeball" on the graph.

Table 30. Second calculation of mean impact resistance of data of Fig. 44 by method given on page 10-23 of Natrella (NBS Handbook 91)

y	r	j	j^2	rj	rj^2
194	0				
190	3	3	9	9	27
186	5	2	4	10	20
182	2	1	1	2	2
178	1	0	0	0	0
174	0				
	11			21	49
				A	B

$y_o = 178$
$R = 11$
$A = 21$
$B = 49$
$d = 4$

$$\bar{v} = m = y_o + d\left(\frac{A}{R} - \frac{1}{2}\right)$$

$$= 178 + 4\left(\frac{21}{11} - \frac{1}{2}\right)$$

$$= 183.6$$

$$S_x = 1.62d\left(\frac{RB - A^2}{R^2} + .029\right)$$

$$= 5.4$$

sophisticated enough to try to find it as this final report is written, because it would serve little useful purpose under this contract for the following reasons:

1. If the speedle test were to be used in a performance standard then it would be used as a pass-fail test. In this case gas pressure of the air gun would be set by trial-and-error to the correct pressure to give the desired velocity, and the small standard deviation in velocities given by Table 16 would apply.

2. If the speedle test is used, as under this contract, to appraise or survey the impact resistance of products, then the additional uncertainty in velocity with each change in pressure setting comes into play. This results in the test levels becoming somewhat more "blurred" or broadened than the less than 1% coefficient of variation given in Table 16. As we see from Table 30, this problem can be handled in data reduction by grouping the data points using appropriately sized test level spacing - appropriate test level spacing for analysis can be determined by an "eyeball" line through the data points plotted on probability paper.

3. A more exact analysis would not alter conclusions reached in Task 2 about the applicability of the speedle test or the relative impact resistance of products surveyed. This conclusion was reached after comparing "eyeball" line data with properly grouped data points for two other impact tests in the series reported on in Task 2. A more exact analysis would alter numerical results by only a few percent at most.

4. A more exact analysis would have delayed this report.

In conclusion, the fact that an approximate method of statistical analysis was used to reduce data in the impact-resistance survey of Task 2 has no bearing on use of the speedle in a go - no go performance test. As discussed earlier, we feel the speedle test to be very worthwhile for any future standard on impact resistance.

BIBLIOGRAPHIC DATA SHEET	1. Report No.	2.	3. Recipient's Accession No. PB276818
4. Title and Subtitle *DEVELOPMENT OF CRITERIA AND TEST METHODS FOR EYE AND FACE PROTECTION DEVICES*			5. Report Date *August 1977* 6.
7. Author(s) *David A. LaMarre*			8. Performing Organization Rept. No.
9. Performing Organization Name and Address *American Optical Corporation* *14 Mechanic Street* *Southbridge, Massachusetts 01550*			10. Project/Task/Work Unit No. 11. Contract/Grant No. *210-75-0058*
12. Sponsoring Organization Name and Address *National Institute for Occupational Safety and Health* *4676 Columbia Parkway* *Cincinnati, Ohio 45226*			13. Type of Report & Period Covered *Final* 14.

15. Supplementary Notes

16. Abstracts: *Eye and face protection devices required by OSHA for use by industrial employees must comply with the performance and design specifications of American National Standards Institute Standard Practice for Occupational and Educational Eye and Face Protection ANSI Z87.1-1968. Some of the requirements and test methods of Z87.1 have been unchanged for many years or are not clearly defined, hence there exists a need to determine whether performance requirements are adequate and to improve test methods. Following description of a program of analytical and experimental work on three specific aspects of eye and face protection devices, recommendations are presented for significant changes in attenuation properties of light-absorptive materials such as welding plates, for a high-speed impact test employing a pointed missile, and for improved test methods for optical attributes.*

17. Key Words and Document Analysis. 17a. Descriptors

Protection
Protective clothing
Goggles
Safety engineering
Safety devices
Industrial hygiene
Headgear
Optical properties
Mechanical properties

17b. Identifiers/Open-Ended Terms

Absorbing lenses
Impact resistance
Optical tolerance and test methods

17c. COSATI Field/Group *06/J*

18. Availability Statement	19. Security Class (This Report)	21. No. of Pages
Release unlimited	UNCLASSIFIED	*198*
	20. Security Class (This Page) UNCLASSIFIED	22. Price *PC-A09/MF-A01*